STUDY OF THE ALTERATIONS OF MINERAL METABOLISM AND BONE DISORDERS ASSOCIATED WITH CHRONIC KIDNEY DISEASE (Estudio de las Alteraciones del Metabolismo Mineral y de los Trastornos Óseos asociados a la Enfermedad Renal Crónica)

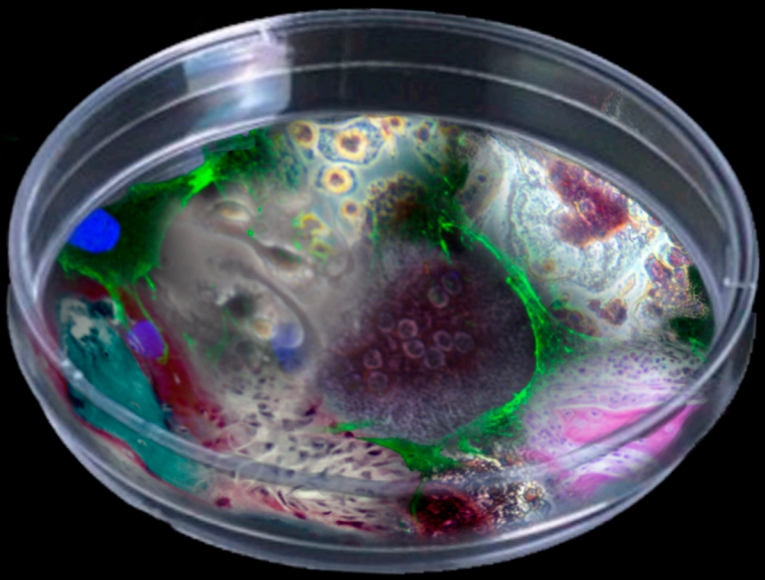

AUTHOR: Juan Miguel Díaz Tocados

DIRECTORS: Juan R. Muñoz Castañeda
Yolanda Almadén Peña

TUTOR: Mariano Rodríguez Portillo

PhD Program in Biomedicine
IDEP Submission Date: 10/12/2018

TITULO: *STUDY OF THE ALTERATIONS OF MINERAL METABOLISM AND BONE DISORDERS ASSOCIATED WITH CHRONIC KIDNEY DISEASE*

AUTOR: *Juan Miguel Díaz Tocados*

Campus de Rabanales
Ctra. Nacional IV, Km. 396 A
14071 Córdoba

https://www.uco.es/ucopress/index.php/es/
ucopress@uco.es

STUDY OF THE ALTERATIONS OF MINERAL METABOLISM AND BONE DISORDERS ASSOCIATED WITH CHRONIC KIDNEY DISEASE

(Estudio de las Alteraciones del Metabolismo Mineral y de los Trastornos Óseos asociados a la Enfermedad Renal Crónica)

Author: Juan Miguel Díaz Tocados

Directors: Juan R. Muñoz Castañeda
Yolanda Almadén Peña

Tutor: Mariano Rodríguez Portillo

PhD Programme in Biomedicine IDEP Submission Date: 10/12/2018

JUNTA DE ANDALUCIA

UNIVERSIDAD D CORDOBA

IMIBIC
MAIMONIDES BIOMEDICAL RESEARCH INSTITUTE OF CORDOBA

TÍTULO DE LA TESIS: STUDY OF THE ALTERATIONS OF MINERAL METABOLISM AND BONE DISORDERS ASSOCIATED WITH CHRONIC KIDNEY DISEASE (Estudio de las alteraciones del metabolismo mineral y de los trastornos óseos asociados a la enfermedad renal crónica)

DOCTORANDO/A: JUAN MIGUEL DÍAZ TOCADOS

INFORME RAZONADO DEL/DE LOS DIRECTOR/ES DE LA TESIS
(se hará mención a la evolución y desarrollo de la tesis, así como a trabajos y publicaciones derivados de la misma).

El doctorando Juan Miguel Díaz Tocados se incorporó al grupo en 2013 e inició sus estudios de doctorado en 2014 en el grupo de investigación de Metabolismo del Calcio. Calcificación Vascular de IMIBIC. Desde su incorporación ha participado activamente en todas las actividades del grupo mostrando gran resolución en las tareas en las que ha participado. Fruto de su vinculación al grupo y de su trabajo ha publicado 11 artículos científicos. En 4 de los 11 artículos publicados el doctorando participa como primer firmante. Además hay que resaltar que todos sus artículos con posición de liderazgo, la mayoría derivados de su tesis doctoral, son de contrastada calidad científica al estar publicados en revistas de primer decil y primer cuartil.
Del mismo modo, derivado de su labor investigadora es miembro de la Sociedad Española de Nefrología y de la Sociedad Española de Investigación Ósea y de Metabolismo Mineral participando activamente en los congresos nacionales e internacionales derivados de ambas especialidades.
En cuanto a su formación el doctorando ha realizado 2 estancias pre-doctorales con una duración global de 8 meses en el laboratorio del Dr. João Frazão en Porto, Portugal en donde ha tenido la oportunidad de profundizar en el estudio de la histomorfometría ósea en condiciones de uremia.
La presente Tesis Doctoral, llevada a cabo bajo nuestra dirección y supervisada por el Tutor Mariano Rodríguez Portillo se ha desarrollado durante el período comprendido entre 2014 y 2018 y está encuadrada en el Programa de Doctorado en Biomedicina de la Universidad de Córdoba.
A continuación se detalla la producción científica derivada del programa de doctorado del doctorando.

Indicadores generales de calidad de la producción científica

Total de Publicaciones: 14
Índice H: 5
Promedio de citas por elemento: 5,43
Total de veces citado: 76 (Sin citas propias: 73)
Artículos en que se cita: 72 (Sin citas propias: 70)

Publicaciones científicas indexadas

Díaz-Tocados JM, Rodríguez-Ortiz ME, Almadén Y, Pineda C, Martínez-Moreno JM, Herencia C, Vergara N, M. Pendón-Ruiz de Mier MV, Santamaría R, Rodelo-Haad C, Casado-Díaz A, Lorenzo V, Carvalho CG, Frazão JM, Felsenfeld AJ, Richards WG, Aguilera-Tejero E, Rodríguez M, López I, Muñoz-Castañeda JR. Calcimimetics Maintain Bone Turnover in Uremic Rats despite the concomitant decrease in Parathyroid Hormone concentration. Kidney Int. 2018 Dec. *In Press*

Santamaría R, **Díaz-Tocados JM**, Pendón-Ruiz de Mier MV, Robles A, Salmerón-Rodríguez MD, Ruiz E, Vergara N, Aguilera-Tejero E, Raya A, Ortega R, Felsenfeld A, Muñoz-Castañeda JR, Martín-Malo A, Aljama P, Rodríguez M. Increased Phosphaturia Accelerates The Decline in Renal Function: A Search for Mechanisms. Sci Rep. 2018 Sep 12;8(1):13701. doi: 10.1038/s41598-018-32065-2. **(Primera autoría compartida)**

Díaz-Tocados JM, Herencia C, Martínez-Moreno JM, Montes de Oca A, Rodríguez-Ortiz ME, Vergara N, Blanco A, Steppan S, Almadén Y, Rodríguez M, Muñoz-Castañeda JR. Magnesium Chloride promotes Osteogenesis through Notch signaling activation and expansion of Mesenchymal Stem Cells. Sci Rep. 2017 Aug 10;7(1):7839. doi: 10.1038/s41598-017-08379-y.

Díaz-Tocados JM, Peralta-Ramirez A, Rodríguez-Ortiz ME, Raya AI, Lopez I, Pineda C, Herencia C, Montes de Oca A, Vergara N, Steppan S, Pendon-Ruiz de Mier MV, Buendía P, Carmona A, Carracedo J, Alcalá-Díaz JF, Frazao J, Martínez-Moreno JM, Canalejo A, Felsenfeld A, Rodriguez M, Aguilera-Tejero E, Almadén Y, Muñoz-Castañeda JR. Dietary magnesium supplementation prevents and reverses vascular and soft tissue calcifications in uremic rats. Kidney Int. 2017 Nov;92(5):1084-1099. doi: 10.1016/j.kint.2017.04.011. Epub 2017 Jul 29.

Muñoz-Castañeda JR, Herencia C, Pendón-Ruiz de Mier MV, Rodriguez-Ortiz ME, **Díaz-Tocados JM**, Vergara N, Martínez-Moreno JM, Salmerón MD, Richards WG, Felsenfeld A, Kuro-O M, Almadén Y, Rodríguez M. Differential regulation of renal Klotho and FGFR1 in normal and uremic rats. FASEB J. 2017 Sep;31(9):3858-3867. doi: 10.1096/fj.201700006R. Epub 2017 May 17.

Martínez-Moreno JM, Herencia C, de Oca AM, **Díaz-Tocados JM**, Vergara N, Gómez-Luna MJ, López-Argüello SD, Camargo A, Peralbo-Santaella E, Rodríguez-Ortiz ME, Canalejo A, Rodriguez M, Muñoz-Castañeda JR, Almadén Y. High phosphate induces a pro-inflammatory response by vascular smooth muscle cells and modulation by vitamin D derivatives. Clin Sci (Lond). 2017 Jun 28;131(13):1449-1463. doi: 10.1042/CS20160807. Print 2017 Jul 1.

Lopez I, Pineda C, Raya AI, Rodriguez-Ortiz ME, **Díaz-Tocados JM**, Rios R, Rodríguez JM, Aguilera-Tejero E, Almaden Y. Leptin directly stimulates parathyroid hormone secretion. Endocrine. 2017 Jun;56(3):675-678. doi: 10.1007/s12020-016-1207-z. Epub 2016 Dec 16.

Herencia C, **Díaz-Tocados JM**, Jurado L, Montes de Oca A, Rodríguez-Ortiz ME, Martín-Alonso C, Martínez-Moreno JM, Vergara N, Rodríguez M, Almadén Y, Muñoz-Castañeda JR. Procaine Inhibits Osteo/Odontogenesis through Wnt/β-Catenin

Inactivation. PLoS One. 2016 Jun 3;11(6):e0156788. doi: 10.1371/journal.pone.0156788. eCollection 2016.

Martínez-Moreno JM, Herencia C, Montes de Oca A, Muñoz-Castañeda JR, Rodríguez-Ortiz ME, **Díaz-Tocados JM**, Peralbo-Santaella E, Camargo A, Canalejo A, Rodriguez M, Velasco-Gimena F, Almaden Y. Vitamin D modulates tissue factor and protease-activated receptor 2 expression in vascular smooth muscle cells. FASEB J. 2016 Mar;30(3):1367-76. doi: 10.1096/fj.15-272872. Epub 2015 Dec 23.

Herencia C, Rodríguez-Ortiz ME, Muñoz-Castañeda JR, Martínez-Moreno JM, Canalejo R, Montes de Oca A, **Díaz-Tocados JM**, Peralbo-Santaella E, Marín C, Canalejo A, Rodriguez M, Almaden Y. Angiotensin II prevents calcification in vascular smooth muscle cells by enhancing magnesium influx. Eur J Clin Invest. 2015 Nov;45(11):1129-44. doi: 10.1111/eci.12517. Epub 2015 Sep 13.

Guerrero F, Herencia C, Almadén Y, Martínez-Moreno JM, Montes de Oca A, Rodriguez-Ortiz ME, **Díaz-Tocados JM**, Canalejo A, Florio M, López I, Richards WG, Rodriguez M, Aguilera-Tejero E, Muñoz-Castañeda JR. TGF-β prevents phosphate-induced osteogenesis through inhibition of BMP and Wnt/β-catenin pathways. PLoS One. 2014 Feb 27;9(2):e89179. doi: 10.1371/journal.pone.0089179. eCollection 2014.

Comunicaciones a Congresos Internacionales

Título del trabajo: FGF23 impairs osteocyte maturation by inhibition of Wnt/b-catenin pathway and is associated with bone alterations in early CKD
Nombre del congreso: ASBMR annual meeting 2018
Ciudad de celebración: Montreal, Canadá
Fecha de celebración: 28/09/2018
Fecha de finalización: 01/10/2018
Entidad organizadora: The American Society for Bone and Mineral Research
Autores: **Juan Miguel Díaz Tocados**; Maria Encarnación Rodríguez Ortíz; Yolanda Almadén Peña; Julio Manuel Martínez Moreno; Carmen Herencia Bellido; Noemi Vergara Segura; Catarina Carvalho; João Miguel Frazão; Mariano Rodríguez Portillo; Juan Rafael Muñoz Castañeda.

Título del trabajo: Dietary Magnesium Supplementation Prevents and Reverses Vascular and Soft Tissue Calcifications in Uremic Rats (Comunicación Oral)
Nombre del congreso: Kidney Week 2016. American Society of Nephrology Annual Meeting
Ciudad de celebración: Chicago, Estados Unidos de América
Fecha de celebración: 15/11/2016
Fecha de finalización: 20/11/2016
Entidad organizadora: American Society of Nephrology
Autores: Mariano Rodríguez Portillo; Juan Rafael Muñoz Castañeda; Alan Peralta Ramírez; Yolanda Almadén Peña; Maria Encarnación Rodríguez Ortiz; Ignacio Lopez; Carmen Herencia Bellido; Noemi Vergara Segura; Sonja Steppan; Julio Manuel Martínez Moreno; **Juan Miguel Díaz Tocados**; Antonio Canalejo; Escolástico Aguilera Tejero.

Título del trabajo: In Uremic Rats, the Calcimimetic Maintains Bone Turnover in a Parathyroid Hormone-Independent Manner (Comunicación Oral)
Nombre del congreso: Kidney Week 2016. American Society of Nephrology Annual Meeting
Ciudad de celebración: Chicago, Estados Unidos de América
Fecha de celebración: 19/10/2016

Fecha de finalización: 21/10/2016
Entidad organizadora: American Society of Nephrology
Autores: Mariano Rodríguez Portillo; **Juan Miguel Díaz Tocados**; Maria Encarnación Rodríguez Ortiz; Yolanda Almadén Peña; Carmen Pineda; Eduardo Salido; Victor Lorenzo; Catarina Carvalho; João Miguel Frazão; Juan Rafael Muñoz Castañeda; Escolástico Aguilera Tejero; Ignacio Lopez.

Título del trabajo: High doses of calcitriol lead to alterations in osteogenesis and bone disease
Nombre del congreso: 52nd European Renal Association-European Dialysis and Transplant Association Congress
Ciudad de celebración: Londres, Inner London, Reino Unido
Fecha de celebración: 28/05/2015
Fecha de finalización: 31/05/2015
Entidad organizadora: European Renal Association-European Dialysis and Transplant Association
Autores: Maria Encarnación Rodriguez Ortiz; Juan Rafael Muñoz Castañeda; Carmen Herencia Bellido; **Juan Miguel Díaz Tocados**; Julio Manuel Martinez Moreno; Addy Rosa Montes de Oca González; Noemi Vergara Segura; Yolanda Almadén Peña; Juan Mariano Rodríguez Portillo. "Póster".

Título del trabajo: DUODENAL IRON AFTER FERRIC CITRATE ADMINISTRATION IN UREMIC RATS
Nombre del congreso: 52nd Congress of the European-Renal-Association-European-Dialysis-and-Transplant-Assocation
Ciudad de celebración: London,
Entidad organizadora: European Renal Assoc; European Dialysis & Transplant Assoc
Forma de contribución: Artículo científico
Vergara, Noemi; **Diaz-Tocados, Juan Miguel**; Encarnacion Rodriguez-Ortiz, Maria; Almaden, Yolanda; Rafael Munoz-Castaneda, Juan; Rodriguez, Mariano. "NEPHROLOGY DIALYSIS TRANSPLANTATION". 30, 01/05/2015. ISSN 0931-0509, ISSN 1460-2385

Título del trabajo: MAGNESIUM PROMOTES OSTEOGENESIS OF MESENCHYMAL STEM CELLS VIA NOTCH SIGNALING
Nombre del congreso: 51st Congress of the European-Renal Association(ERA)/European-Dialysis-and-Transplant-Association (EDTA)
Ciudad de celebración: Amsterdam,
Entidad organizadora: European Renal Assoc; European Dialysis & Transplant Assoc
Forma de contribución: Artículo científico
Diaz-Tocados, Juan Miguel; Herencia, Carmen; Martinez-Moreno, Julio M.; Montes De Oca, Addy; Encarnacion Rodriguez-Ortiz, Maria; Gundlach, Kristina; Buechel, Janine; Steppan, Sonja; Passlick-Deetjen, Jutta; Rodriguez, Mariano; Almaden, Yolanda; Munoz-Castaneda, Juan R."NEPHROLOGY DIALYSIS TRANSPLANTATION". 29, pp. 380 - 380. 01/05/2014. ISSN 0931-0509, ISSN 1460 2385

Título del trabajo: PHOSPHATE RESTRICTION PRESERVES BONE VOLUME IN EARLY AND LATE STAGES OF CKD IN RATS
Nombre del congreso: 52nd Congress of the European-Renal-Association-European-Dialysis-and-Transplant-Assocation
Ciudad de celebración: London,
Entidad organizadora: European Renal Assoc; European Dialysis & Transplant Assoc
Forma de contribución: Artículo científico

Diaz Tocados, Juan Miguel; Rodriguez Ortiz, Maria Encarnacion; Herencia, Carmen; Martinez-Moreno, Julio Manuel; Montes de Oca, Addy; Vergara, Noemi; Carvalho, Catarina G.; Rodriguez, Mariano; Frazao, Joao M.; Almaden, Yolanda; Munoz Castaneda, Juan Rafael. "NEPHROLOGY DIALYSIS TRANSPLANTATION". 30, 01/05/2015. ISSN 0931-0509, ISSN 1460-2385

Título del trabajo: SEVERE DIETARY PHOSPHORUS RESTRICTION IS ASSOCIATED WITH REDUCED FGF23 LEVELS IN UREMIC RATS
Nombre del congreso: 52nd Congress of the European-Renal-Association-European-Dialysis-and-Transplant-Assocation
Ciudad de celebración: London,
Entidad organizadora: European Renal Assoc; European Dialysis & Transplant Assoc
Forma de contribución: Artículo científico
Rodriguez Ortiz, Maria Encarnacion; **Diaz Tocados, Juan Miguel**; Munoz Castaneda, Juan Rafael; Herencia, Carmen; Martinez Moreno, Julio Manuel; Montes de Oca, Addy; Alcala Diaz, Juan Francisco; Ortiz, Alberto; Aguilera Tejero, Escolastico; Felsenfeld, Arnold J.; Rodriguez, Mariano; Almaden, Yolanda. "NEPHROLOGY DIALYSIS TRANSPLANTATION". 30, 01/05/2015. ISSN 0931-0509, ISSN 1460-2385

Comunicaciones a Congresos nacionales

Título del trabajo: En ratas urémicas la adición de calcimimético incrementa el remodelado óseo independientemente de su acción sobre la PTH
Nombre del congreso: XLVII CONGRESO NACIONAL DE LA S.E.N.
Ciudad de celebración: Burgos, Castilla y León, España
Fecha de celebración: 06/10/2017
Fecha de finalización: 09/10/2017
Entidad organizadora: Sociedad Española de Nefrología
Autores: **Juan Miguel Díaz Tocados**; María Encarnación Rodríguez Ortíz; Yolanda Almadén Peña; Víctor Lorenzo Sellarés; João Miguel Frazão; Escolástico Aguilera Tejero; Ignacio López Villalba; Juan Rafael Muñoz Castañeda; Mariano Rodríguez Portillo.

Título del trabajo: Efecto PTH-independiente de la administración de calcitriol sobre el hueso de ratas urémicas (Comunicación Póster)
Nombre del congreso: Congreso de la Sociedad Española de Investigación Ósea y Metabolismo Mineral 2016
Ciudad de celebración: Gran Canaria, Canarias, España
Fecha de celebración: 19/10/2016
Fecha de finalización: 21/10/2016
Entidad organizadora: Sociedad Española de Investigación Ósea y Metabolismo
Autores: **Juan Miguel Díaz Tocados**; María Encarnación Rodríguez Ortiz; Carmen Herencia Bellido; Julio Manuel Martínez Moreno; Noemi Vergara Segura; Catarina Carvalho; João Miguel Frazão; Ignacio Lopez; Escolástico Aguilera Tejero; Yolanda Almadén Peña; Mariano Rodríguez Portillo; Juan Rafael Muñoz Castañeda.

Título del trabajo: El suplemento dietético de magnesio previene y revierte la calcificación vascular en ratas urémicas (Comunicación Oral)
Nombre del congreso: XLVI CONGRESO NACIONAL DE LA S.E.N.
Ciudad de celebración: Oviedo, Principado de Asturias, España
Fecha de celebración: 19/10/2016
Fecha de finalización: 21/10/2016
Entidad organizadora: Sociedad Española de Nefrología
Autores: Juan Rafael Muñoz Castañeda; María Encarnación Rodríguez Ortiz; Carmen Herencia Bellido; Ignacio Lopez; Noemi Vergara Segura; Julio Manuel Martínez

Moreno; **Juan Miguel Díaz Tocados**; Yolanda Almadén Peña; Escolástico Aguilera Tejero; Mariano Rodríguez Portillo.

Título del trabajo: Efecto del suplemento de Magnesio sobre el remodelado óseo y mineralización en ratas urémicas (Comunicación E-Póster)
Nombre del congreso: XLVI CONGRESO NACIONAL DE LA S.E.N.
Ciudad de celebración: Oviedo, Principado de Asturias, España
Fecha de celebración: 08/10/2016
Fecha de finalización: 11/10/2016
Entidad organizadora: Sociedad Española de Nefrología
Autores: **Juan Miguel Díaz Tocados**; Maria Encarnación Rodríguez Ortiz; Carmen Herencia Bellido; Julio Manuel Martinez Moreno; Noemi Vergara Segura; Catarina Carvalho; João Miguel Frazão; Yolanda Almadén Peña; Mariano Rodríguez Portillo; Juan Rafael Muñoz Castañeda.

Título del trabajo: El daño renal inducido por fósforo durante la enfermedad renal crónica es previo a la hiperfosfatemia
Nombre del congreso: XLV Congreso Nacional de la Sociedad Española de Nefrología
Ciudad de celebración: Valencia, Comunidad Valenciana, España
Fecha de celebración: 03/10/2015
Fecha de finalización: 06/10/2015
Entidad organizadora: Sociedad Española de Nefrología
Autores: **Juan Miguel Díaz Tocados**; Maria Encarnación Rodríguez Ortiz; Carmen Herencia Bellido; Julio Manuel Martínez Moreno; Addy Rosa Montes de Oca González; Noemi Vergara Segura; Rosa Ortega Salas; Mariano Rodríguez Portillo; Yolanda Almadén Peña; Juan Rafael Muñoz Castañeda. "Comunicación Oral".

Título del trabajo: El incremento de la fracción de excreción de fósforo induce FGF23 resistencia a través del descenso de Klotho
Nombre del congreso: XLV Congreso Nacional de la Sociedad Española de Nefrología
Ciudad de celebración: Valencia, Comunidad Valenciana, España
Fecha de celebración: 03/10/2015
Fecha de finalización: 06/10/2015
Entidad organizadora: Sociedad Española de Nefrología
Autores: Juan Rafael Muñoz Castañeda; Carmen Herencia Bellido; Maria Encarnación Rodríguez Ortiz; **Juan Miguel Díaz Tocados**; Julio Manuel Martínez Moreno; Addy Rosa Montes de Oca González; Noemi Vergara Segura; William G. Richards; Yolanda Almadén Peña; Juan Mariano Rodríguez Portillo. "Comunicación Oral".

Título del trabajo: La restricción de fósforo preserva el volumen óseo durante las fases tempranas de la enfermedad renal crónica
Nombre del congreso: XLV Congreso Nacional de la Sociedad Española de Nefrología
Ciudad de celebración: Valencia, Comunidad Valenciana, España
Fecha de celebración: 03/10/2015
Fecha de finalización: 06/10/2015
Entidad organizadora: Sociedad Española de Nefrología
Autores: **Juan Miguel Díaz Tocados**; Maria Encarnación Rodríguez Ortiz; Carmen Herencia Bellido; Julio Manuel Martínez Moreno; Addy Rosa Montes de Oca González; Noemi Vergara Segura; João M. Frazão; Yolanda Almadén Peña; Juan Mariano Rodríguez Portillo; Juan Rafael Muñoz Castañeda. "Póster".

Título del trabajo: Normalización de FGF23 con restricción de fósforo en la uremia. Efecto de la inflamación.
Nombre del congreso: XLV Congreso Nacional de la Sociedad Española de Nefrología
Ciudad de celebración: Valencia, Comunidad Valenciana, España

Fecha de celebración: 03/10/2015
Fecha de finalización: 06/10/2015
Entidad organizadora: Sociedad Española de Nefrología
Autores: Maria Encarnación Rodríguez Ortiz; **Juan Miguel Díaz Tocados**; Juan Rafael Muñoz Castañeda; Carmen Herencia Bellido; Julio Manuel Martínez Moreno; Addy Rosa Montes de Oca González; Alberto Ortiz Arduán; Arnold J. Felsenfeld; Juan Mariano Rodríguez Portillo; Yolanda Almadén Peña. "Póster".

Título del trabajo: Efecto diferencial de calcitriol y paricalcitol sobre la osteogénesis de células madre mesenquimales de médula ósea
Nombre del congreso: XLIV Congreso Nacional de la Sociedad Española de Nefrología
Ciudad de celebración: Barcelona, Cataluña, España
Fecha de celebración: 04/10/2014
Fecha de finalización: 07/10/2014
Entidad organizadora: Sociedad Española de Nefrología
Autores: Carmen Herencia Bellido; **Juan Miguel Díaz Tocados**; Julio Manuel Martínez Moreno; Addy Rosa Montes de Oca González; Maria Encarnación Rodríguez Ortiz; Yolanda Almadén Peña; Juan Mariano Rodríguez Portillo; Juan Rafael Muñoz Castañeda. "Comunicación Oral".

Título del trabajo: El magnesio promueve la osteogénesis de células madre mesenquimales a través de la ruta Notch
Nombre del congreso: XLIV Congreso Nacional de la Sociedad Española de Nefrología
Ciudad de celebración: Barcelona, Cataluña, España
Fecha de celebración: 04/10/2014
Fecha de finalización: 07/10/2014
Entidad organizadora: Sociedad Española de Nefrología
Autores: **Juan Miguel Díaz Tocados**; Carmen Herencia Bellido; Julio Manuel Martínez Moreno; Addy Rosa Montes de Oca González; Maria Encarnación Rodríguez Ortiz; Janine Gundlach; Jutta Passlick Deetjen; Juan Mariano; Rodríguez Portillo; Yolanda Almadén Peña; Juan Rafael Muñoz Castañeda. "Comunicación Oral".

Título del trabajo: FGF23 disminuye la osteogénesis de células madre mesenquimales mediante la inhibición de la ruta Wnt/β-catenin
Nombre del congreso: XLIV Congreso Nacional de la Sociedad Española de Nefrología
Ciudad de celebración: Barcelona, Cataluña, España
Fecha de celebración: 04/10/2014
Fecha de finalización: 07/10/2014
Entidad organizadora: Sociedad Española de Nefrología
Autores: **Juan Miguel Díaz Tocados**; Carmen Herencia Bellido; Julio Manuel Martínez Moreno; Addy Rosa Montes de Oca González; Maria Encarnación Rodríguez Ortiz; Juan Mariano Rodríguez Portillo; Yolanda Almadén Peña; Juan Rafael Muñoz Castañeda. "Póster".

Patentes

Título propiedad industrial registrada: Lisados de células madre mesenquimales para el tratamiento de lesiones musculo esqueléticas
Inventores/autores/obtentores: Juan Rafael Muñoz Castañeda; **Juan Miguel Díaz Tocados**; Juan Manuel Domínguez Pérez

Nº de solicitud: PCT/ES2015/070797
País de inscripción: España, Comunidad de Madrid
Fecha de registro: 13/11/2015

Título propiedad industrial registrada: Magnesium enhanced MSC differentiation
Inventores/autores/obtentores: Juan Rafael Muñoz Castañeda; **Juan Miguel Diaz Tocados**; Herencia Bellido C; Maria Encarnación Rodríguez Ortiz; Addy Rosa Montes de Oca González; Julio Manuel Martínez Moreno; Yolanda Almadén Peña; Mariano Rodríguez Portillo; Pedro Aljama Garcia; Kristina Gundlach; Peter Mirjam; Janine Büchel; Sonja Steppan; Jutta Passlick-Deetjen
Nº de solicitud: 14 152 494.2
País de inscripción: Alemania
Fecha de registro: 29/07/2015

Título propiedad industrial registrada: Lisados de células madre mesenquimales para el tratamiento de lesiones musculo esqueléticas
Inventores/autores/obtentores: Juan Rafael Muñoz Castañeda; **Juan Miguel Diaz Tocados**; Juan Manuel Dominguez Pérez
Nº de solicitud: P201431630
País de inscripción: España, Comunidad de Madrid
Fecha de registro: 06/11/2014

Premios

VIII Lección Conmemorativa Maimónides. Premio IMIBIC 2018. Enrique Aguilar Benítez de Lugo a la publicación de mayor relevancia científica publicada en 2017 por el artículo titulado **"Dietary magnesium supplementation prevents and reverses vascular and soft tissue calcifications in uremic rats"**.

Por todo ello, se autoriza la presentación de la tesis doctoral.

Córdoba, 30 de Noviembre de 2018

Firma del/de los director/es

Fdo.: Juan Rafael Muñoz Castañeda

Fdo.: Yolanda Almadén Peña

JUAN RAFAEL MUÑOZ CASTAÑEDA, DOCTOR EN BIOQUIMICA, INVESTIGADOR SENIOR PROGRAMA NICOLAS MONARDES, CONSEJERIA SALUD, JUNTA DE ANDALUCIA, ADSCRITO AL GRUPO "METABOLISMO DEL CALCIO. CALCIFICACION VASCULAR" DEL INSTITUTO MAIMÓNIDES DE INVESTIGACION BIOMEDICA DE CORDOBA

INFORMA

Que D. Juan Miguel Díaz Tocados, licenciado en Biología, ha realizado bajo mi dirección en el Instituto de Investigaciones Biomédicas de Córdoba (IMIBIC) el trabajo titulado: "STUDY OF THE ALTERATIONS OF MINERAL METABOLISM AND BONE DISORDERS ASSOCIATED WITH CHRONIC KIDNEY DISEASE (Estudio de las alteraciones del metabolismo mineral y de los trastornos óseos asociados a la enfermedad renal crónica)", y que a mi criterio dicho trabajo reúne los méritos suficientes para optar al grado de Doctor.

Y para que así conste y surta los efectos oportunos , firmo el presente informe en Córdoba a treinta de Noviembre de dos mil dieciocho.

Fdo. Juan Rafael Muñoz Castañeda

YOLANDA ALMADEN PEÑA DOCTORA, EN BIOLOGIA, INVESTIGADORA SENIOR PROGRAMA NICOLAS MONARDES, CONSEJERIA SALUD, JUNTA DE ANDALUCIA, ADSCRITA AL GRUPO "NUTRIGENÓMICA. SINDROME METABÓLICO" DEL INSTITUTO MAIMÓNIDES DE INVESTIGACION BIOMEDICA DE CORDOBA

INFORMA

Que D. Juan Miguel Díaz Tocados, licenciado en Biología, ha realizado bajo mi dirección en el Instituto de Investigaciones Biomédicas de Córdoba (IMIBIC) el trabajo titulado: "STUDY OF THE ALTERATIONS OF MINERAL METABOLISM AND BONE DISORDERS ASSOCIATED WITH CHRONIC KIDNEY DISEASE (Estudio de las alteraciones del metabolismo mineral y de los trastornos óseos asociados a la enfermedad renal crónica)", y que a mi criterio dicho trabajo reúne los méritos suficientes para optar al grado de Doctor.

Y para que así conste y surta los efectos oportunos , firmo el presente informe en Córdoba a treinta de Noviembre de dos mil dieciocho.

Fdo. Yolanda Almadén Peña

PREFACE

At the moment we have almost finished the writing of this thesis I have much more doubts than at the beginning. All the past years studying, discussing and researching only were useful to increase the uncertainties. I remember the first day of my connection with the research group, when I met Yolanda Almadén, the key that opened the door of research for me and one of the most beautiful spirits I encountered in my life. I will be ever grateful for this coincidence.

At the end of 2012, I became a member of the IMIBIC-Calcium Metabolism and Vascular Calcification research group. All the interactions and experiences with my group were somehow constructive.

Along this thesis I was led by Juan Muñoz, the principal person responsible for the development of my scientific and critical thinking. During the time we shared, we enjoyed lovely moments, but also we had conflicts. I am well aware that to instruct PhD students is a hard responsibility that severely tire yourself. I really appreciate all the effort and every advice. I was not better student than Juan was professor.

We worked together several days and longer time, and the results were not what we expected the most of the time. Those situations were very frustrating and I felt happy when I got the support of my colleagues. That's why I get a personal feeling and I thank their patience. Unfortunately, I recognize that I could have been much better lab mate than I was.

My stays at Porto, where Professor Frazão's team introduced me to the world of the renal osteodystrophy and bone histomorphometry, were critical in the development of our studies and they all were very kind with me. All I learnt is the biggest gift.

During the time I was dedicated to this thesis I disregarded a lot of people, but I will never forgive myself not sharing the last years of my grandparents with them.

My friends and family know that I was a very enthusiastic PhD student, but they ignore how long I spent in the lab. In the most cases it was not mandatory, just an addiction.

In these pages I expound, with the help of my directors Juan Muñoz, Yolanda Almadén and Mariano Rodríguez, and the writing assistance of Marien Rodríguez and my brother Rafa, our studies focused on bone homeostasis in renal insufficiency, my doctoral thesis.

In loving memory of my grandparents

“The map is not the territory”
(Alfred Korzybski)

INDEX

ABSTRACT

Chronic Kidney Disease (CKD) affects million people worldwide and is a risk factor for morbidity and mortality. CKD patients have poor bone mineral density due to mineral metabolism imbalance and secondary hyperparathyroidism resulting in an increased fracture incidence. Bone, despite its well-known function on mineral storage and organ protection, plays an important role as endocrine organ controlling several system functions and metabolic pathways. In this respect, bone status have been associated with cardiovascular diseases and mortality in both, the general and CKD populations. Moreover, Fibroblast Growth Factor 23 (FGF23), a phosphaturic hormone secreted by osteocytes and mature osteoblasts has been associated with increased mortality and left ventricular hypertrophy.

In clinical practice, mineral abnormalities are commonly treated with calcitriol, phosphate binders and calcimimetics, to maintain plasma parathyroid hormone (PTH) and phosphate levels within the normal range. Among the distinct types of phosphate binders available, those based on magnesium have additional benefits, preventing vascular smooth muscle cells calcification.

As bone disorders are involved in adverse outcomes, we consider of interest the study of the abnormalities of mineral and bone disorders associated with CKD and how calcitriol, magnesium, calcimimetic and FGF23 affect bone cells and bone homeostasis in the context of renal insufficiency.

To address this issue we used animal models of renal insuficiency and *in vitro* models of osteoblasts and osteoclasts and we found that 1) moderate doses of calcitriol decrease osteoblast acitivity and increase mineralization *in vivo* whereas high doses of calcitriol impair osteogenic differentiation *in vitro*; 2) dietary magnesium supplementation increases osteoblast activity and may impair mineralization *in vivo* and magnesium supplementation promotes osteogenic differentiation *in vitro* through Notch signaling activation; 3) treatment with calcimimetic maintains bone turnover despite the concomitant decrease in PTH concentration *in vivo* and increased osteogenesis and mineralization *in vitro* and 4) high FGF23 concentrations produce bone changes in a model of uni-nefrectomized rats and impair osteocyte maturation whereas promote osteoclast differentiation *in vitro*.

Altogether, our results demonstrate a potential role of these molecules on bone homeostasis in CKD by targeting directly bone cells.

RESUMEN

La Enfermedad Renal Crónica (ERC) afecta a millones de personas mundialmente y es un factor de riesgo para morbilidad y mortalidad. Los pacientes con ERC tienen pérdida de densidad mineral ósea debido al desequilibrio del metabolismo mineral y al hiperparatiroidismo secundario que resulta en un incremento del índice de fracturas. El hueso, además de sus conocidas funciones como almacén de minerales y soporte y protección de órganos, juega un importante papel como órgano endocrino controlando el funcionamiento de varios sistemas y procesos metabólicos. En este sentido, el estado del hueso ha sido asociado con enfermedades cardiovasculares y mortalidad tanto en la población general como en pacientes con ERC. Además, el Factor de Crecimiento Fibroblástico 23 (FGF23), una hormona fosfatúrica secretada por osteocitos y osteoblastos maduros ha sido asociada con el incremento de mortalidad y la hipertrofia de ventrículo izquierdo.

En la clínica, el tratamiento con calcitriol, quelantes de fósforo y calcimiméticos es a menudo usado para controlar los niveles plasmáticos de hormona paratiroidea (PTH) y fósforo. Entre los distintos quelantes de fósforo, los que contienen magnesio ofrecen beneficios adicionales, previniendo la calcificación de células de músculo liso vascular.

Ya que los trastornos óseos están implicados en eventos adversos, consideramos de interés el estudio de las alteraciones del metabolismo mineral y los trastornos óseos asociados con la ERC y como el calcitriol, magnesio, calcimimético y FGF23 afectan las células del hueso y la homeostasis ósea en el contexto de la insuficiencia renal.

Para abordar este trabajo usamos modelos animales de insuficiencia renal y modelos *in vitro* de osteoblastos y osteoclastos y encontramos que 1) dosis moderadas de calcitriol mejoran la mineralización y disminuyen la actividad osteoblástica *in vivo* mientras altas dosis bloquean la diferenciación osteogénica *in vitro*; 2) el alto magnesio en la dieta incrementa la actividad osteoblástica y puede afectar la mineralización *in vivo*, mientras que *in vitro* el suplemento con magnesio promueve la diferenciación osteogénica a tráves de la activación de la ruta Notch; 3) el tratamiento con calcimimético mantiene el remodelado óseo a pesar de la consecuente disminución de los nivels de PTH *in vivo* e incrementa la osteogénesis

y la mineralización *in vitro* y 4) altas concentraciones de FGF23 provocan cambios en el hueso en un modelo de ratas uninefrectomizadas mientras que *in vitro* inhiben la maduración de los osteocitos y promueven la diferenciación osteoclástica.

En general, nuestros resultados demuestran el potencial papel de estas moléculas en la homeostasis del hueso en la ERC, afectando directamente las células del hueso.

INTRODUCTION

Chronic kidney disease (CKD) is a growing global problem affecting million people worldwide. In CKD patients, the loss of renal function leads to a mineral metabolism imbalance that compromises several organs. Due to mineral abnormalities, most of CKD patients develop secondary hyperparathyroidism (SHPT) resulting also in bone disorders.

In addition to its mechanical and organs protection functions, bone orchestrates a wide number of interactions with other organs, acting as a sender/receptor of many hormones and cytokines that take part in physiological processes such as cardiovascular status[1,2], glucose metabolism[3], immune response[4], gonadal sex steroid interaction[5], brain function[6,7], etc.

In CKD, bone contribution to cardiovascular diseases has been largely studied. For example, bone mineral density has been associated inversely to vascular calcification. Other specific bone factors such as fibroblast growth factor 23 (FGF23), has been also associated with the induction of left ventricular hypertrophy and heart failure[8–10]. Additionally, bone health is dramatically compromised in CKD patients. In this respect, the terminus CKD-Mineral and Bone Disorders (MBD) has been proposed to include the systemic abnormalities of mineral metabolism due to CKD.

Due to the fact that bone is an important contributor to mineral and cardiovascular disorders associated with CKD, we consider that the study of bone is key to understand globally the pathophysiology of CKD-MBD and propose new therapeutic tools.

In the introduction of this thesis, we summarize the current knowledge about the mineral metabolism alterations in CKD, focused on the abnormalities in bone structure and bone cells.

1. *Calcium and phosphate stores in the body*

The major reservoir in the body for calcium (Ca) and phosphate (P) is bone, containing 99% and 85% of the total content respectively in the form of hydroxyapatite. In the extracellular fluid, the amount of these elements only represents a very small part of the total body content.

In healthy individuals, blood Ca concentration varies from ~8.6 to 10.4 mg/dL. The 40% is protein-binding Ca and the 6% is linked to P, citrate and bicarbonate. The metabolic actions of Ca are attributed to its ionized form, which represents the 54% of the total blood Ca and it is tightly ranged between ~4.4 and 5.4 mg/dL (1.1-1.35 mM).

Plasma P concentration is around 3.0-4.5 mg/dL and, in normal conditions, it is inversely correlated to plasma Ca concentration. P levels vary depending of age, gender, diet and acid-base status. P is necessary to catalyze a wide number of reactions; it forms part of organic molecules and cellular structures and plays a critical role in intermediary metabolism and energy-transfer mechanisms (protein phosphorylation, ATP synthesis, etc)[11]. The distribution of the content of Ca and P in the body is shown in Table 1.

	Extracellular Fluids	Cells	Bone	Total body content*
Calcium	1%	negligible	99%	1000grs
Phosphate	0.1%	15%	85%	542grs

Table 1. Calcium and phosphate content and distribution in the body.
*Content in a 70kg adult human. Data from Favus MJ. Primer of the Metabolic Bone Disease and Disorders of Mineral Metabolism. 6th edition, 2006[10].

2. *Bone and bone cells*

Bone is the principal store of Ca and P in the body and commonly it is considered as an individual organ. The term bone could be controversial, due to it may be referred to the mineralized tissue (hard tissue), the sum of mineralized bone and the not-yet-mineralized collagen matrix or osteoid (sometimes called as pre-bone), and the whole organ including bone marrow and soft tissues. The American Society for Bone and Mineral Research (ASBMR) adopted the term bone as the sum of both, mineralized bone and osteoid.

Structurally, bone compartments are divided in two types, cortical bone that is the hard-outer layer and represents approximately the 80% of total bone mass in the adult human skeleton, and trabecular bone, also referred as spongy or cancellous bone which is an internal bone that forms a skeletal porous network. The thin structures which form the trabecular bone are called trabeculae. Figure 1 shows the bone structures of a longitudinal section of the mouse distal femur.

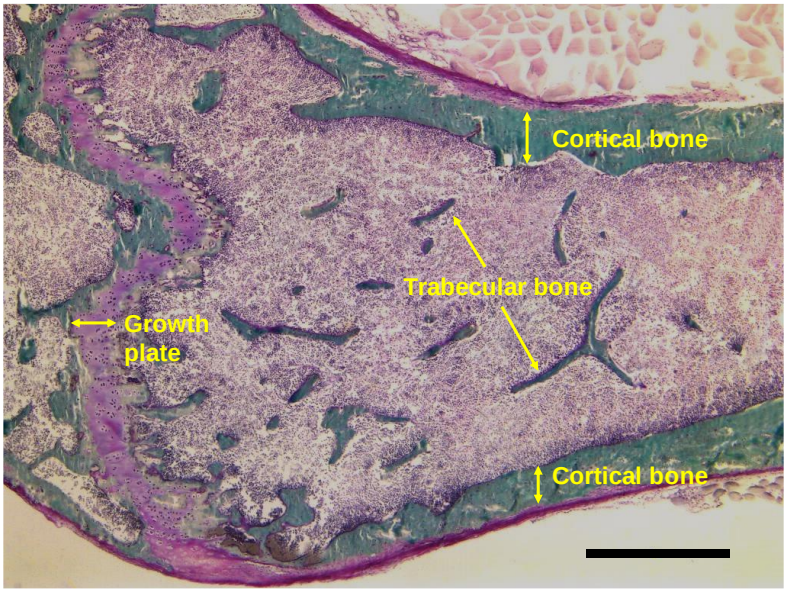

Figure 1. Goldner's trichrome image showing cortical and trabecular bone in the distal femur of a female mouse. Augmentation: 40x. Scale bar: 500µm. Image from our laboratory.

The growth plate, or epiphyseal plate, is the area of growing tissue near the ends of the long bones (fuchsia band). It is constituted by chondrocytes embedded into cartilaginous matrix which became mineralized in the zone close to the bone marrow (ossification zone). Bone is formed by several types of cells with different functions. Following, the main cells participating in bone remodeling are defined.

2.1. *Osteoblasts*

Osteoblasts are bone forming cells. This term is strictly referred to the cells, generally with cuboidal morphology, which produce bone matrix (osteoid), mainly composed by collagen fibers. The flat cells that remain quiescent are called lining cells. The osteoblast progenitor cells are mesenchymal stem cells (MSC) and they are found into the bone marrow[12]. Furthermore, MSC are also chondrocyte and adipocyte progenitors. In the bone marrow, it has been well studied that MSC differentiation into osteoblasts is inversely related to MSC differentiation into adipocytes[13,14]. With aging, bone marrow MSC tend to be differentiated into adipocytes instead of osteoblasts and it is a feature in the process of osteoporosis[15].The main stimulus for osteoblast differentiation and activity is PTH[16]. In this regard, the pharmaceutical companies have developed human recombinant PTH analogues (fragment 1-34 and 1-84) as osteoanabolic agent for the treatment of osteoporosis[17].

Osteoblast differentiation is characterized by the expression of specific bone proteins. Figure 2 illustrates the gene expression profile changes during osteoblastic/osteocytic differentiation. In early stages of differentiation, when MSC are led to be committed osteoprogenitor cells, there is an increase in the expression of Collagen Type I (COL1A1), Alkaline Phosphatase (ALP) and Runx2 genes, generating preosteoblasts. Then, preosteoblasts upregulate the expression of Osterix, an important transcription factor for osteoblast maturation[18], and Osteocalcin, a protein secreted into the bone matrix and blood stream, which participates in bone development and also has an important role in energy balance[19], and they achieve the state of mature osteoblasts. Some of the osteoblasts may be trapped into the mineralized matrix and differentiated into osteocytes, the terminal

stage of osteogenic differentiation[20]. Osteocytes highly express specific genes such as SOST, the gene responsible for the production of sclerostin.

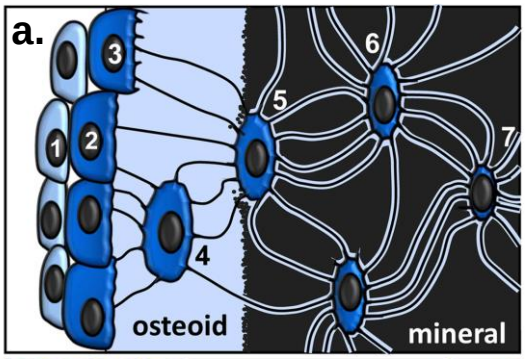

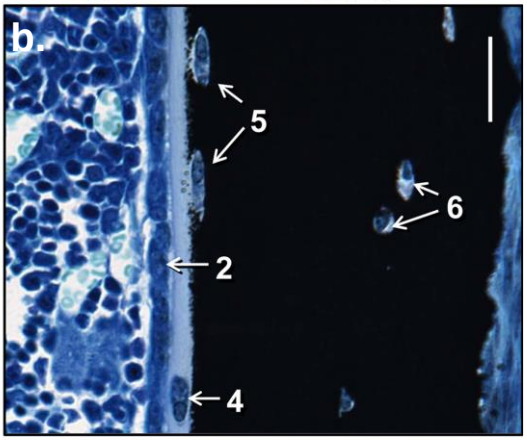

c.	1	2	3	4	5	6
RUNX2	+	+	-	-	-	-
OCN	-	+	+	+	+	-
E11	-	-	+	+	+	-
DMP1	-	-	+	+	+	+
PHEX	-	-	+	+	+	+
MEPE	-	-	-	+	+	+
Sclerostin	-	-	-	-	-	+
CapG	-	-	+	+	+	+
ORP150	-	-	-	-	-	+

Figure 2. Transitional stages during osteocyte differentiation (**a** and **b**). 1 = preosteoblast; 2 = osteoblast; 3 = embedding osteoblast; 4 = osteoid osteocyte; 5 = mineralizing osteocyte; 6 and 7 = mature osteocytes. Scale bar = 25 µm. Marker genes for the different stages of osteogenic differentiation are shown in (**c**). From Dallas SL. et al [21].

2.2. *Osteocytes*

Osteocytes are the main cell type in the adult bone and represent about the 90% of the bone cells. They can live for decades into the bone matrix and they are one of the longest-lived cells in the body and are important endocrine cells participating in mineral homeostasis and other processes. Furthermore, they act as mechanosensors and regulate bone formation and strength[21]. Osteocytes express high amounts of some specific proteins such as Dentin Matrix Protein 1 (DMP1), which participates in bone mineralization, Sclerostin, an endogenous inhibitor of Wnt signaling or Fibroblast Growth Factor 23 (FGF23), a potent regulator of phosphate metabolism. The study of the bone effects of FGF23 will be a key point in this thesis. In spite of they are embedded into the mineralized bone, osteocytes are very well connected to whole body signals. Actually, the harvesian system or osteon (Fig.3 **a**) is a very organized structure found in compact bone, measuring 0.2 mm of diameter approximately and several millimeters of length. In the center of the system exists a tunnel where blood capillaries and nerves, which transport nutrients and signals to the cells and collect waste and signals from the bone cells to the circulation. Around the harvesian canal, osteocytes are disposed in concentric circles, called lamellae. Harvesian system can contain up to 20 lamellae. Osteocytes (Fig.3 **b**) are embedded into mineralized bone, each one into their own cavity, named lacuna. Osteocytic lacunae are connected by canals, named canaliculi and they spread their dendrites along the canaliculi to connect with the dendrites of the neighbor osteocytes forming gap junctions, which only allow the transport of small molecules (intracellular signals as Ca^{2+}, cAMP, IP3). Bone canaliculi are not completely occupied by the osteocytes, the remaining space is called periosteocytic space and contains fluid and large molecules[22]. Altogether, osteocytes are tightly connected to the systemic signals and form an extremely organized network to convey information from the whole body to the bone environment and vice versa.

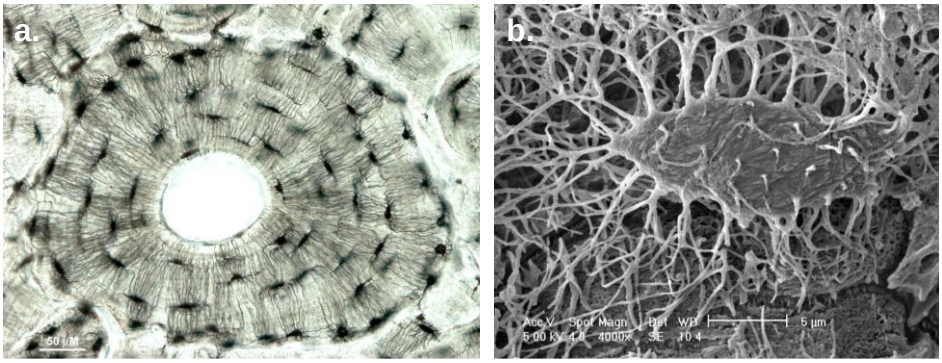

Figure 3. In (**a**) is shown a microphotograph of the harvesian system. In the middle is found the harvesian canal. Surrounding the harvesian canal, it can be appreciated a very organized network of osteocytes connected by cannaliculi (Image adapted from the gallery of the Bone Research Society). In (**b**) is shown a scanning electron microscopy (SEM) microphotograph of a mouse osteocyte showing filopodia by Bonewald LF. (Image from Pajevic PD. IBMS BoneKEy 2009)[23].

2.3. *Osteoclasts*

Osteoclasts are the bone resorbing cells. The osteoclast progenitor cells are monocytes/macrophages[24]. Several monocytes fuse to form a large multinucleated cell termed osteoclast. Although osteoclasts are multinucleated, containing from 2 to several nuclei, in a histological preparation of bone we may observe osteoclasts with only one or no nucleus because of the sectional view of the slice. Osteoclasts contain abundant lysosomes and tartrate-resistant acid phosphatase (TRAP), which is typically used as histochemical staining for osteoclast identification[25]. Osteoclast life spam is a few days[26]. Osteoclasts differentiation and their activity are regulated by the osteoblasts and osteocytes, which produce receptor activator of nuclear factor kappa-B ligand (RANKL) that binds the receptor activator of nuclear factor kappa-B (RANK) in the monocyte surface and promotes their recruitment and fusion to form osteoclasts[27]. Osteoblasts also produce Osteoprotegerin (OPG), a soluble receptor for RANKL that intercept the protein and inhibits its ability to bind RANK, preventing osteoclast differentiation and activity[28,29] (Fig.4).

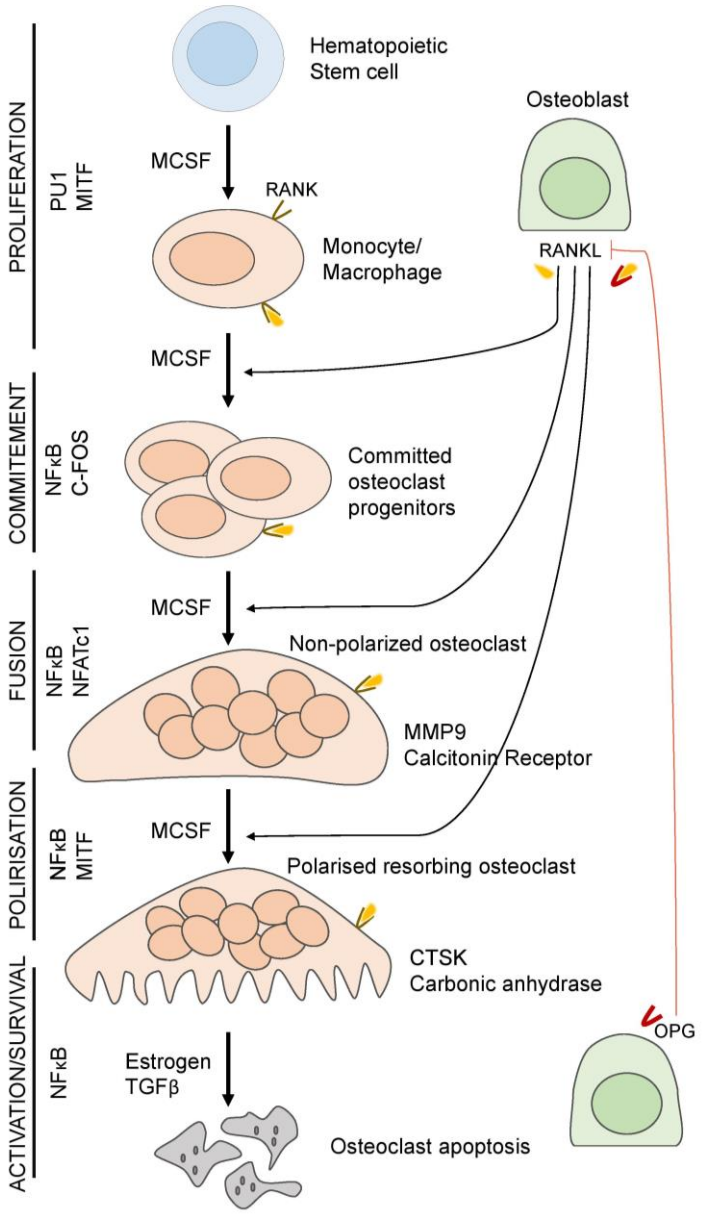

Figure 4. Stages of osteoclast differentiation. Monocytes/macrophages are cells from hematopoietic lineage. The binding of the RANKL secreted by osteoblasts to the receptor RANK in the osteoclast surface activates pathways such as NFκB and NFATc1 that lead to monocyte recruitment and osteoclast differentiation. OPG prevents RANKL actions. At contrary, estrogen and TGFβ induce osteoclast apoptosis.

In bone resorption, osteoclasts mainly release two enzymes, Cathepsin K (CTSK) which degrades the osteoid[30], and TRAP which decreases the pH level and promotes the hydroxyapatite crystals dissolution[31].

The typical situation of bone remodeling is a set of osteoblasts in a row forming bone following an osteoclast resorbing bone ahead. In a healthy bone, osteoclasts are not abundant and bone remodeling remains almost quiescent. Figure 5 shows osteoblasts in the process of bone formation and an osteoclast during bone resorption.

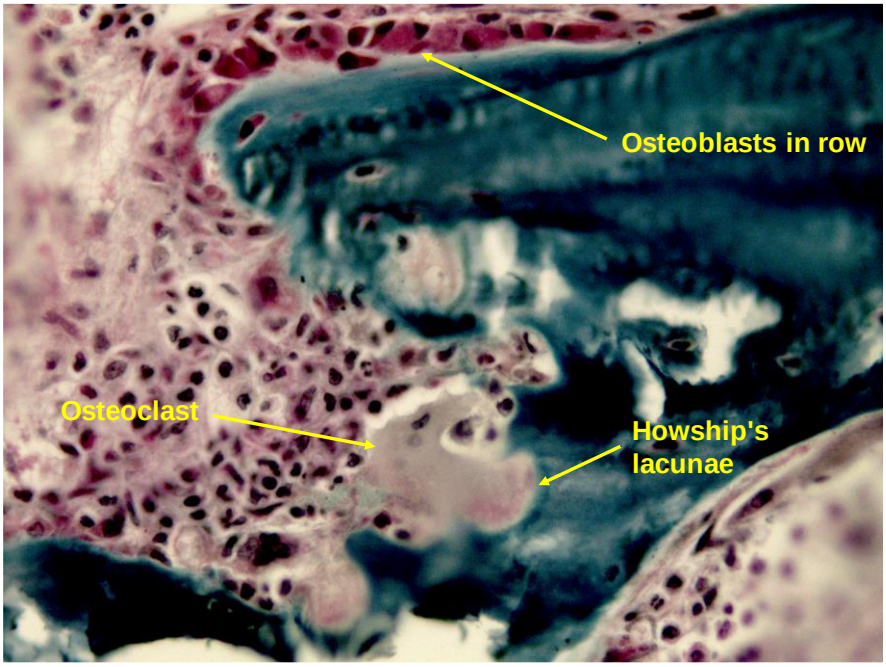

Figure 5. Example of a Goldner's trichrome staining picture showing high bone remodeling with active osteoblasts and osteoclasts. Augmentation: 400x. Image from our laboratory.

3. *Signaling pathways involved in osteoblast differentiation*

Among others biochemical pathways, Wnt/β-catenin or Notch signaling have a critical role during MSC differentiation into osteoblasts. Following, both signaling pathways are briefly described.

3.1. *Notch signaling pathway*

In addition to the Wnt/β-catenin pathway, Notch signaling activation has been associated with bone formation. Notch signaling is also a conserved pathway in multicellular organisms and it is critical in proliferation, differentiation and cell polarity in embryonic and postnatal development. To activate Notch signaling, a communication between two adjacent cells is needed. Notch receptor is a single pass transmembrane receptor consistent in an extracellular domain, a transmembrane domain and a Notch Intracellular Domain (NICD)[32]. When the extracellular domain of a receiving cell binds the surface ligand Delta or Jagged of a sender cell, the Notch receptor is cleaved intracellularly by a γ-secretase and the NICD fragments are translocated into the nucleus activating the transcription factor CSL (CBF1, Suppressor of Hairless, Lag-1), responsible for the Notch target genes expression, such as *HES* (hairy and enhancer of split-1) and *HEY* (Hairy/enhancer-of-split related with YRPW motif) genes[33]. See Figure 6.

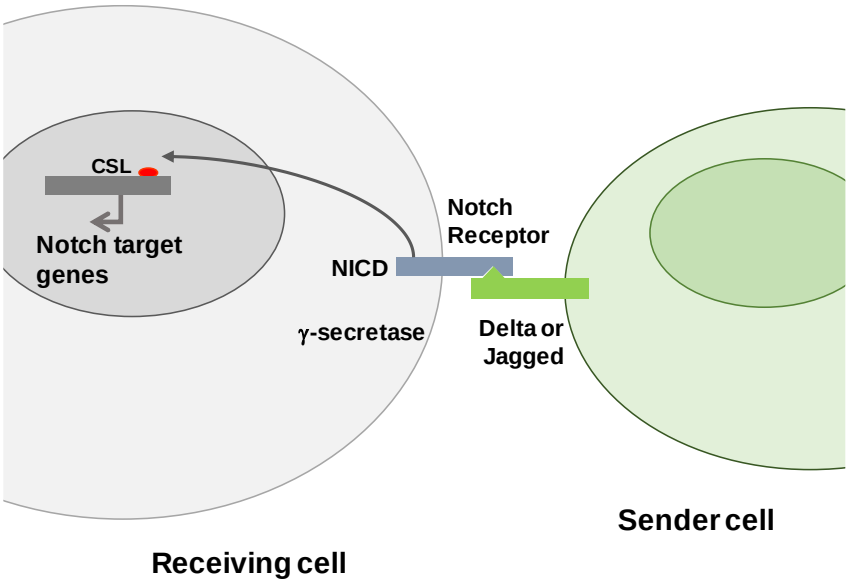

Figure 6. Simplified scheme of Notch signaling pathway. NICD: Notch intracellular domain. CSL: CBF1, Suppressor of Hairless, Lag-1 transcription factor.

In vitro, it has been reported that Notch signaling activation increases mineralization and osteoblastic differentiation[34,35]. *In vivo*, it was demonstrated that Notch signaling regulates osteoblast differentiation by maintaining the osteoblast progenitor cell pool[36,37]. Additionally, it has been shown that specific ablation of Notch in osteocytes decreases sclerostin and increases trabecular bone volume. In these mice, cortical and trabecular bone were indistinguishable, indicating that Notch exerts functions in osteocytes to determine the structure of the different bone compartments[38]. More recently, other studies have confirmed an osteoanabolic response of Notch activation in osteocytes[39–41], suggesting that there exists controversy about the role of Notch signaling during osteogenesis.

3.2. *Wnt-β/catenin pathway*

Wnt signaling pathways are highly conserved evolutionarily. The common feature of all of them is that they depend of the binding of the Wnt ligands to the receptors of the Frizzled family. The Wnt signaling pathway that involves β-catenin nuclear translocation and the activation of the target genes via T cell factor/lymphoid enhancer binding factor (TCF/LEF) transcription factors is termed canonical Wnt pathway. Its co-receptors are Lipoprotein-receptor related protein 5 (LRP5) and LRP6 and mainly participates in proliferation and differentiation. The non-canonical Wnt pathways are those not dependent of β-catenin-TCF/LEF and the most studied branches are the non-canonical Wnt/Ca^{2+} pathway, which participates in cell fate and migration, via intracellular Ca^{2+}; and the non-canonical Wnt planar cell polarity (PCP) signaling pathway which controls morphogenesis, cell polarity and migration[42]. In addition to its role in embryonic development, the canonical Wnt/β-catenin signaling pathway is critical in bone formation in adults, since mutations affecting the functionality of the LRP5 receptor have been identified as causes for skeletal disorders[43,44]. In general, sustained activation of the Wnt/β-catenin pathway in osteoblasts leads to an increase of bone mineral density.

For the canonical pathway, in the absence of soluble Wnt protein ligands, the protein Axin forms a complex with the proteins adenomatous polyposis coli (APC), Casein

kinase 1 isoform α (CK1α) and glycogen synthase kinase 3 (GSK3). Axin and APC act as scaffold proteins for GSK3β that binds and phosphorylates β-catenin, which is degraded by the proteasome. The activation of the Wnt/β-catenin pathway occurs with the binding of the Wnt ligands to the receptor Frizzled and the co-receptor LRP5 or LPR6, following the recruitment of the protein Dishevelled that sequesters Axin and prevents the complex formation. In these conditions, β-catenin is not phosphorylated and is stabilized, promoting its nuclear translocation. In the nucleus, it activates the transcription of the Wnt target genes through the interaction with the transcription factors TCF/LEF[45].

There exist a number of proteins that regulate the Wnt/β-catenin pathway by inhibition of the binding between the Wnt ligands and the co-receptors. The members of the secreted frizzled related protein (sFRP) are proteins that contains a cysteine-rich domain homologous to the putative Wnt-binding site of Frizzled proteins. Crystallographic resolution and biochemical analysis have shown that sFRPs are able to prevent the bound of the Wnt proteins to the Frizzled receptors by a) binding to the cysteine-rich domain of the Frizzled proteins and forming inactive homo or heterodimers complexes or b) binding the Wnt ligands acting as antagonist and impeding the activation of the canonical Wnt pathway[46,47].

Other proteins as Sclerostin (the product of the SOST gene) and Dickkopf related proteins (DKK), interact with LRP5/6 working as Wnt signaling inhibitors. Sclerostin binds the LRP5/6 receptors, impairs the LRP5/6-Frizzled interaction and the interaction of the Wnt signaling proteins to the receptors[48,49]. DKK binds also the LRP5/6 receptor and prevents the activation of the Wnt/β-catenin pathway[50]. (See Figure 7)

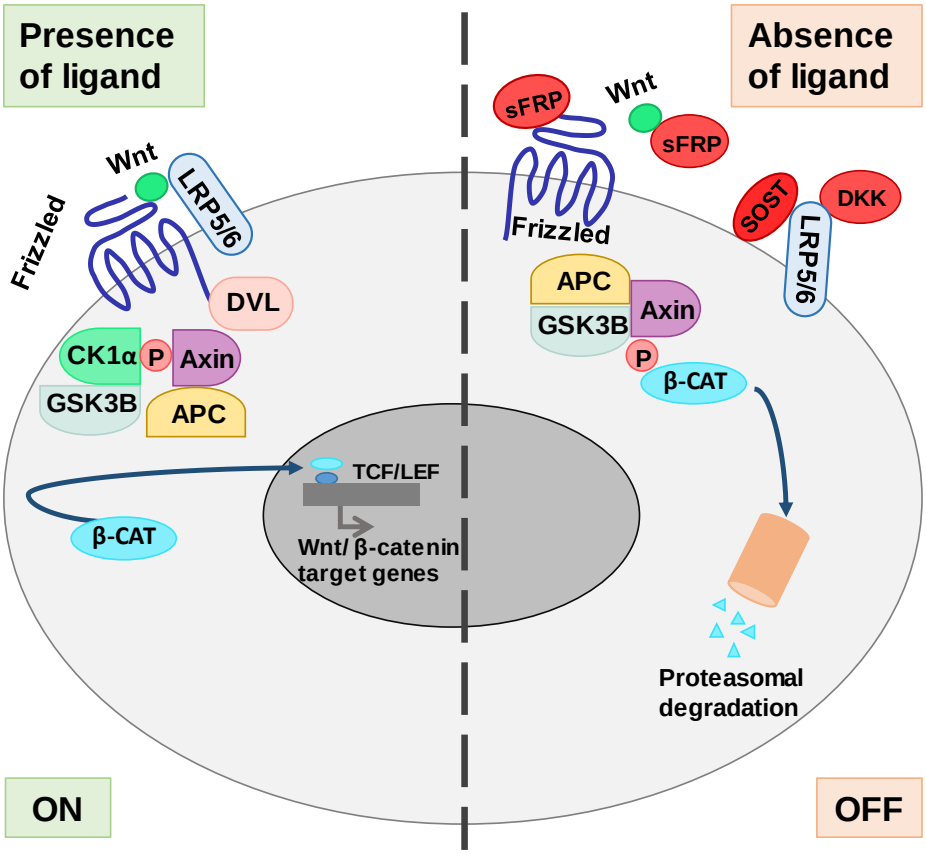

Figure 7. Simplified scheme of the Wnt/β-catenin signaling pathway. In the presence of the Wnt ligand (left), the protein Dishevelled (DVL) binds the Frizzled receptor and sequester the protein complex for β-catenin degradation, which in turn translocates into the nucleus and activates the TCF/LEF transcription factor. In the absence of the Wnt ligand or under the action of the Wnt inhibitors (right), β-catenin is phosphorylated and led for proteasomal degradation.

Historically, the participation of the Wnt-β-catenin pathway in bone disorders have been widely documented. In 1955, a rare case of osteopetrosis was defined by Van Buchem as “Hyperostosis Corticalis Generalisata Familiaris”, nowadays called Van Buchem syndrome. Van Buchem Syndrome patients show extremely increased bone mineral density with hyperostosis of the jaw and syndactyly[51]. In 2001, a loss-of-function mutations in the *SOST* gene, was identified as the cause leading to the development of the Van Buchem syndrome[52,53]. Thus, the canonical Wnt pathway is

critical in bone formation and its modulation could be beneficial for the treatment of bone disorders.

In CKD, two inhibitors of the canonical Wnt pathway have been investigated: DKK1 and Sclerostin[54]. Paradoxically, despite to both molecules inhibit Wnt ligand-LRP5/6-Fzd interaction, the downstream responses are different, unrevealing the complexity of this pathway. In CKD patients, the correlation of serum DKK1 with mineral and bone parameters is inexistent in the most studies[55,56], suggesting that DKK1 might have a weak relation with renal osteodystrophy. Nevertheless, the serum sclerostin levels increase early in CKD before renal osteodystrophy is established. It is associated with increased expression in osteocytes, which indicates a relationship between bone and kidney in CKD patients[57]. Serum sclerostin levels increase as glomerular filtration rate declines in CKD patients, and also correlate with gender and age[58]. The effects of these elevated levels of sclerostin on bone are unknown and the causes and consequences whereby the levels of serum sclerostin increase in CKD are not well understood. Paradoxically, it has been reported a positive association of serum sclerostin levels with bone mineral density in hemodialysis patients[59]. Additionally, the treatment with neutralizing antibodies against sclerostin in a murine model of CKD only resulted beneficial in low PTH conditions[60].

In vitro studies in our laboratory have reported the involvement of the canonical Wnt pathway also in pathologic processes as vascular smooth muscle cells calcification[61] and renal cells deterioration[62].

Altogether, Wnt/β-catenin pathway is largely involved on the regulation of bone formation. Considering that Wnt inhibitors are increased in CKD, it is a very attractive mechanism to look for treatments for the management of renal osteodystrophy. Similarly, it results of interest to study the relationship between bone metabolism parameters altered during CKD and the activation or inhibition of this important pro-osteogenic pathway.

4. *Calcium and phosphate balance in health*

Kidneys, gut, parathyroid glands and bone are the organs responsible for the tight regulation of Ca and P levels in the body. Thus, the main mechanisms involved in Ca and P homeostasis are intestinal absorption, renal reabsorption and bone turnover. These processes are regulated by a set of key elements, including parathyroid hormone (PTH), 1,25-hydroxyvitamin D or calcitriol ($1,25(OH)_2D_3$), fibroblast growth factor 23 (FGF23), and receptors, as calcium sensing receptor (CaSR), PTH receptor (PTHR, mainly PTHR1), Vitamin D receptor (VDR) and the complex FGFR1-α-klotho.

Parathyroid glands are the responsible organ for PTH production and secretion and the control of Ca concentration. Mechanistically, the parathyroid glands sense the Ca concentration in the blood through the CaSR, a G protein coupled-receptor that detects ionized calcium (iCa) concentration and activates a downstream signaling that regulates the PTH production and secretion[63]. When plasma Ca concentration decreases, the CaSR downstream signaling is inactivated and PTH releasing is increased (Fig.8).

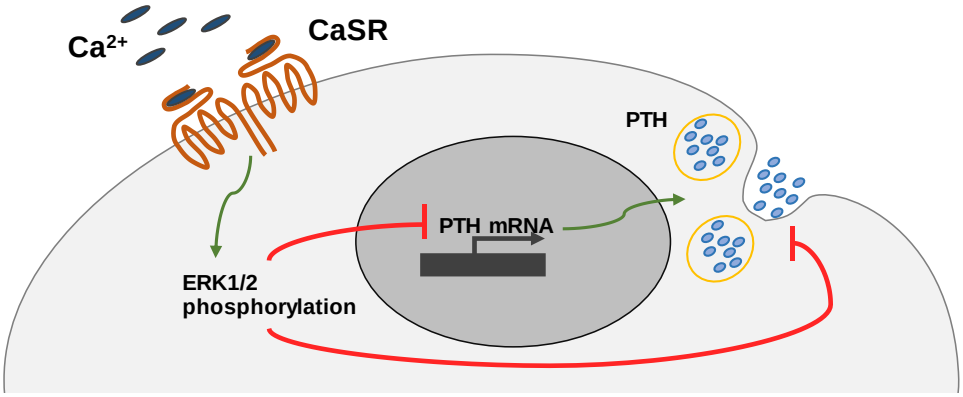

Figure 8. Mechanism of action of the CaSR in parathyroid cells.

Circulating PTH targets the kidneys and the bone, binds the PTH receptor 1 (PTHR1) and exerts its actions to normalize blood Ca concentration. In the kidney, PTH promotes Ca reabsorption through activation of the Transient Receptor Potential

Vanilloid 5 (TRPV5)[64]. Additionally, PTH induces the expression of the renal 25-hydroxyvitaminD-1-α-hydroxylase (1α-OHase), the enzyme responsible for the hydroxylation of the 25-hydroxyvitamin D to $1,25(OH)_2D_3$. Active vitamin D acts in the gut to promote the absorption of Ca through the TRPV6 channels, and P absorption through the NaPi-IIb[65].

In the bone, PTH increases the osteoclastic differentiation, proliferation and activity, by decreasing osteoprogerin (OPG) and increasing RANKL in osteoblasts, which subsequently targets the monocytes (osteoclast precursors) and promotes their recruitment and differentiation into osteoclasts[66]. Consequently, osteoclasts increase bone reabsorption and mobilize Ca from the bone-mineralized matrix to the bloodstream. At the same time, osteoblasts produce protein-bone matrix or osteoid (mainly collagen) which works as scaffold for hydroxyapatite crystals[67]. The process by which osteoblasts and osteoclasts form and resorb mineralized bone is called bone turnover or bone remodeling. Finally, the CaSR in the parathyroid glands senses again normal Ca concentrations and its activation decreases the PTH secretion, closing the loop.

In normal adults, the Ca content in the bone is net, nevertheless, this content decreases in processes such as aging or in the pathological process called osteoporosis where participate other mechanisms[68].

It is interesting to note that in normal conditions, plasma P and Ca concentrations are indirectly correlated. As well as low iCa concentration, high plasma P levels also increase PTH secretion that triggers actions in the kidneys increasing phosphaturia[69]. The *ex vivo* studies using intact parathyroid glands have been key to reveal the direct effects of P and other molecules on PTH releasing[70,71]. However, in addition to PTH, other molecules such as FGF23 has been also involved in the maintenance of P homeostasis and bone is thought to be the organ responsible for FGF23 production[72]. In osteocytes and mature osteoblasts, stimuli such as PTH or calcitriol, promote FGF23 production and secretion to the bloodstream to maintain P homeostasis through its action in the target organs[73]. The bone actions of both, calcitriol and FGF23 will be examined in this thesis.

In pathologic conditions, such as loss of kidney functionality, the regulation of the Ca and P levels is severely compromised, finding an imbalance of the mineral metabolism, which disrupts the hormonal equilibrium and leads to decreasing bone mineral density, high incidence of fractures and cardiovascular complications.
In the next section, the disorders in mineral metabolism due to kidney dysfunction are summarized.

5. *Chronic Kidney Disease-Mineral and Bone Disorders*

Nowadays, CKD is a worldwide problem without cure and only palliative treatments are used until the patients receive a renal transplant or die. After organ transplantation, treatment with immunosuppressive drugs is needed to prevent organ rejection and graft-versus-host disease. In the most cases, the transplanted organ is rejected in less than 10 years[74], therefore the problem is still far from being solved. An epidemiologic study about the incidence of CKD in Europe reported a prevalence in CKD (stages 1 to 5) from 3.3% in Norway to 17.3% in Northeast Germany[75]. In Spain, the EPIRCE study reported an overall prevalence of CKD (stages 1 to 5) of 9.09%[76].
The principal causes for CKD establishment are diabetes mellitus, hypertension and glomerulonephritis[77]. There are not specific symptoms at the beginning of the disease and often it remains undetectable until serum creatinine or proteinuria is increased. The progression of this pathology leads to alterations and changes in other organs such as heart, parathyroid glands or bone. Actually, cardiovascular complications are very common in uremic patients and are inversely associated with the decreased renal function[78]. In this respect, bone abnormalities contributes importantly to the development of mineral and cardiovascular disorders in CKD[79].
The main focus of this thesis will be the study of bone changes associated with CKD and the implications of potential treatments such as magnesium (Mg), calcimimetic and calcitriol on the development of bone disorders. Furthermore, the study of the bone effects of FGF23 in early CKD will be also addressed.

The CKD-MBD syndrome is a broad group of abnormalities related to a mineral metabolism imbalance in the context of renal disease. The progression of CKD leads to alterations in the mineral metabolism and its severity increases as the disease advances. One of the first pathophysiological events that occurs in the early stages of CKD, when the loss of glomerular filtration rate is still marginal, is a renal α-klotho down-regulation[80]. The causes for this renal α-klotho reduction is unclear yet although they are largely attributed to kidney deterioration. It has been suggested that plasma FGF23 concentration increases progressively, in part promoted by a FGF23-resistance caused by a loss of its co-receptor α-klotho which is decreased, at least in part, by an excessive P load in the renal tubular cells[62,81]. In Figure 9 are shown the changes in the mineral metabolism parameters in blood according to CKD progression.

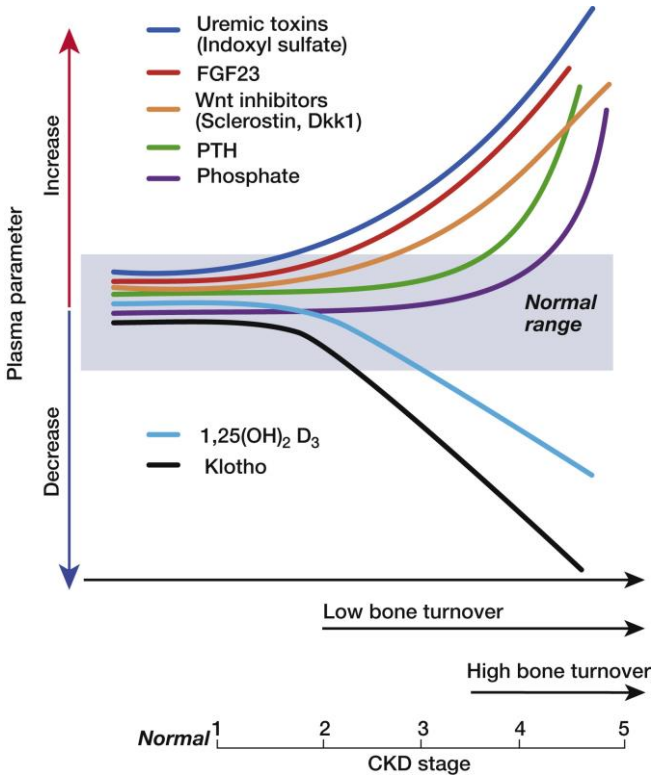

Figure 9. Changes in plasma and renal parameters with CKD progression (From Drueke T. and Massy Z.)[82].

The loss of the renal function and the high FGF23 levels decrease the renal 1α-hydroxylase expression and activity and reduces the active $1,25(OH)_2D_3$ synthesis[83]. Consequently, the lower $1,25(OH)_2D_3$ levels induce a decrease in the plasma iCa and stimulate the secretion of PTH, which additionally increases the FGF23 concentration that further suppress the expression of the renal 1α-hydroxylase and $1,25(OH)_2D_3$ production. Serum FGF23 concentration increases before PTH and becomes extremely high in end-stage renal disease (ESRD) patients[84].

The high levels of plasma PTH in uremia are not able to produce sufficient active $1,25(OH)_2D_3$ due to the loss of the functional renal mass and plasma Ca levels fall below the normal range while plasma P concentration becomes abnormally high. Moreover, FGF23 is unable to decrease PTH releasing due to the loss of the FGFR1 and α-klotho receptors in the hypertrophic parathyroid glands[85]. Furthermore, there is a feedback response by bone cells to high PTH levels that induces a direct increase of FGF23 in osteoblasts[73]. These alterations lead to the development of SHPT that dramatically affects bone homeostasis[86]. The lack of a functional kidney maintains an open cycle in progressive worsening leading to extra-renal complications (Fig.10).

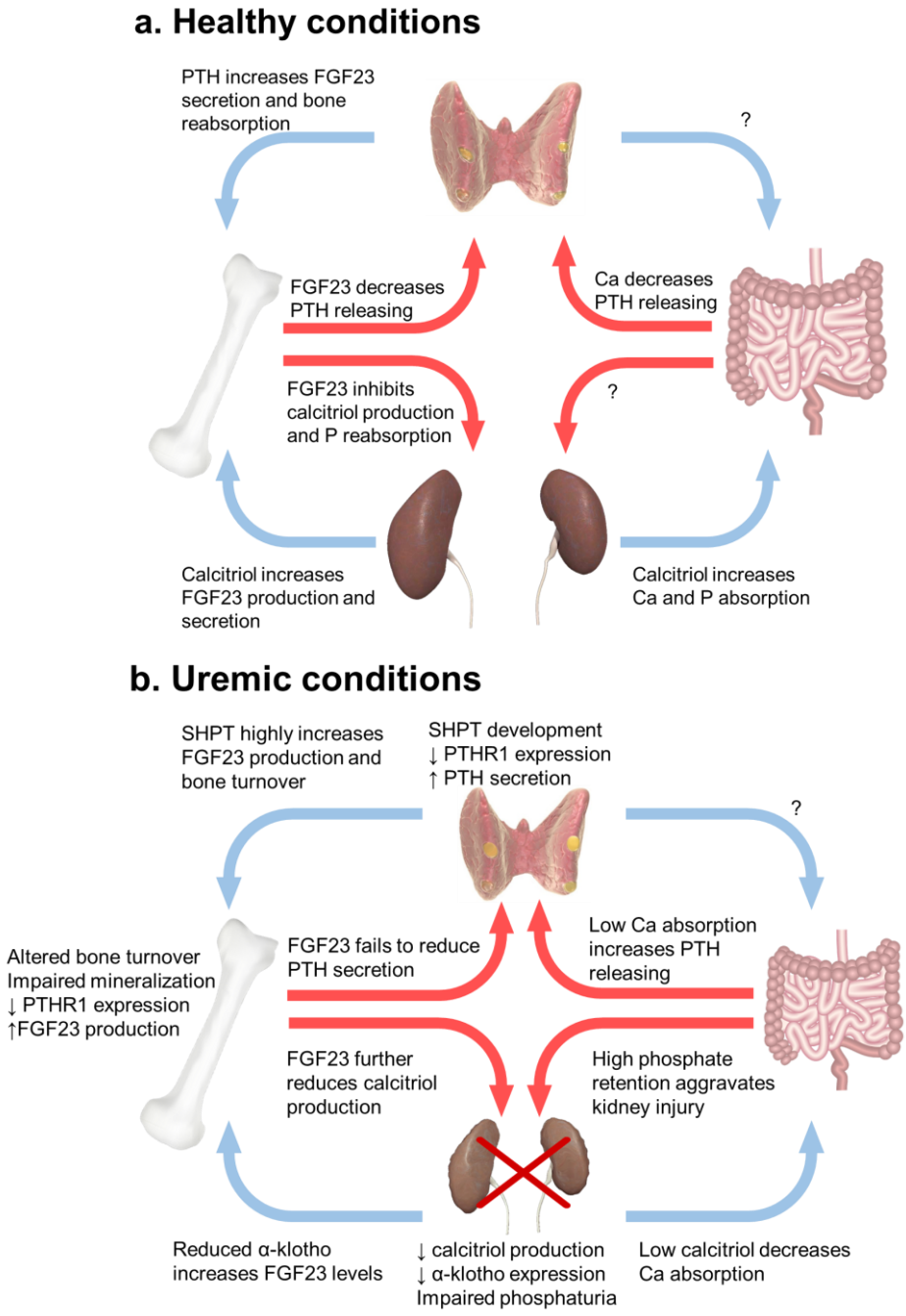

Figure 10. Scheme of endocrine interactions in the regulation of mineral metabolism in health (**a**) and renal dysfunction (**b**).

Bone disorders in CKD are heterogeneous. To provide basic understanding, the next section summarizes the main types of bone abnormities found during CKD and their potential causes.

5.1. *Renal osteodystrophy*

Renal osteodystrophy is the term that includes the different skeletal abnormalities in the CKD context[87]. Bone disorders associated with albuminuria were recognized in the year 1883[88], but it was since 60's when skeletal abnormalities emerged due to the beginning of the dialysis and the increased lifespan of the patients[89]. Nowadays, renal osteodystrophy represents a serious health problem worldwide and both, the bone contribution to renal disease progression and its relationship with cardiovascular disorders constitute a challenge in the nephrology field.

Bone disorders in renal insufficiency are largely attributed to both, the high PTH levels or the lack of responsiveness to PTH[90]. Due to the lower plasma levels of $1,25(OH)_2D_3$ and iCa, plasma PTH concentration increases and consequently also bone turnover. In these conditions, osteoclast activity may be higher than osteoblast activity, thus bone volume is reduced. Extremely high PTH levels promote also the differentiation of pre-osteoblasts into fibroblasts and lead to the development of osteitis fibrosa[91].

On the other hand, bone resistance to PTH and the increased levels of uremic toxins in early stage of renal disease lead to low bone turnover and low bone volume, this form of renal osteodystrophy is named adynamic bone disorder[92].

Renal osteodystrophy have been divided into different types based on bone turnover, bone volume and bone mineralization. The classification of the types of renal osteodystrophy is following detailed.

5.1.1. Adynamic bone disease

Nowadays, adynamic bone is the most common form of renal osteodystrophy[93]. Adynamic bone is a form of renal osteodystrophy characterized by decreased bone

volume, normal mineralization and very low or inexistent bone turnover. Both, PTH over-suppression due to an excessive pharmacological control, and the reduction in the PTHR1 expression in bone cells in CKD patients, contribute to the development of adynamic bone disorder[94]. To avoid this fact, guidelines recommend maintaining PTH levels moderately elevated[87], however in many cases this proceeding is insufficient yet.

5.1.2. Osteomalacia

Other type of bone abnormaties associated with CKD are those related to defective mineralization such as Osteomalacia. Osteomalacia is defined by an abnormal mineralization (mineralization lag time > 100 days and Osteoid thickness > 12.5µm) and low bone turnover. It commonly appears due to inadequate Ca-P ratio, insufficient $1,25(OH)_2D_3$ or factors that impair hydroxyapatite crystal formation (e.g. Aluminum). In bone histology, osteomalacia is appreciated as a high accumulation of osteoid due to impaired mineralization of the new bone matrix (See Figure 11).

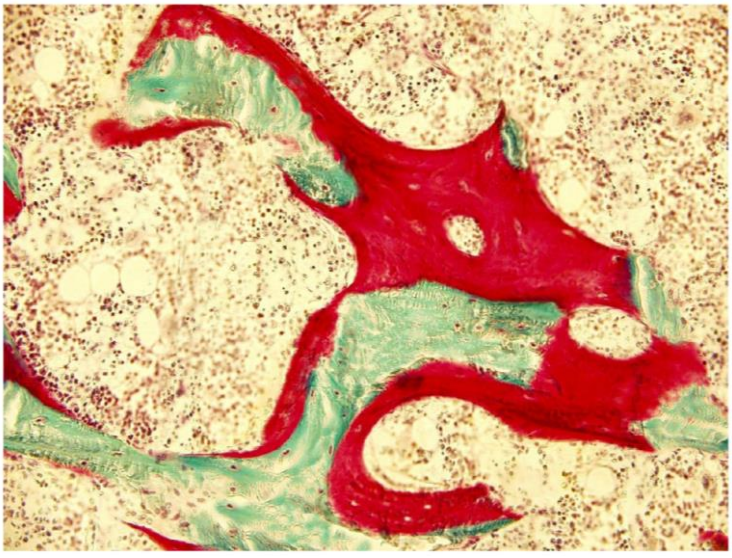

Figure 11. Goldner trichrome staining of trabecular bone showing osteomalacia in a rat with renal insufficiency (5/6Nx) for 14 days. Note the accumulation and thickness of osteoid (red). Image from our laboratory.

5.1.3. Mixed uremic osteodystrophy

On the other hand, high levels of PTH accompanied by defective mineralization may also cause Mixed Uremic Osteodystrophy, where increased osteoid, unmineralized bone matrix, and a high activity of bone cells co-exist. Mixed uremic osteodystrophy is variably defined internationally. Table 2 summarizes the different types of bone disorders in CKD.

	Volume	**Turnover**	**Mineralization**
Adynamic Bone	↓↓↓	↓↓↓	normal
Mild Hyperparathyroidism	↓	↑↑	normal
Osteotis Fibrosa	↓	↑↑↑	normal
Osteomalacia	↓	↓	↓↓↓
Mixed Uremic Osteodystrophy	↓	↑↑	↓↓

Table 2. Classification of the different forms of renal osteodystrophy according to bone turnover, mineralization and volume (TMV *turnover/mineralization/volume*) classification.

6. *Fractures Prevalence in CKD*

CKD is an important risk factor for hip fracture independently of age and gender, and the incidence ratios increase according to the time since the first dialysis treatment[95]. In addition to the risk factors in the general population, peripheral vascular disease was also independently associated with hip fractures in hemodialysis patients[96]. This risk of fractures increases as CKD progresses[97] (See Figure 12) being higher in dialysis patients[98].

Nickolas TL et al showed that the decrease of glomerular filtration rate (GFR) below 60 mL/min significantly increases the prevalence of hip fracture, particularly in younger patients[99]. In a retrospective study in CKD men, it has been showed that the increased fractures risk was dependent to the CKD stage and the age.

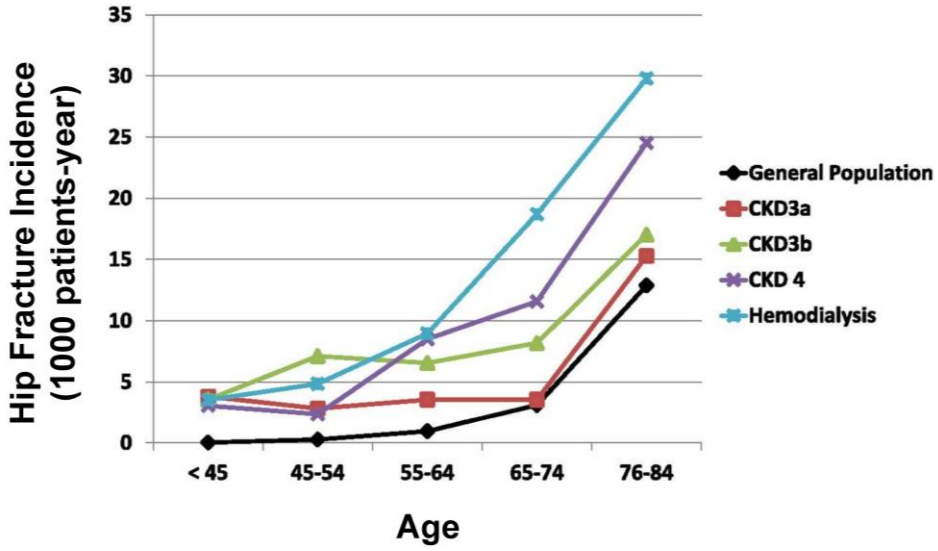

Figure 12. Hip fracture incidence have a higher incidence with age and progressive CKD increases this incidence. (From Moe SM. and Nickolas T.)[97].

In CKD patients, out of range plasma PTH levels (high or low) have been associated with fractures[100,101], so there must be other additional factors that contribute to the development of fractures in CKD. Altogether indicates that low bone mineral density and fractures are very common in CKD and optimal control of PTH levels must be a potential factor to reduce fracture and to improve survival, yet not the only one.

Of note, there exist a close relationship between the increased risk of fractures and mortality in elderly adults[102–104], and the incidence of all-cause mortality and overall survival for hip fracture is comparable to those for myocardial infarction or stroke[105]. Therefore bone analysis is critical in order to avoid fractures and complication in renal disease patients.

In the diagnosis and classification of the types of renal osteodystrophy, bone biopsy is the gold standard. Although it is not extensively used in the clinic, considering that

it is an invasive technique and requires specialized processing, bone histomorphometry is a very useful tool in clinical research, giving information about bone turnover, mineralization and volume. Moreover, the new KDIGO Guidelines 2017 Update indicates performing a bone biopsy prior to antiresorptive and other osteoporosis therapies in CKD patients from CKD-3 to CKD-5D[106].

7. *Bone histomorphometry for evaluation of renal osteodystrophy*

In 1987, Parfitt AM. et al[107], reported for the first time a set of parameters and nomenclature to encourage bone researchers to standardize the manner in which data are reported in the field of bone histology. To study bone histomorphometry accurately, specific parameters comprising bone cells number and surface, bone structure and mineralization should be included. In 2013 the guidelines were updated in by Dempster DM et al with scarce changes[108].

The specific measurement must be related to a referent and the most commonly used are Tissue Volume (TV), Bone Volume (BV), Bone Surface (BS), Osteoid Surface (OS) and their corresponding two-dimensional areas and perimeters. The three dimensional/Surface ratios are commonly referred to TV or BV.

For some case, a subdivision of bone surface is needed as a referent for bone cell number and activity. Thus, Osteoblast surface (Ob.S), the surface of bone covered by osteoblasts, and the mineralizing surface are often related to osteoid surface, while for osteoclasts, osteoid as referent is avoided. Osteoid thickness should be also specified. Eroded surface (ES) is the irregular bone surface as result of osteoclasts resorption and comprises the osteoclasts surface (Oc.S) and the reversal surface (Rv.S). Unfortunately, bone resorption cannot be measured directly by histomorphometry, however can be estimated indirectly as the bone formation rate increased or decreased by an assumed or measured rate of change of bone volume.

Respect to, derived indices can be either structural or kinetic. The structural ones are Trabecular number (Tb.N), Trabecular Separation (Tb.S) and Trabecular thickness (Tb.Th). To obtain a value for derived kinetic indices, a labeling of the

surface active in mineralization at a time of the label administration is needed. Double labeling provide information about the mineralized bone deposition. The most commonly used fluorochromes for labeling in bone histomorphometry are tetracycline and calcein compounds (See Figure 13).

Figure 13. Image shows double calcein labeling in rat trabecular bone. Interlabel period: 7days. Augmentation: 200x. Image from our laboratory.

The term Mineralizing Surface (MS) is the mean of the double labels and the half of the single labels. MS can be expressed as MS/OS, equivalent to the fraction of osteoid seam life span during which mineralization occurs or to the BS. Bone Formation Rate (BFR) relative to BV determines bone age-dependent properties. The mineral apposition rate (MAR) is a parameter of bone formation that represents the distance between labels divided by the time between both labeling. In addition, the concept of Adjusted Apposition Rate (Aj.AR) is the MAR*MS/OS and represents the best estimate available in a biopsy of the mean rate of osteoid (or matrix) apposition in the absence of osteomalacia. Others parameters are used to express the timing of mineralization. The interval between osteoid secretion and its subsequent mineralization, in days, is the mineralization lag time (Mlt). The MS is

also used to calculate bone formation rate (BFR) and the volume of mineralized bone formed per unit time. BFR relative to BS seems most logical when are being considered hormonal effects on bone remodeling. The principal parameters for bone histomorphometry are displayed in Table 3.

Despite bone histomorphometry could be applied to many types of materials, the most common are cylindrical biopsies of iliac crest in humans and sections of long bones in experimental murine models, usually femurs. Surgical biopsy for bone histomorphometry analysis is a painful intervention and is only used for diagnosis of renal osteodystrophy and research. However, as it has been already mentioned, KDIGO guidelines for CKD-MBD suggests a more extended use of bone biopsy to consider with more precision the pathophysiological alterations of bone in CKD[106].

Parameter	Abbreviation	Units
Cortical Thickness	Ct.Th	µm
Trabecular Thickness	Tb.Th	µm
Osteoid Thickness	O.Th	µm
Trabecular Separation	Tb.Sp	µm
Trabecular Number	Tb.N	/mm
Bone Volume	BV/TV	%
Osteoid Volume	OV/TV	%
Osteoid Surface	OS/BS	%
Osteoblast surface	Ob.S/BS	%
Osteoblast Number	N.Ob/B.Pm	/mm
Eroded Surface	ES/BS	%
Osteoclast Surface	Oc.S/BS	%
Osteoclast number	Oc.N/B.Pm	/mm
Mineralizing Surface	MS/BS	%
Mineralizing Surface per Osteoid	MS/OS	%
Mineral Apposition Rate	MAR	µm/day
Adjusted Apposition Rate	Aj.AR	µm/day
Mineralization lag time	Mlt	Days
Osteoid Maturation Time	Omt	Days
Bone Formation Rate	BFR/BS	µ/day
Bone Formation Rate	BFR/BV	%/year

Table 3. Nomenclature and units for bone histomorphometry parameters according to the ASBMR guidelines[107,108].

8. *Treatments for the management of CKD-MBD*

The causes for the establishment of the broad spectrum of bone disorders in CKD are poorly understood. Nevertheless, the maintenance of mineral metabolism parameters in CKD-MBD is critical to avoid bone abnormalities. In clinical practice, the use of calcitriol, CaSR agonists (calcimimetics) and P binders is frequent to maintain the mineral parameters within a narrow range in CKD patients.

Due to the fact that $1,25(OH)_2D_3$ levels are very low in CKD patients with the high levels of PTH, the most if not all the CKD patients are treated with any form of vitamin D, vitamin D receptor (VDR) agonists or calcimimetics in order to decrease PTH levels. However, despite of its effects on PTH regulation are well studied, those effects independent of PTH on bone are unknown. Therefore, both calcitriol and calcimimetic are particularly important in this thesis, and their PTH-independent effects on bone will be studied.

Regarding to P binders, there is a growing interest in the effects of Mg-based P binders on mineral metabolism. This thesis is aimed on the study of the direct actions of calcitriol, calcimimetic and magnesium on bone homeostasis in CKD, and in bone cells. To attempt this proposal we performed *in vivo* experiments using animal models of renal insufficiency, and *in vitro* models of osteoblasts and osteoclasts.

On the other hand, as mentioned above, besides PTH levels, FGF23 concentration is also deregulated in CKD and, although some direct actions of FGF23 on bone cells has been reported, its contribution to bone abnormalities in CKD have not been clearly studied yet. Another key point raised in this thesis will be the study of FGF23 effects on bone.

Following a brief introduction to the role of calcitriol, calcimimetic, magnesium, and FGF23 on bone and mineral metabolism will be summarized with a focus on CKD.

8.1. *Calcitriol*

Calcitriol or $1,25(OH)_2D_3$ is the active form of vitamin D. In 1971, it was discovered the pivotal role of the kidney in the activation of $1,25(OH)_2D_3$ [109], and the reduction of $1,25(OH)_2D_3$ induced by the loss of renal mass proposed a feasible explanation for the frequency of rickets in patients with renal insufficiency. Afterwards, patients with CKD were treated with exogenous $1,25(OH)_2D_3$, resulting in the elevation of serum Ca and the lowering of PTH levels[110]. Nowadays, $1,25(OH)_2D_3$ is commonly used to reestablish the $1,25(OH)_2D_3$ deficiency and control the SHPT. The metabolism of the vitamin D is shown in Figure 14.

The effects of vitamin D on renal osteodystrophy have been largely described. In 1977, an experiment using dogs with experimental renal insufficiency showed that restriction of P, decreased the levels of PTH and ameliorated the osteoid accumulation, however, when P restriction was accompanied by treatment with vitamin D, PTH levels further decreased and signs of renal osteodytrophy were not observed, although the animals became hypercalcemic. In that moment, the reduction of the PTH levels was attributed to the high levels of plasma Ca[111]. However, after the discovery of the existence of the VDR in the parathyroid glands, a direct action of $1,25(OH)_2D_3$ in the regulation of PTH levels was demonstrated in dialysis patients[112].

It has been reported that, in addition to the kidneys, bone cells also possess the enzyme 1-α hydroxylase, responsible for the $1,25(OH)_2D_3$ synthesis[113]. Of note, it is known since the birth of vitamin D that calcitriol increases bone reabsorption[114], however there exists controversy about its actions in bone in renal disease patients. Long-term treatment with calcitriol also decreased bone alkaline phosphatase without changes in PTH levels in eight ESRD patients, but only four showed improvement of bone mineral density that remained below normal[115], suggesting PTH-independent effects of CTR in bone. This issue will be explored in this thesis.

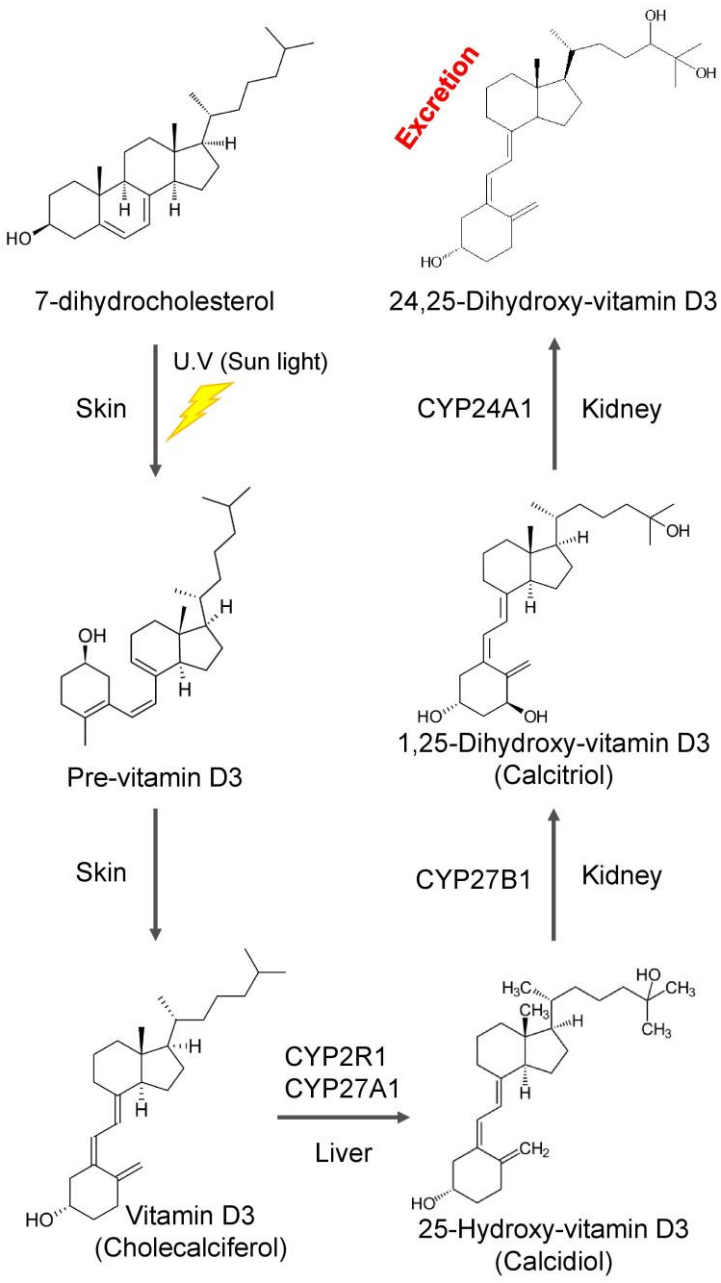

Figure 14. Scheme for Vitamin D synthesis. Vitamin D is synthesized in the skin by the action of the ultraviolet light of the sun. Calcidiol is produced in the liver by 25-hydroxylation of Vitamin D3. Calcitriol is the active form of the vitamin D and is mainly produced in the kidney by 1α-hydroxylation of the 25-hydroxyvitamin D3. 24-hydroxylation of calcitriol or calcidiol is performed in the kidney and it has been proposed that this product is excreted.

Nowadays, calcitriol is widely used in the general population, alone or in combination, for the treatment of osteoporosis. In the most cases calcitriol supplementation prevents or even reverses the loss of bone mineral density, and these effects could be related to its calcemic function[116]. At contrary, a meta-analysis review about the association between vitamin D and bone mineral density showed that vitamin D supplementation has marginal effects in bone mineral density when administered to individuals who do not present Vitamin D deficiency[117]. In animals, it has been showed that very high calcitriol treatment to rats with normal renal function increases cortical porosity[118].

In summary, the previous information illustrates the controversial effects of calcitriol on bone. Whether calcitriol effects on bone cells are mediated by its direct actions through VDR or by the modulation of plasma PTH and Ca levels are unknown. This issue will be studied *in vivo* in an experimental model of uremia with clamped PTH and *in vitro* during osteogenesis of mesenchymal stem cells and osteoclastogenesis of hematopoietic cells.

It is well known that Vitamin D enhances blood Ca concentration by increasing the Ca uptake in gut[119]. Due to the fact that the CaSR is also expressed in bone, we hypothesized that the activation of this receptor, by both, Ca or calcimimetics, might participate in the transduction of the Ca signaling, orchestrating bone homeostasis. In this context, CaSR activation may contribute to bone turnover in CKD and the effects of calcimimetic in bone independently of its action on PTH secretion *in vivo* and *in vitro* in bone cells must be clarified.

8.2. *CaSR and bone*

In 1993, the CaSR was identified by the first time in bovine parathyroid glands[63]. In this sense, positive and negative allosteric modulators of the CaSR have been developed for the management of the PTH secretion[120–122]. Additionally, CaSR is also expressed in the kidney, and there it regulates calciuria[123]. In addition to iCa, the CaSR can be activated in a minor intensity by other divalent ions as Mg[124]. Activation of CaSR by its ligands triggers a rapid respond via MAPK[125,126], which

promotes the transcription of the specific target genes. Figure 15 shows a scheme of the downstream pathways of CaSR in cells.

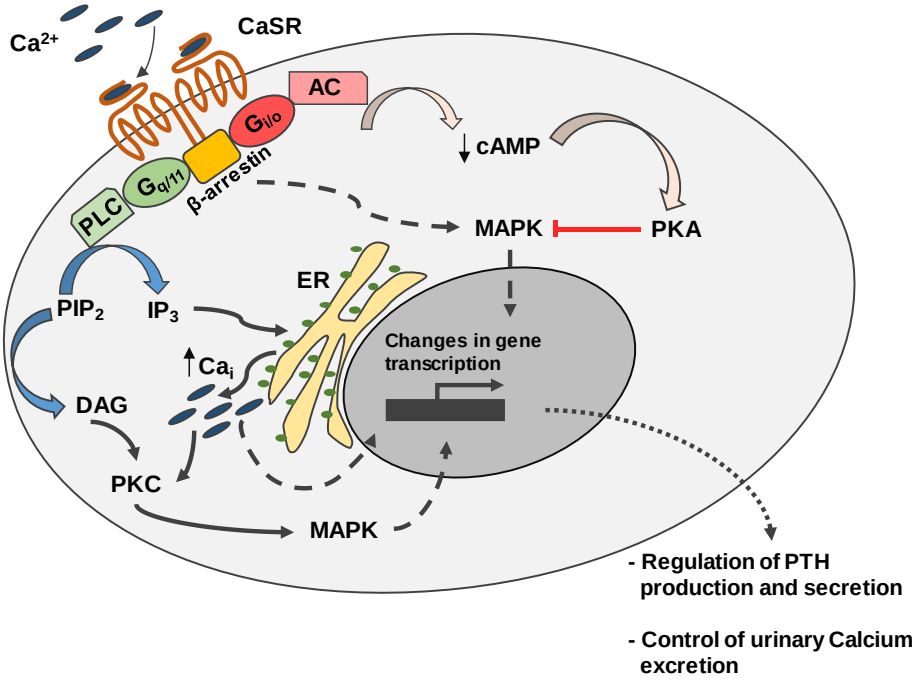

Figure 15. Summary figure showing the principal downstream pathways of the CaSR. Ionized Ca^{2+} in blood, binds the homodimeric CaSR and rapidly activates $G_{q/11}$ and $G_{i/o}$ pathways (2-5 minutes). The $G_{q/11}$ activates mainly phospholipase C (PLC) that metabolizes phosphatidylinositol 4,5-biphosphate (PIP_2) into inositol triphosphate (IP_3) and diacylglycerol (DAG). DAG activates protein kinase C (PLC) and mitogen-activated protein kinase (MAPK). IP_3 binds the IP_3 receptor in the endoplasmic reticulum (ER) and promotes calcium releasing into the cytoplasm, which can also activate the MAPK pathway. The activation of the $Gi_{/o}$ that inhibits the adenylate cyclase (AC), leading to decreasing cAMP levels and protein kinase A (PKA) activation. The reduction in PKA activity prevent the inhibition of MAPK and further increases the MAPK pathway. Adapted from Gorvin C. et al[126].

An interesting study by Miao D. et al suggested a regulation of the 1α-hydroxylase by Ca independently of PTH. They observed that PTH knockout mice developed a phenotype similar to that found in hypoparathyrodism (i.e. hypocalcemia, hyperphosphatemia and low levels of circulating $1,25(OH)_2D_3$) when feed in a normal

P diet. However, PTH-KO mice fed on a low Ca diet increased the synthesis of $1,25(OH)_2D_3$, consistent with a higher expression of the renal 1α-hydroxylase[127].

In vitro studies have also demonstrated the existence of the CaSR in osteoblasts[128], and its activation promotes proliferation and chemotaxis, suggesting a key role of CaSR in the organization and mobilization of the osteoblasts to the site of resorption[129]. In addition, it has been observed in calvaria cells and others models of osteoblasts, that high Ca concentration (1.25-1.8mM) or gadolinium, a trivalent cation with similar ionic radius to Ca, activate the CaSR downstream signaling and increase the mineralized bone formation[130].

The role of a functional CaSR in bone tissue has been also studied *in vivo*. Mice with conditional ablation of the CaSR in osteoblasts show delayed osteoblast differentiation and defective mineralization. In addition, in these mice RANKL was also increased, and consequently the number of osteoclasts[131]. Other studies have shown that mice with specific ablation of the CaSR under the promotor of Col (II) or Osterix displayed important defects in bone development, demonstrating the crucial role of CaSR in osteoblasts at different stages[132].

In this respect, calcimimetics and Ca, through the activation of CaSR, might also exerts relevant actions directly in bone cells in CKD although this issue has not been clearly studied.

8.2.1. Calcimimetics in CKD

Calcimimetics are positive agonist of the CaSR and are used in the clinic to decrease PTH secretion[133,134]. These molecules induce a conformational change in the extracellular domain of the CaSR and make the receptor more sensitive to plasma Ca concentration[135]. The mechanism of action of the calcimimetics is summarized in Figure 16.

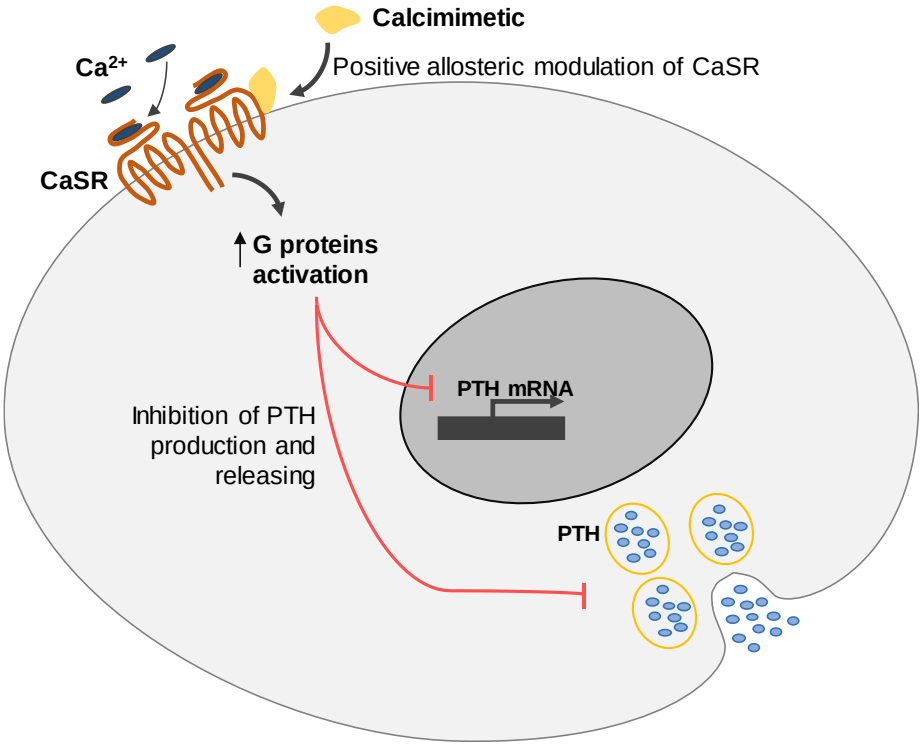

Figure 16. Simplified scheme for the action of calcimimetic in the parathyroid cells.

In hemodialysis patients with established SHPT, administration of the calcimimetic R-568 also reduced PTH plasma concentration[121]. In CKD patients, several clinical studies have demonstrated that hemodialysis patients treated with the second generation of calcimimetics Cinacalcet (Mimpara) showed decreased PTH levels as well as lower serum P concentration[122,136,137]. In 2004, FDA approved the clinical use of Cinacalcet for the treatment of hyperparathyroidism.

Generally, the effects of calcimimetics in bone in CKD are largely attributed to its action on PTH regulation[138]. The hypothesis that CaSR activation promotes bone changes independently of PTH has not been explored or quantified yet. More recently, the expression of the CaSR have been also confirmed in a variety of tissues and calcimimetic may exert its functions in others cells. Thus, CaSR modulation is being investigated in other fields “not related” to calcium metabolism, as cancer[139–141], hypertension[142,143], asthma[144] or inflammation[145] among others.

The bone effects of calcimimetic have been widely documented. Yajima A. et al[146], in a histomorphometric study, reported that treatment with cinacalcet during 1 year decreased bone turnover markers and fibrosis in four hemodialysis patients. Undoubtedly, these results could be influenced by the lower PTH levels after treatment. In the EVOLVE study, cinacalcet vs placebo was compared in a cohort of hemodialysis patients with established SHPT. At the beginning, the study was planned to investigate the effects of cinacalcet in cardiovascular diseases and mortality and the authors recognized limitations in the bone study. However, they observed a significant decrease in the incidence of fractures when adjusted for differences in baseline characteristics, multiple fractures, and/or events prompting discontinuation of the study drug. Nevertheless, the action of cinacalcet as suppressor of PTH releasing may be involved in the reduction of fracture events[147]. In the same way, in the Bonafide study, bone cells activity decreased according to the reduction of PTH levels after treatment with calcimimetic[138]. In a recent study, the administration of the novel second generation calcimimetic Etelcalcetide (Parsabiv) maintained the bone turnover in rats that underwent subtotal Nx despite of the decrease in serum PTH levels[148]. Therefore, these studies suggest a specific role of CaSR activation, although it is difficult to separate a direct effect of CM from the decreased levels of PTH. In this way, directs effects of the calcimimetics on bone during CKD must be evaluated.

Another critical issue in CKD is to maintain plasma P levels within the normal range. In this respect, it has been reported that the control of P absorption in the gut decreases plasma P concentration in CKD patients[149] and dietary intervention has showed beneficial effects[150]. However, poor adherence to P restriction diet is frequent in patients with renal disease[151]. To solve this problem, P binders have been developed for managing plasma P levels in CKD patients. Particularly, Mg-based P binders have shown important beneficial effects. Another key item in this thesis is the evaluation of the bone effects of dietary magnesium as P binder in a murine model of renal insufficiency and vascular calcification. Furthermore, the *in vitro* effects of magnesium on osteogenesis and osteoclastogenesis will be also examined in this thesis.

8.3. *Phosphate Binders*

The control of P levels in CKD patients is a key challenge nowadays. High plasma levels of P have been associated with mortality and morbidity in people with normal[152] and reduced renal function[153]. The plasma P concentration is highly associated with the P content in the diet and even the source of P[154]. The benefits of P restriction in the diet for the management of SHPT in renal insufficiency were firstly examined by Slatopolsky E. et al[155] in 1973. They observed that P restriction in the diet prevents the increase of plasma PTH concentration at different ranges of Glomerular Filtration Rate (GFR) in a model of renal insufficiency in dogs. More recently the benefits of dietary P restriction in CKD patients have been also demonstrated[150]. However, due to the fact that the management of the diet in patients with CKD is difficult, pharmaceutical corporations have developed compounds capable to decrease P absorption in the gut, thus reducing plasma P levels; these drugs are called P binders and there are a wide variety of them (i.e. Aluminum Hydroxide, Calcium carbonate, Calcium acetate, Calcium acetate-Magnesium carbonate, Lanthanum carbonate, Sevelamer Hydrochloride).

At the beginning, aluminum-based P binders showed to be efficient reducing serum P levels, however, the clinical use of aluminum was stopped after the discovery of its implication in the “uremic encephalopathy” and osteomalacia, due to the accumulation of aluminum in the cerebral and osseous tissues respectively[156]. Magnesium hydroxide was proposed as an alternative for aluminum[157,158], nevertheless later was changed to calcium carbonate because of its poor gastrointestinal tolerability and laxative effects[159]. Nowadays other magnesium-based P binders are efficiently used in the control of hyperphosphatemia[160]. In addition, Mg has other beneficial effects regarding vascular calcification and SHPT. In this respect, Mg results of interest for our studies due to the fact that its effects on bone homeostasis and osteogenesis have not been investigated in depth. In this thesis, we attempt to shed light on the actions of Mg in bone homeostasis.

8.3.1. Magnesium and bone

About the 66% of the total Mg in the body is located in bone, nevertheless the impact of Mg supplementation on bone in the context of CKD has been poorly studied. In 1973, Alfrey CA suggested that the accumulation of Mg in bone might be involved in the development of renal osteodystrophy[161]. Additionally, *in vitro* studies have reported that a concentration of 2 mM of Mg promotes amorphous hydroxyapatite crystal formation[162] which could contribute to the development of osteomalacia and defective mineralization. More recently, in the CALMAG study, the authors compared the effects of Mg-based P binder (Calcium Acetate/Magnesium Carbonate) or Sevelamer on serum bone turnover markers in a cohort of hemodialysis or online hemodiafiltration patients. Calcium Acetate/Magnesium Carbonate administration increased the levels of serum Ca and Mg after 9 weeks of treatment and reduced serum P. In this period, Mg-based P binder administration decreased the serum β-crosslap collagen type I C-telopeptides, a marker of bone resorption, and increased the bone-specific alkaline phosphatase. These effects were not observed in the sevelamer group, despite the fact that both groups showed lower PTH levels, indicating that Mg may affect bone cells activity[163].

In the other side of the spectrum, several studies have reported a deleterious effect of Mg deficiency on bone. Rude et al reported that Mg depletion in the diet by the 50% increased the number of osteoclasts in rats[164]. In elderly men and women, Mg intake has been related to higher bone mineral density[165].

However, despite the fact that the use of Mg supplementation seems to be beneficial for the treatment of CKD, there exist controversy about its effects in bone. One key point in this thesis will be the study of the effects of dietary Mg supplementation on bone in an animal model of renal insufficiency and vascular calcification and *in vitro* on the differentiation of mesenchymal stem cells into osteoblasts.

Finally, despite FGF23 is not properly a treatment, we consider of interest the study of the role of this molecule on bone homeostasis. FGF23 plays a critical role on P metabolism and, importantly FGF23 levels increase according to the loss of the glomerular filtration rate. As FGF23 is a key participant in mineral metabolism

homeostasis by regulating PTH production and secretion in parathyroid glands and renal vitamin D metabolism, we hypothesized that it may also exerts actions in bone cells, considering relevant the study of the effects of FGF23 in bone. Following, a brief introduction to this molecule is detailed.

8.4. *FGF23. Definition, functions and contribution to mineral metabolism*

Before FGF23 identification, the existence of molecules responsible for the regulation of P levels, in addition to PTH and Vitamin D, was supposed. These molecules were called "phosphatonins". In 1994, a potent phosphatonin was identified as a low molecular weight and heat-sensitive protein, released by a sclerosing hemangioma which induces osteomalacia, decreases serum P and $1,25(OH)_2D_3$ levels and increases P wasting by inhibition of the apical expression of the NaPi-IIa and NaPi-IIc in the renal proximal tubule. After excision of the tumor, P and $1,25(OH)_2D_3$ levels became within the normal range[166]. Therefore, this protein was considered as a key factor to maintain P homeostasis. Subsequently, Shimada identified FGF23 as the causative protein for hypophosphatemia in Tumor Induced Osteomalacia. In this way, subcutaneous implantation of cells overexpressing FGF23 induced a decrease in serum P and renal 1α-hydroxylase expression, and increased phosphaturia, bone alkaline phosphatase, osteoid accumulation and the widening of the growth plate. Characterization of FGF23 showed a soluble secreted protein of approximately 30 KDa, however, two fragments resulting from FGF23 cleavage were also identified[72]. The tumor responsible for osteomalacia showed an elevated FGF23 expression in bone, although this was also detected in at lesser extent in other tissues such as heart, liver, lymph node and thymus[72].

At bone level, it has been described that the disruption of FGF23 production promotes pathologic bone features with defective mineralization and decreased bone turnover. Using FGF23-null mice, Shimada et al showed that the absence of FGF23 increased $1,25(OH)_2D_3$ production due to 1α-hydroxylase activation in the kidney. Moreover, plasma P and Ca were increased and PTH levels decreased[83]. FGF23 also acts on the parathyroid glands and inhibits PTH production and

secretion through FGFR/α-klotho/MAPK signaling activation[167]. Furthermore, FGF23 directly participates in the Ca homeostasis, increasing Ca reabsorption by activation of the TRPV5 apical expression in the distal renal tubules[168].

Mutations affecting the FGF23 metabolism have been studied in hypophosphatemic cases (i.e X-linked hypophosphatemia (XLH)[169], autosomal dominant hypophosphatemic rickets (ADHR)[170] and hyperphosphatemic (i.e hyperphosphatemic familial tumoral calcinosis (HFTC)[171] disorders, leading to bone defects. The Phosphate-regulating neutral Endopeptidase, X-linked (PHEX) is an enzyme that participates in the cleavage of FGF23 in two fragments[172]. Loss-of-function mutations in the PHEX gene develop XLH, the most common of the hypophosphatemic rickets affecting 1:20000. In XLH patients, due to the high plasma intact FGF23 levels, serum P concentration is low because of the increased renal P wasting. Additionally, hypophosphatemia is not solved due to the resulting low $1,25(OH)_2D_3$ and PTH levels. These patients developed severe rickets at early age and ectopic calcification in adulthood[173]. Similarly, ADHR is caused by a mutation in the FGF23 gene resulting in a site of cleavage unable to be identified for PHEX, protecting FGF23 from proteolysis and leading to increased levels of plasma intact FGF23[174]. FGF23 degradation by PHEX may be prevented by intact FGF23 O-glycosylation, in the site of cleavage. The enzyme responsible for this process is the polypeptide N-acetylgalactosaminyltransferase 3 (GalNAc-T3). Loss-of-function mutations in the gene encoding GalNAc-T3 result in HFTC, characterized by increased cleavage of the FGF23 protein, hyperphosphatemia and ectopic calcifications[175]. Additionally, the Family with Sequence Similarity 20, Member C (FAM20C or DMP4) is a kinase that phosphorylates FGF23 and inhibits the action of GalNAc-T3, yet proteolysis is enhanced[176]. Figure 17 shows the different fragments of FGF23 found in the blood (Fig.17 **a**) and the principal enzymes participating on FGF23 processing (Fig.17 **b**). The previous findings reveal the complexity in the FGF23 metabolism.

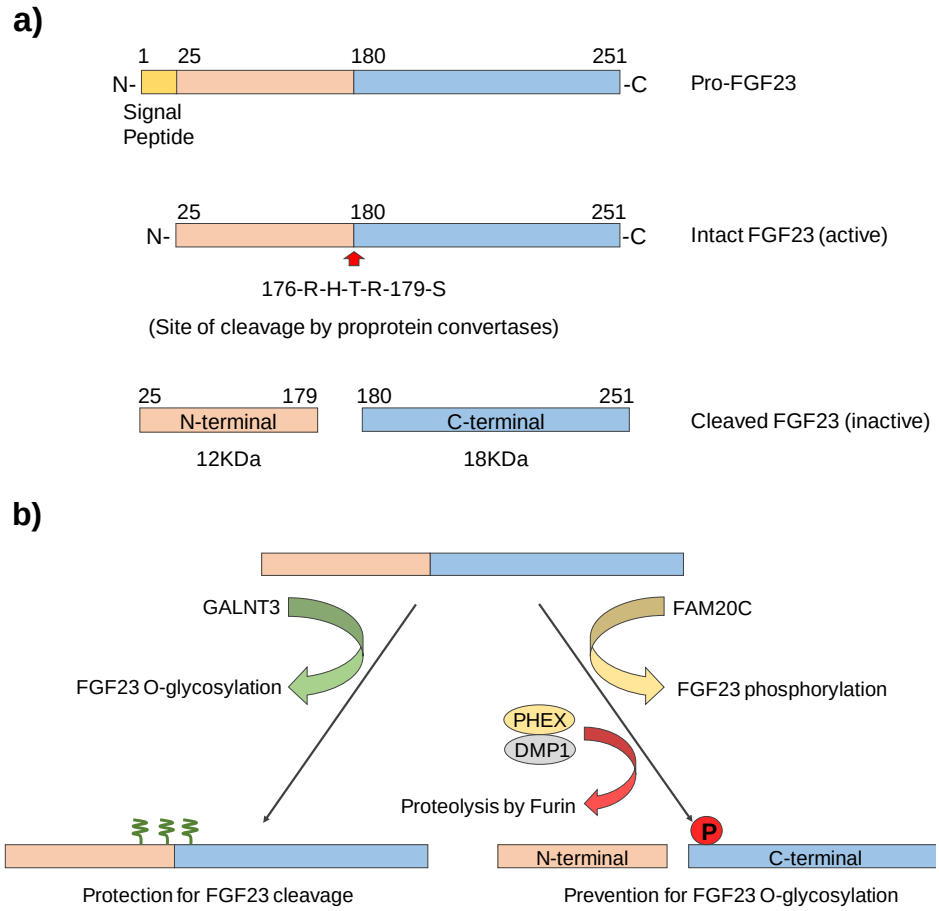

Figure 17. Scheme for FGF23 processing. **a**) FGF23 is synthesized as a pro-protein. The 1-24 signal peptide is excised and the protein become active. The intact FGF23 can undergo proteolysis at the site 176-Arg-His-178-Thr-179-Arg-Ser-180, resulting in two inactive fragments N-terminal, (12 KDa) and C-terminal (18 KDa). **b**) Intact FGF23 can be O-Glycosylated by the enzyme GALNT3 in various sites and also in theThr-178 preventing the proteolysis. At contrary, the kinase FAM20C phosphorylates FGF23 at the Ser-180 and inhibits the O glycosylation in favor of the FGF23 proteolysis by Furin.

Overall there exists a direct role of high FGF23 on bone turnover and mineralization, however, whether FGF23 could contribute to renal osteodystrophy is still unclear. There are a growing number of evidences suggesting that FGF23 triggers different effects in bone cells[177,178]. The *in vivo* e *in vitro* effects of high levels of FGF23 will be explored during this thesis.

OBJECTIVES

The main aim of this thesis is the study of the potential effects of treatments generally used in CKD patients (such as CTR, calcimimetic or Mg) and molecules abnormally altered in renal insufficiency (such as FGF23) on bone alterations. Following, the specific aims in this work are pointed out:

Calcitriol:

1. To evaluate the direct effects of calcitriol on bone histomorphometry in a model of renal insufficiency with parathyroidectomy and subcutaneous constant infusion of PTH

2. To determine *in vitro* the effects of calcitriol supplementation on the differentiation of mesenchymal stem cells into osteoblasts and on osteoclasts differentiation of bone marrow hematopoietic cells.

Calcimimetic:

3. To investigate the role of calcimimetic on bone histomorphometry in a model of parathyroidectomy and subcutaneous constant infusion of PTH in rats with normal of reduced renal function.

4. To study *in vitro* the direct effects of CaSR modulation by calcimimetic and calcilytics in a cell line of osteoblast and on bone marrow mesenchymal stem cells differentiation into osteoblasts.

Magnesium:

5. To evaluate the preventive effects of dietary magnesium supplementation as phosphate binder in a rat model of renal insufficiency and its involvement in the development of vascular calcification, renal deterioration and bone disorders.

6. To investigate the direct effects of magnesium supplementation in the differentiation of the bone marrow mesenchymal stem cells into osteoblasts and osteoclasts differentiation of bone marrow hematopoietic cells *in vitro*.

FGF23:

7. To analyze the role of high FGF23 levels on pathophysiological changes in bone turnover in a rat model of early CKD.

8. To study *in vitro* the effects of high concentrations of FGF23 on bone marrow mesenchymal stem cells differentiation into osteoblasts and on osteoclast differentiation from bone marrow hematopoietic cells.

MATERIALS AND METHODS

This part has been divided into four separate sections for each elements/molecules that we have considered as potential contributors to bone alterations associated with CKD.
Every section comprises *in vivo* experiments using a rat model of renal insufficiency as well as *in vitro* experiments using different types of bone cells.

Therefore, methodology will be described as follows:

Section 1: Calcitriol and bone
Section 2: Calcimimetic and bone
Section 3: Magnesium and bone
Section 4: FGF23 and bone

Animal care and proceedings

10-12-week old male Wistar rats weighing 250–300 g were used to carry out the *in vivo* experiments. This strain was chosen on the basis of its feasibility to resemble CKD features. Animals were purchased from Charles River (Wilmington, Massachusetts) and individually housed in 33.5 x 56 x 19 cm cages with 450 cm^2 floor area per rat, applying a 12h/12h light/dark cycle. Before starting the experiments, all rats were given *ad libitum* access to a standard diet (Ca 0.6%, P 0.6% and Mg 0.1%) and tap water. Appropriate measures were taken to ensure animal welfare and to address the basic behavioral and physiological needs of the animals. All experimental protocols were reviewed and approved by the Ethics Committee for Animal Research of IMIBIC in accordance with the ethical guidelines of the Institution and the EC Directive 86/609/EEC for animal experimentation and the University of Cordoba, and all rats received humane care in compliance with the guiding principles in the “Guide for the Care and use of laboratory animals: Eight edition”.

Research ethics to obtain human samples

Human bone marrow mesenchymal stem cells were obtained from bone marrow aspirates taken from the iliac crest of adult donors after written informed consent. Donors were patients of the Hematology Service of the Reina Sofia University Hospital on diagnosis or follow-up. All protocols were approved by the Ethical Committee of Reina Sofia University Hospital in agreement with the ethical principles of the Declaration of Helsinki.

SECTION 1: CALCITRIOL AND BONE

1.1. *IN VIVO EXPERIMENTS*

As previously detailed, calcitriol (CTR) administration is widely used for the treatment of SHPT, thus increasing plasma Ca concentration and decreasing PTH levels. To examine *in vivo* the bone effects of CTR independently of PTH, we used an experimental model of uremia based on 5/6 nephrectomy and total parathyroidectomy.

1.1.1. Model of 5/6 nephrectomy in rats

Uremia was induced by 5/6 nephrectomy (5/6Nx), a two-step procedure that reduces the original functional renal mass by five-sixths. On the basis of our previous studies[179], animals were anesthetized using sevoflurane (Sevorane, Abbott laboratories, Chicago, IL, USA). In the first step of the nephrectomy, a 5 to 8 mm incision was made on the left mediolateral surface of the abdomen. The left kidney was exposed, and the two poles (2/3 of renal mass) were ablated. The kidney was inspected and returned to an anatomically neutral position within the peritoneal cavity. The abdominal wall and skin incisions were closed with sutures, and the rat was placed back into its home cage. After 1 week of recovery, the animal was reanesthetized and a 5 to 8 mm incision was made on the right mediolateral surface of the abdomen. The right kidney was exposed and unencapsulated, the renal pedicle was clamped and ligated, and the kidney was removed. The ligated pedicle was returned to a neutral anatomical position and the abdomen and skin incisions closed with suture materials. Fentanyl 0.01mg/kg; i.p (Fentanest, Kern Pharma, Barcelona, Spain) was used as analgesic agent.

1.1.2. Parathyroidectomy and PTH clamp in rats

Total parathyroidectomy (PTx) was performed using a dissecting microscope as previously reported[180], Briefly, rats were anesthetized with sevoflurane, a surgical incision was made in the skin of the ventral part of the neck and subsequently

another incision was made carefully in the muscular tissue until the thyroid was exposed. Using a stereoscopic microscope, parathyroid glands were removed from the thyroid gland, vessels were cauterized and both surgical cuts were stitched with absorbable suture. After surgery, rats received analgesia using fentanyl (0.01mg/kg; i.p.). One day after PTx, rats were re-anesthetized using sevoflurane and blood (0.7 ml) was drawn by puncture of the jugular vein to measure serum Ca levels. PTx was considered successful in rats with iCa levels below 0.8mM.

Subsequently, a miniosmotic pump (ALZET model 2004 purchased from Charles River Laboratories, Barcelona, Spain) was implanted subcutaneously between the shoulders. The osmotic pump was loaded with rat recombinant PTH (1-34 fragment) (Sigma-Aldrich CO, St. Louis, MO, USA) diluted in isosmotic saline with 2% cysteine (pH 1.4) in aseptic conditions. As a decrease in plasma iCa levels was expected due to the reduction in the renal mass, these groups of rats received a constant infusion of a 6-fold the dose of the rat recombinant PTH 1-34 necessary to maintain plasma iCa levels in rats with normal renal function (0.132 µg/100g/hr)[181].

1.1.3. Experimental design for the in vivo study

To evaluate the PTH-independent effects of CTR in bone, we used male wistar rats that underwent 5/6Nx and total PTx. As PTH requirements in uremic conditions must be higher than in normal conditions, it was administered a constant infusion of rat recombinant PTH higher than the necessary dose to maintain plasma iCa concentration in PTx rats with normal renal function (1-34 fragment; 0.132 µg/100g/hr). In addition, CTR (Calcijex, Abbott Laboratories, Chicago, IL, USA) was administered at 20, 40 or 60 ng/kg/48h; i.p. during 28 days. Calcein (Sigma-Aldrich, 25mg/kg; i.p.) was administered 9 and 2 days before sacrifice to evaluate bone mineralization. Animals were fed with a 0.6% Ca and 0,9% P diet (Altromin GmbH & CO. KG, Lage, Germany).Rats receiving a simulated surgery (Sham) were included in all the experiments as control animals. Sham operation consist of the exposition of the target organs to be mobilized and then returned to the animal. Sham rats were fed on a diet containing Ca 0.6%, P 0.6%, and Mg 0.1% (Altromin GmbH & CO. KG)

and were not treated with calcitriol or any other treatment different of those used in the surgery.

The experimental groups were as follows:

1. Sham Operated (n=5)
2. 5/6Nx (n=7)
3. 5/6Nx plus PTx and PTH replacement (Nx+PTx+PTHx6+Vehicle, n=9)
4. Nx+PTx+PTHx6+CTR 20ng/kg (n=10)
5. Nx+PTx+PTHx6+CTR 40ng/kg (n=5)
6. Nx+PTx+PTHx6+CTR 60ng/kg (n=9)

At the end of the study, blood was obtained by aortic puncture under general anesthesia with sodium thiopental 50mg/kg (B. Braun, Melsungen, Germany) and femurs were dissected to evaluate bone histomorphometry. A visual timeline of the experiment is shown in Fiure 18.

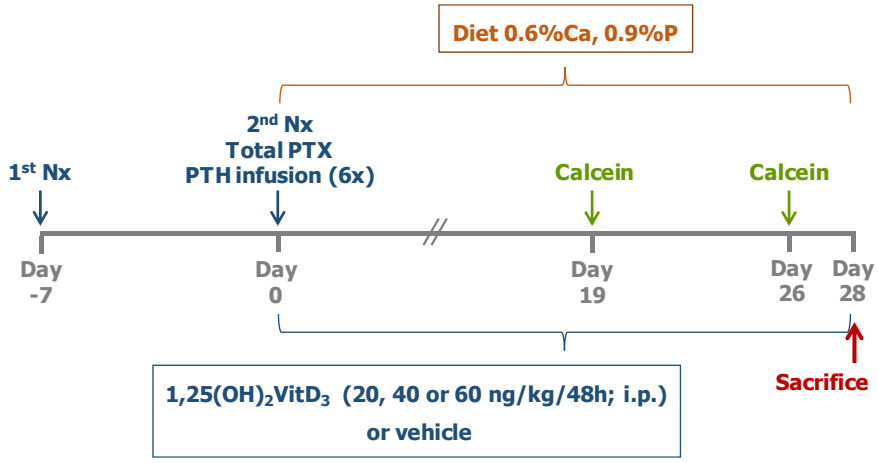

Figure 18. *E*xperimental design for the in vivo study with CTR.

1.1.4. Plasma biochemical analysis

To confirm the PTx, blood for measurements of iCa levels was collected in heparinized syringes and immediately analyzed using a Ciba- Corning 634 ISE Ca2+18 /pH analyzer (Ciba-Corning, Essex, UK) or a Spotlyte Ca^{2+}/pH Analyzer (Menarini Diagnostics, Barcelona, Spain). Afterwards, blood samples were centrifuged 2000 x g for 10 minutes at 4ºC for plasma separation, aliquoted and stored at -20ºC for biochemical analysis.

At the end of the study, blood was obtained by aortic puncture under general anesthesia with sodium thiopental (50mg/kg; i.p.). Plasma P, Mg and creatinine were measured by spectrophotometry using commercially available kits (BioSystems SA, Barcelona, Spain).

Plasma levels of circulating intact FGF23 were determined using a rat FGF23 sandwich enzyme-linked immunosorbent assay (ELISA) kit (Kainos Laboratories, Tokyo, Japan). In this ELISA kit, wells are coated with an antibody against N-terminal FGF23 length that capture both intact and N-terminal FGF23; then another monoclonal HRP-conjugated antibody is added to detect the C-terminal length, thus only intact FGF23 is recognized by the measurement.

Plasma CTR concentration was measured with a radioimmunoassay (RIA) kit (Immunodiagnostic Systems (IDS) Ltd, Boldon, UK). Briefly, plasma samples was delipidated and $1,25(OH)_2D_3$ extracted from potential cross-reactants by incubation for 3 hours with a highly specific solid phase monoclonal antibody against $1,25(OH)_2D_3$. The immunoextraction gel is then washed and purified $1,25(OH)_2D_3$ eluted directly into glass assay tubes. Reconstituted eluates and calibrators are incubated overnight with a highly specific sheep anti-$1,25(OH)_2D_3$. Then, ^{125}I-$1,25(OH)_2D_3$ is added and incubation continued for 1 hour. Separation of bound from free is achieved by a short incubation with Sac-Cel®, a binder reagent developed by the company, followed by centrifugation, decantation and counting. Bound radioactivity is inversely proportional to the concentration of $1,25(OH)_2D_3$.

Plasma intact PTH concentration was quantified according to the manufacturer's instructions using a rat PTH (1–84) sandwich ELISA kit (Immutopics, San Clemente, CA, USA). To detect intact PTH the ELISA kit uses two antibodies, the capture

antibody is a polyclonal rat avidin-biotin-conjugated antibody against the PTH (39-84) fragment coated in wells and for detection was used a PTH (1-34) polyclonal antibody raised against epitopes in the PTH (1-34) fragment.

Infused rat recombinant PTH (1-34 fragment) was not recognized by the intact PTH assay. To determine the plasma concentration of PTH (1-34) fragment, we used a specific competitive ELISA kit (Phoenix Pharmaceuticals, Inc. Burlingame, CA, USA). In this kit, the plate is pre-coated with a capture antibody that binds both the biotinylated antibody and the PTH (1-34) peptide at the same time. The antigen and antibody therefore "compete" for the binding sites. The biotinylated peptide interacts with streptavidin-horseradish peroxidase which catalyzes the substrate solution, thus the intensity of the yellow is inversely proportional to the amount of the PTH (1-34) peptide. The amount of the PTH (1-34) peptide was determined by extrapolation with a standard curve.

Plasma sclerostin concentration was measured with a sandwich ELISA kit (R&D System, Inc. Minneapolis, USA), consistent in a pre-coated microplate with a murine monoclonal antibody against sclerostin for protein capture and once rinsed, a polyclonal HRP-conjugated antibody specific for murine sclerostin was added for detection by colorimetry.

1.1.5. Bone histomorphometry

After sacrifice, right femurs were dissected, adjacent soft tissues were removed and bones were placed into 10 ml crystal bottles with 70% ethanol and then femurs were dehydrated with 100% ethanol. Each ethanol solution was replaced every 24 hours during three days at room temperature. Subsequently, samples were cleared with xylene overnight at room temperature, and bones were embedded in 75% methyl methacrylate (Merck KGaA, Darmstadt, Germany), 25% dibutyl phthalate (Sigma-Aldrich) (Solution A), then in Solution A plus 1% w/v benzoyl peroxide (Merk) and finally in Solution A plus 2.5% w/v benzoyl peroxide. Each methyl methacrylate solution was replaced every 24 hours during three days and stored at 4ºC. After the last replacement, samples were maintained at 37ºC. Once solution became solid,

crystal bottles were broken and the blocks with the embedded samples were cutting with a tungsten knife.

5µm sections of the undecalcified distal femurs were stained with a modified Masson-Goldner trichrome method as previously reported[182]. In detail, slices were fixed with 50% ethanol and slides were maintained at 37ºC overnight. Samples were rehydrated and stained with 1:1 hematoxylin-ferric chloride during 10 minutes and subsequently rinsed with tap water for 5 minutes. Then, slices were cleared with 1% HCl, and turned blue with a solution of saturated $LiCO_3$. After rinsing with water, slices were stained with Goldner trichrome dye for 20 minutes and then rinsed with 1% acetic acid. Subsequently, samples were dehydrated with 95% ethanol (twice, 1.5 minutes each), and stained with an ethanol solution of 1% w/v saffron for 5 minutes. Afterward slices were subsequently rinsed with 95% and 100% ethanol, 1 minutes each, and cleared with xylene. A non-aqueous xylene-containing mounting medium was used to adhere to the coverslips. Green stained areas were considered as mineralized bone and red stained areas measuring at least 1.5 µm were considered as osteoid.

Bone histomorphometric parameters were assessed in cancellous bone within the secondary spongiosa (0.25 mm distance from endocortical bone and growth plate) under 200x magnification as previously described[183] using OsteoMeasure™ software (OsteoMetrics, Decatur, IL, USA) and derived indices were determined by standard calculations[108].

The following parameters were analyzed: BV/TV: Bone Volume/Tissue Volume, OV/TV: Osteoid Volume/Tissue Volume, OS/BS: Osteoid Surface/Bone Surface, Ob.S/BS: Osteoblast Surface/Bone Surface, ES/BS: Eroded Surface/Bone Surface, Oc.S/BS: Osteoclast Surface/Bone Surface, BFR/BS: Bone Formation Rate/Bone Surface, MS/BS: Mineralizing Surface/Bone Surface.

The bone dynamic parameters were calculated by measurement of the single and double fluorescent calcein labelling lines in undecalcified 10 µm serial sections.

1.2. *IN VITRO EXPERIMENTS*

1.2.1. In vitro study of the effects of calcitriol on osteogenesis of rat bone marrow MSC

The effects of CTR on osteogenesis of bone marrow mesenchymal stem cells (MSC) were also analyzed. Thus, different concentrations of calcitriol (10^{-12}, 10^{-11}, 10^{-10}, 10^{-9} and 10^{-8} M) were used.

1.2.1.1. Isolation and primary culture of rat bone marrow MSC

2-month male Wistar rats weighting 200-250 g were euthanized by aortic puncture under general anesthesia with pentobarbital sodium (50 mg/kg; i.p.). Tibiae and femurs were cut at the epiphyses and subsequently perfused with alpha minimal essential medium (α-MEM; Sigma-Aldrich) containing 15% FBS (Lonza Inc., Walkersville, MD, USA), 1% ultraglutamine (Lonza), 100 U/ml penicillin and 100 µg/ml streptomycin. Cell aggregation was reduced by filtration through 70 µm cell strainer (BD Biosciences, San Jose, CA, USA). Following centrifugation and washing with α-MEM, bone marrow cells were cultured in 25 cm^2 flasks (NUNC A/S, Roskilde, DE, USA) with α-MEM containing 15% FBS, 1% ultraglutamine, 100 U/ml penicillin, 100 µg/ml streptomycin and 1 ng/ml rat recombinant basic fibroblast growth factor (bFGF; PeproTech EC Ltd., London, UK) in a humidified atmosphere with 5% CO_2 at 37ºC. MSC were isolated according to their plastic adherence properties. Fresh α-MEM with 10% FBS, 1% ultraglutamine, 100 U/ml penicillin, 100 µg/ml streptomycin and rat recombinant 1 ng/ml bFGF was added after 24 hours and replaced every 3 days. Once 85-90% confluence was reached, cells were collected using Trypsin-EDTA (Lonza). Briefly, supernatant was discarded and cells were rinsed with saline twice. 1.5 ml of Trypsin-EDTA was added per 25 cm^2 flask and cells were maintained at 37ºC in the incubator for 5 minutes. After we had checked that adherent cells were detached from the surface, trypsin was inactivated with 5 ml of supplemented α-MEM and cells were collected. Subsequently, cells were centrifuged at 450 x *g*, 4 ºC for 10 minutes and pellets suspended in supplemented α-MEM. Cells were counted using a Neubauer chamber in a Motic AE31 inverted microscope (MoticEurope S.L.U, Barcelona, Spain). Cells were seeded in 6-well

plates (NUNC) at 13000 cells/cm^2. Treatments were started as described below when cells reached 90% confluence.

1.2.1.2. Osteogenic differentiation of MSC and treatments

MSC were cultured in α-MEM with 10% FBS, 1% ultraglutamine, 100 U/ml penicillin, 100 µg/ml streptomycin and an osteogenic stimuli based on the addition of 1 µM dexamethasone (Sigma-Aldrich), 10 mM β-glycerol phosphate (Sigma-Aldrich) and 0.2 mM ascorbic acid (BAYER, Barcelona, Spain). Cells were maintained in osteogenic medium during 21 days. Undifferentiated MSC at 0 and 21 days were used as control cells. CTR was added throughout osteogenic differentiation of rat bone marrow MSC at concentrations of 10^{-12}, 10^{-11}, 10^{-10}, 10^{-9} and 10^{-8} M.
Osteoblastic differentiation and mineralization of *in vitro* cultures were evaluated through the measurement of the expression of specific osteogenic genes, alkaline phosphatase activity, Ca content and alizarin red staining. In addition, the role of pro-osteogenic pathways was also analyzed through confocal microscopy. Methodology is shown in Figure 19. Experiments were performed at least three times.

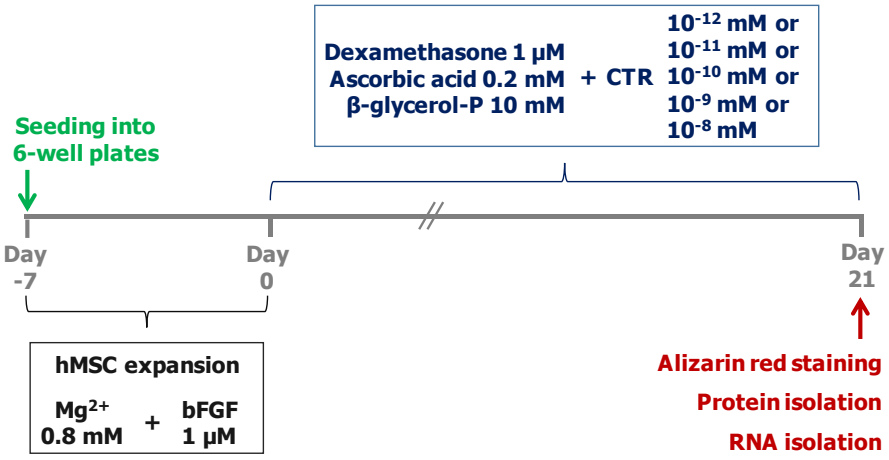

Figure 19. Experimental design for the *in vitro* study of the effects of calcitriol on osteogenesis of MSC.

1.2.1.3. RNA isolation from cell cultures

Total RNA from cell cultures was extracted using TRI Reagent® (Sigma-Aldrich). Briefly, cells were lysed and collected with 1 ml of TRI Reagent® and stored at -80 ºC until procedure.

To isolate total RNA, 200 µl of chloroform was added, samples were mixed with vortex and then centrifuged at 15000 x *g*, 4 ºC for 15 minutes. Following, clear supernatant containing the RNA fraction was separated and mixed with 500 µl of isopropanol and maintained at -80ºC for 10 minutes to allow RNA precipitation. Then, samples were centrifuged at 15000 x g, 4 ºC for 10 minutes and the resultant pellet was rinsed with 1 ml of 70% ethanol and centrifuged at 15000 x *g*, 4 ºC for 5 minutes. Ethanol was discarded, pellet was air-dried and RNA was dissolved in RNAse- and DNAse-free water.

Final RNA concentration was quantified by spectrophotometry (ND-1000, Nanodrop Technologies, Wilmington, DE, USA).

1.2.1.4. RNA treatment with DNase

1 µg of RNA was treated with a DNase I amplification grade kit (Sigma-Aldrich) to eliminate possible DNA contamination. Then, RNA concentration was quantified again. Briefly, 1 µg of RNA was suspended in a final volume of 10 µl containing 0.1 unit of DNase I, 20mM Tris-HCl, 2 mM $MgCl_2$ and incubated for 25 minutes at room temperature. Then, 1 µl of 50 mM EDTA was added to prevent metal ion catalyzed hydrolysis of the RNA and samples were heated at 70 ºC for 10 minutes to denature both DNase I and RNA. Subsequently, samples were placed into ice, RNA was quantified by spectrophotometry and then stored at -80 ºC until analysis.

1.2.1.5. Two-step RT-PCR

In these experiments, RT-PCR was performed using a two-step protocol. Firstly, cDNA was synthesized from total RNA and, in a second step, quantitative PCR was performed. Briefly, total RNA was extracted with 1 ml of TRI Reagent® and quantified by spectrophotometry. cDNA was synthesized from 1 µg of total RNA with a first strand cDNA synthesis kit (Qiagen, Hilden, Germany) in the presence of random

hexamers in a final volume of 20 µl at 25 °C for 10 minutes, followed by 42 °C for 15 minutes and 95 °C for 3 minutes. PCR SYBR Green kit (Qiagen N.V., Hilden, Germany) was used to quantify mRNA expression levels. Primers for *Runx2*, *Osterix*, *Osteocalcin* and *18S* were synthesized with Oligo software and used at a final concentration of 1 µM. Primers sequences are listed in Table 4. The expression of these genes was evaluated by quantitative RT-PCR using Lightcycler 480 (Roche Diagnostics, Basel, Switzerland). The relative expression was calculated by the $2^{-\Delta\Delta Ct}$ method, using ribosomal 18S RNA expression as housekeeping control.

	Primer sequences	**NCBI gene ID**
Rat *Runx2*	Fw 5'-CGGGAATGATGAGAACTACTC-3'	367218
	Rv 5'-CGGTCAGAGAACAAACTAGGT-3'	
Rat *Osterix*	Fw 5'-GTACGGCAAGGCTTCGCATCTGA-3'	300260
	Rv 5'-TCAAGTGGTCGCTTCGGGTAAAG-3'	
Rat *Osteocalcin*	Fw 5'-TCTGAGTCTGACAAAGCCTTCATG-3'	25295
	Rv 5'-TGGGTAGGGGGCTGGGGCTCC-3'	
Rat *18S*	Fw 5'-GTAACCCGTGAACCCCATT-3'	100861533
	Rv 5'-CCATCCAATCGGTAGTAGCG-3'	

Table 4. Sequences of the primers used in the *in vitro* study of the effects of calcitriol on osteogenesis.

1.2.1.6. Enriched fractions of cytosolic and nuclear proteins isolation

Enriched fraction of cytosolic proteins was isolated from cells in lysis buffer A, containing 10 mM HEPES, 10 mM KCl, 0.1 mM EDTA, 0.1 mM EGTA, 1 mM Dithiothreitol (DTT), 0.5 mM phenylmethylsulfonyl fluoride (PMSF), 15 µL/ml Protease Inhibitor Cocktail and 0.5% Igepal CA-630, pH 7.9. All the reagents were purchased from Sigma-Aldrich. The suspension was centrifuged at 15000 *g*, 4º C for 3 minutes, and the supernatant (cytosolic extract) was stored at -80ºC. Nuclear extracts were obtained by incubating the pellet obtained from the cytosolic extract in

lysis buffer B for 20 minutes, containing 20 mM HEPES, 0.4 M NaCl, 1 mM EDTA, 1 mM EGTA, 1 mM DTT, 0.5 mM PMSF and 15 µL/ml Protease Inhibitor Cocktail, pH 7.9. Suspension was centrifuged at 15000 *g*, 4º C for 5 minutes. Supernatants were collected and stored at -80ºC. Protein concentration was determined by Bradford assay (Bio-Rad Laboratories, Hercules, CA, USA).

1.2.1.7. Western blot analysis

To analyze the amount of specific cytosolic or nuclear protein, cell lysates were analyzed by immunoblotting. Briefly, loading buffer containing glycerol, sodium dodecyl sulfate (SDS), β-mercaptoethanol and bromophenol blue were added to protein samples and denaturalization was carried out at 70 ºC for 10 minutes. Following, samples were placed in ice and samples were loaded in polyacrylamide gels. Electrophoresis were performed in a commercial chamber (Bio-Rad Laboratories) at 150 V, 90 mA until the blue front line reached the end of the gel. A pre-stained ladder (Bio-Rad Laboratories) was used as an indicator of molecular weight. Thereafter, proteins were transferred from gel to nitrocellulose membranes using a trans-blot turbo (Bio-Rad Laboratories). Then, membranes were blocked in TBS-T with 5% dry milk to avoid unspecific binding and subsequently incubated with primary antibodies against proliferating cell nuclear antigen (PCNA; Santa Cruz Biotechnology / SC-56; 1:100 dilution) and Cyclin D1 (Cell signaling Technology / #2978; 1:500 dilution). Following, primary antibodies were removed, membranes were rinsed with TBS-T three times and incubated with HRP-conjugated goat anti-mouse and goat anti-rabbit (Santa Cruz Biotechnology) as secondary antibodies. Antibody for detection of Transcription factor II B (TFIIB; Cell signaling Technology / #4169; 1:1000 dilution) were used for loading control.

ECL Advance Detection Reagents (GE Healthcare Bio-Sciences, Uppsala, Sweden) were used to detect chemiluminiscence in a LAS 4000 imager (GE Healthcare Europe GmbH, Barcelona, Spain). Band areas were quantified with Image J software.

1.2.1.8. Immunofluorescence analysis

Cells were cultured upon glass coverslips in 6-well plates. After 14 days of treatment cells were fixed with cold methanol for 20 minutes and subsequently rinsed with PBS three times. Fixed cells were incubated in the diluted antibodies in 1% BSA (Sigma-Aldrich) in PBS. β-catenin primary antibody (BD Biosciences; dilution 1:75) was incubated for 1 hour at 4ºC. Subsequently, cells were washed with PBS and incubated with Alexa Fluor 488 anti-mouse (Invitrogen, Ltd., Paisley, UK. / Ref A21204; 1:500 dilution) diluted in 1% BSA in PBS. Cell nuclei were visualized with the nuclear stain 4',6-diamino-2-phenylindole dihydrochloride (DAPI; Invitrogen). Pictures were obtained at 400x in a Zeiss LSM 710 inverted confocal microscope (Carl Zeiss, Jena, Germany). ImageJ software (National Institutes of Health, Bethesda, MD, USA) was used to analyze the confocal images. Co-localization analysis was performed by quantifying the mean of intensity of fluorescence (β-catenin-488 Green) in each nucleus of the different treatments. Briefly, channels for both colors were split into separate images and blue channel (DAPI) was used to select a region of interest (ROI) comprising the nuclei. Then, ROI were placed onto the green image (β-catenin) and pixels into the region were measured. Values are showed as fold change vs undifferentiated MSC control.

1.2.1.9. Quantification of alkaline phosphatase activity

2 µg of cytoplasmic cell lysates were incubated in 2 mM p-nitrophenyl phosphate (Sigma-Aldrich) for 30 minutes at 37 °C. The reaction was stopped by adding 3 M NaOH, and alkaline phosphatase (ALP) activity was measured by quantifying absorption at 405 nm. ALP activity was expressed as µmol of hydrolyzed p-nitrophenyl phosphate per min and per mg of protein versus undifferentiated control cells.

1.2.1.10. Alizarin red S staining

In differentiated MSC treated or not with the different CTR concentrations, matrix mineralization was evaluated by alizarin red S staining. Cells were washed twice with PBS, fixed with 2% para-formaldehyde and 1% sucrose for 15 minutes and

subsequently washed 3 times with PBS. Then, cells were stained with 40 mM Alizarin Red S pH 4.1 Sigma-Aldrich for 20 minutes, and washed 4 times for 5 minutes with water at pH 7. Finally, water was removed and samples were dried at room temperature. Plates were scanned in a WIFI OKI Scanner (Madrid, Spain).

1.2.1.11. Measurement of calcium content in cell cultures

Demineralization of the calcified matrix was carried out by incubating cell cultures with 0.6 M HCl for 24 hours. Ca content in the supernatant was determined by the phenolsulfonphthalein method using a commercial assay (QuantiChrom™ Calcium Assay Kit, BioAssay Systems, CA, USA). Cells were washed three times with PBS (Sigma Aldrich) and protein content was isolated with a 0.1 M NaOH and 0.1% SDS solution. Protein content was quantified using the Bradford method and Ca content was normalized according to total protein and expressed as µg Ca/mg protein.

1.2.2. In vivo study of the effects of calcitriol supplementation on osteoclastogenesis

The effects of CTR (10^{-11} and 10^{-9} M) were determined in an *in vitro* model of osteoclasts.

1.2.2.1. Osteoclast differentiation of hematopoietic bone marrow cells

10 Male wistar rats weighing 250 g approximately were anesthetized with sodium thiopental (50mg/kg; i.p) and sacrificed by aortic puncture. Rat femurs and tibias were extracted, the adjacent soft tissues were removed and bones were placed in α-MEM. In a laminar flow chamber, bones were cut at the epiphyses and bone marrow was extracted by perfusion with α-MEM supplemented with 10% FBS with a sterile syringe as described in the section 1.2.1.1. Bone marrow cells from each rat were isolated separately to avoid immune response among different animals. Cell aggregation was prevented by filtration using a 70 µm cell strainer. Then, cells were centrifuged at 450 x *g* for 5 minutes at room temperature and the resultant pellet was re-suspended in ACK lysing buffer, incubated for 2-3 minutes at room temperature and centrifuged at 450 x *g* for 5 minutes at room temperature. Subsequently,

supernatant was removed and cell pellets were re-suspended in α-MEM with 10% FBS plus rat recombinant 10 ng/ml M-CSF (PeproTech) and incubated at 37 ºC, 5% CO_2 with saturated humidity. After 24 hours, non-adherent cells were collected and centrifuged at 450 x *g* for 5 minutes at room temperature and cell pellets were re-suspended in supplemented α-MEM with 10% FBS. At this time, a fraction of the cells was collected for characterization by flow cytometry and the remaining cells were seeded on 6-well plates and incubated at 37%, CO_2 5% with saturated humidity with supplemented α-MEM with 10% FBS containing rat recombinant 30 ng/ml M-CSF. After 3 days, adherent cells were collected carefully using a scrapper, counted in a Neubauer chamber and seeded on 24-well plates at $4x10^4$ cells/cm^2 with α-MEM with FBS 10% containing rat recombinant 30 ng/ml M-CSF and rat recombinant 100 ng/ml RANKL. Additionally, CTR was added at concentrations of 10^{-11} and 10^{-9} M. Cells were incubated at 37%, CO_2 5% with saturated humidity for 5 days. Medium was replaced every 2 days. At the end of the experiments cells were processed for determination of osteoclastic gene expression (Cathepsin K) or tartrate-resistant acid phosphatase (TRAP) staining, commonly used as histochemical marker for osteoclasts. Figure 20 summarizes the methodology of this study. Experiments were performed at least three times.

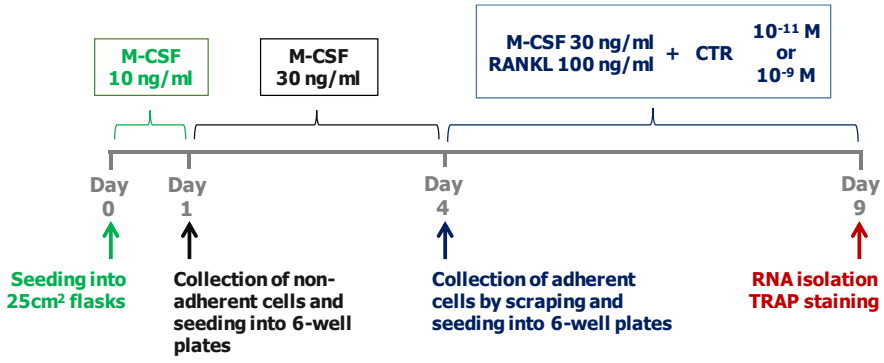

Figure 20. Experimental design for the *in vitro* study of the effects of CTR on osteoclastogenesis.

1.2.2.2. Characterization of non-adherent osteoclast-precursor cells

Non-adherent cells were processed for characterization by flow cytometry using a MACs Quant cytometer (Miltenyi Biotec S.L., Madrid, Spain). Briefly, cells were suspended in 800 µl of PBS at $4x10^6$ per tube and subsequently labeled with FITC-conjugated anti-rat CD34, FITC-conjugated anti-rat CD45, FITC-conjugated anti-rat Sca-1 or an isotype control antibody (Negative control IgG) for 15 minutes protected from light exposure. The expression of the cell surface proteins CD34, CD45 and Sca-1 is used for characterization of bone marrow cells. Dilution for all the antibodies was 1:150. Then, cells were centrifuged at 450 x *g*, 4 ºC for 5 minutes, the supernatant was discarded and cell pellets were re-suspended in PBS for acquisition in the cytometer using the software BD CellQuest™ (BD Biosciences, San Jose, CA, USA).

1.2.2.3. RNA isolation and DNase treatment

RNA isolation and treatment with DNase was carried out as aforementioned in sections 1.2.1.3 and 1.2.1.4, respectively.

1.2.2.4. RT-PCR (one-step protocol)

A one-step RT-PCR kit was used for quantification of *Cathepsin K* (*CTSK*) mRNA expression, using *GAPDH* as housekeeping gene. Cathepsin K is a protease highly expressed in osteoclasts. Cathepsin K is secreted by osteoclasts to degrade bone collagen matrix. RT-PCR was performed with 50 ng of DNase-treated RNA using SensiFAST SYBR No-ROX One-Step Kit (Bioline Reagents Limited, London, UK) as indicated by the manufacturer. Primers for PCR are shown in Table 5. Final concentration of the forward and reverse primer mix was 1 µM. Primer sequences were designed with the Oligo software or pre-designed oligonucleotides were purchased from IDT (Integrated DNA Technologies Inc., Coralville, IA, USA). PCR amplification was performed using Lightcycler 480 (Roche Molecular Systems, Inc., Indianapolis, USA). The expression of target genes was normalized with the $2^{-\Delta\Delta Ct}$ method using GAPDH as housekeeping gene.

	Primer sequences	NCBI gene ID
Rat *CTSK*	Fw 5'-TCTCTGTACCCTCTGCACTTAG-3'	29175
	Rv 5'-ATTGACTCTGAAGACGCTTACC-3'	
Rat *GAPDH*	Fw 5'-AGGGCTGCCTTCTCTTGTGAC-3'	24383
	Rv 5'-TGGGTAGAATCATACTGGAACATGTAG-3'	

Table 5. Primers sequences used in the study of the calcitriol effects on osteoclastogenesis

1.2.2.5. TRAP staining

Osteoclasts are TRAP-positive cells. TRAP is an enzyme highly expressed by osteoclasts. It is secreted to bone surface by osteoclasts and participates in bone resorption.

For TRAP staining, a commercially available kit was used (Sigma–Aldrich) with modifications. Briefly, cells were fixed according to manufacturer instructions with a citrate-paraformaldehyde-acetone solution for 30 seconds at room temperature. Then, fixative solution was removed and cells were rinsed three times with 37 ºC pre-warmed deionized distillated water (ddH_2O). Subsequently, ddH_2O was removed and cells were incubated in TRAP-staining solution as indicated by the manufacturer (0.25 M Acetate, 0.7 mg/ml Diazotized Fast Garnet GBC, 1.25 mg/ml Naphtol AS-BI phosphate and 0.67 M tartrate) at 37ºC. After 1 hour, TRAP-staining solution was removed and cells were rinsed with ddH_2O twice. Then, cells were counterstained with hematoxylin for 2 minutes, rinsed with tap water and air-dried.

SECTION 2: CALCIMIMETIC AND BONE

2.1. *PTH-INDEPENDENT EFFECTS OF CALCIMIMETICS IN BONE: IN VIVO STUDIES*

Calcimimetics (CM) are used alone or in combination with CTR to reduce PTH levels and treat SHPT. The effects of CM independently of their action in parathyroid glands are unknown. To examine *in vivo* the PTH-independent effects of CM in bone we used rats with normal renal function and an experimental model of uremia based on 5/6 nephrectomy. Both rat models underwent total parathyroidectomy and received constant infusion of rat recombinant PTH (1-34 fragment) capable of maintaining plasma Ca and P levels.

2.1.1. Experimental procedure for the in vivo study

Firstly, CM effect was evaluated in PTx rats with normal renal function. Parathyroidectomy was performed according to the protocol described in 1.1.2. Subsequently, two subgroups of PTx rats received a physiological dose of 1-34 PTH (0.022 µg/100g per hour) released from miniosmotic pumps. Additionally, the PTx rats with PTH (1-34) infusion were divided in two subgroups, one of them received calcimimetic AMG 641 (1.5 mg/kg/48h; subcutaneously) and the other one received vehicle. The physiological dose of PTH (0.022 µg/100g per hour) was previously defined by its ability to maintain serum iCa within a normal range (1.15-1.25 mM) in PTx rats fed a 0.6% Ca and 0.6% P diet[181]. The calcimimetic AMG 641 was reconstituted in 12% p/v Captisol (Ligand Pharmaceuticals, Inc. San Diego, CA), pH 3. The dose of AMG 641 administered to the rats was demonstrated to be efficient decreasing PTH levels in Nx rats[184]. In these conditions animals were maintained on a 0,6% Ca and 0,9% P diet for 28 days. The experimental groups of animals for the study with normal renal function were as follows:

1. Sham-operated (Sham, n=6)
2. PTx rats (PTX, n=7)
3. PTX rats with PTH replacement (PTX-PTH, n=5)
4. PTx rats with PTH replacement plus CM (PTX-PTH-CM, n=6).

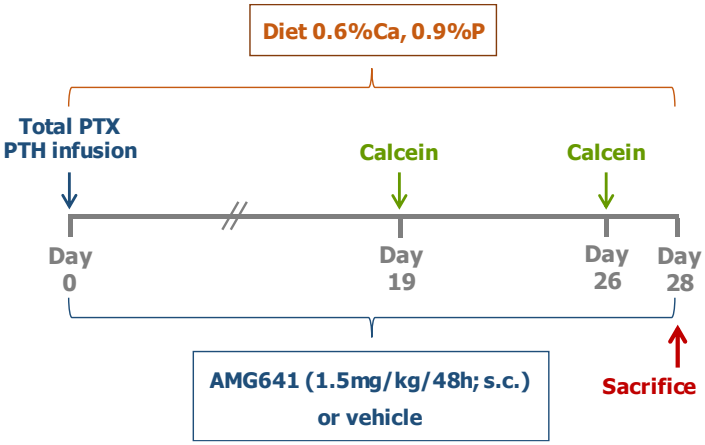

Figure 21. Experimental design of the *in vivo* experiment of the effects of calcimimetic on bone in rats with normal renal function.

To assess the effects of the CM on bone in the context of CKD, a second experiment was performed in uremic PTx rats. Uremia was induced by 2-step subtotal nephrectomy (5/6Nx) as described in section 1.1.1. After the second surgery, the standard diet was switched to a moderately high P diet (Ca 0.6% and P 0.9%). An additional group of Nx rats was treated with CM (1.5 mg/kg/48h; subcutaneously). As a decrease in plasma iCa levels was expected due to the reduction in the renal mass, these groups of rats received a constant infusion of a 6-fold (0.132 µg/100g per hour) or 9-fold (0.198 µg/100g per hour) the dose of rat recombinant PTH 1-34 needed to maintain plasma iCa levels within a normal range in rats with normal renal function through ALZET osmotic pumps in combination with vehicle or CM (1.5 mg/kg/48h, subcutaneously). Therefore, experimental groups were the following:

5. Sham (Sham, n=6)
6. 5/6 Nx rats (5/6Nx, n=7)
6. 5/6 Nx rats and CM (5/6Nx, n=6)
7. 5/6 Nx-PTx and PTH replacement x6 (5/6Nx-PTx-PTHx6, n=8)
8. 5/6 Nx-PTx, PTH replacement x6 and CM (5/6Nx-PTx-PTHx6-CM, n=5)
9. 5/6 Nx-PTx and PTH replacement x9 (5/6Nx-PTx-PTHx9, n=5)
10. 5/6 Nx-PTx, PTH replacement and CM x9 (5/6Nx-PTx-PTHx9-CM, n=6).

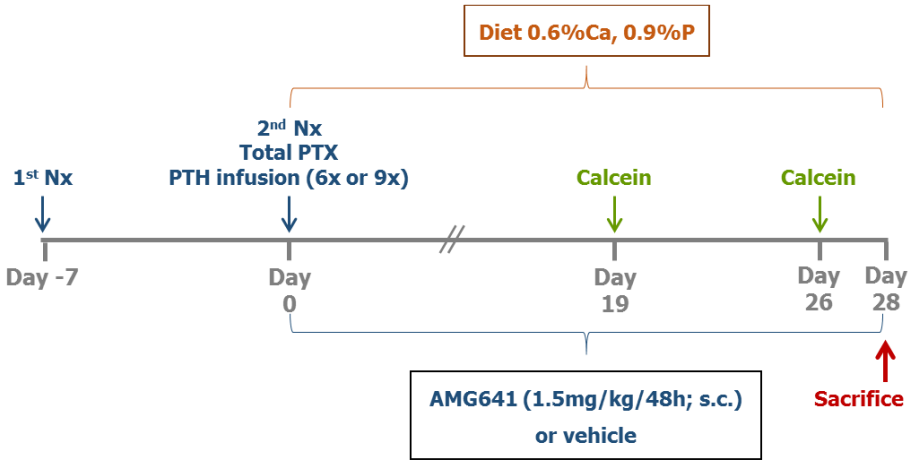

Figure 22. Experimental design for the study of the effect of calcimimetic on bone in rats with renal insufficiency.

To evaluate bone mineralization, double calcein labeling was performed by administering calcein (25 mg/kg; i.p.) at days 9 and 2 before sacrifice. On day 28, twenty-four hours after the last dose of CM, animals were sacrificed by aortic puncture under general anesthesia with sodium thiopental (50mg/kg, i.p). Blood samples were collected in heparinized tubes for biochemistry and femurs were collected to study bone histomorphometry.

2.1.2. Plasma and biochemistry

Blood ionized Ca concentration was determined using a Spotlyte Ca^{2+}/pH Analyzer. Plasma was separated by centrifugation at 2000 x *g* for 10 minutes at 4 ºC, and P, creatinine, CTR, intact PTH and intact FGF23 concentrations were measured as described in section 1.1.4. The plasma concentration of the PTH (1-34) fragment, was measured with a specific ELISA kit (Phoenix Pharmaceuticals, Inc. Burlingame, CA, USA).

2.1.3. Bone histomorphometry

Bone histomorphometric analysis of distal left femurs was assessed as previously described in section 1.1.5. The following parameters were analyzed: BV/TV: Bone

Volume/Tissue Volume, OV/TV: Osteoid Volume/Tissue Volume, OS/BS: Osteoid Surface/Bone Surface, Ob.S/BS: Osteoblast Surface/Bone Surface, ES/BS: Eroded Surface/Bone Surface, Oc.S/BS: Osteoclast Surface/Bone Surface, BFR/BS: Bone Formation Rate/Bone Surface, MS/BS: Mineralizing Surface/Bone Surface, Osteoid Thickness (O.Th), Mineralizing Surface related to Osteoid Surface (MS/OS), mineral apposition rate (MAR), adjusted apposition rate (Aj.AR), mineralization lag time (Mlt) and osteoid maturation time (Omt).

2.1.4. Bone immunohistochemistry

To confirm the activation of the CaSR in bone cells, ERK1/2 phosphorylation, a CaSR downstream signaling pathway, was examined. Tissue phospho-ERK1/2 expression was evaluated in decalcified 5-µm bone sections. Briefly, bone sections were deacrylated in a 1:1 mixture of xylene and chloroform for 30 minutes and rehydrated with graded ethanol to tap water. Subsequently, slices were decalcified with 14% EDTA, pH 7.4 for 1 hour and rinsed with distilled water for 10 minutes. Then, immunohistochemistry was performed using the Novolink Polymer detection System kit (Leica Biosystems Newcastle Ltd, UK) according to the manufacturer's instructions. Briefly, endogenous peroxidase was neutralized with hydrogen 4% peroxidase for 5 minutes and rinsed twice with PBS. Then, protein was blocked with 0.4% casein for 5 minutes to avoid non-specific binding of primary antibody and polymer and rinsed twice with PBS. Subsequently, slices were incubated with anti-phospho-p44/42 MAPK (Cell signaling Technology / Ref. #4370; 1:400 dilution) at 37 ºC for 2 hours. To localize osteoblasts in bone tissue, the distribution of the osteoblast marker osteocalcin was determined using a monoclonal antibody against rat osteocalcin (R&D Systems Inc. MN, USA / Ref. MAB1419; 10 µg/ml dilution). Then, samples were rinsed twice with PBS and a post-primary antibody (rabbit anti mouse; <10 µg/ml) was added for 30 minutes. Then, slices were incubated with a polymer solution (poly-HRP-conjugated antibody raised against rabbit; <25 µg/ml), rinsed twice with PBS and protein detection was performed by incubating with 3, 3 - diaminobenzidine (DAB) for 5 minutes. Subsequently, slices were rinsed with water and counterstained with hematoxylin for 15 minutes. Finally, samples were rinsed

with tap water, dehydrated with ethanol, cleared with xylene and mounted with coverslips using a non-aqueous mounting medium. Images were taken with a Leica DM2000 LED microscope with a Leica MC190 HD camera using the Leica Application Suite 4.8.0 software.

2.2. *IN VITRO EXPERIMENTS*

2.2.1. Effects of calcimimetic on osteogenesis

The *in vitro* effects of AMG641 were evaluated in UMR-106 cells and in osteogenesis of bone marrow mesenchymal stem cells.

2.2.1.1. Effects of calcimimetic in UMR-106 cells

To test the effects of the treatment with CM in mature osteoblasts, we used the rat osteosarcoma cell line UMR-106 (ATCC, Manassas, VA, USA) which displays osteoblastic properties. UMR-106 cells were cultured in a Ca-free DMEM (Gibco™, Grand Island, NY, USA), supplemented with 10% FBS, 2 mM ultraglutamine, 1 mM sodium pyruvate, 20 mM HEPES, 100 U/ml penicillin, 100 µg/ml streptomycin. $CaCl_2$ (Sigma-Aldrich) was used to adjust the Ca concentration at 0.5 mM (low Ca conditions). Once cells reached ~90% confluence, CM was added at 1 µM and 100 µM. Protein and RNA samples were collected after 6 and 24 hours, respectively.
To further confirm that the CM actions are mediated by the CaSR, Calhex 231, a negative allosteric modulator of the CaSR was added at 1 µM and 10 µM to UMR cells cultured in Ca-free DMEM (Gibco™) supplemented with $CaCl_2$ to achieve a Ca concentration of 1.8mM (high Ca conditions). Cells were processed for protein isolation after 6 hours and for RNA isolation after 24 hours. Experiments were performed at least three times.

2.2.1.2. In vitro study of the calcimimetic effects on osteogenesis of human bone marrow MSC

Additionally, human MSC were obtained from excess bone marrow collected during diagnosis or routine follow-up of patients in the Hematology service of Reina Sofía University Hospital. Human samples of bone marrow MSC were collected from patients after obtaining the corresponding signed informed consent. These MSC from the iliac crest were isolated by their plastic adherence properties. Briefly, 750 µl of total bone marrow aspirate were cultured in 75 cm^2 flasks with α-MEM containing 15% FBS, 2 mM ultraglutamine, 100 U/ml penicillin, 100 µg/ml streptomycin and 1 ng/ml human recombinant bFGF (PeproTech). Cells were

incubated in a humidified atmosphere of 5% CO_2 at 37ºC. Fresh α-MEM supplemented as above and with 10% FBS was added after 24 hours and replaced every 3 days. Once 85-90% confluent, cells were collected using Trypsin-EDTA, seeded in 6-well plates at a density of

13000 cells/cm^2 and cultured with Ca-free DMEM supplemented as described above and under osteogenic stimuli based on dexamethasone, β-glycerol phosphate and ascorbic acid. Additionally, 100 µM of CM were added to osteogenic media with low 0.5 mM Ca throughout the differentiation period. After 21 days, cells were processed for analysis of protein and mRNA expression. A graphical scheme sumarizing the methodology of this experiment is shown in Figure 23. Experiments were carried out at least three times.

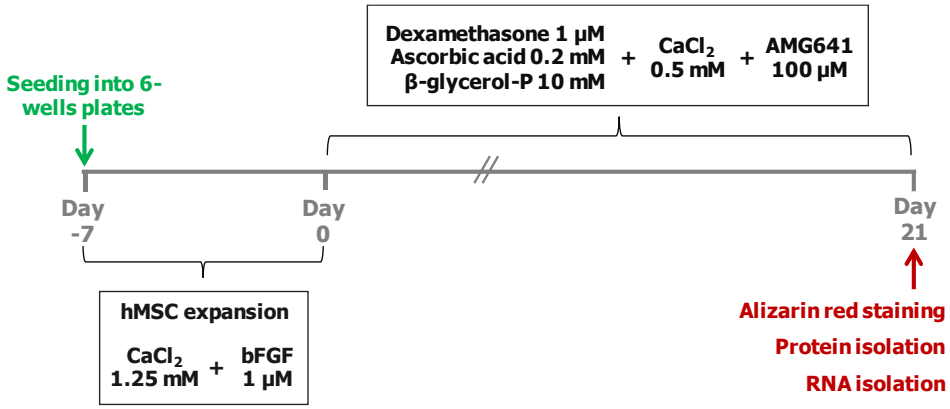

Figure 23. Experimental design for the *in vitro* study of the effects of calcimimetic on human MSC osteogenesis.

2.2.1.3. Total protein isolation

Total protein was isolated from cells in a lysis buffer, containing 20 mM Tris/HCl, 150 Mm NaCl, 1 Mm EDTA, 0.5 Mm PMSF, 70 µg/ml Protease Inhibitor Cocktail, 0.5% Igepal CA-630, 1 µl/ml Phosphatase Inhibitor Cocktail 2 (Sigma-Aldrich) and 1 µl/ml Phosphatase Inhibitor Cocktail 3 (Sigma-Aldrich), Ph 7.6. Suspension was centrifuged and supernatant (protein extract) was stored at -80 ºC. Protein concentration was determined by Bradford assay (Bio-Rad Laboratories).

2.2.1.4. Western blotting

50 µg of total protein were analyzed by immunoblotting as described in the section 1.2.7 using antibodies for CaSR (Abcam plc, Cambridge, UK. Ref. ab19347; 2 µg/ml dilution), p44/42 MAPK (total ERK1/2; Cell signaling Technology / Ref. #4695; 1:1000 dilution) and phospho-p44/42 MAPK (phospho-ERK1/2; Cell signaling Technology Ref. #4370; 1:2000 dilution) as primary antibodies, and horseradish peroxidase-conjugated goat anti-mouse and goat anti-rabbit (Santa Cruz Biotechnology) as secondary antibodies. β-actin (Antibody for detection Santa Cruz Biotechnology / Ref. SC-47778; 1:500 dilution) was used as loading control .

2.2.1.5. RNA extraction, DNAse treatment and RT-PCR

RNA isolation, DNase treatment and RT-PCR analysis for rat *Runx2*, *Osterix* and *Osteocalcin* and human *Runx2*, *Osterix*, *Osteocalcin* and *BMP2* were determined as described in sections 1.2.1.3, 1.2.1.4 and 1.2.2.4, respectively. *GAPDH* expression was used as housekeeping gene. Primers sequences are listed in Table 6.

2.2.1.6. Calcium content in the matrix of the cell cultures

At the end of the experiment with MSC differentiated into osteoblasts, Ca concentration in the mineralized matrix was quantified as in section 1.2.11. Representative microphotographs showing nodules of calcifications were taken using an inverted microscope Nikon eclipse Ti-S (Nikon Instruments Europe B.V., Amsterdam, Netherlands).

	Primer sequences	NCBI gene ID
Rat *Runx2*	Fw 5'-CGGGAATGATGAGAACTACTC-3'	367218
	Rv 5'-CGGTCAGAGAACAAACTAGGT-3'	
Rat *Osterix*	Fw 5'-GTACGGCAAGGCTTCGCATCTGA-3'	300260
	Rv 5'-TCAAGTGGTCGCTTCGGGTAAAG-3'	
Rat *Osteocalcin*	Fw 5'-TCTGAGTCTGACAAAGCCTTCATG-3'	25295
	Rv 5'-TGGGTAGGGGGCTGGGGCTCC-3'	
Rat *GAPDH*	Fw 5'-AGGGCTGCCTTCTCTTGTGAC-3'	24383
	Rv 5'-TGGGTAGAATCATACTGGAACATGTAG-3'	
Human *Runx2*	Fw 5'-CCGGAGTGGACGAGGCAAGAGTT-3'	860
	Rv 5'-AGCTTCTGTCTGTGCCTTCTGGG-3'	
Human *Osterix*	Fw 5'-ATCTGCCTGGCTCCTTGGGACCCG-3'	121340
	Rv 5'-TGCTTTGCCCAGAGTTGTTGAGTC-3'	
Human *Osteocalcin*	Fw 5'-GCAGAGTCCAGCAAAGGTGCAGCC-3'	632
	Rv 5'-GCCTCCTGAAAGCCGATGTGGTCA-3'	
Human *BMP2*	Fw 5'-AGGAGGCAAAGAAAAGGAACGGAC-3'	650
	Rv 5'-GGAAGCAGCAACGCTAGAAGACAG-3'	
Human *GAPDH*	Fw 5'-TGATGACATCAAGAAGGTGGTGAAG-3'	2597
	Rv 5'-TCCTTGGAGGCCATGTGGGCCAT-3'	

Table 6. Primers sequences for RT-PCR in the experiments with calcimimetics *in vitro*.

2.2.2. Effects of calcimimetic on osteoclastogenesis: In vitro study

The effects of low calcium concentration (0.5mM) and calcimimetic (10 and 100 µM) during osteoclastic differention of bone marrow hematopoietic cells were also examined as indicated previously in the section 1.2.2.

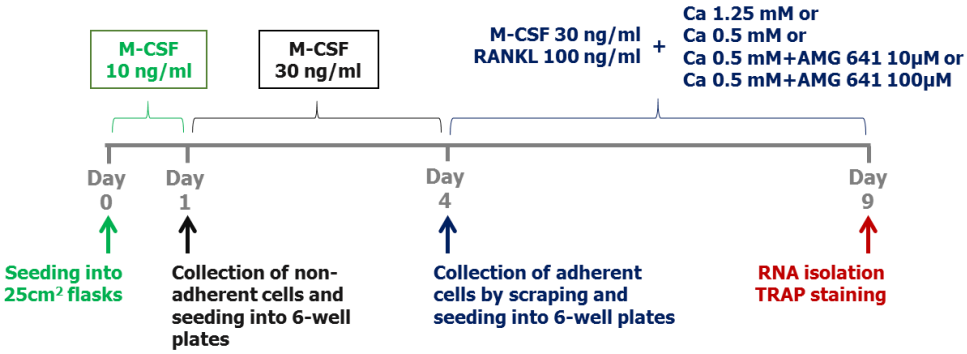

Figure 24. Scheme of the *in vitro* experiment for the study of the effects of calcium and calcimimetic on the osteoclastic differentiation of rat bone marrow hematopoietic cells.

SECTION 3: MAGNESIUM AND BONE

3.1. *IN VIVO EXPERIMENTS*

Mg-based compounds are commonly used as P binders to reduce serum P levels and vascular calcifications. Moreover, Mg-based phosphate binders also increase serum Mg levels, with unknown effects on bone homeostasis. In this section, we studied the effects of Mg supplementation in bone *in vivo* in a rat model of renal osteodystrophy and *in vitro* on osteogenesis of mesenchymal stem cells and osteoclast differentiation of bone marrow hematopoietic stem cells.

3.1.1. In vivo experimental procedure

To induce uremia in rats, the 5/6 nephrectomy model was used (detailed in section 1.1.1). One day after the second kidney surgery, rats were fed a high P diet (Ca 0.6% and P 1.2%). 5/6Nx animals received CTR (80ng/kg/48h; i.p). Rats were randomly divided into groups (n=10-14) which were fed with diets containing different Mg content: 0.1, 0.3 or 0.6% for 14 days. All diets were purchased from Altromin (Altromin GmbH, Lage, Germany).

The following animal groups were studied in this section:

1. Sham operated (n=15)
2. 5/6Nx+P 1.2%+Mg 0.1% (n=21)
3. 5/6Nx+P 1.2%+Mg 0.3% (n=22)
4. 5/6Nx+P 1.2%+Mg 0.6% (n=24)

At the end of the experiments rats were euthanized and exsanguinated by aortic puncture under general anesthesia with sodium thiopental (50mg/kg; i.p.). Blood samples were collected, processed for plasma separation and subsequently stored at -80 ºC until determination of biochemical parameters. Femurs were placed into ethanol 70% for histomorphometric analyses.

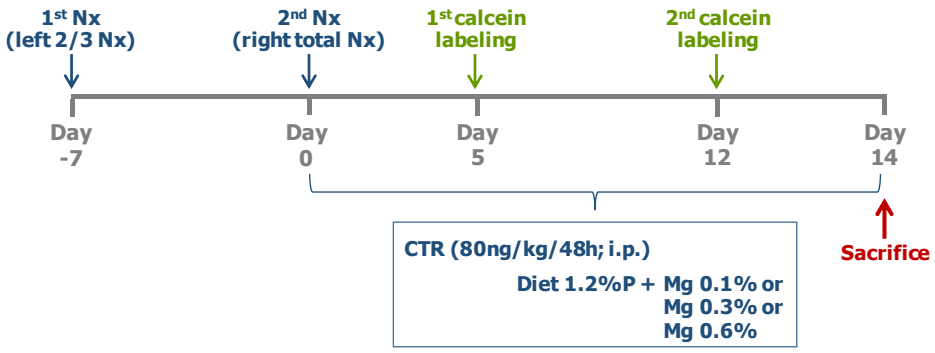

Figure 25. Experimental design for the study of the effects of magnesium on bone in 5/6Nx rats.

3.1.2. Plasma and urine biochemistry

Three days before sacrifice, rats were housed into metabolic cages for urine collection and maintained on the same diet. Urine samples from the two first days were discarded and only urine from the 24h before sacrifice was used to determine Ca, P, Mg and creatinine by spectrometry using commercial kits (Biosystem S.A.).

Blood samples were collected during the sacrifice in heparinized tubes and processed to obtain plasma by centrifugation at 2000 x *g*, 4 ºC for 10 minutes. Samples were divided in aliquots and stored at -20ºC.

Creatinine, ionized Ca, P, Mg, PTH, CTR and FGF23 plasma concentrations were measured as described in section 1.1.4.

3.1.3. Bone histomorphometry

Femurs were dehydrated, embedded in methyl-methacrylate and processed for histomorphometric analysis as detailed in section 1.1.5. Bone volume, turnover and were assessed using Osteometrics™ software according to the established system[108].

3.2. *IN VITRO EXPERIMENTS*

3.2.1. Magnesium effects on MSC osteogenic differentiation

The *in vitro* effects of Mg supplementation were evaluated on osteogenesis of bone marrow MSC.

3.2.1.1. Experimental design

Basal Mg^{2+} concentration in α-MEM was 0.8 mM. To increase Mg^{2+} content in the pro-osteogenic medium, α-MEM was supplemented as indicated in section 1.2.1.2 and $MgCl_2$ (Carlo ErbaReagentiSpA, Milano, Italy) was added to achieve final Mg^{2+} concentrations of 1.2 and 1.8 mM during the osteogenic stimulus. Fresh medium alone or osteogenic medium supplemented with $MgCl_2$ was replaced every 3 days.

Furthermore, 2-aminoethoxydiphenyl borate (2-APB; 50 µM; Tocris Bioscience, Bristol, UK), was added to the osteogenic medium containing 0.8 mM of Mg^{2+} during differentiation to determine the effects of inhibiting the Mg^{2+} channel Transient Receptor Potential cation channel, subfamily M, member 7 (TRPM7). To examine the direct effects of Mg^{2+}, $MgCl_2$ at 1.2 and 1.8Mm, or 2-APB at 50 µM was added for 24 hours to undifferentiated MSC, to MSC at early osteogenic differentiation (first 24 hours of osteogenic stimuli) or to MSC at a late stage of differentiation (last 24 hours on day 21). At the end of the experiments cells were processed for protein and RNA isolation.

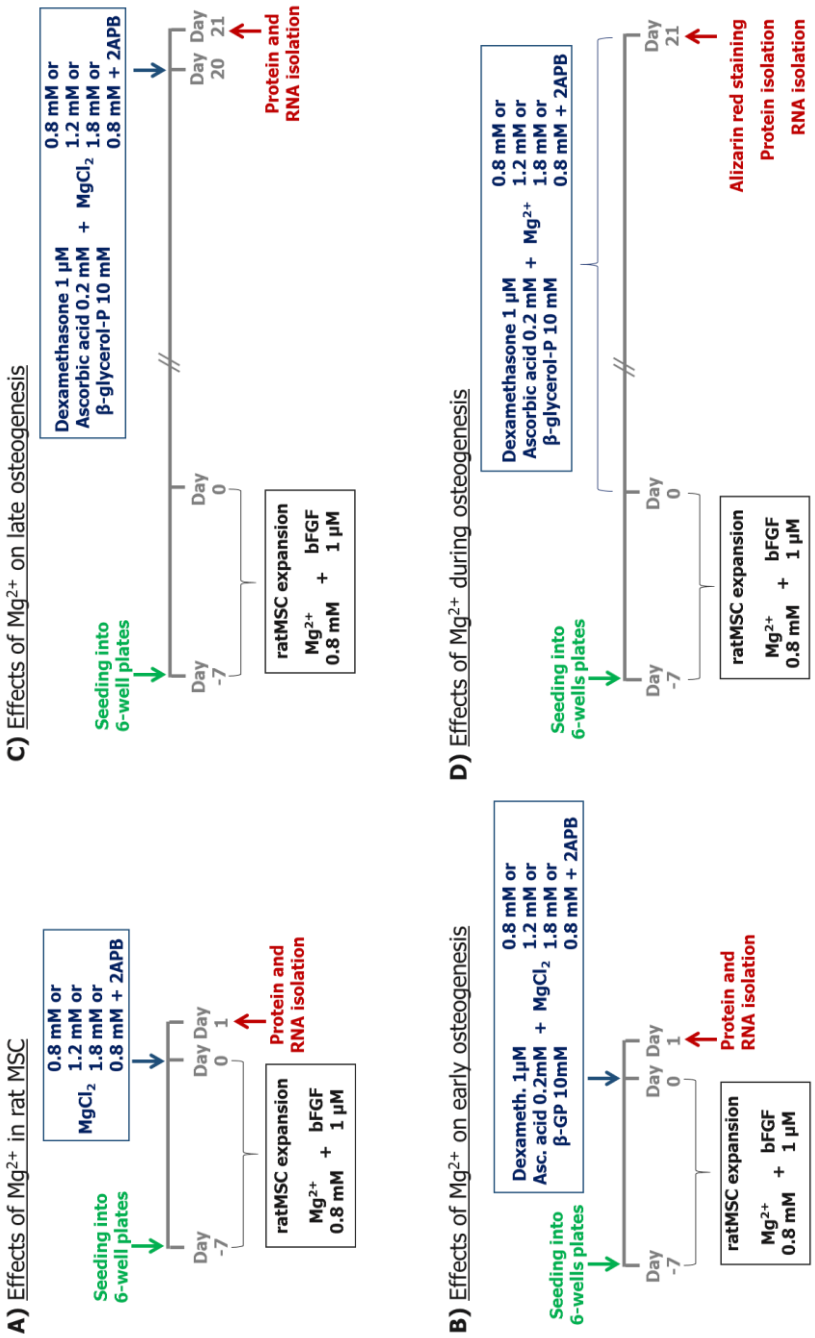

Figure 26. Design for the *in vitro* study of the effects of magnesium on osteogenesis

3.2.1.2. Protein isolation and western blotting

Isolation of enriched fractions of cytoplasmic and nuclear proteins was carried out as previously described in section 1.2.1.6. Protein expression of cleaved Notch, β-catenin, PCNA and Cyclin D1 was measured by western blotting as described in section 1.2.1.7 using 20 µg of nuclear-enriched protein extracts. Primary antibodies were anti Cleaved Notch1 (Val1744) (Cell signaling Technology / Ref. #2421; 1:200 dilution), anti-β-catenin (Cell signaling Technology / Ref. #9562; 1:1000 dilution), anti-PCNA (Santa Cruz Biotechnology / Ref. SC-56; 1:100 dilution) and anti-Cyclin D1 (Cell signaling Technology / Ref. #2978; 1:500 dilution). TFIIB protein expression was used as loading control (Cell signaling Technology / Ref. #4169; 1:1000 dilution). All experiments were repeated at least three times.

3.2.1.3. RNA isolation and RT-PCR (two-step protocol)

RNA samples were obtained at the end of the experiments and treated with DNase as previously described in sections 1.2.1.3 and 1.2.1.4 respectively. For these experiments RT-PCR was performed for the osteogenic genes *Runx2*, *Osterix*, *Osteocalcin* using a two-step protocol as indicated previously in 1.2.1.5. Ribosomal *18S* RNA expression was used as housekeeping control. Primers sequences are listed in Table 7.

3.2.1.4. Quantification of ALP activity

Determination of ALP activity was conducted as described in the section 1.2.1.9 using the p-nitrophenyl phosphate method.

3.2.1.5. Alizarin red S staining

Matrix mineralization was assessed by alizarin red staining. Protocol and image processing were performed as previously detailed in section 1.2.1.10.

	Primer sequences	NCBI gene ID
Rat *Runx2*	Fw 5'-CGGGAATGATGAGAACTACTC-3'	367218
	Rv 5'-CGGTCAGAGAACAAACTAGGT-3'	
Rat *Osterix*	Fw 5'-GTACGGCAAGGCTTCGCATCTGA-3'	300260
	Rv 5'-TCAAGTGGTCGCTTCGGGTAAAG-3'	
Rat *Osteocalcin*	Fw 5'-TCTGAGTCTGACAAAGCCTTCATG-3'	25295
	Rv 5'-TGGGTAGGGGGCTGGGGCTCC-3'	
Rat *HEY2*	Fw 5'-TCCAATGCTCATAAAGTCCGT-3'	155430
	Rv 5' -TCTGCAAATGACAGTGGATCA-3'	
Rat *18S*	Fw 5'-GTAACCCGTGAACCCCATT-3'	100861533
	Rv 5'-CCATCCAATCGGTAGTAGCG-3'	

Table 7. Sequences for primers used in the in vitro experiments with magnesium.

3.2.1.6. Immunoflurescence analysis

Protein amount and location for Notch intracellular domain and β-catenin were analyzed by confocal microscopy as previously described in section 1.2.1.8.

3.2.1.7. Decellularization of rat bones for scaffold preparation

Bone scaffolds were obtained as it was previously reported Shahabipour[185]. Briefly, rat femurs and tibiae were cut longitudinally in 5 mm pieces. Subsequently, bone pieces were boiled 4 times for 5 minutes to remove fat tissues. Pieces were stored overnight at -20ºC before decellularization. Bone specimens were thawed at room temperature, washed with PBS and placed in liquid nitrogen for 2 minutes. Then, pieces were maintained in distilled water at room temperature and washed with PBS. The freeze-thaw process was repeated five times to lysate the cells. Bone scaffolds were decellularized in 2.5% SDS (Sigma-Aldrich) for 24h at 37 ºC with gentle shaking. Then, bone specimens were washed twice with PBS for 15 minutes to

remove SDS, washed in ethanol (70%) and maintained in PBS (Sigma-Aldrich) for 30 minutes with shaking at room temperature. Pictures shown the processing and the resulting decellularized scaffolds are shown in Figure 27.

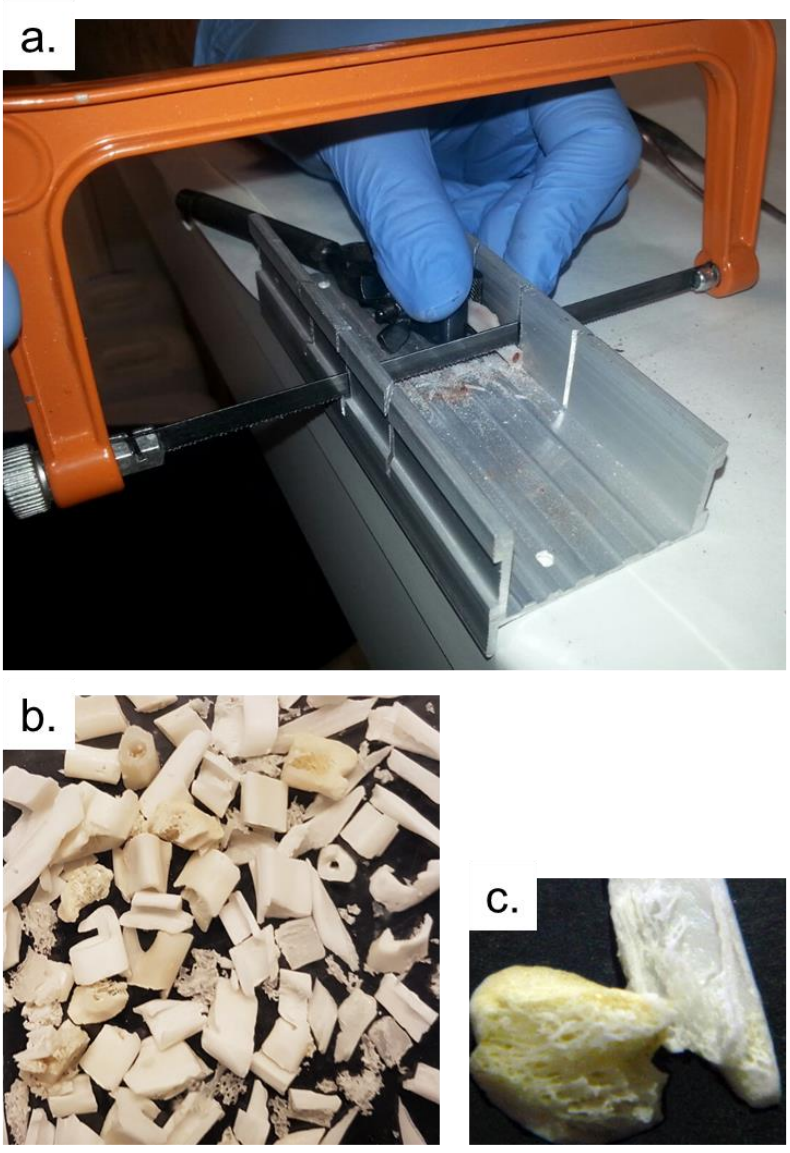

Figure 27. Photograph of processing and resulting decellularized rat bone scaffolds. Rat bones were cut using a saw (**a**), and processed for decellularization. Decellularized rat bones pictures were taken with a conventional camera using different zoom (**b** and **c**).

3.2.1.8. Transmission Electron Microscopy (TEM)

Bone marrow MSC were cultured in the presence of different concentrations of $MgCl_2$ (0.8, 1.2 and 1.8 Mm) on rat femur scaffolds. After 21 days of culture, the cellular layer was removed from the surface of the bone scaffolds and they were analyzed by electronic microscopy. For the ultrastructural study, randomly selected samples of decellularized bone scaffolds were primarily fixed in a glutaraldehyde 2% solution in phosphate buffer 0.1 M pH 7.4 overnight at 4ºC and then re-fixed in osmium tetroxide 1% in phosphate buffer 0.1 M pH 7.4 for 30 minutes. After dehydration in graded ethanol series and embedding in an epoxy adhesive, semi-thin and ultra-thin sections were cut with a LKB ultramicrotome. Ultra-thin sections were viewed and photographed in a Philips CM10 transmission electron microscope.

3.2.1.9. Scanning Electron Microscopy (SEM)

Bone marrow MSC were cultured in the presence of different concentrations of $MgCl_2$ (0.8, 1.2 and 1.8 Mm) on rat femur scaffolds. After 21 days of culture, decellularized bone fragments without MSC, differentiated cells and differentiated cells plus $MgCl_2$ were kept in glutaraldehyde 2.5%. Bone scaffolds were mounted on the SEM specimen stubs with carbon tape and were carbon-coated. Samples were analyzed and photographed with a Hitachi S520 SEM (Hitachi, Tokyo, Japan).

3.2.2. Effects of magnesium on osteoclastogenesis

The effects of high doses of Mg were determined in an *in vitro* model of osteoclasts.

3.2.2.1. Experimental design

Osteoclast differentiation was performed as abovementioned in section 1.2.2.1. Magnesium chloride was added at the time of osteoclastic differentiation to achieve concentrations of 1.4 and 2.6 mM (Fig. 28). After 5 days of differentiation and once the presence of multinucleated cells was confirmed in an inverted microscope, cells were processed for RNA isolation and TRAP staining.

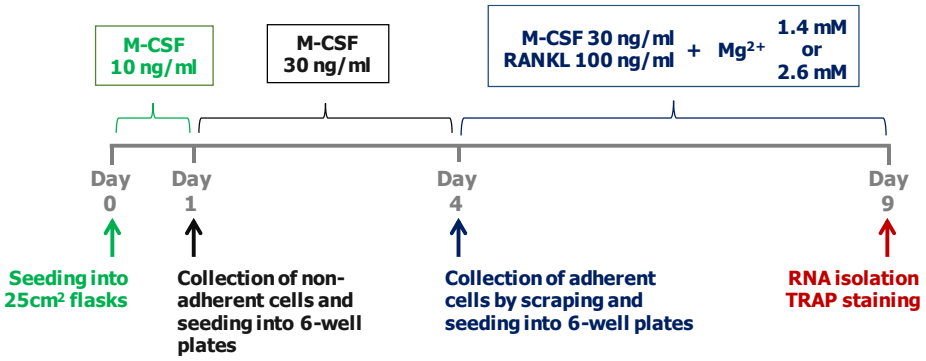

Figure 28. Experimental design for the *in vitro* study of the effects of magnesium addition on osteoclastogenesis.

3.2.2.2. RNA isolation and RT-PCR

RNA isolation and DNAse treatment was determined as aforementioned in sections 1.2.1.3 and 1.2.1.4, respectively. mRNA expression of *CTSK* was quantified using a one-step protocol as indicated previously in section 1.2.2.4.

3.2.2.3. TRAP staining

TRAP staining was performed at the end of the experiment as previously described in section 1.2.2.4.

SECTION 4: FGF23 AND BONE

4.1. *IN VIVO STUDIES*

Serum levels of FGF23 increase dramatically during CKD. This hormone is produced mainly by mature osteoblasts and osteocytes; however, currently it is unknown whether FGF23 controls osteogenesis or whether excessive FGF23 promotes changes in bone homeostasis. In this section, the effect of FGF23 on bone at early stage of CKD will be evaluated.

A heminephrectomy model with modifications in the P content of the diet was performed to generate a uremic model with a low and high FGF23 levels without additional changes in other important parameters of mineral metabolism.

4.1.1. Experimental procedure

Male wistar rats weighing 250 g approximately were anesthetized using sevoflurane and underwent total right kidney ablation (1/2Nx). Briefly, rats were anesthetized with sevoflurane, an excision was made in the right lateral side of the abdomen and the right kidney was exposed, the vessels and the ureter were ligated and the kidney was ablated. A group of rats received sham-operation in which the right kidney was exposed, moved and returned to approximately the same place in the abdominal cavity. Animals were analgesized with fentanyl 10 µg/kg/i.p. After surgery, rats were housed using a 12h/12h light/dark cycle and given *ad libitum* access to tap water. All animals fed a 1.2% P, 0.6% Ca diet (Fig.29). Therefore, the following groups of rats were studied:

1. Sham+ P 1.2% (n=8)
2. 1/2Nx+P 1.2% (n=13).

After three weeks, rats were euthanized and exsanguinated by aortic puncture under general anesthesia by sodium thiopental (50mg/kg; i.p.). Blood samples were collected in heparinized tubes and right femurs were placed in 70% ethanol for bone histomorphometry. Right tibias were also stored at -80 ºC for RNA isolation and quantification of gene expression.

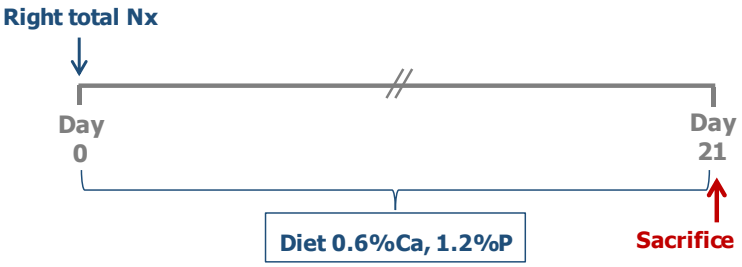

Figure 29. Experimental design for the *in vivo* study of 1/2Nx rat model. Sham rats were included.

4.1.2. Plasma and urine biochemistry

Plasma determinations of ionized Ca, P, creatinine, intact PTH, intact FGF23 and sclerostin concentrations were assayed as previously described in section 1.1.4.

4.1.3. Bone histomorphometry

Bone histomorphometric analysis was performed in undecalcified right femurs as previously described in section 1.1.5.

4.1.4. Bone RNA isolation and RT-PCR

To prevent tissue degradation, frozen tibias were cut and the proximal parts were used for RNA isolation. Samples were maintained in liquid nitrogen during tissue homogenization using a mortar. Then, the ground tissue was placed in 1 ml of TRI Reagent® and homogenized using a vortex during at least 10 seconds. RNA isolation and DNase treatment were performed as shown in sections 1.2.1.3 and 1.2.1.4, respectively.

RT-PCR was performed for the genes *Runx2*, *Osterix*, *Ostecalcin*, *DMP1* and *SOST* as described in the section 1.2.2.4, using *GAPDH* as housekeeping gene. Primer sequences are listed in Table 8.

	Primer sequences	NCBI gene ID
Rat *Runx2*	Fw 5'-CGGGAATGATGAGAACTACTC-3' Rv 5'-CGGTCAGAGAACAAACTAGGT-3'	367218
Rat *Osterix*	Fw 5'-GTACGGCAAGGCTTCGCATCTGA-3' Rv 5'-TCAAGTGGTCGCTTCGGGTAAAG-3'	300260
Rat *DMP1*	Fw 5'-GGCTGTCCTGTGCTCTCC-3' Rv 5'-ACTGCTGTCCGTGTGGTC-3'	25312
Rat *SOST*	Commercially acquired from Qiagen Ref. QT00418558	80722

Table 8. Primer sequences for RT-PCR in the study of the effects of FGF23 on bone homeostasis *in vivo*.

4.2. *IN VITRO STUDIES*

4.2.1. Effects of FGF23 on osteogenesis of bone marrow MSC

The effects of high FGF23 on osteogenic differentiation of bone marrow MSC or in mature osteoblasts/osteocytes were investigated *in vitro*.

4.2.1.1. Experimental design

Bone marrow MSC isolation and osteogenic differentiation was performed as previously detailed in sections 1.2.1.1 and 1.2.1.2, respectively. A high rat recombinant FGF23 (R176Q) (rFGF23, 15 ng/ml) concentration was added during osteogenic differentiation to assess the effects along differentiation, or 24 hours before lysis, to evaluate the effects on mature osteocytes (Fig.30).

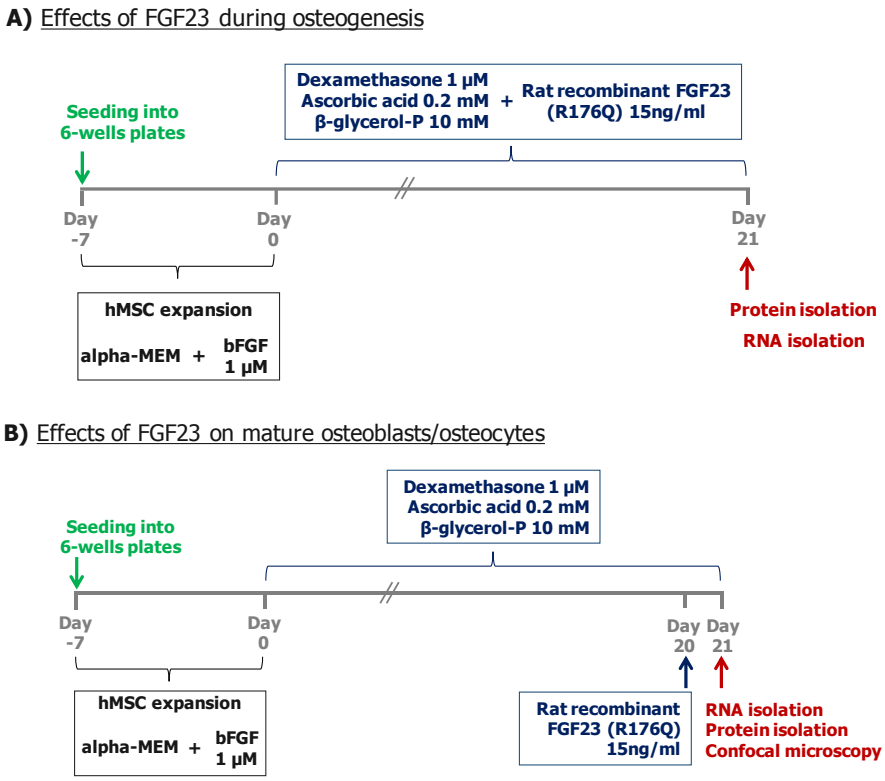

Figure 30. Experimental designs for the *in vitro* study of the effects of FGF23 on osteogenesis.

At the end of the experiments cells were processed for RNA or protein isolation. Experiments were repeated at least three times.

4.2.1.2. RNA isolation and RT-PCR

RNA isolation, DNAse treatment and the quantification of *Runx2*, *Osterix*, *Osteocalcin*, *DMP1*, *SOST*, *OPG* and *RANKL* mRNA expressions, using *GAPDH* as housekeeping gene, was performed as previously described in sections 1.2.1.3, 1.2.1.4 and 1.2.2.4, respectively. Primers sequences are shown in Table 9.

	Primer sequences	**NCBI gene ID**
Rat *Runx2*	Fw 5'-CGGGAATGATGAGAACTACTC-3' Rv 5'-CGGTCAGAGAACAAACTAGGT-3'	367218
Rat *Osterix*	Fw 5'-GTACGGCAAGGCTTCGCATCTGA-3' Rv 5'-TCAAGTGGTCGCTTCGGGTAAAG-3'	300260
Rat *Osteocalcin*	Fw 5'-TCTGAGTCTGACAAAGCCTTCATG-3' Rv 5'-TGGGTAGGGGGCTGGGGCTCC-3'	25295
Rat *DMP1*	Fw 5'-GGCTGTCCTGTGCTCTCC-3' Rv 5'-ACTGCTGTCCGTGTGGTC-3'	25312
Rat *OPG*	Fw 5'-CACCAGAACACTCAGCCAAT-3' Rv 5'-CCGGAAACAGAGAAGCAACT-3'	25341
Rat *RANKL*	Fw 5'-ACGAACCTTCCATCATAGCTG-3' Rv 5'-GAAGACACAGAAGCACTACCT-3'	117516
Rat *SOST*	Commercially acquired from Qiagen Ref. QT00418558	80722

Table 9. Sequences of the primers used for RT-PCR analysis in the *in vitro* study of the effects of FGF23 on osteogenesis.

4.2.1.3. ALP activity quantification

As protein extracts were not collected in these experiments, ALP activity was measured in the supernatants. At the end of the experiment, supernatants were collected and 20 µl were incubated in 2 mM p-nitrophenyl phosphate using the protocol detailed in section 1.2.1.9.

4.2.1.4. Immunofluorescence analysis

Confocal microscopy analysis for the location and quantification of β-catenin was performed as described in section 1.2.1.8.

4.2.2. Effects of FGF23 on osteoclastogenesis

The effects of high doses of rFGF23 (0.1 and 10 ng/ml) were determined in an *in vitro* model of osteoclasts.

4.2.2.1. Experimental design

Osteoclast differentiation was performed as described previously in section 1.2.2.1. Additionally rFGF23 was added at 0.1 and 10 ng/ml along with the osteoclastogenic stimuli. Cells were incubated at 37 ºC, 5% CO_2 with saturated humidity for 5 days. Figure 31 shows a visual timeline of this study.

Medium was replaced every 2 days. At the end of the experiments cells were processed for determination of mRNA expression and TRAP staining. Experiments were performed at least three times.

4.2.2.2. RNA isolation and RT-PCR

RNA isolation, DNAse treatment and quantification of *CTSK* mRNA expression were carried out as described in sections 1.2.1.3, 1.2.1.4 and 1.2.2.4.

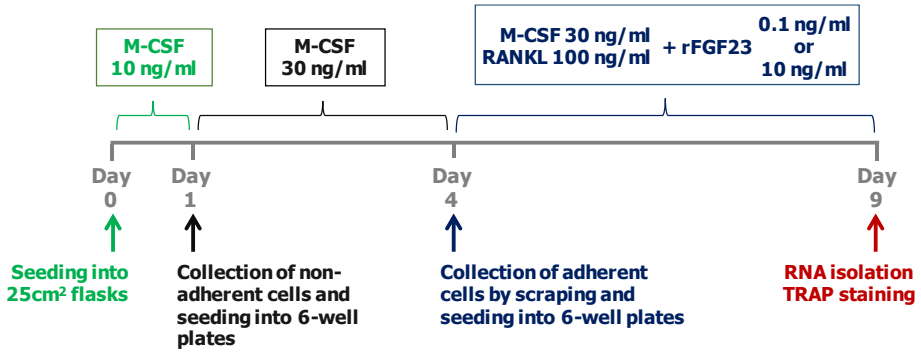

Figure 31. Experimental design for the *in vitro* study of the effects of FGF23 on osteoclastogenesis.

4.2.2.3. TRAP staining

TRAP staining was performed at the end of the experiment as previously detailed in section 1.2.2.4.

4.2.2.4. Length measurement of osteoclasts

As an increase in the size of the osteoclasts was observed in the cells treated with high rFGF23, we considered to measure the length of differentiated osteoclasts. Osteoclast differentiation was evaluated using an inverted microscope Nikon eclipse Ti-S. Intense red-stained (TRAP-positive) cells with more than 3 nuclei were considered osteoclasts. Cells nuclei were counted and the length of the minor and major axis were measured using Image J software.

RESULTS

SECTION 1: CALCITRIOL

1.1 IN VIVO STUDY OF THE CALCITRIOL EFFECT ON BONE

In these experiments, the effect of different concentrations of CTR (20, 40 and 60 ng/kg) were evaluated in 5/6 nephrectomized (5/6Nx) and parathyroidectomized (PTx) rats, receiving a constant infusion of rat recombinant PTH (1-34 length) through Alzet pumps and fed on a 0.9% P diet. Thus, the actions of CTR on bone were separated from those mediated by CTR-dependent PTH modulation. Sham rats and 5/6Nx-PTx-PTH rats receiving vehicle were also included.

1.1.1. Plasma biochemistry

Biochemical data of this study are shown in Table 10. As compared with Sham animals, 5/6Nx rats showed a significant increase in plasma creatinine, P, PTH and intact FGF23, while plasma iCa was significantly decreased. In 5/6Nx rats with PTx and PTH replacement by 6-fold (5/6Nx-PTx-PTHx6), plasma iCa levels were similar to those observed in the 5/6Nx group. Administration of CTR dose-dependently increased plasma P and iCa, being statistically significant at the dose of 60 ng/kg. The group receiving the dose of CTR 60 ng/kg also showed higher plasma creatinine than the others 5/6Nx groups. Furthermore, it was found that plasma FGF23 and sclerostin levels resulted significantly increased according to CTR dose. Exogenous PTH (1,34 length) could not be detected by the assay for intact PTH detection.

	Sham n=7	**5/6Nx** n=7	**5/6Nx-PTx-PTHx6** n=8	**5/6Nx-PTx-PTHx6-CTR20** n=10	**5/6Nx-PTx-PTHx6-CTR40** n=5	**5/6Nx-PTx-PTHx6-CTR60** n=9
Creatinine (mg/dl)	0.49±0.03	0.88±0.06[a]	0.91±0.03 [a]	1.02±0.05 [a]	1.03±0.06 [a]	1.46±0.15 [a,b,c,d,e]
P (mg/dl)	6.2±0.2	8.73±0.39 **[a]**	7.77±0.43 [a]	8.49±0.66 [a]	9.28±0.65 [a]	13.6±2.17 [a,b,c,d]
iCa (mM)	1.21±0.02	1.10±0.02[a]	1.02±0.03 [a]	1.04±0.03 [a]	1.23±0.04 [c,d]	1.32±0.01 [b,c,d]
Intact PTH (pg/ml)	47±4.4	540±96 [a]	n.a	n.a	n.a	n.a
FGF23 (pg/ml)	130±31	1522±217 [a]	471±105 **[a,b]**	908±138 **[a,b,c]**	5143±2264 **[a,b,c]**	28930±9608 [a,b,c,d,e]
Sclerostin (pg/ml)	215±20	261±43	288±39	253±24	374±112	713±179 [a,b,c]

Table 10. Plasma biochemistry. Values are mean ±SEM. One-way ANOVA with tukey test. a: p<0.05 vs Sham; b: p<0.05 vs 5/6Nx; c: p<0.05 vs 5/6Nx-PTx-PTHx6; d: p<0.05 vs 5/6Nx-PTx-PTHx6-CTR20; e: p<0.05 vs 5/6Nx-PTx-PTHx6-CTR40. Sham rats fed a 0.6%P, 0.6%Ca Diet. 5/6Nx groups fed a 0.9%P, 0.6%Ca diet.

1.1.2. Bone histomorphometry

Bone histomorphometry parameters were evaluated in the trabecular bone of the distal right femurs (Fig.32). 5/6Nx rats showed reduced BV/TV (Fig.32 **a**) and increased OV/BV, OS/BS (Fig.32 **b** and **c** respectively) and osteoblast activity (Fig.32 **d**) as compared with Sham animals. The ES/BS and the bone surface covered by osteoclasts were increased in the 5/6Nx group as compared with Sham rats (Fig.32 **e** and **f**). 5/6Nx-PTx-PTHx6 rats receiving vehicle showed similar BV/TV and OV/BV than the 5/6Nx group (Fig.32 **a** and **b** respectively), while bone cell activity was lower as assessed by the OS/BS and ES/BS (Fig.32 **c** and **e**) and the bone surface covered by osteoblasts and osteoclasts (Fig.32 **d** and **f**). CTR administration at 40 ng/kg body weight prevented the decrease in BV/TV. However, CTR at the dose of 60 ng/kg did not further increased the BV/TV. Osteoid amount was reduced by CTR administration at 20 and 40 ng/kg, consistent with a decrease in the bone surface covered by osteoblasts (Fig.32 **d**). It is interesting to note that the highest dose of CTR (60 ng/kg body weight) increased the osteoid amount respect to lower CTR doses. In 5/6Nx-PTx-PTHx6, CTR administration did not induce significant effects on osteoclast activity (Fig 32.**e** and **f**).

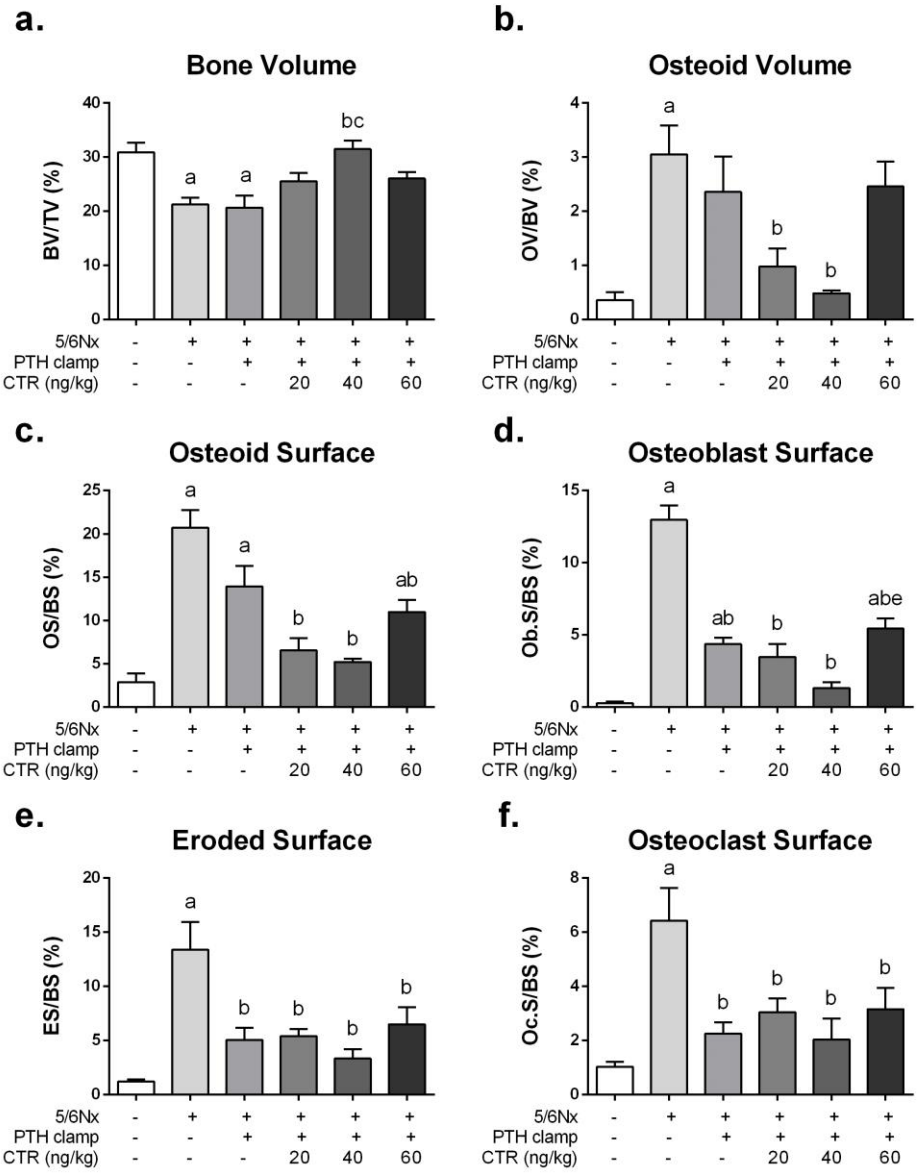

Figure 32. Effect of CTR on bone volume and turnover. CTR induces alterations in bone volume and bone cell activity independently of PTH in uremia. One-way ANOVA with Tukey test. a: $p<0.05$ vs Sham; b: $p<0.05$ vs 5/6Nx; c: $p<0.05$ vs 5/6Nx-PTx-PTH-vehicle; d: $p<0.05$ vs 5/6Nx-PTx-PTH-CTR 20 ng/kg; e: $p<0.05$ vs 5/6Nx-PTx-PTH-CTR 40 ng/kg. Sham rats fed a 0.6%P, 0.6%Ca Diet. 5/6Nx groups fed a 0.9%P, 0.6% Ca diet.

5/6Nx rats showed higher trabecular separation (Fig.33 **c**) and decreased trabecular number (Fig.33 **d**) than Sham animals. Bone structural parameters in 5/6Nx-PTx-PTHx6 were similar to those in 5/6Nx group. There was a significant increase in the osteoid thickness in 5/6Nx-PTx-PTHx6 rats treated with CTR at the dose of 60 ng/kg as compared with all the groups (Fig.33 **b**). A tendency to prevent the loss of trabecular bone was observed according to CTR administration. Trabecular thickness remained similar in all experimental groups (Fig.33 **a**).

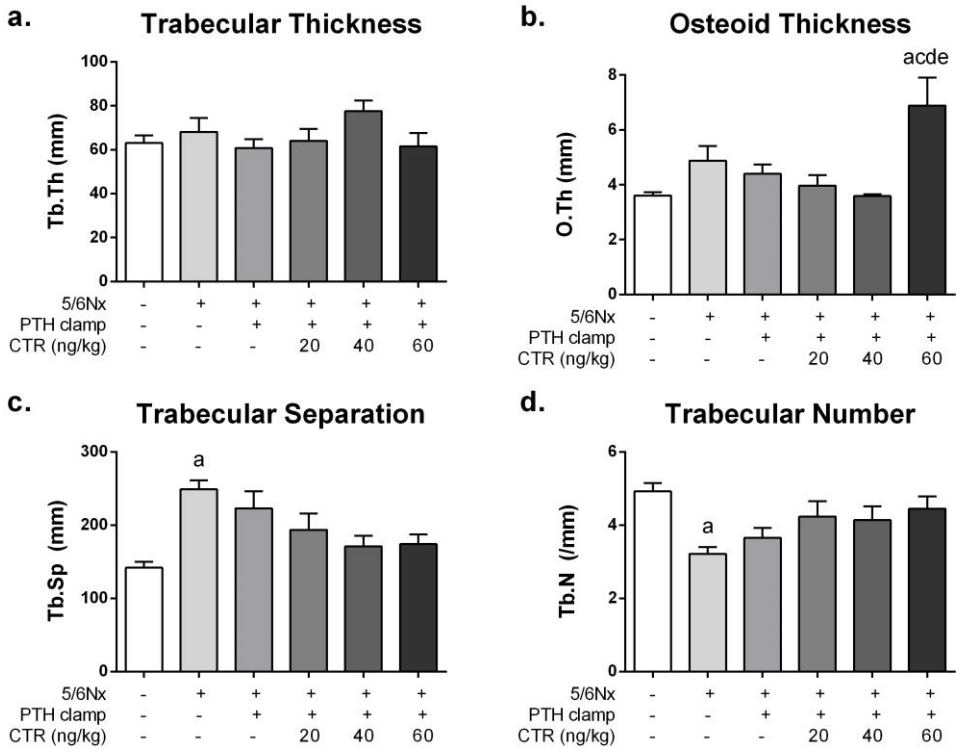

Figure 33. Effect of CTR on bone microstructure. CTR produces changes in bone structure and thickness independently of PTH. One-way ANOVA with Tukey test. a: $p<0.05$ vs Sham; c: $p<0.05$ vs 5/6Nx-PTx-PTHx6; d: $p<0.05$ vs 5/6Nx-PTx-PTHx6-CTR20; e: $p<0.05$ vs 5/6Nx-PTx-PTHx6-CTR40. Sham rats fed a 0.6%P, 0.6%Ca Diet. 5/6Nx groups fed a 0.9%P, 0.6%Ca diet.

As compared with Shan animals, bone mineralization assessed by calcein labelling showed higher mineralizing surface (MS/BS, Fig.34 **a**) and bone formation rate

(BFR/BS, Fig.34 **c**) in the 5/6Nx group. A tendency to increase the time of mineralization was observed in the 5/6Nx group respect to Sham animals (Fig.34 **d**). 5/6Nx-PTx-PTHx6 rats showed significantly lower BFR/BS than 5/6Nx and a tendency to decrease MS/BS. CTR administration at 60 ng/kg body weight produced a significant increase in the mineral apposition rate (MAR) as compared with the other 5/6Nx-PTx-PTHx6 groups (Fig.34 **b**). CTR administration did not modify bone formation significantly (Fig.34 **c**). Mineralization lag time was similar among all groups, however CTR administration at 20 and 40 ng/kg showed a tendency to decrease the time of mineralization, while it was observed delayed mineralization with the dose of 60 ng/kg (Fig.34 **d**), consistent with the accumulation of osteoid.

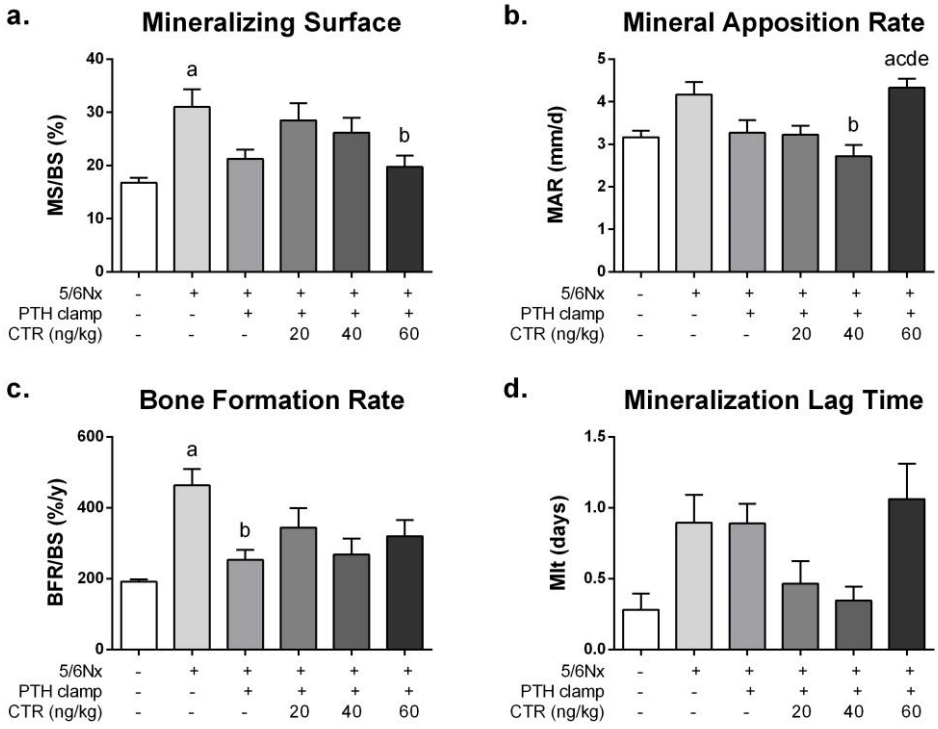

Figure 34. Bone formation and mineralization is affected by 1,25(OH)2D3 at the same plasma PTH levels. One-way ANOVA with Tukey test. a: $p<0.05$ vs Sham; b: $p<0.05$ vs 5/6Nx; c: $p<0.05$ vs 5/6Nx-PTx-PTHx6; d: $p<0.05$ vs 5/6Nx-PTx-PTHx6-CTR20; e: $p<0.05$ vs 5/6Nx-PTx-PTHx6-CTR40. Sham rats fed a 0.6%P, 0.6%Ca Diet. 5/6Nx groups fed a 0.9%P, 0.6%Ca diet.

Figure 35 shows representative pictures of Goldner's trichrome staining and calcein labeling of trabecular bone for each group. Note the increased resorption in the 5/6Nx group (Fig.35 **b**) and the increased bone formation (Fig.35 **e**) as compared with Sham animals (Fig.35 **a** and **d**). CTR administration by 20 ng/kg (Fig.35 **g** and **j**) and 40 ng/kg (Fig.35 **h** and **k**) decreased the osteoid amount as compared with vehicle (Fig.35 **c** and **f**), however, CTR at 60ng/kg increased osteoblast activity and osteoid amount (Fig.35 **i** and **l**). CTR did not exert significant effects on osteoclast activity and bone formation, however decreased bone mineralization and increased time of mineralization were observed in the group treated with CTR at 60ng/kg.

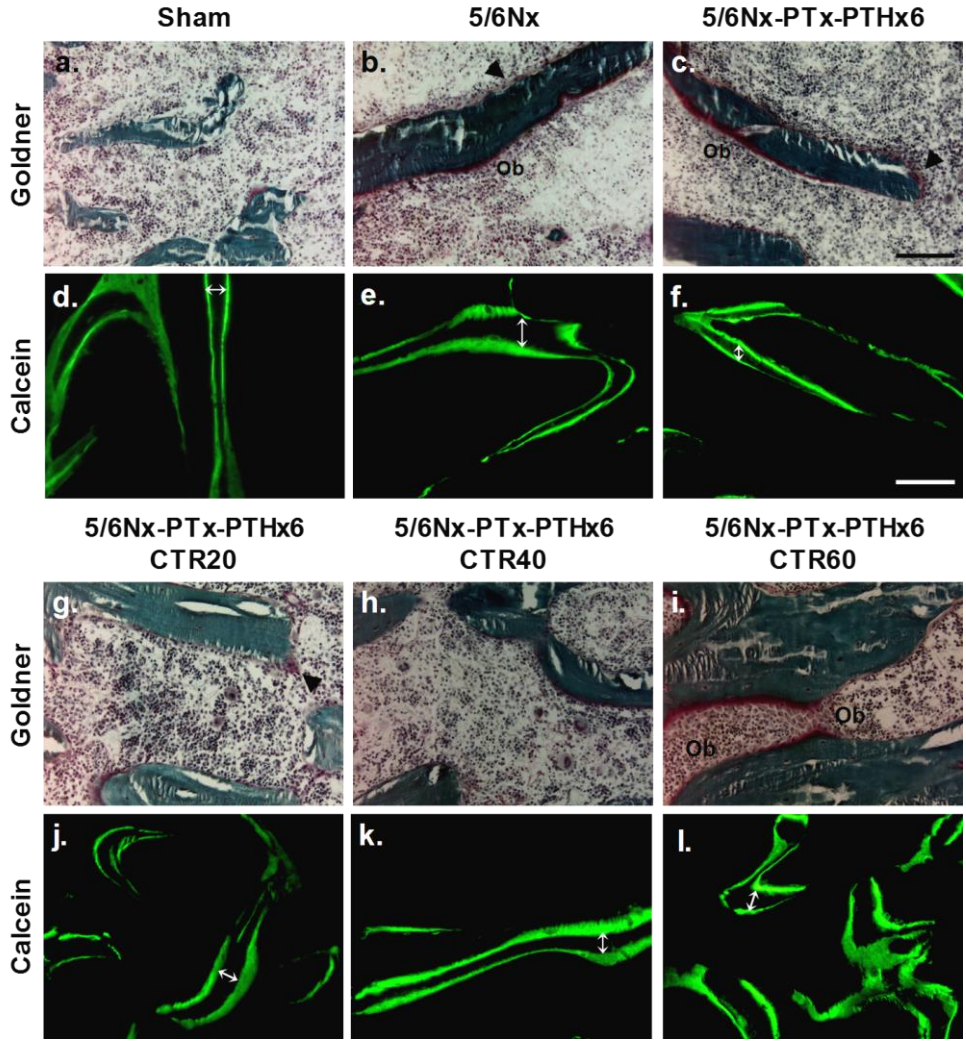

Figure 35. Representative pictures of Goldner's trichrome staining and calcein labeling of trabecular bone. 5/6Nx rats (**b** and **e**) showed an increased bone remodeling and bone formation as compared with Sham animals (**a** and **d**). PTH replacement maintained bone formation in parathyroidectomized rats receiving vehicle (**c** and **f**). CTR administration by 20 (**g** and **j**) and 40 ng/kg (**h** and **k**) decreased the osteoid amount in 5/6Nx-PTx-PTHx6 rats, while CTR at 60 ng/kg induced an increase in osteoblast activity and diffuse bands of calcein were observed (**i** and **l**). Sham rats fed a 0.6%P, 0.6%Ca Diet. 5/6Nx groups fed a 0.9%P, 0.6%Ca diet. Double-headed arrows indicate distance between both calcein labels.
Ob: Osteoblasts. Arrowhead: Osteoclast. Magnification: 200x. Bars represent 100µm.

1.2. *IN VITRO STUDY OF THE CALCITRIOL EFFECTS ON OSTEOGENESIS*

The direct actions of CTR supplementation were studied *in vitro* on osteogenesis and osteoclastogenesis models with bone marrow stem cells. Firstly, our *in vitro* model of osteoblast differentiation was based on rat bone marrow mesenchymal stem cells (MSC) treated with dexamethasone, β-glycerol-phosphate and ascorbic acid for 21 days. To evaluate whether CTR acts directly on osteogenesis, we measured its effects at different doses, from 10^{-12} to 10^{-8} M, during osteogenic differentiation of MSC.

1.2.1. Effects of calcitriol supplementation on MSC osteogenesis

As expected, osteogenic stimuli in the culture medium promoted MSC differentiation into osteoblast-like cells (OB), increasing the amount of mineralized matrix (Fig.36 **a**). Alizarin red staining at 21 days showed lower intensity at high doses of CTR, supporting the previous results. At the concentration of CTR 10^{-8} M mineralization was inexistent. Of note, the addition of CTR suppressed MSC differentiation dose-dependently, as confirmed by decreased calcium content in the mineralized matrix and the lower alkaline phosphatase activity (Fig.36 **b** and **c** respectively).

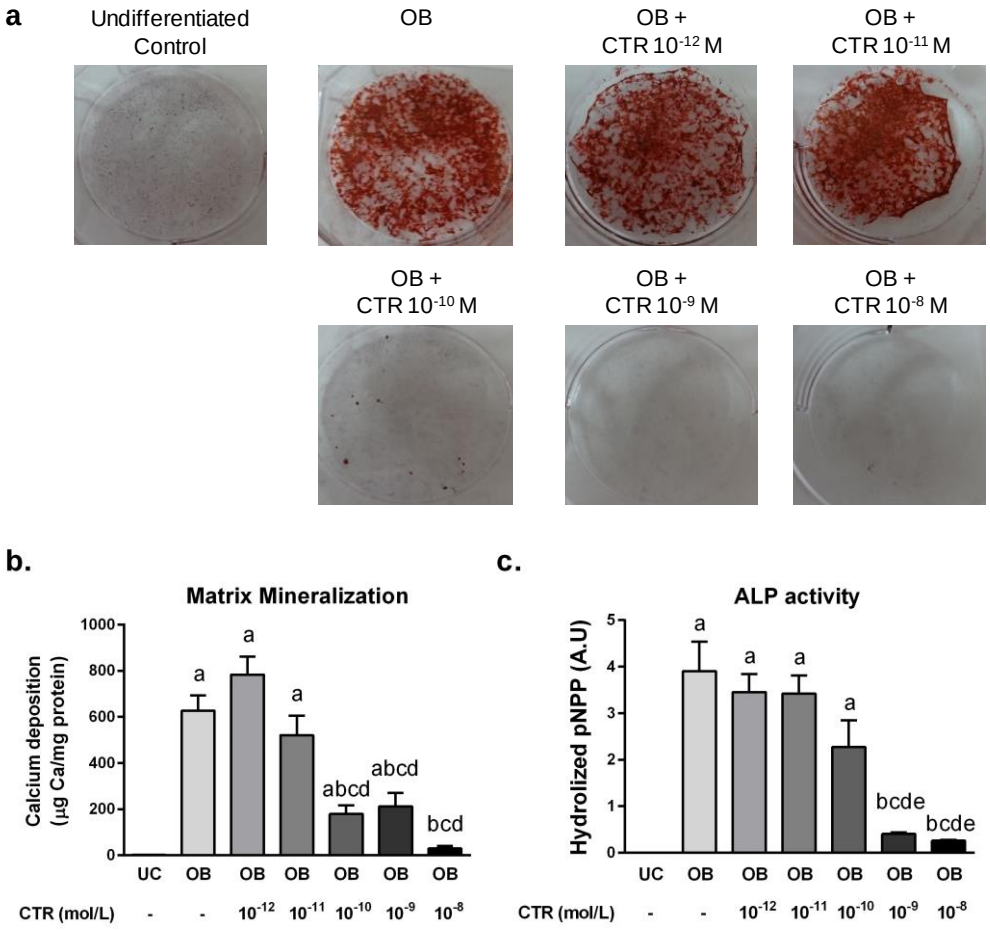

Figure 36. Effect of CTR on mineralization during osteogenesis *in vitro*. Representative pictures of alizarin red staining and microphotographs of MSC cultured with different experimental conditions after 21 days (**a**). UC: undifferentiated control. CTR dose-dependently decreased the amount of Ca in the mineralized matrix (**b**) and ALP activity (**c**). Bars are mean ± SEM. One-way ANOVA with Tukey test. a: $p<0.05$ vs UC; b: $p<0.01$ vs OB; c: $p<0.001$ vs OB+CTR 10^{-12} M; d: $p<0.001$ vs OB+CTR 10^{-11} M; e: $p<0.01$ vs OB+CTR 10^{-10} M. ALP: Alkaline phosphatase. pNPP: p-nitrophenyl phosphate. A.U: Arbitrary units.

In addition, treatment with CTR at doses from 10^{-10} to 10^{-8} M decreased the expression of the osteogenic master genes *Osterix* and *Osteocalcin* (Fig.37 **a** and **b** respectively), however CTR addition at lower dose (10^{-11} and 10^{-12} M) increased the

expression of both genes, resembling a reverse J-shaped curve that suggests a hormetic dose-response. Similar results were observed respect to the expression of the Vitamin D receptor (VDR) (Fig.37 **c**).

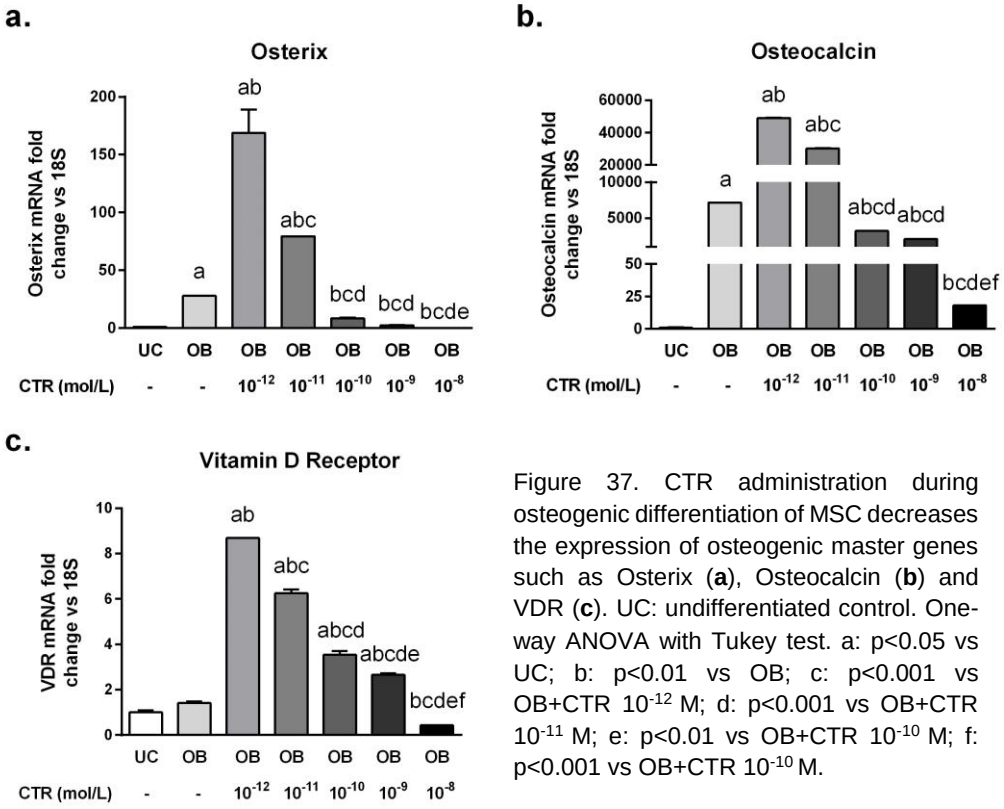

Figure 37. CTR administration during osteogenic differentiation of MSC decreases the expression of osteogenic master genes such as Osterix (**a**), Osteocalcin (**b**) and VDR (**c**). UC: undifferentiated control. One-way ANOVA with Tukey test. a: $p<0.05$ vs UC; b: $p<0.01$ vs OB; c: $p<0.001$ vs OB+CTR 10^{-12} M; d: $p<0.001$ vs OB+CTR 10^{-11} M; e: $p<0.01$ vs OB+CTR 10^{-10} M; f: $p<0.001$ vs OB+CTR 10^{-10} M.

Moreover, high doses of CTR during osteogenic differentiation reduced the cellular proliferation, assessed by the decreased protein amount of PCNA and Cyclin D1 in western blot analysis (Fig.38).

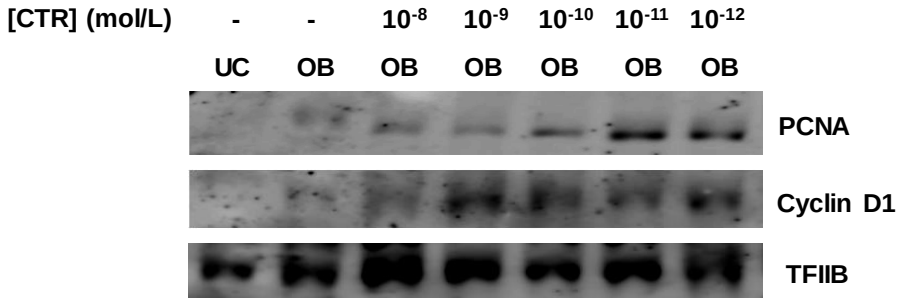

Figure 38. Effects of CTR supplementation on proliferation during MSC osteogenesis. CTR addition throughout osteogenesis decreased the amount of nuclear PCNA and Cyclin D1. TFIIB was used as housekeeping protein.

1.2.2. Effects of calcitriol on β-catenin nuclear translocation during osteogenesis of MSC

In order to evaluate the mechanism whereby high doses of CTR achieve its anti-osteogenic effect, the participation of the canonical Wnt/β-catenin pathway was examined by confocal microscopy.

High doses of CTR during osteogenic differentiation decreased the nuclear traslocation of β-catenin. Co-localization analysis of the confocal microphotographs clearly showed that the number of green pixels (β-catenin labeling) overlapping with blue pixels (DAPI, nuclear labeling) were lower in MSC differentiated into osteoblasts as CTR concentration increases (Fig.39).

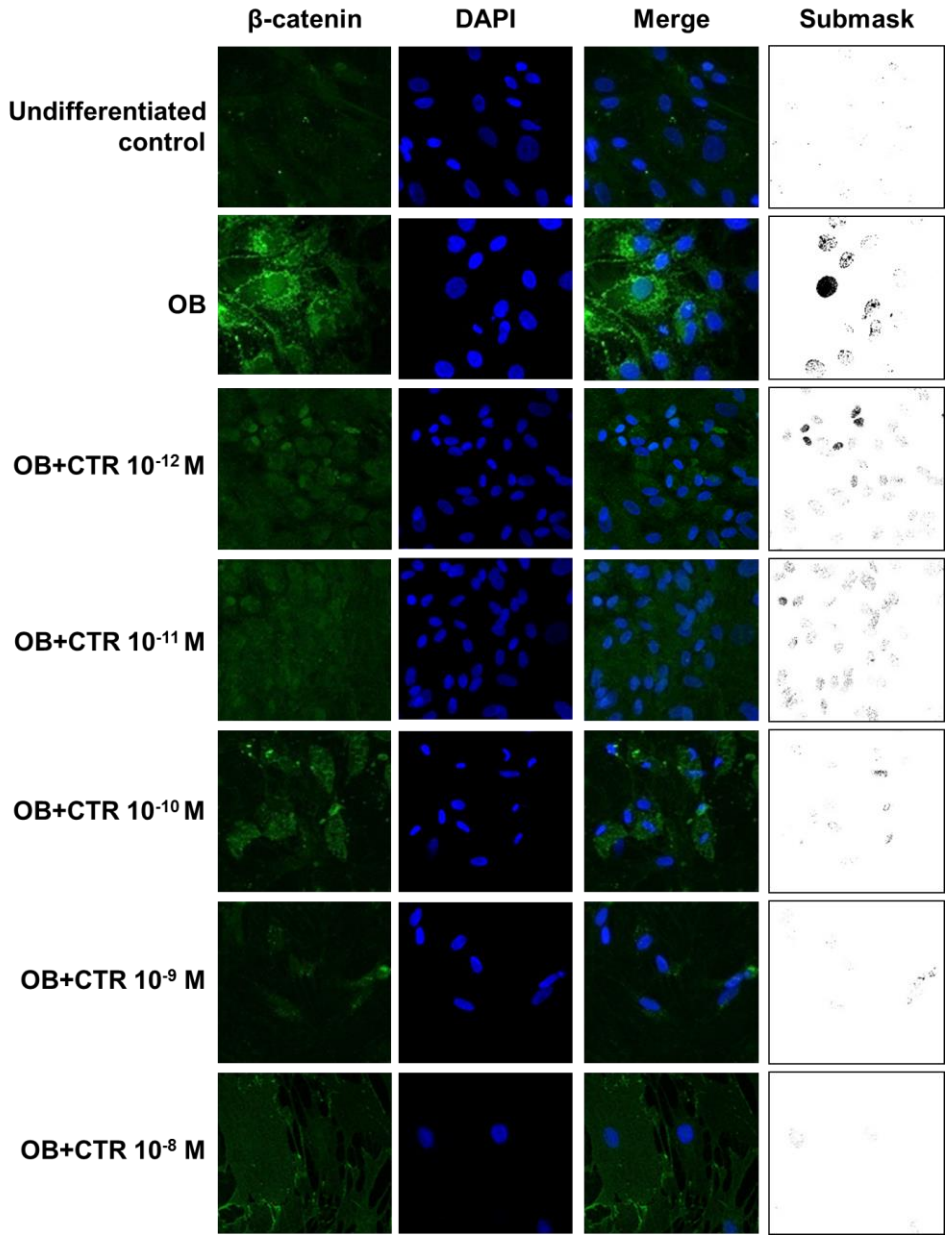

Figure 39. Representative pictures of β-catenin immunofluorescence. Submask images were performed for clearly identifying the co-localization for blue and green pixels co-localization. Green: β-catenin-488. Blue: DAPI.

1.3. *IN VITRO EFFECTS OF CALCITRIOL ON OSTEOCLASTOGENESIS*

To develop the *in vitro* model of osteoclast differentiation, we isolated non-adherent bone marrow hematopoietic stem cells from rat tibias and femurs, subsequently monocyte-macrophage differentiation was induced with M-CSF and differentiated into osteoclasts with M-CSF and RANKL during 5 days approximately. CTR was added along the differentiation process.

1.3.1. Osteoclast differentiation of bone marrow hematopoietic cells

Firstly, we characterized by immunophenotyping the osteoclast precursor cells. At the time of characterization, the non-adherent osteoclast precursor cells showed the immunophenotype of rat hematopoietic stem cell (Table 11).

	CD34	**CD45**	**Sca1**
Positive cells (%)	0.07±0.015	77.1±6.73	1.05±0.12

Table 11. Immunophenotype of the osteoclast precursor cells.

Undifferentiated control cells were mono-nuclear TRAP-negative cells (Fig.40 **a** and **b**). Osteoclastogenic stimulus promoted the recruitment of the precursor cells and osteoclastic differentiation (Fig.40 **b**). Multinucleated cells and positive for TRAP staining were considered well differentiated into osteoclasts (Fig.40 **d**). Moreover, osteoclastogenic medium induced an increase in the *Cathepsin K* (*CTSK*) mRNA expression after 5 days (Fig.40 **e**), an enzyme highly expressed in osteoclast that participates in extracellular matrix degradation.

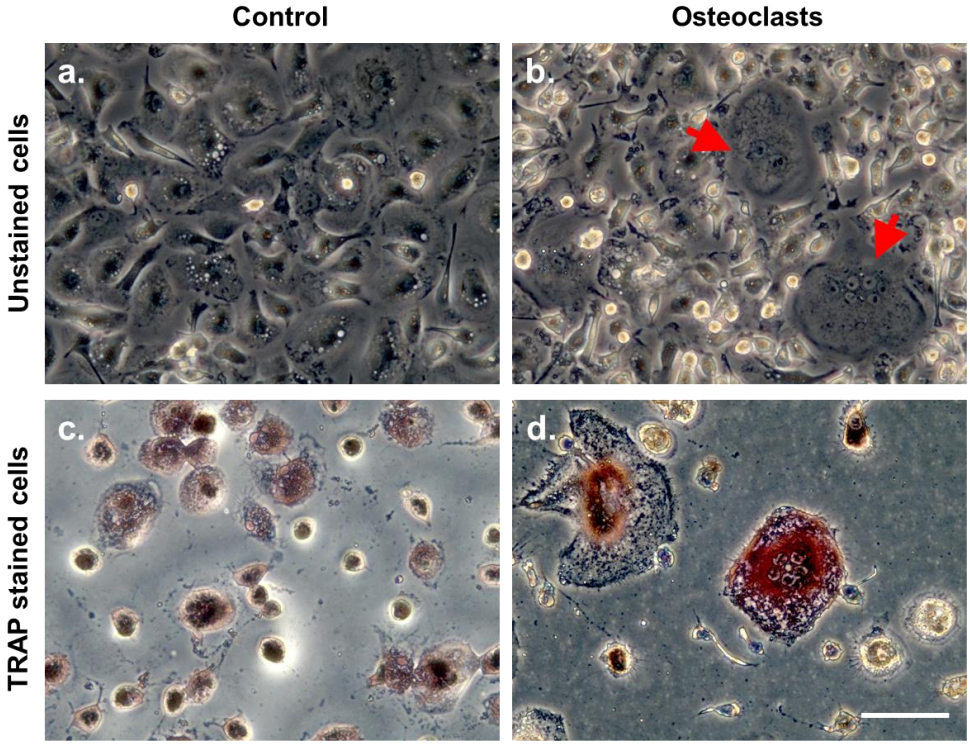

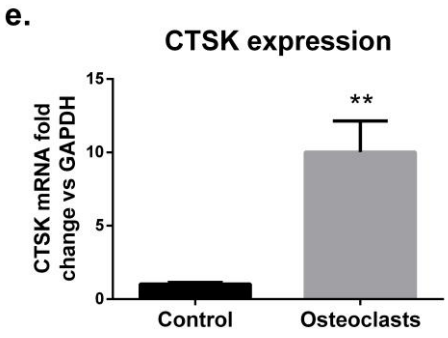

Figure 40. Osteoclastogenic stimulus produced multinucleated TRAP-positive cells. Bright field microscopy showed control cells (**a**) and lager multinucleated cells after 5 days of osteoclastogenic stimulus (**b**). Scarce or absence of TRAP stained cells were observed in the undifferentiated control cells (**c**), while multinucleated cells were positive for TRAP staining (**d**). *CTSK* expression increased after 5 days of osteoclastogenic stimuli (**e**).

Arrowheads indicate nuclei in osteoclast-like hematopoietic cells. T-test ** $p<0.01$. Augmentation 400x. Scale bar: 50 µm.

1.3.2. Calcitriol supplementation increases osteoclast differentiation

We evaluated a physiological (10^{-11} M) and supraphysiological (10^{-9} M) concentrations of CTR during osteoclast differentiation of bone marrow hematopoietic cells and we observed that CTR supplementation increased the expression of *CTSK* as compared with osteoclasts (OC), consistent with a higher number of multinucleated TRAP positive cells (Fig.41).

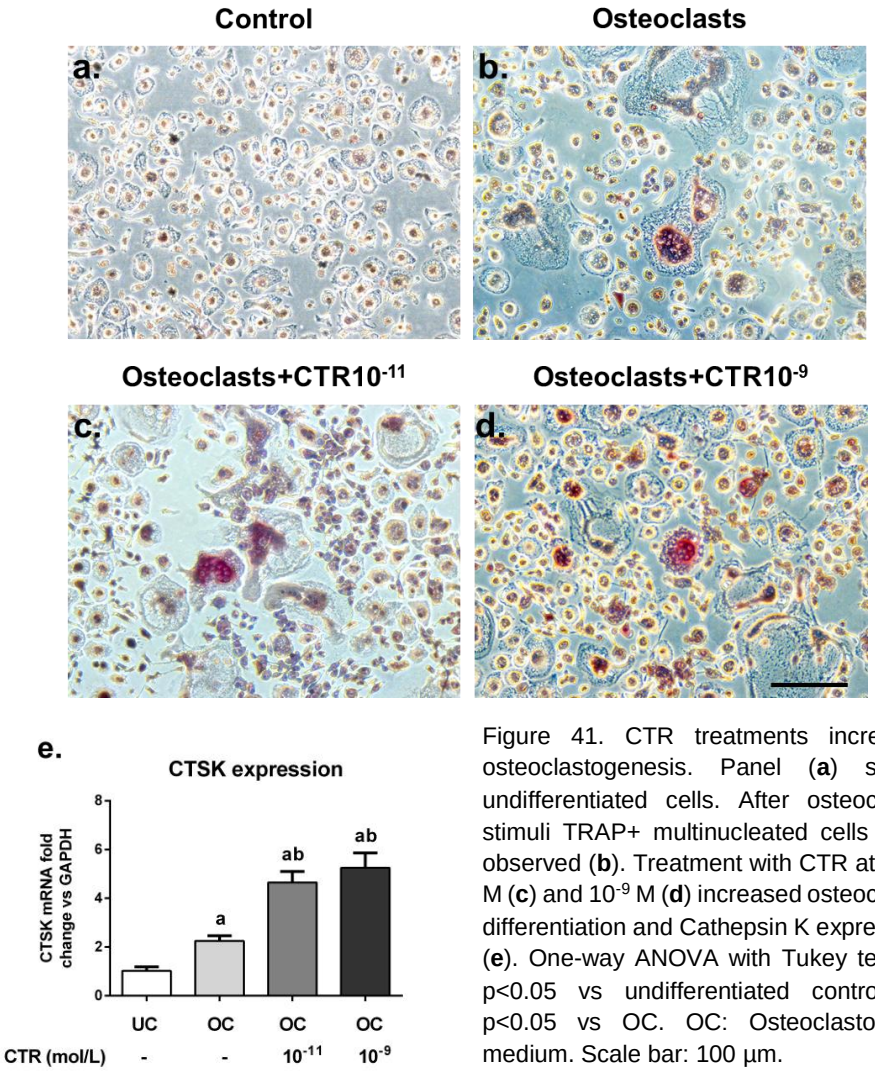

Figure 41. CTR treatments increased osteoclastogenesis. Panel (**a**) shows undifferentiated cells. After osteoclastic stimuli TRAP+ multinucleated cells were observed (**b**). Treatment with CTR at 10^{-11} M (**c**) and 10^{-9} M (**d**) increased osteoclastic differentiation and Cathepsin K expression (**e**). One-way ANOVA with Tukey test. a: $p<0.05$ vs undifferentiated control; b: $p<0.05$ vs OC. OC: Osteoclastogenic medium. Scale bar: 100 µm.

SECTION 2: CALCIMIMETIC

2.1. *PTH-INDEPENDENT EFFECTS OF CALCIMIMETIC: IN VIVO STUDIES*

To separate the specific bone effects of calcimimetic from those triggered by the treatment decreasing PTH levels, we used rats that underwent total parathyroidectomy with PTH replacement to maintain blood calcium. After 28 days, animals were sacrificed and blood and bone (femurs) samples were collected for biochemical and bone histomorphometric analysis.

2.1.1. Plasma biochemistry of rats with clamped PTH and normal renal function treated with calcimimetic

Biochemical data are shown in Table 12. PTx rats showed lower plasma iCa and higher P levels than sham-operated rats ($^{a}p<0.05$). PTH replacement (PTx-PTH) restored plasma iCa and P concentration to normal levels. The administration of calcimimetic (PTx-PTH-CM) did not modify plasma iCa and P levels significantly, however plasma calcium showed a tendency to decrease as compared with the PTx-PTH group. Plasma 1,25(OH)2D3 levels were similar among Sham, PTx and PTx-PTH groups, however PTx-PTH-CM rats showed significantly higher levels of 1,25(OH)2D3 than this other groups ($^{abc}p<0.05$ vs all groups). Plasma intact FGF23 concentration was decreased in PTx rats as compared with Sham; and PTH replacement increased FGF23 concentration. PTx-PTH-CM group showed significantly lower plasma FGF23 concentration than PTx-PTH rats.

	Sham	PTx	PTx-PTH	PTx-PTH-CM
	n=6	n=7	n=5	n=6
iCa (mM)	1.21±0.02	0.59±0.02 [a]	1.13±0.04	1.07±0.04
P (mg/dl)	6.2±0.2	11.6±0.9 [a]	5.6±0.4 [b]	5.4±0.6 [b]
$1,25(OH)_2D_3$ (pg/ml)	192±35	126±20	163±25	252±30 [a,b,c]
FGF23 (pg/ml)	130±34	68±6[a]	129±20 [b]	88±13 [c]

Table 12. Plasma biochemistry of rats with normal renal function. One-way ANOVA with Tukey test. a: p<0.05 vs Sham; b: p<0.05 vs PTx; c: p<0.05 vs PTx-PTH.

2.1.2. Calcimimetic effects in bone histomorphometry of rats with clamped PTH and normal renal function

Bone volume (BV/TV) was similar in all groups (Fig.42 **a**). In PTx rats, the osteoid volume, osteoid surface and bone surface covered by osteoblasts (OV/BV, OS/BS and Ob.S/BS respectively) were significantly reduced as compared with the Sham group (Fig.42 **b**, **c** and **d** respectively). In addition, the bone surface covered by osteoclast was decreased in comparison with Sham rats (Fig.42 **f**) without changes in the eroded surface (Fig.42 **e**). PTH replacement (PTx-PTH) restored bone histomorphometric parameters to values similar than those found in sham-operated animals. The administration of CM (PTx-PTH-CM) did not alter bone parameters as compared with Sham and PTx-PTH, however a tendency to increase the osteoblast surface and activity was observed.

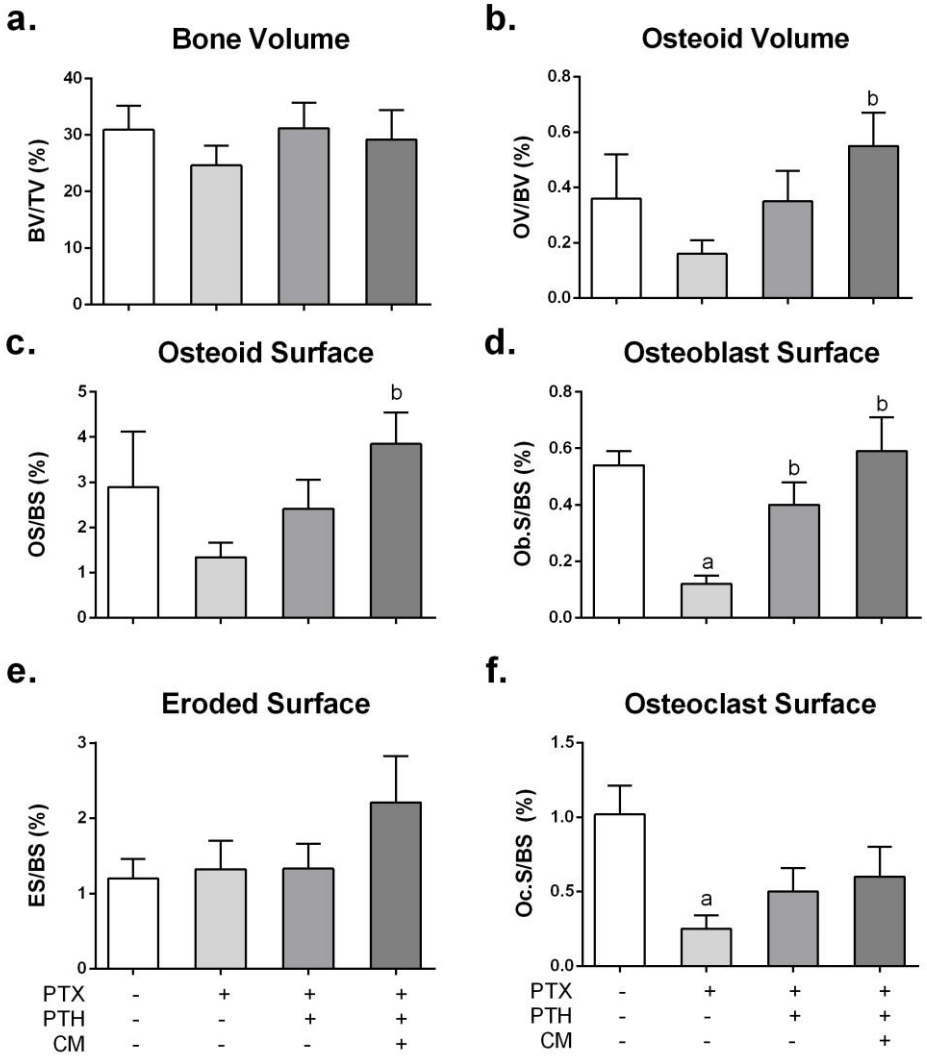

Figure 42. Bone histomorphometry parameters in rats with normal renal function. One-way ANOVA with Tukey test. a: $p<0.05$ vs Sham; b: $p<0.05$ vs PTx. Rats fed a 0.6%P, 0.6%Ca diet.

2.1.3. Effects of calcimimetic administration on bone in rats with renal insufficiency and clamped PTH

As shown in Table 13, plasma concentration of creatinine was increased significantly in all 5/6Nx groups as compared with Sham rats ($^{a}p<0.05$) with no differences among the other 5/6Nx groups. Plasma P, intact PTH and intact FGF23 concentration increased also in 5/6Nx rats as compared with Sham while plasma iCa levels decreased ($^{a}p<0.05$). CM administration to 5/6Nx animals, decreased plasma intact PTH, $1,25(OH)_2D_3$ and intact FGF23 concentration as compared with 5/6Nx group. In 5/6Nx rats with PTx, the PTH infusion in an amount 6-fold the normal replacement dose (5/6Nx-PTx-PTHx6) was sufficient to maintain plasma Ca and P at levels similar to those in 5/6Nx rats. The treatment with CM in 5/6Nx-PTx-PTHx6 rats (5/6Nx-PTx-PTHx6-CM) did not affect the plasma Ca concentration, and plasma biochemistry was similar to the 5/6Nx-PTx-PTHx6 group. PTH replacement by 9-fold induced a significant increase in plasma iCa and intact FGF23 concentrations as compared with 5/6Nx-PTx-PTHx6 group, while plasma $1,25(OH)_2D_3$, and P levels remained similar to those with PTH replacement by 6-fold. CM administration did not alter plasma biochemistry between both 5/6Nx-PTx-PTHx9 groups. The amount of plasma PTH 1-34 in the 5/6Nx-PTx-PTHx6 groups was significantly lower than in 5/6Nx rats. PTH replacement by 9-fold increased significantly the plasma concentration of PTH 1-34 as compared with 5/6Nx and 5/6Nx-PTx-PTHx6 groups ($p<0.01$).

	Sham n=6	**5/6Nx** n=7	**5/6Nx-CM** n=6	**5/6Nx-PTx-PTHx6** n=8	**5/6Nx-PTx-PTHx6-CM** n=5	**5/6Nx-PTx-PTHx9** n=5	**5/6Nx-PTx-PTHx9-CM** n=6
Creat (mg/dl)	0.49±0.03	0.88±0.06 [a]	0.9±0.05 [a]	0.91±0.03	0.9±0.05	0.9±0.05	0.85±0.04
iCa (mM)	1.21±0.02	1.10±0.02 [a]	1.00±0.02 [a]	1.02±0.03 [a]	1.08±0.06	1.15±0.07	1.17±0.06
P (mg/dl)	6.2±0.2	8.73±0.39 [a]	7.35±0.32 [a]	7.77±0.43	6.32±0.40	7.58±0.80	7.94±0.76
Intact PTH (pg/ml)	47±4.4	540±96 [a]	144±40 [a,b]	n.a	n.a	n.a	n.a
PTH 1-34 (pg/ml)	-	386±44	-	304±23	295±12	541±63	599±56
$1,25(OH)_2D_3$ (pg/ml)	192±35	159±18	131±9.0 [a]	162±10	158±7	153±17	152±22
FGF23 (pg/ml)	130±31	1522±217 [a]	826±178 [a,b]	471±105	491±87	1209±280	1005±140

Table 13. Plasma biochemistry. Values are mean±SEM. T-test between paired treatments. a: $p<0.05$ vs sham, b: $p<0.05$ vs 5/6Nx. n.a.: infused PTH not recognized by the intact PTH assay. Sham rats fed a 0.6%P, 0.6%Ca diet. 5/6Nx groups fed a 0.9%P, 0.6%Ca diet.

2.1.4. PTH-independent effects of calcimimetic in bone histomorphometry in uremic rats

5/6Nx rats showed a significant reduction in BV/TV as compared with the sham group ($p<0.001$, Fig.43 **a**) and increased bone cell activity (Fig.43 **b**-**h**). Bone histomorphometric parameters in 5/6Nx rats treated with CM did not differ significantly from those in the 5/6Nx group treated with vehicle. 5/6Nx-PTx-PTHx6 rats showed lower bone cell activity than the 5/6Nx group as assessed by the OS/BS, Ob.S/BS, ES/BS and Oc.S/BS (Fig.43 **c**, **d**, **e** and **f** respectively). In these conditions of relatively low PTH replacement (5/6Nx-PTx-PTHx6), CM administration increased significantly the osteoid surface (23.3±1.27 vs 13.9±2.39 %, $p<0.05$) and the bone surface covered by osteoblasts (11.7±1.44 vs 4.35±0.46, $p<0.05$). Similarly, in comparison with 5/6Nx-PTx-PTHx6, CM also increased the bone formation rate and mineralizing surface (Fig.43 **g** and **h** respectively). In parathyroidectomized 5/6Nx rats with PTH replacement by 9-fold the normal dose, bone turnover was higher than in 5/6Nx-PTx-PTHx6 rats and similar to 5/6Nx group. With the highest PTH infusion, the osteoanabolic action of calcimimetic was not observed, being the bone histomorphometric parameters similar between both 5/6Nx-PTx-PTHx9 groups.

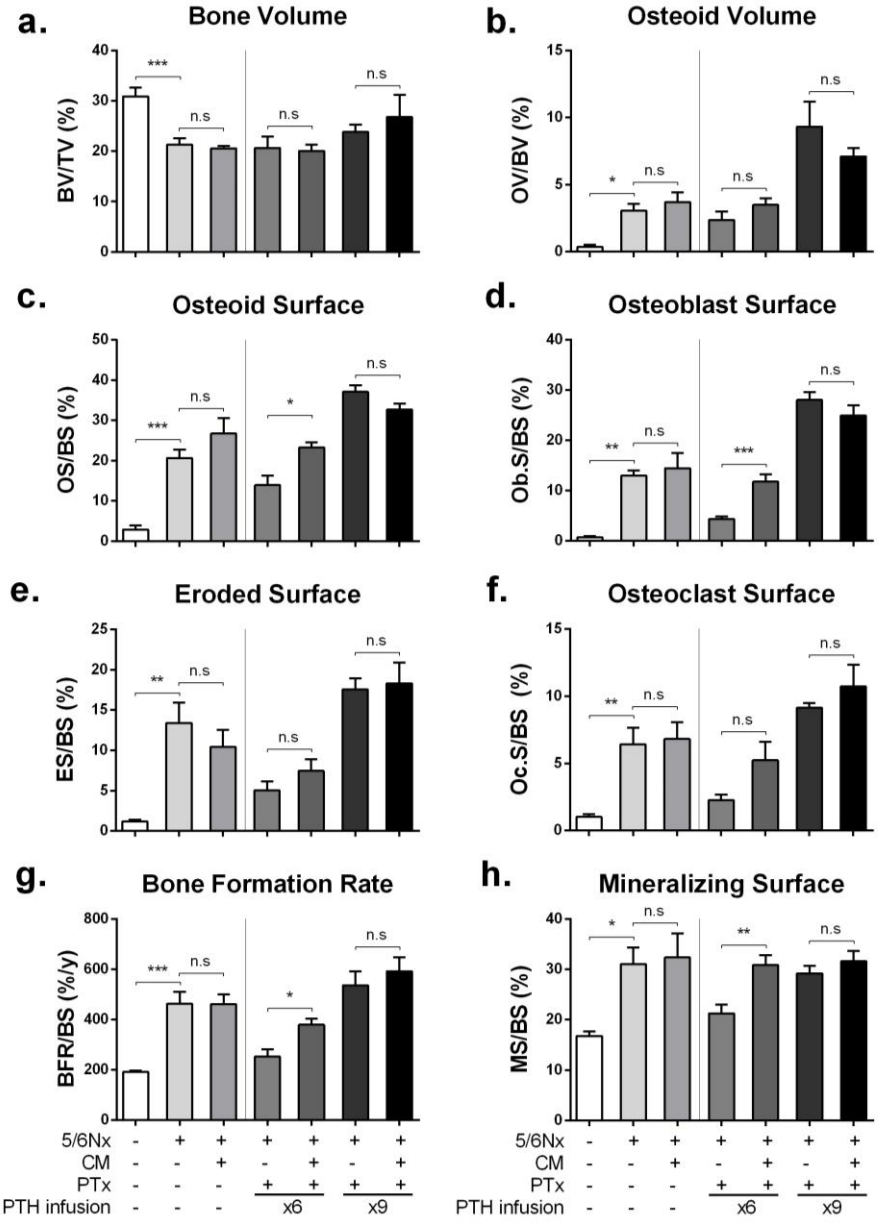

Figure 43. Bone histomorphometry in 5/6Nx rats with clamped PTH and calcimimetic treatment. Bars show mean±SEM. T-test. *: p<0.05; **: p<0.01; ***: p<0.001; n.s: no significant differences.

5/6Nx animals showed higher mineral apposition rate and mineralization lag time (Fig.44 **c** and **e**) and lower mineralizing surface related to osteoid surface and adjusted apposition rate (Fig.44 **b** and **d**) than Sham rats ($p<0.05$). However, CM administration did not induce significant changes in osteoid thickness, mineralizing surface related to osteoid Surface, mineral apposition rate, adjusted apposition rate, mineralization lag time or osteoid maturation time as compared with the corresponding vehicle treatment (Fig.44 **a**-**f**).

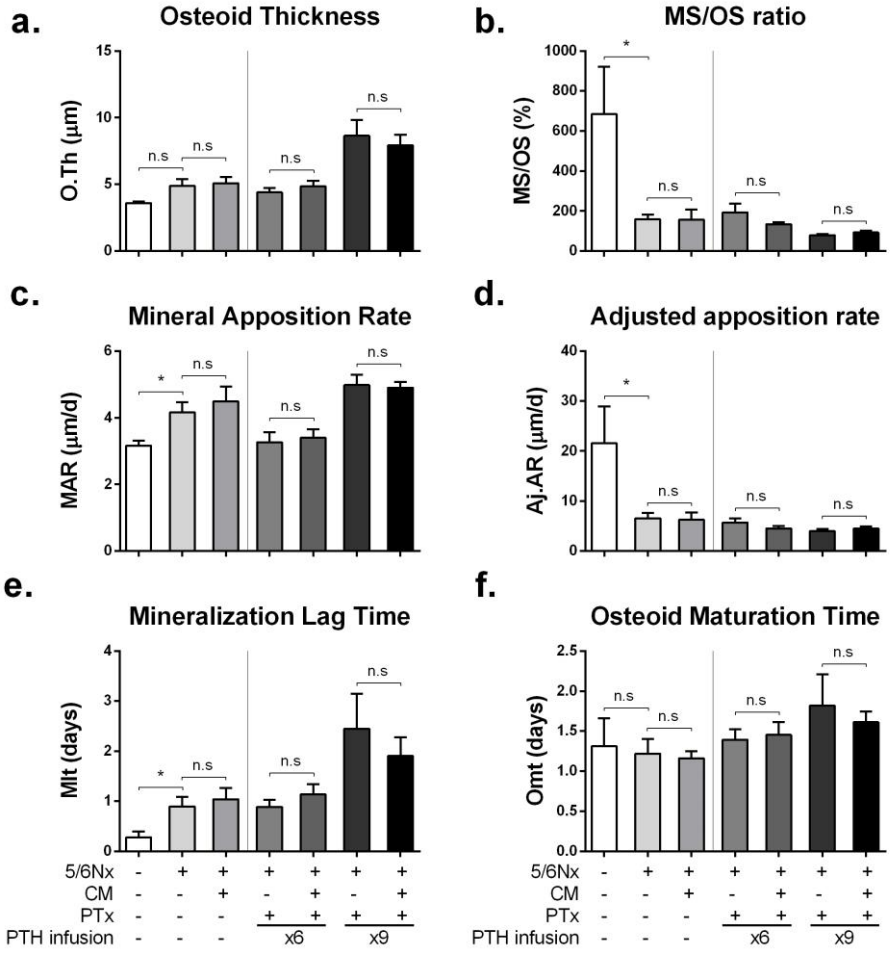

Figure 44. Bone histomorphometry. Mineralization indices in 5/6Nx rats with clamped PTH and CM treatment. Bars show mean±SEM. T-test. *: $p<0.05$; n.s: non-significant.

Representative samples of Goldner's trichrome staining of the undecalcified bone histology from the seven groups of rats are also shown in Figure 45.

As CaSR activation triggers ERK1/2 phosphorylation, we investigated the CaSR downstream signaling in bone cells and we found that rats receiving CM showed increased phosphorylation of ERK1/2 in the osteoblasts, indicating a potential activation of the CaSR. ERK1/2 phosphorylation was observed in both, cytoplasm and nuclei of osteoblasts (Fig.46 and 47).

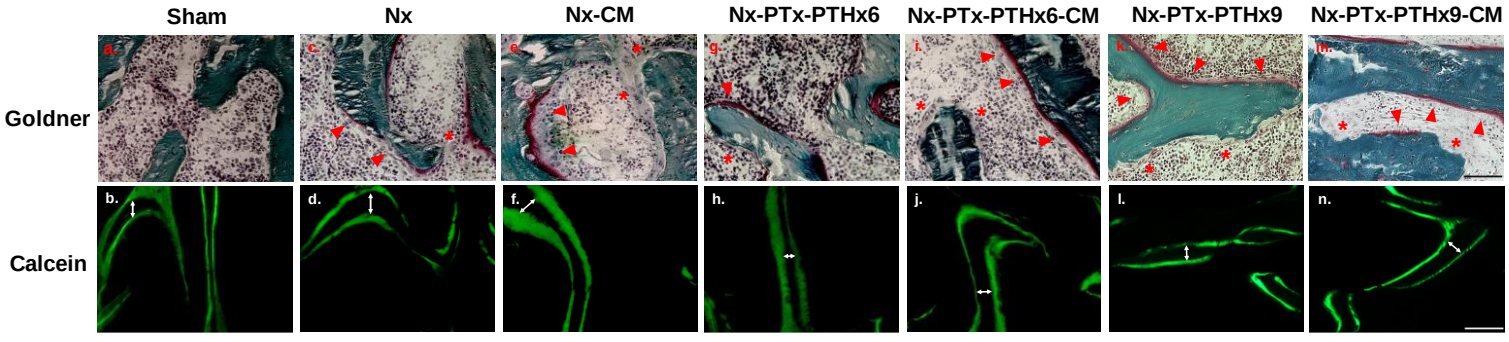

Figure 45. Representative photographs of Goldner's trichrome staining and double calcein labeling in trabecular bone. In Sham animals, an almost quiescent state of bone cells was observed (**a**), with normal mineralization (**b**). In 5/6Nx rats, an increase in bone cell activity was observed (**c**), accompanied by an increase in bone formation (**d**). 5/6Nx rats treated with CM maintained a similar bone cell activity (**e**) and mineralization (**f**) than 5/6Nx rats. In Nx-PTx-PTHx6 animals, was detected a low bone turnover (**g**) and bone formation (**h**) respect to 5/6Nx group. Treatment with CM increased the number of osteoblasts and osteoclasts (**i**) as well as mineralization and bone formation (**j**). In Nx-PTx-PTHx9 group was observed a similar bone turnover (**k**) and mineralization (**l**) than 5/6Nx group. In 5/6Nx-PTX-PTHx9 plus CM, bone cells activity (**m**) and bone formation (**n**) were similar to those observed in the 5/6Nx-PTX-PTHx9. Double-head arrows show the bone distance between both calcein labels (time interval: 7 days). Magnification: 200x. Scale bar: 100µm. Ob: Osteoblasts. Arrowheads: Osteoclasts.

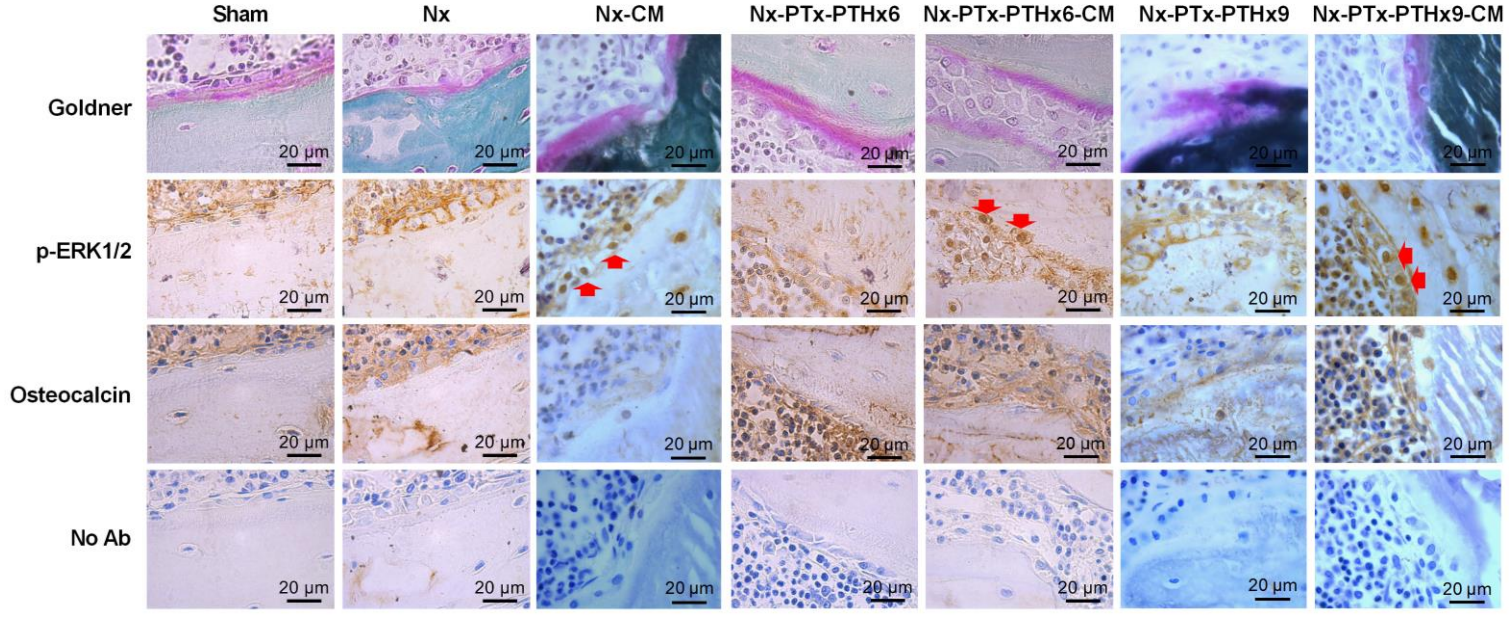

Figure 46. The administration of CM triggered Erk1/2 phosphorylation in osteoblasts. Goldner's staining of undecalcified bone sections shows cuboidal osteoblasts covering osteoid on the bone surface. Immunohistochemistry for phospho-Erk1/2 showed intense nuclear staining in osteoblasts in the Nx-CM, Nx-PTx-PTHx6-CM and Nx-PTx-PTHx9-CM groups and scarce nuclear staining in the bone cells of the other groups. To determine that the target cells are osteoblasts, serial undecalcified bone sections were also stained for osteocalcin. Running the immunohistochemistry without primary antibody in undecalcified bone samples showed no positive staining. Arrowheads indicate nuclear phospho-Erk1/2. Magnification 1000x. Scale bar: 20µm.

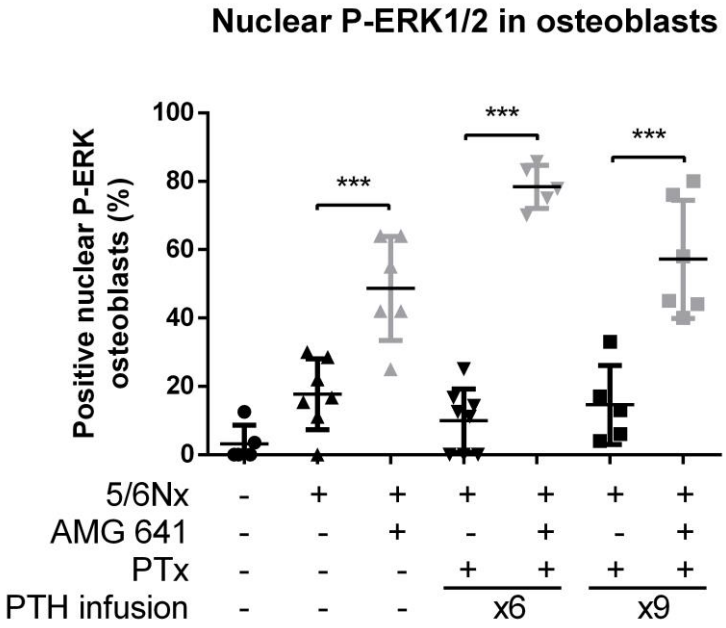

Fig 47. Osteoblasts with positive phospho-Erk1/2 staining were counted in 3 random fields of each sample and were expressed as the percentage of total osteoblasts. T-test. *** $p<0.001$.

2.2. *IN VITRO STUDY OF THE CALCIMIMETIC EFFECT ON OSTEOBLASTS*

To further confirm the direct actions of CaSR in bone cells, we studied the effects of CaSR allosteric modulation by calcimimetic and calcilytic drugs in *in vitro* models of osteoblasts.

2.2.1. Effects of the modulation of CaSR by calcimimetic and calcilytic in UMR-106 cells

To evaluate the direct effect of the positive allosteric modulation of CaSR on the osteoblastic phenotype of cell line UMR106, CM was added in the medium with a low Ca^{2+} concentration, which in turn mimics the *in vivo* effects of CM decreasing PTH with the resulting decrease in plasma Ca^{2+} concentration. Firstly, the presence of CaSR in UMR106 was proven by western blot and the addition of CM did not affect its expression (Fig.48 **a**). CaSR activation by CM led to an increase in ERK1/2 phosphorylation (Fig.48 **b**), demonstrating that CaSR is functional and modulated by CM. After 48 hours of treatment, CM administration (100μM) significantly increased ($^{a}p<0.05$ vs all groups) the expression of the osteogenic markers *Runx2*, *Osterix* and *Osteocalcin* (Fig.48 **c**, **d** and **e** respectively).

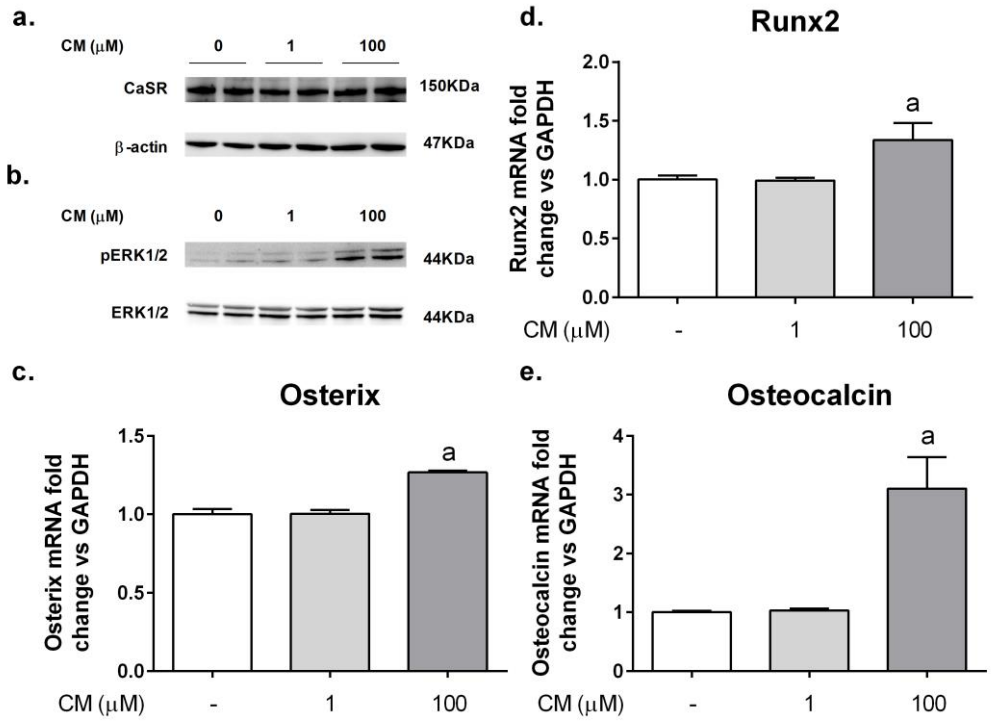

Figure 48. CM addition activated CaSR downstream signaling and up-regulated osteogenic marker genes expression. Western blots of total protein extracts showed positive expression of CaSR in UMR106 cells (**a**) and induced ERK1/2 phosphorylation (**b**). The gene expression of Runx2 (**c**), Osterix (**c**) and osteocalcin (**e**) were up-regulated with the dose of 100 μM of CM. Bars show mean±SEM. ANOVA with Tukey test. a: $p<0.05$ vs all groups. $[Ca^{2+}]=0.5mM$.

At contrary, the administration of the calcilytic Calhex 231 to UMR-106 cells inhibited the MAPK pathway, as assess by the reduction in ERK1/2 phosphorylation (Fig.49 **a**). The decrease in the CaSR signaling was also accompanied by a down-regulation in the expression of the osteogenic genes *Runx2*, *Osterix* and *Osteocalcin* (Fig.49 **b**, **c** and **d** respectively).

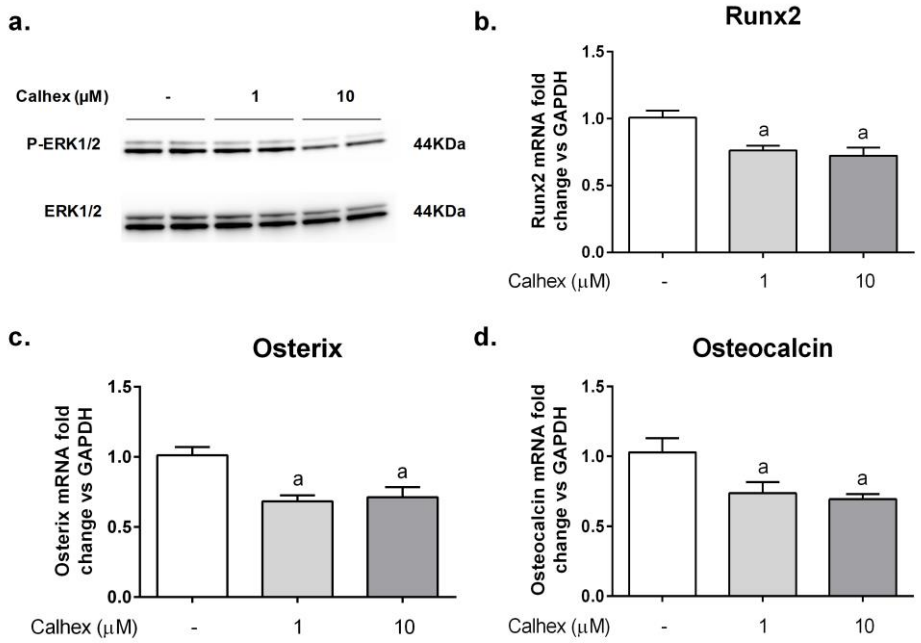

Figure 49. Treatment with calcilytic decreased osteogenic genes expression in UMR-106 cells. ERK1/2 phosphorylation was reduced by the treatment with Calhex 231 **(a)**. CaSR inhibition with Calhex 231 induced a down-regulation of *Runx2* (**b**), *Osterix* (**c**) and *Osteocalcin* (**d**). Bars show mean±SEM. ANOVA with Tukey test. a<0.05 vs Control. $[Ca^{2+}]$=1.8 mM.

2.2.2. Effects of calcimimetic on osteoblastic differentiation and mineralization of human MSC

Human bone marrow mesenchymal stem cells (MSC) were differentiated into osteoblasts in a medium with a low Ca^{2+} concentration (Ca 0.5 mM). Results show that CaSR was constitutively expressed in MSC (Fig.50 **a**). After 21 days, Ca^{2+} deposition (Fig.50 **b**) and the number of calcification nodules (Fig.50 **c**) were increased in osteoblasts cultured with CM.

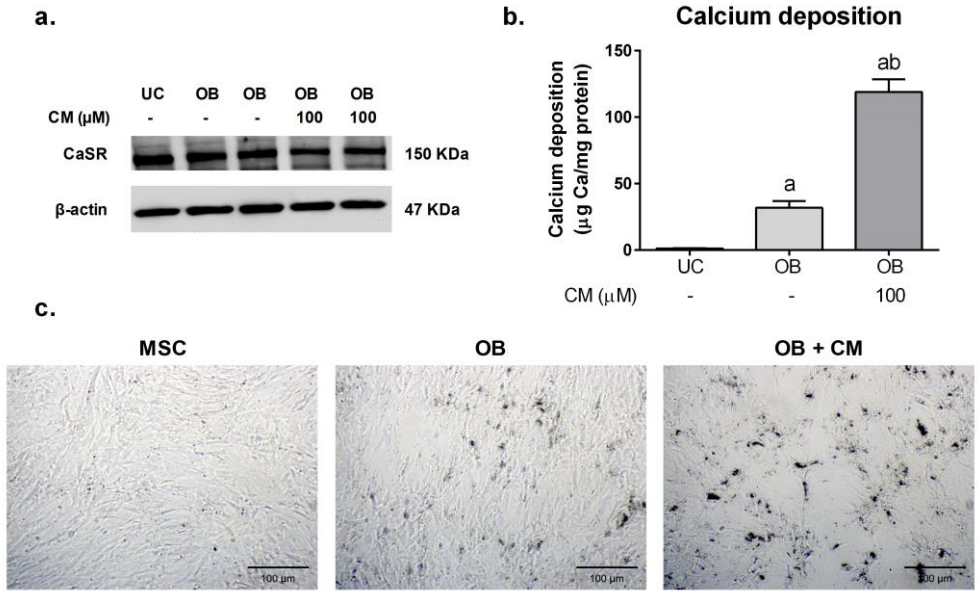

Figure 50. CM (100 μM) increases calcification of human MSC differentiated into osteoblasts. CaSR was expressed in MSC and Osteoblast-like MSC and CM did not significantly alter its expression (**a**). CM administration increased the calcium content in the mineralized matrix (**b**) and the number and size of the calcification nodules (**c**) after 21 days of osteogenic differentiation. One-way ANOVA with Tukey test. a: $p<0.05$ vs MSC; b: $p<0.05$ vs OB. Bars in microphotograph represent 100μm.

Consistently, the addition of CM also increased the expression of the early osteoblast markers *Runx2* and *Osterix* (Fig.51 **a** and **b** respectively) and mature genes such as

osteocalcin (Fig.51 **c**). Furthermore, CM addition enhanced the expression of *BMP2* (Fig.51 **d**), other well-known pro-osteogenic factor.

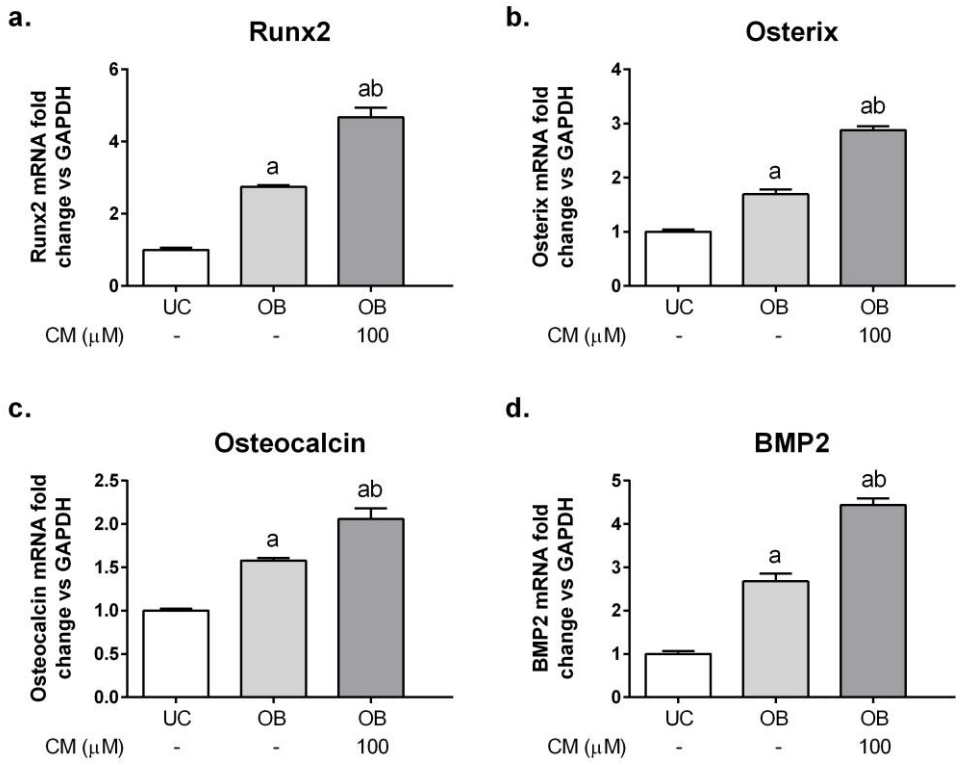

Figure 51. Treatment with CM (100 µM) increases osteogenic genes expression of MSC differentiated into osteoblasts. One-way ANOVA with Tukey test. a: $p<0.05$ vs UC; b: $p<0.05$ vs OB. UC: undifferentiated control. OB: Osteogenic medium.

2.3. *IN VITRO EFFECTS OF CALCIMIMETIC ON OSTEOCLASTOGENESIS*

The direct effects of calcimimetic administration throughout osteoclastogenesis was also studied with a low calcium (0.5 mM Ca^{2+}) in the culture medium.

2.3.1. Calcimimetic effects on osteoclastic differentiation

Firstly, we evaluated the role of different Ca^{2+} concentrations (low 0.5 mM vs normal 1.25 mM) during osteoclastogenesis of bone marrow hematopoietic stem cells. Osteoclastogenic stimuli in normal Ca^{2+} conditions produced TRAP positive multinucleated cells (Fig.52 **b**), while with low Ca^{2+} (0.5 mM) (Fig.52 **c**) were not detected significant differences in TRAP staining as compared with undifferentiated cells (Fig.52 **a**). Furthermore, despite of some cells were multinucleated, rarely cells with more than 3 nuclei were found with low Ca^{2+} condition. Similarly, the pro-osteoclastogenic stimulus did not increase the expression of *CTSK* (Fig.52 **d**), indicating that low Ca^{2+} may suppress osteoclastic differentiation.

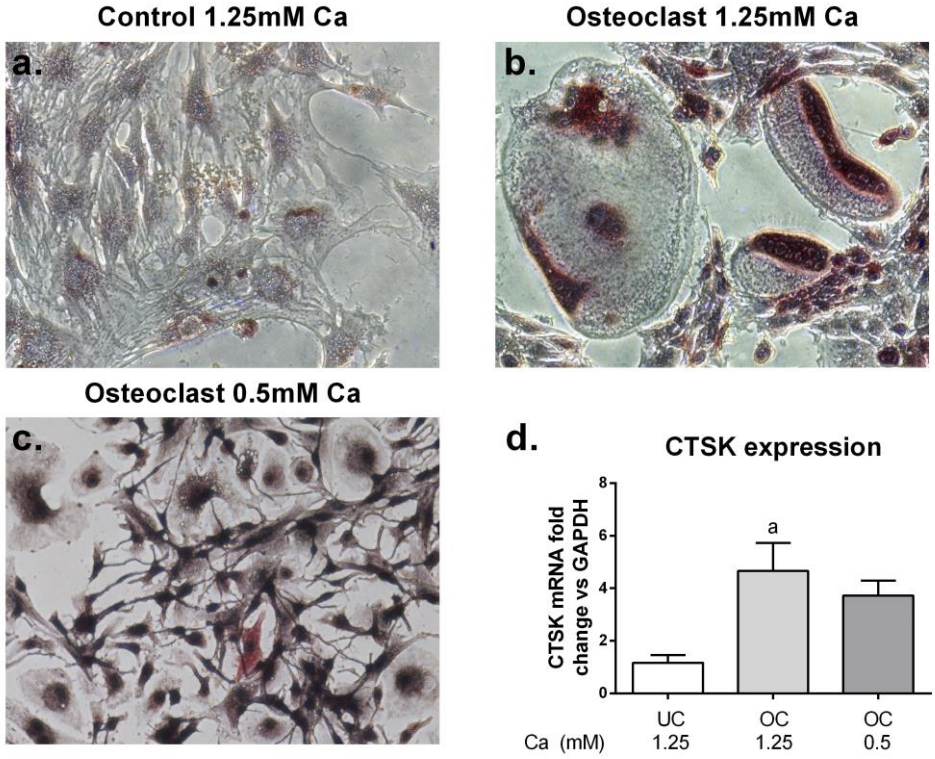

Figure 52. Effects of low calcium on osteoclastogenesis. TRAP staining was negative in undifferentiated cells (**a**) and osteoclastogenic medium induced differentiation with Ca 1.25 mM, as assessed by the increased number of multinucleated TRAP-positive cells (**b**). Low Ca prevented osteoclastic differentiation (**c**). *CTSK* expression (**d**) support these results. a: $p<0.05$ vs undifferentiated control.

Once the influence of low Ca was examined, we evaluate the effect of CM administration at 10 and 100 µM on osteoclastic differentiation. In low Ca conditions (Ca 0.5 mM), osteoclast differentiation did not induce an increase in the size of the multinucleated cells, which did not have more than 3-4 nuclei (Fig.53 **a**, **b** and **c**). Despite CM (at 100µM) significantly increased the expression of *CTSK* as compared with the group treated with osteoclastogenic medium (OC, Fig.53 **d**), CTSK expression was not more increased than in undifferentiated cells.

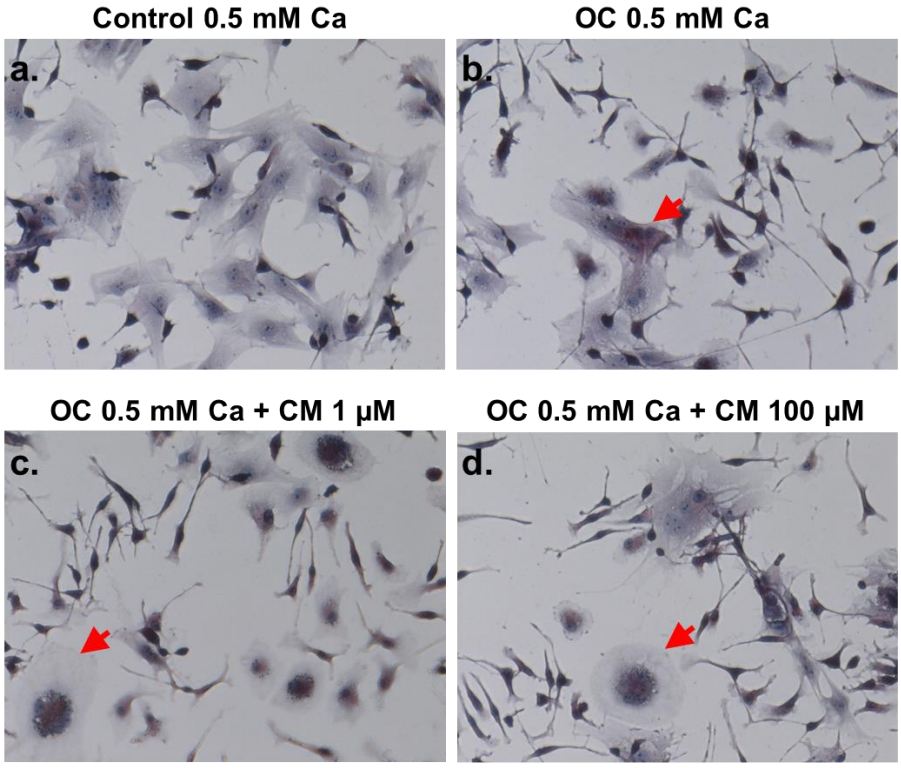

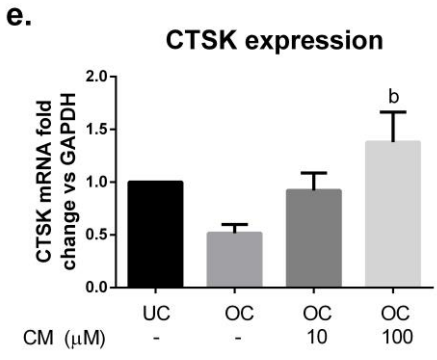

Figure 53. Effect of CM on osteoclastic differentiation of hematopoietic cells in low Ca^{2+} conditions. Control cells were TRAP negative and mononuclear cells (**a**). A scarce TRAP staining was observed in multinucleated cells, with no more than 3-4 nuclei (**b**). Treatment with CM by 10 (**c**) and 100 µM (**d**) did not induce significant differences in the number or intensity of TRAP-positive cells after 5 days. The expression of *CTSK* in osteoclasts was significantly increased with CM at 100 µM (**e**). C*TSK* expression was quantified in three replicas. OC: osteoclastogenic medium. b: $p<0.05$ vs OC. Arrows: osteoclasts.

SECTION 3: MAGNESIUM

3.1. *IN VIVO STUDY OF THE EFFECTS OF DIETARY MAGNESIUM SUPLEMENTATION ON BONE*

Despite the beneficial effects of Mg supplementation in renal disease had been reported in the last decades, there exist controversy about the actions of Mg on bone cells *in vitro* and *in vivo*. In this part of the results, the effects of dietary Mg supplementation on bone of uremic rats were examined.

3.1.1. Plasma biochemistry

5/6Nx rats were fed on diets with increased Mg content (0.1%, 0.3% and 0.6%) for 14 days. At the moment of sacrifice all animals with 5/6Nx showed a lower body weight than sham rats without significant differences among them. Plasma biochemistry is shown in Table 14. The reduction of the renal mass in the 5/6Nx groups produced an increase in plasma creatinine levels as compared with the Sham group. Both Mg-supplemented diets prevented the increase in plasma creatinine levels, suggesting a protective renal effect of dietary Mg. The levels of plasma Mg increased in 5/6Nx rats as compared with Sham rats and significantly increased according to the Mg content in the diet although it was statistically significant alone with 0.6% Mg diet. Plasma P was increased in 5/6Nx rats fed on 0.1% Mg diet as compared with Sham animals. In comparison with these 5/6Nx rats, both 0.3% and 0.6% Mg diets, decreased plasma P levels. In addition, iCa concentration was decreased in 5/6Nx rats as compared with Sham rats and 0.3% Mg showed similar iCa levels to those observed in Sham rats. Plasma PTH concentration was increased in the 5/6Nx+0.1% Mg group as compared with the Sham group. Rats on dietary Mg supplementation showed lower plasma PTH levels than 5/6Nx + 0.1% Mg, which were statistically significant with a 0.6% Mg diet. CTR concentration was reduced in all 5/6Nx groups as compared with Sham animals without significant changes among them and Mg diets. Plasma intact FGF23 increased in 5/6Nx+0.1% Mg as compared

with Sham; lower levels of FGF23 were found in 5/6Nx rats fed on Mg supplementation.

	Sham n=10	**5/6Nx+0.1% Mg** n=14	**5/6Nx+0.3% Mg** n=10	**5/6Nx+0.6% Mg** n=10
Body Weight (g)	306±34	235±40 [a]	242±20 [a]	236±31 [a]
Creat (mg/dl)	0.41±0.06	1.71±0.2 [a]	1.11±0.12 [a,b]	1.10±0.16 [a,b]
Mg (mg(dl)	2.14±0.09	2.97±0.3 [a]	2.98±0.2 [a,b]	3.31±0.4 [a,b]
P (mg/dl)	6.5±0.3	10.7±1.4 [a]	8.0±0.8 [a,b]	7.9±0.9 [a,b]
iCa (mM)	1.20±0.01	1.07±0.03 [a]	1.19±0.02 [b]	1.13±0.03 [a,b]
PTH (pg/ml)	21±7	529±171 [a]	401±170 [a]	79±46 [a,b]
1,25(OH)2D3 (pg/ml)	318±29	110±23 [a]	120±25 [a]	89±25 [a]
FGF23 (pg/ml)	218±147	100311± 158105 [a]	783±814 [a,b]	16253± 9121 [a,b]

Table 14. Plasma biochemical analysis. Sham fed a 0.6% P, 0.6% Ca, 0.1% Mg diet. 5/6Nx groups fed a 1.2% P, 0.6% Ca and the indicated Mg percentage. Values show mean±SEM. ANOVA with Tukey test. [a] $p<0.05$ vs Sham; [b] $p<0.05$ vs 5/6Nx + Mg0.1%.

Urinary parameters are shown in Table 15. Consistent with plasma biochemistry, creatinine clearance decreased in 5/6Nx groups as compared with Sham, and the reduction was lower in the 5/6Nx + 0.6% Mg. Urinary calcium was similar among all 5/6Nx groups, however there was a significant increase respect to Sham animals group ($p<0.05$ vs Sham). According to plasma FGF23 and PTH levels, urinary P excretion, assessed by P/creatinine ratio and FEPi, increased in 5/6Nx + 0.1% Mg as compared with Sham animals. Dietary Mg supplementation (0.6% Mg) decreased the urinary P/Creat ratio. On the other hand, Mg content in the urine decreased in the 5/6Nx+0.1% Mg group as compared with Sham. In the 5/6Nx groups receiving Mg supplementation in the diet, urinary Mg was also increased.

	Sham n=10	5/6Nx+0.1% Mg n=14	5/6Nx+0.3% Mg n=10	5/6Nx+0.6% Mg n=10
Creat Clearance	3.25±0.30	0.57±0.11[a]	0.68±0.14 [a]	1.16±0.21 [a,b]
FEPi (%)	4.9±0.80	95.0±17.2 [a]	86.5±7.1 [b]	44.8±6.0 [a,b]
P/Creat Ratio	0.68±0.06	6.12±0.83 [a]	6.11±0.70 [a]	3.47±0.44 [b]
Mg/Creat Ratio	1.04±0.10	0.45±0.06 [a]	1.48±0.16 [a,b]	1.72±0.25 [a,b]
Ca/Creat Ratio	0.05±0.01	0.11±0.07[a]	0.18±0.03[a]	0.15±0.04[a]

Table 15. Urinary parameter analysis. a: p<0.05 vs Sham; b: p<0.05 vs 5/6Nx+Mg0.1%. Sham fed a 0.6% P, 0.6% Ca, 0.1% Mg diet. 5/6Nx groups fed a 1.2% P, 0.6% Ca and the indicated Mg percentage. ANOVA with Tukey test. [a] p<0.05 vs Sham; [b] p<0.05 vs 5/6Nx+ Mg 0.1%.

3.1.2. Bone histomorphometry

Cancellous bone histomorphometry parameters were studied in the distal right femurs. We found that with respect to Sham animals, bone volume was decreased in 5/6Nx+0.1% Mg. Importantly, dietary Mg supplementation by 0.6% significantly prevented this loss of bone volume (Fig.54 **a**). Respect to Sham animals, osteoid volume and osteoid surface were also increased in 5/6Nx rats fed on basal Mg in the diet (0.1% Mg). Mg supplementation by 0.3% reduced both osteoid volume and osteoid surface. However, 5/6Nx rats fed on 0.6% Mg showed similar osteoid volume and osteoid surface than the 5/6Nx+0.1% Mg group (Fig.54 **b** and **c**). The high osteoid observed in the 5/6Nx+0.6% Mg was also associated with an increase in the osteoid thickness, suggesting that high Mg content in the diet might reduce bone mineralization (Fig.54 **d**). Bone turnover in 5/6Nx+0.1% Mg was higher than in Sham rats. The bone surface covered by osteoblasts was similar among all the 5/6Nx groups, (Fig.54 **e**). Additionally, the bone surface covered by osteoclasts was reduced in the 5/6Nx+0.6% Mg as compared with both, 5/6Nx+0.1% Mg and 5/6Nx+0.3% Mg groups (Fig.54 **f**).

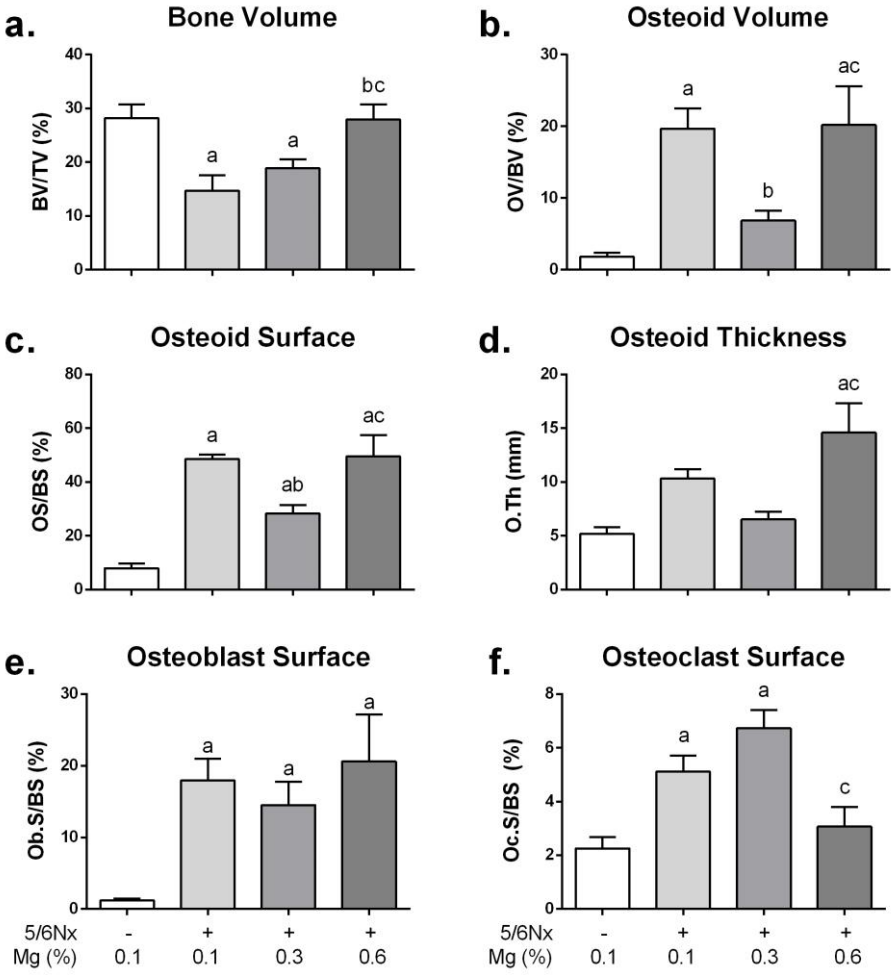

Figure 54. Dietary Mg alters bone histomorphometric parameters in 5/6Nx rats. a: $p<0.05$ vs Sham; b: $p<0.05$ vs Nx+0.1% Mg; c: $p<0.05$ vs Nx+0.3% Mg. Sham fed a 0.6% P, 0.6% Ca, 0.1% Mg diet. 5/6Nx groups fed a 1.2% P, 0.6% Ca and the indicated Mg percentage.

Goldner's trichrome representative pictures are shown in the Figure 55.

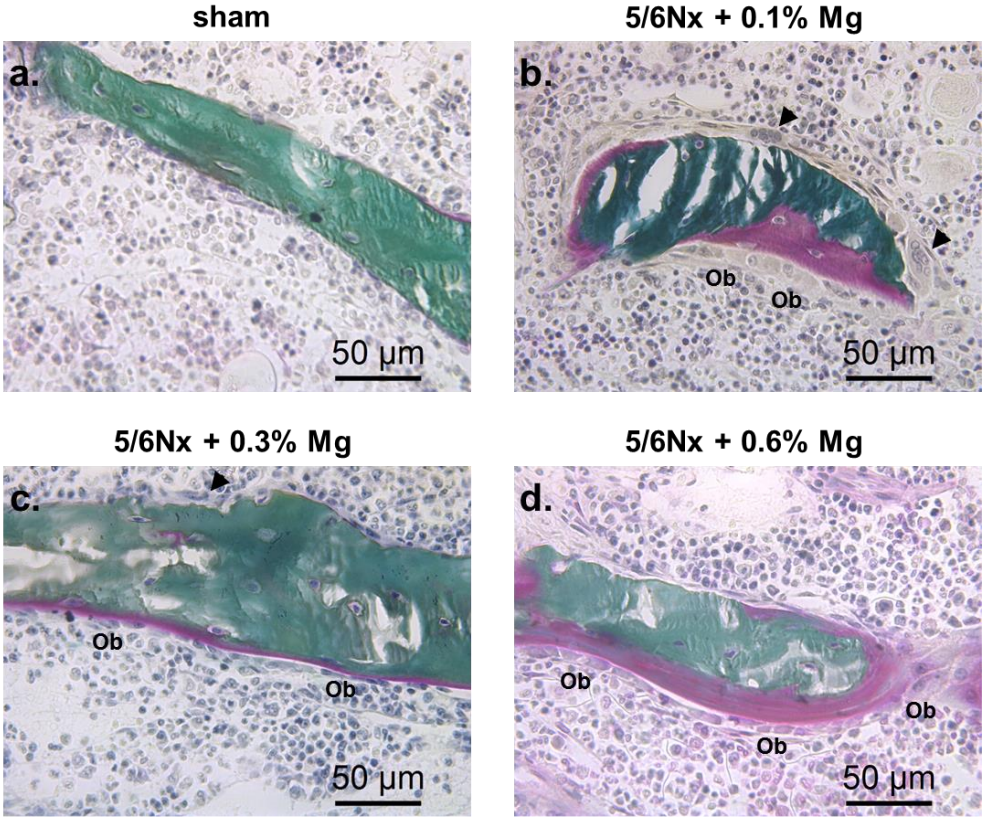

Figure 55. Effect of Mg suplementation on bone. Representative pictures of Goldner's trichrome staining. Sham fed on a 0.6% P, 0.6% Ca and 0.1% Mg diet showed normal bone turnover (**a**). 5/6Nx group fed on a 1.2% P, 0.6% Ca and 0.1% Mg showed increased number of osteoblasts (Ob) and osteoclasts (arrowhead), and increased osteoid and resorption surface (**b**). 5/6Nx rats on 0.3% Mg showed a decrease in osteoid volume (**c**) and dietary Mg by 0.6% resulted in an increased osteoid thickness (**d**). Arrowhead: Osteoclast. Ob: Osteoblasts. Magnification: 400x.

3.2. *IN VITRO STUDY OF THE EFFECTS OF MAGNESIUM ON OSTEOGENIC DIFFERENTIATION*

To examine the direct actions of Mg supplementation in bone cell differentiation and activity we used an *in vitro* model of osteogenesis. Thus, bone marrow MSC (from adherent fraction) were differentiated into osteoblasts. In addition, Mg content in the

culture medium was increased with $MgCl_2$ up to 1.2 or 1.8 mM. Basal Mg in the culture medium is 0.8 mM.

3.2.1. Effects of moderately high concentrations of magnesium on osteogenesis and mineralization of rat bone marrow MSC

After the addition of osteogenic stimuli for 21 days, MSC displayed osteoblast phenotype increasing the expression of osteogenic marker genes. Osteogenic medium supplementation with Mg^{2+} at 1.2 mM increased ALP activity by 4.2-fold while the addition of Mg^{2+} 1.8 mM elevated this activity by 6-fold vs basal Mg content (0.8 mM) (Fig.56 **a**). The increased ALP activity was consistent with higher matrix mineralization, assessed by Alizarin Red staining (Fig.56 **b**).

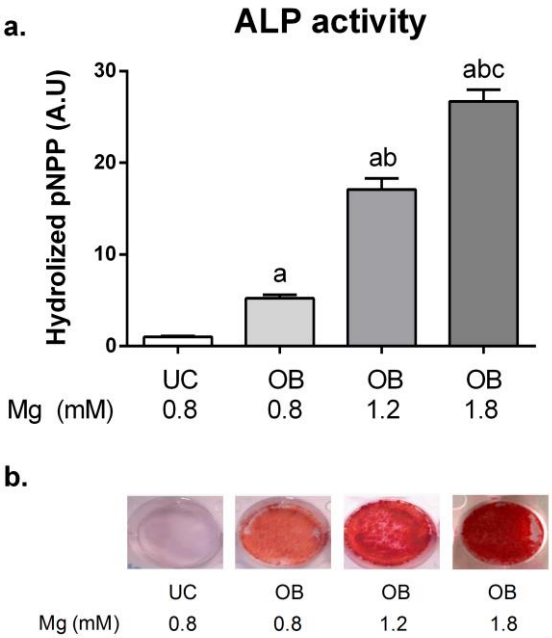

Figure 56. $MgCl_2$ supplementation increases mineralization of MSC differentiated into osteoblasts. Alkaline Phosphatase activity (**a**) was increased according to Mg concentration, as well as mineralization assessed by alizarin red staining (**b**). ANOVA with Tukey test. a: $p<0.001$ vs UC; b: $p<0.001$ vs OB; c: $p<0.001$ vs OB 1.2. UC: Undifferentiated control. OB: MSC under osteogenic stimuli for 21 days.
pNPP: p-nitrophenyl phosphate. A.U.: arbitrary units.

In addition to an increased mineralization, $MgCl_2$ supplementation achieved a significant increase in the expression of the osteogenic master genes such as *Runx2*, regulator of the early osteoblast differentiation, *Osterix*, transcription factor required for the transition of pre-osteoblasts to osteoblasts, and *Osteocalcin*, produced by mature osteoblasts (Fig.57 **a**, **b** and **c** respectively). These effects of $MgCl_2$ on MSC osteogenesis were observed in dose-dependently.

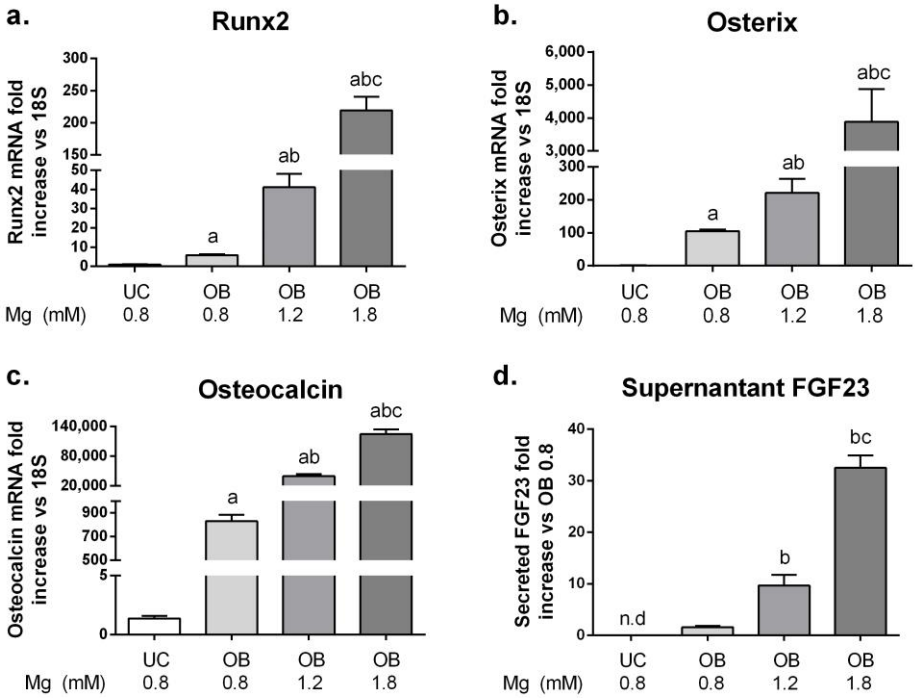

Figure 57. $MgCl_2$ increases the expression of osteogenic markers. The treatment with Mg up-regulated the expression of Runx2 (**a**), Osterix (**b**) and Osteocalcin (**c**), as well as the concentration of intact FGF23 in the supernantant. ANOVA with Tukey test. a: $p<0.001$ vs UC; b: $p<0.001$ vs OB; c: $p<0.001$ vs OB 1.2. UC: Undifferentiated control. OB: MSC under osteogenic stimuli for 21 days. n.d: non-detected.

As FGF23 is released by mature osteoblasts and osteocytes, the amount of intact FGF23 in the supernatant could be also considered as a marker of osteoblast maturation. Culture medium with treatments was replaced and after 24h, supernatant was collected to determine FGF23 secretion during 24h after 21 days

of osteogenic differentiation. As expected, undifferentiated cells did not secrete FGF23. In differentiated MSC into osteoblasts there was a light increase in the FGF23 secretion and after $MgCl_2$ supplementation (1.2 and 1.8 mM) there was significant higher levels of FGF23 in the supernatant as compared with those osteoblasts cultured with basal Mg levels (Fig.57 **d**).

3.2.2. Effects of the inhibition of magnesium transporters TRPM7 on osteogenic differentiation of MSC

The inhibition of the Mg transporter TRPM7 by 2-APB produced a decrease in ALP activity (Fig.58 **a**) accompanied with a reduction of matrix calcification (Fig.58 **b**).

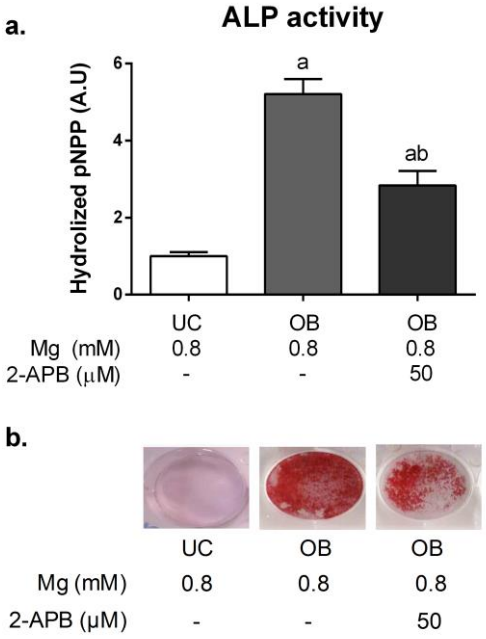

Figure 58. Inhibition of the Mg channel TRPM7 with 2-APB decreases mineralization of MSC differentiated into osteoblasts. (**a**) Alkaline phosphatase activity. (**b**) Alizarin red staining. ANOVA with Tukey test. a: $p<0.05$ vs UC; b: $p<0.05$ vs OB 0.8 mM Mg. pNPP: p-nitrophenyl phosphate. A.U.: arbitrary units.

Moreover, as compared with those osteoblasts cultured with basal Mg^{2+} levels (0.8 mM) TRPM7 inhibition by 2-APB administration diminished significantly the expression of the osteogenic marker genes *Runx2*, *Osterix* and *Osteocalcin* (Fig.59 **a**, **b** and **c**, respectively). Similarly, 2-APB treatment reduced also FGF23 secretion (Fig.59 **d**).

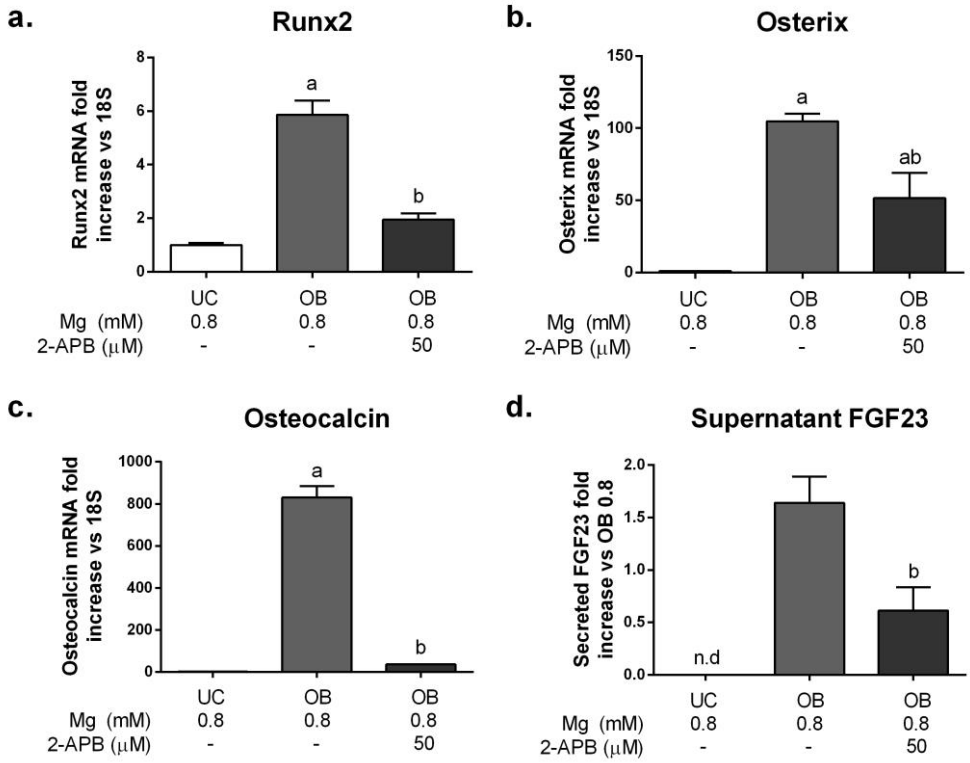

Figure 59. TRPM7 inhibition by 2-APB administration decreased osteogenesis of MSC. ANOVA with Tukey test. a: $p<0.05$ vs UC; b: $p<0.05$ vs OB 0.8. 2-APB: 2-Aminoethoxydiphenyl borate.

3.2.3. Mg supplementation increases proliferation of MSC during osteogenesis

To investigate whether Mg supplementation increases cellular proliferation during MSC differentiation into osteoblasts, Cyclin D1 and PCNA protein levels were analyzed by Western blot after 21 days of treatment. The expression of both proteins

was increased in osteoblasts as compared with undifferentiated cells (UC). In these conditions, $MgCl_2$ supplementation (1.2 and 1.8 mM) enhanced dose-dependently the expression of these proliferation markers. It was interesting to note that 2-APB treatment (50µM), reduced significantly Cyclin D1 and PCNA protein expression, suggesting that Mg exerts its pro-proliferative effects intracellularly through this channel (Fig.60 **a** and **b** respectively).

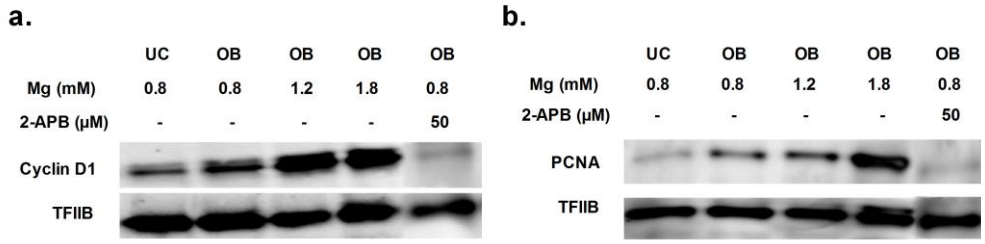

Figure 60. $MgCl_2$ supplementation promotes proliferation of MSC during osteogenesis. Treatment with Mg dose-dependently increased the amount of Cyclin D1 (**a**) and Proliferating Cell Nuclear Antigen (PCNA) (**b**) after 21 days of osteogenesis. At contrary, inhibition of the Mg channel TRPM7 decreased both Cyclin D1 and PCNA.

3.2.4. Effects of magnesium supplementation on Notch1 signaling in MSC

To investigate the mechanism whereby $MgCl_2$ supplementation increases the osteogenic differentiation of MSC, the potential role of two pro-osteogenic pathways, Wnt/β-catenin and Notch, was examined by confocal microcopy. Immunofluorescence analyses showed that osteogenic differentiation promoted the nuclear translocation of β-catenin, however as compared with basal Mg^{2+} treated cells (OB), the addition of $MgCl_2$ to osteogenic medium did not further promote nuclear localization of β-catenin (Fig.61).

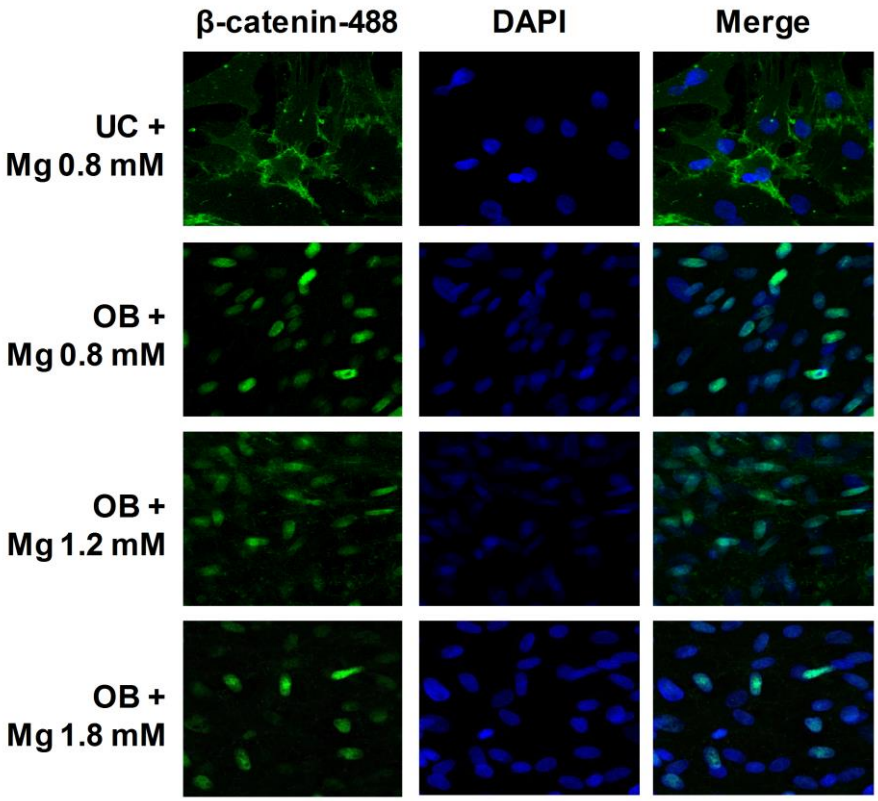

Figure 61. β-catenin nuclear translocation was not affected by $MgCl_2$ supplementation. In undifferentiated MSC, β-catenin was found in the plasma membrane; and osteogenic medium increased the presence of β-catenin in the nuclei, however no significant differences were found with Mg treatments. OB: Osteogenic medium 21 days. DAPI: 4',6-diamidino-2-fenilindol.

These results were also confirmed by western blot analysis of nuclear-enriched protein extracts (Fig.62) confirming that $MgCl_2$ supplementation did not activate the canonical Wnt/β-catenin pathway.

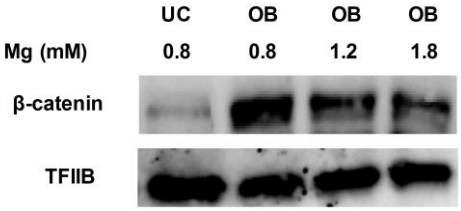

Figure 62. Western blot of nuclear-enriched protein extracts for β-catenin. Osteogenic stimuli induced an increase in the amount of β-catenin in the nuclear-enriched extracts. Magnesium supplementation did not further increase the amount of nuclear β-catenin. TFIIB was used as housekeeping protein.

With respect to Notch signaling, confocal microscopy analysis of Notch1 intracellular domain (NICD), using an antibody that only recognized the truncated (activated) NICD, showed that osteogenic differentiation of MSC with basal levels of Mg decreased the nuclear translocation of NICD as compared with undifferentiated MSC. However, $MgCl_2$ supplementation promoted dose-dependently nuclear colocalization of NICD. At contrary, treatment with 2-APB reduced this nuclear translocation of the NICD that was clearly reduced (Fig.63 **a**). To check this co-localization, green pixels (NICD) matching with blue pixels (DAPI) were analyzed using the Image J software (colocalization finder plugin). As shown in the fourth column (Fig.63 **a**, far right column), $MgCl_2$ supplementation increased the green and blue pixels overlap, while 2-APB decreased it.

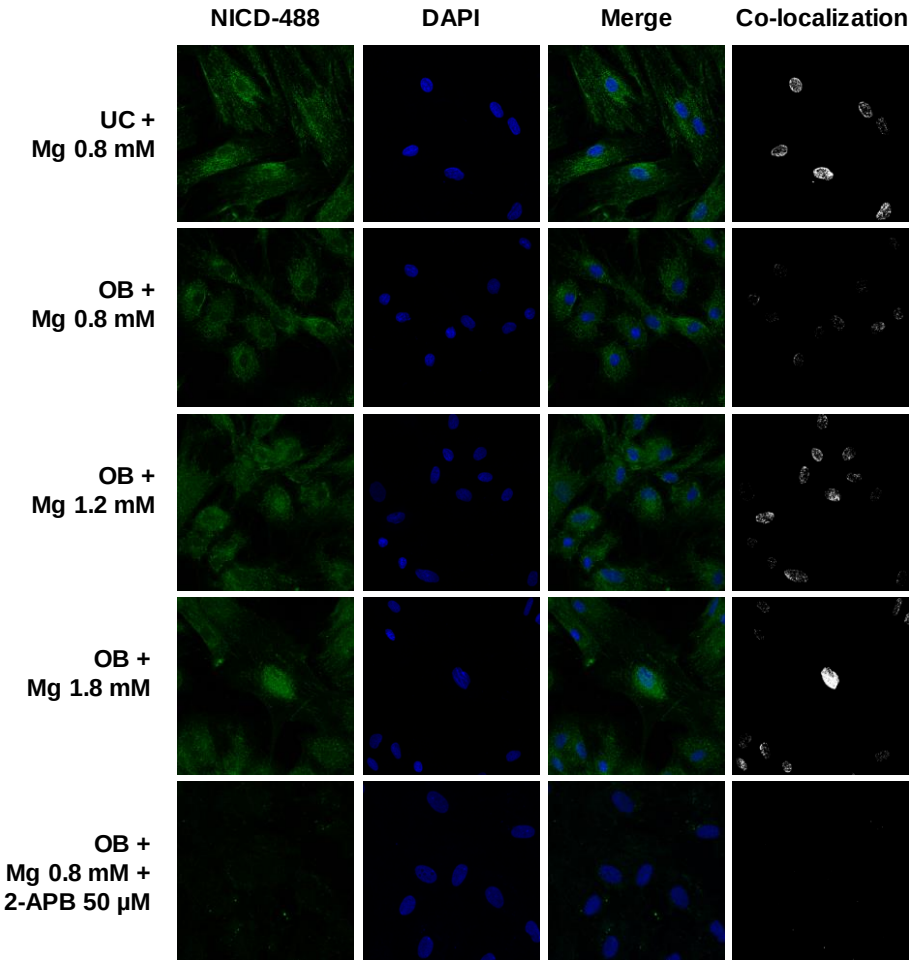

Figure 63. $MgCl_2$ induces NICD nuclear translocation. Confocal microscopy analysis showed intense NICD-green nuclear staining in undifferentiated MSC. Mg addition increased the nuclear NICD translocation dose-dependently respect to differentiated osteoblast with basal Mg (OB 0.8 mM). This presence was reduced in osteoblasts treated with 2-APB. UC: Undifferentiated control. OB: osteogenic medium 21 days. DAPI: 4 ',6-diamino-2-fenilindol. Magnification: 400x.

Additionally, these results were also confirmed by western blot of NICD in a nuclear-enriched protein extracts (Fig.64).

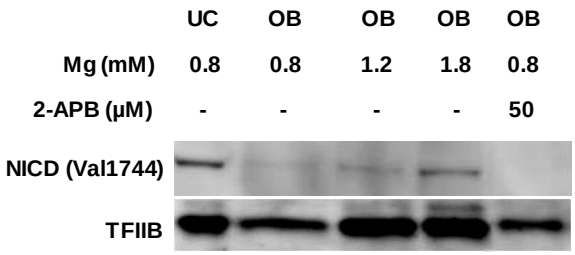

Figure 64. NICD nuclear expression. Western blot analysis showed a decrease in NICD nuclear expression in the OB group respect to undifferentiated cells (UC) after 21 days of osteogenic differentiation. The addition of $MgCl_2$ during osteogenesis increased dose-dependently the amount of nuclear NICD. Treatment with 2-APB during osteogenesis prevented nuclear translocation of NICD protein expression.

The expression of *HEY2*, a well-known Notch target gene, was also quantified to further demonstrate the involvement of this pathway. Consistent with nuclear NICD analysis, the expression of *HEY2* was decreased after osteogenic differentiation as compared with undifferentiated MSC, and the increase of Mg content in the osteogenic medium upregulated the mRNA expression of *HEY2*. Inhibition of the Mg transporter TRPM7 with 2-APB decreased *HEY2* expression (Fig.65).

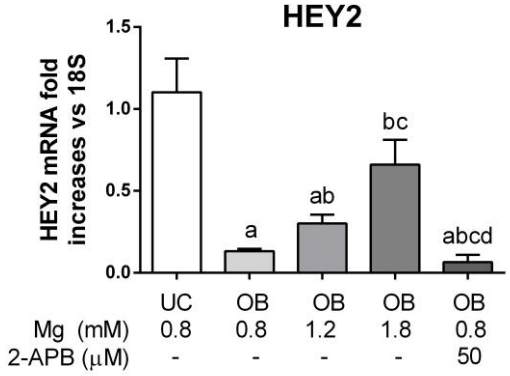

Figure 65. *HEY2* mRNA expression was upregulated according to Mg concentration during osteogenesis. t-test. a: $p<0.05$ vs UC 0.8; b: $p<0.05$ vs OB 0.8; c: $p<0.05$ vs OB 1.2; d: $p<0.05$ vs OB 1.8.

To gain in-depth knowledge with the relationship between Mg, osteogenesis and proliferation, we studied whether $MgCl_2$ supplementation develops its actions preferably in MSC, osteoblasts-committed cells or both. Therefore, the effects of $MgCl_2$ supplementation were evaluated after 24h on MSC or MSC plus osteogenic stimulus at early stage of osteogenic differentiation. Western blotting analysis showed that, in undifferentiated cells, the addition of $MgCl_2$ for 24 h increased the nuclear protein expression of NICD (Fig.66 **a**). However, when $MgCl_2$ was administered for 24 hours to MSC in presence of the osteogenic stimulus the levels of nuclear NICD remained similar to those found with basal Mg^{2+} content (Fig.66 **b**). Similarly, in differentiated osteoblasts for 21 days, the administration of $MgCl_2$ or 2-APB for 24h did not modify the nuclear NICD protein expression (Fig.66 **c**). Of note, high nuclear NICD protein amount was detected in undifferentiated MSC after 21 days, while in differentiated osteoblasts the nuclear NICD was dramatically reduced.

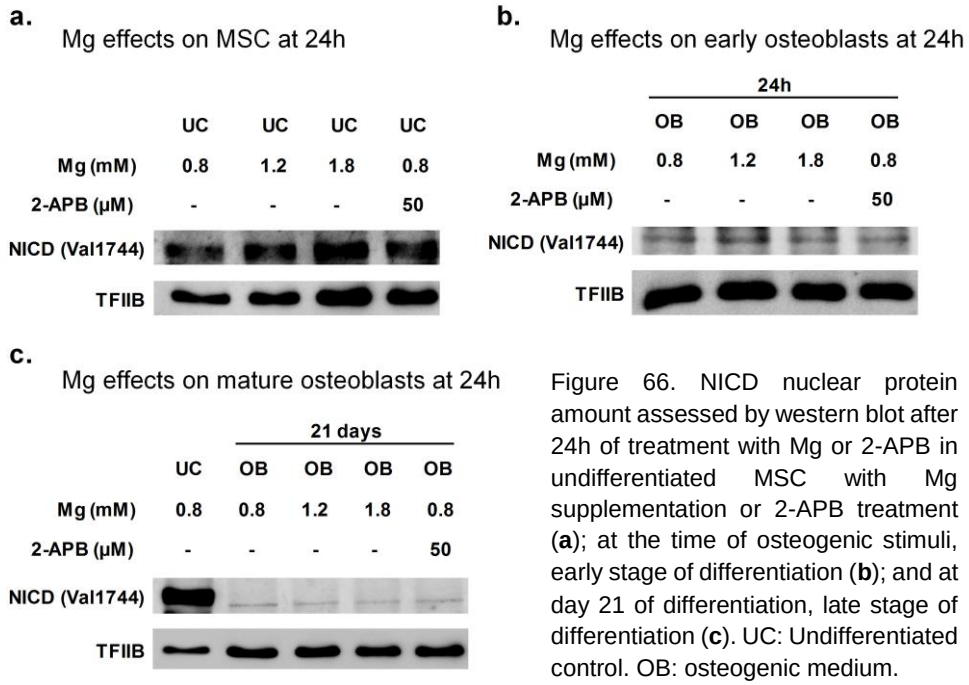

Figure 66. NICD nuclear protein amount assessed by western blot after 24h of treatment with Mg or 2-APB in undifferentiated MSC with Mg supplementation or 2-APB treatment (**a**); at the time of osteogenic stimuli, early stage of differentiation (**b**); and at day 21 of differentiation, late stage of differentiation (**c**). UC: Undifferentiated control. OB: osteogenic medium.

3.3. *IN VITRO STUDY OF THE MAGNESIUM EFFECTS ON OSTEOGENESIS IN DECELLULARIZED BONE SCAFFOLDS*

The role of magnesium on the osteogenesis of MSC cultured over decellularized bone scaffolds was also investigated.

3.3.1. Scanning Electron Microscopy (SEM)

To assess whether $MgCl_2$ supplementation enhances the ability of MSC to repopulate rat bone scaffolds, decellularized rat long bones were cut into 5-10 mm pieces (Fig.67 **a**) and then placed in osteogenic medium with MSC and different Mg content during 21 days. In these decellularized bone scaffolds, SEM images showed osseous matrix as series of uniform and regular depressions corresponding to duct osteons (Fig.67 **a**). With basal Mg, bone scaffolds were covered by MSC differentiated into osteoblasts after 21 days. Abundant cells showed an irregular membrane with an unspecific distribution and presenting a stellate morphology (Fig.67 **b**). After Mg supplementation (1.2 mM), MSC formed an uniformly organized layer over the bone surface, of smooth aspect and with abundant cellular proliferation filling the osteon canals (Fig.67 **c**). In scaffolds treated with 1.8 mM Mg, bone surface was fully occupied by cells showing a continuous and regular layer of germinal bone tissue (Fig.67 **d**).

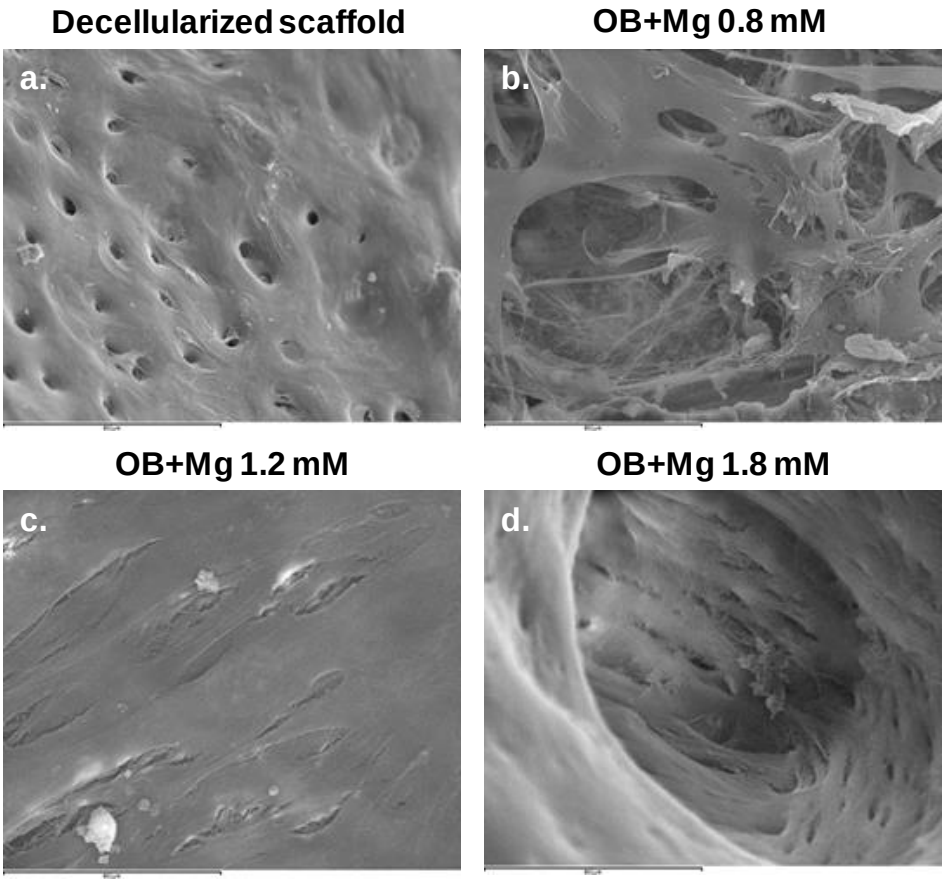

Figure 67. $MgCl_2$ promotes MSC proliferation and cell atachment to bone scaffolds. Representative SEM microphotographs of decellularized rat bone (**a**) and MSC cultured into osteogenic medium with $MgCl_2$ at 0.8 mM (**b**), 1.2 mM (**c**) and 1.8 mM (**d**). Note the surface of the bone scaffold covered by the well-organized cells with the higher Mg concentration. Bars are 800µm.

3.3.2. Transmission Electron Microscopy (TEM)

Additionally, cellular layers from decellularized bone scaffolds were analyzed with TEM after 21 days of differentiation to accurately determine the osteogenic phenotype. During the osteoinduction of MSC with basal Mg levels, cells produced immature matrix, as it can be observed in the poorly organization of the collagen

fibers (Fig.68 **a**). Mg supplementation up to reach 1.2 mM Mg increased the size of the cells, which showed abundant cytoplasm, resembling a phenotype similar to osteoblasts. In addition, cells showed well-structured layers, similar to the appositional growth found in bone, and osteoblasts were observed embedded into the bone matrix, which are considered osteocytes. These osteocytes showed membrane elongations similar to osteocytes and a more organized collagen matrix (Fig.68 **b**). With Mg 1.8 mM, the number of cells further increased, with presence of several osteocytes that showed longer membrane elongations and tunnels similar to bone canaliculi. Furthermore, it was observed well-organized collagen fibers similar to osteoid (Fig.68 **c**).

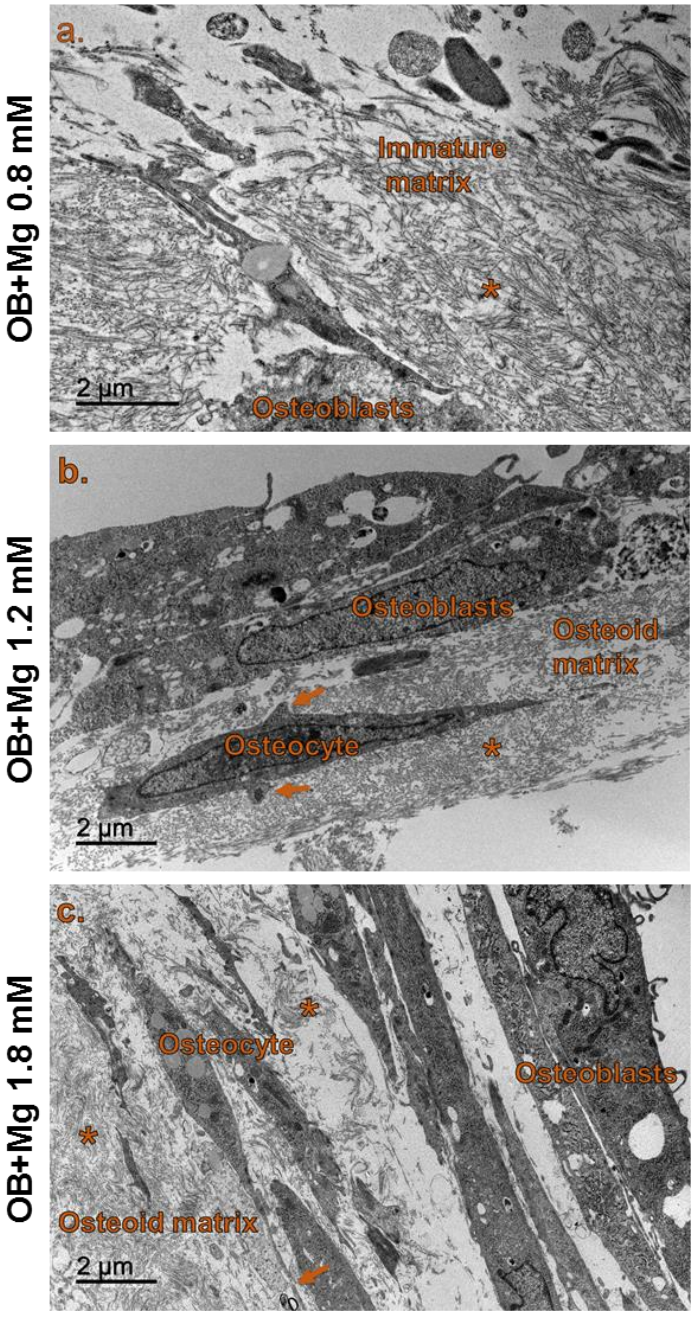

Figure 68. $MgCl_2$ enhances osteoblast differentiation. Representative TEM microphotographs of MSC differentiated into osteoblasts with Mg at 0.8 mM (**a**), 1.2 mM (**b**) and 1.8 mM (**c**). Note the dendrites of the osteocytes with Mg supplementation (Arrows). Asterisks indicate collagen fibers.

3.4. *MAGNESIUM EFFECTS ON OSTEOCLASTOGENESIS IN VITRO*

Additionally, the effects of $MgCl_2$ supplementation by 1.4 and 2.6 mM were examined on osteoclastogenesis *in vitro*. TRAP-positive multinucleated cells were observed with basal Mg concentration (0.8 mM) after 5 days of osteoclastogenic stimuli (OC) as compared with undifferentiated hematopoietic cells (UC) that were unstained (Fig.69 **a-d**). The addition of Mg to osteoclastogenic medium did not modify TRAP staining. Similarly, the expression of *CTSK* increased respect to undifferentiated cells after 5 days of osteoclastogenic stimuli, however increased Mg concentrations did not modify *CTSK* expression levels (Fig.69 **e**).

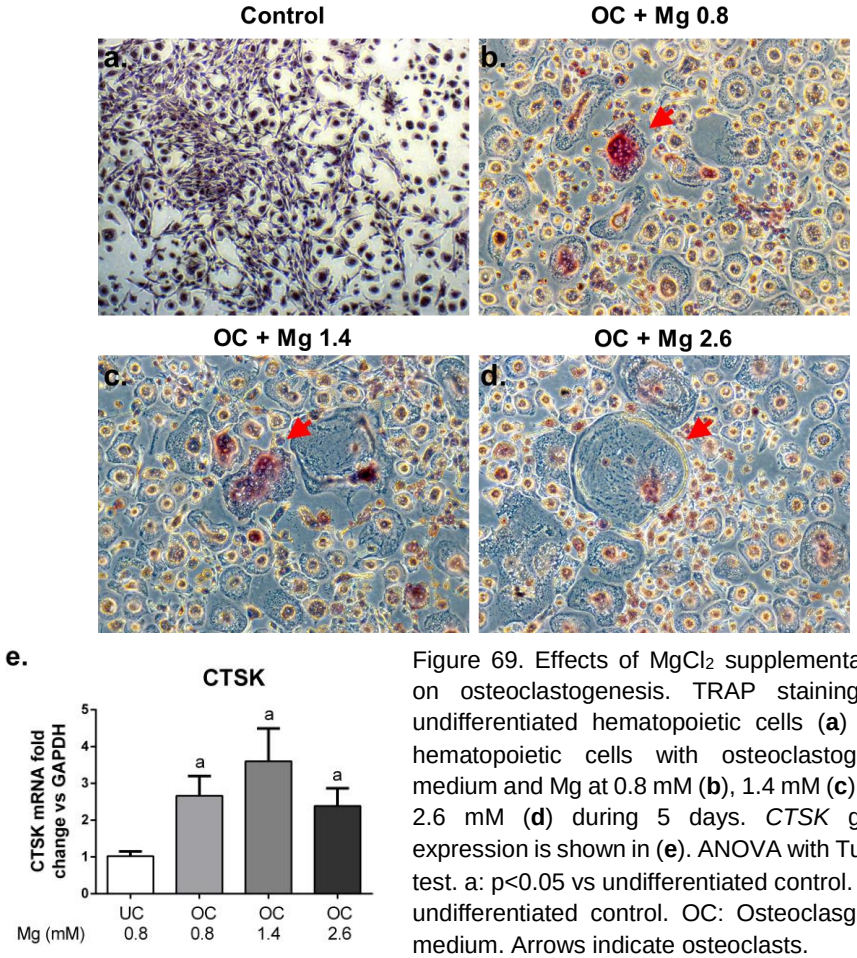

Figure 69. Effects of $MgCl_2$ supplementation on osteoclastogenesis. TRAP staining of undifferentiated hematopoietic cells (**a**) and hematopoietic cells with osteoclastogenic medium and Mg at 0.8 mM (**b**), 1.4 mM (**c**) and 2.6 mM (**d**) during 5 days. *CTSK* gene expression is shown in (**e**). ANOVA with Tukey test. a: $p<0.05$ vs undifferentiated control. UC: undifferentiated control. OC: Osteoclasgenic medium. Arrows indicate osteoclasts.

SECTION 4: FGF23

4.1 IN VIVO STUDY OF THE EFFECTS OF HIGH FGF23 IN BONE IN A RAT MODEL OF EARLY CKD

We developed in our laboratory an animal model with increased plasma FGF23 levels and without alterations of other mineral metabolism or renal parameters such as PTH, P, CTR or creatinine. We took advantage of the early increase of plasma FGF23 to separate it from other parameters that became significantly higher with more severe loss of renal function and end stage of renal disease. In this regard, we used heminephrectomized rats (right kidney, 1/2Nx) fed on a high P diet (1.2%) for three weeks. Sham animals without 1/2Nx fed on the same high P diet were used as control group. With these setting the effects of FGF23 in bone were studied *in vivo*.

4.1.1. Plasma biochemical parameters

Plasma biochemistry of Sham+1.2%P and 1/2Nx+1.2%P groups are shown in Table 15. It is interesting to note that although plasma creatinine levels were different between Sham+1.2%P and 1/2Nx+1.2%P groups (0.52±0.01 vs. 0.66±0.02, ***p<0.001), these ones were within the normal range of creatinine values. Plasma intact FGF23 levels were higher in 1/2Nx+1.2%P as compared with the Sham+1.2%P group (272±25 vs. 454±49.8, **p<0.01). Plasma P, iCa, $1,25(OH)_2D_3$ and PTH concentrations remained similar between both groups. Plasma ALP, a marker of osteoblast activity, also showed a non-significant increase in the 1/2Nx+1.2%P group. A non-significant increase was observed in phosphaturia in 1/2Nx+1.2%P rats as compared with Sham+1.2%P, consistent with the increased levels of plasma intact FGF23. Circulating sclerostin levels, a well-known inhibitor of the canonical Wnt pathway, was increased in 1/2Nx+1.2%P rats.

	Sham+1.2%P n=8	1/2Nx+1.2%P n=13
Creatinine (mg/dl)	0.52±0.01	0.66±0.02***
P (mg/dl)	6.63±0.36	6.77±0.40
iCa (mM)	1.28±0.01	1.25±0.02
PTH (pg/ml)	72.1±7.7	65.9±10.5
FGF23 (pg/ml)	272±25	454±49.8**
1,25(OH)2D3 (pg/ml)	181±21.6	209±6.08
ALP (U/l)	80.4±10.1	114±20.1
Sclerostin (pg/ml)	127±8.16	198±12.1**
FEPi (%)	31.9±7.49	50.2±7.03

Table 15. Plasma biochemistry. ** p<0.01; *** p<0.001 vs Sham+1.2%P group.

4.1.2. Bone histomorphometry parameters in early CKD rats

After 21 days, trabecular bone of the right distal femurs were collected and prepared to analyze bone histomorphometry. A tendency to decrease bone volume was observed in the 1/2Nx+1.2%P group (Fig.70 **a**). Osteoid volume (Fig.70 **b**) and osteoid surface (Fig.70 **c**) were significantly higher in the 1/2Nx+1.2%P group as compared with Sham+1.2%P. Bone surface covered by osteoblasts was also higher in the 1/2Nx+1.2%P group than in Sham+1.2%P animals (Fig.70 **d**). The eroded bone surface was significantly higher in the 1/2Nx+1.2%P group as compared with Sham+1.2%P animals (Fig.70 **e**), however the bone surface covered by osteoclasts only showed a slight but not significant increase (Fig.70 **f**).

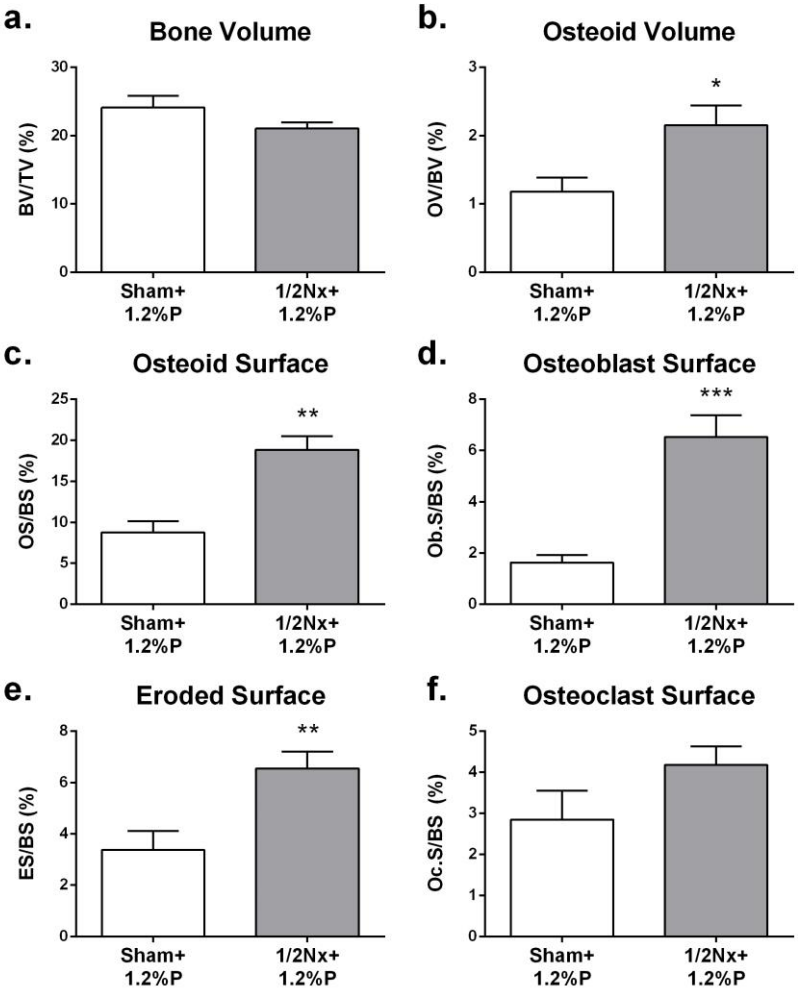

Figure 70. Hemi-nephrectomy produces an increase in bone cells activity. The bone volume showed a tendency to decrease in the 1/2Nx+1.2%P group (**a**). Increased bone remodeling was observed in 1/2Nx+1.2%P rats after 3 weeks, as assessed by the increased osteoid volume and surface (**b** and **c** respectively) and increased resorption surface (**e**); consistent with a higher bone surface covered by osteoblasts (**d**) and osteoclasts (**f**). T-test. * $p<0.05$; ** $p<0.01$; *** $p<0.001$ vs sham+1.2%P.

Representative microphotographs are shown in Figure 71.

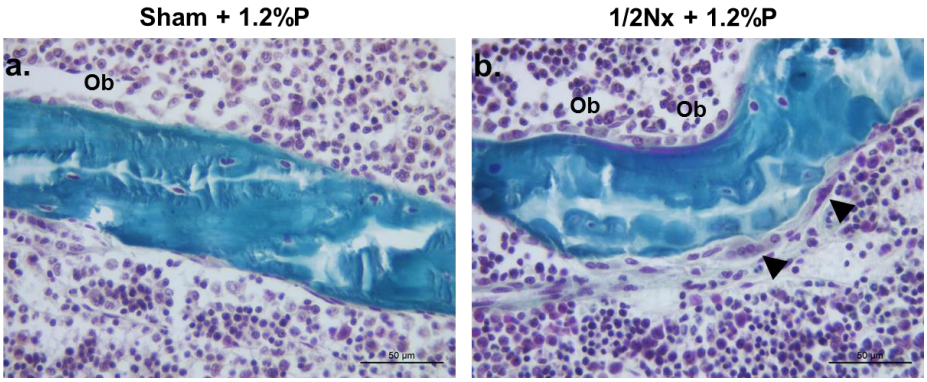

Figure 71. Hemi-nephrectomy increases osteoclast and osteoblast activity. 1/2Nx+1.2% P rats showed higher bone surface covered by osteoblasts and higher osteoclast activity (**b**) as compared with Sham+1.2% P (**a**) Ob: Osteoblasts. Arrowhead: Osteoclast. Augmentation: 400x. Scale bar: 50 µm.

Importantly, despite of the decrease in bone volume was not statistically different, structural parameters showed significant changes in trabecular bone. In this respect, trabecular thickness and trabecular separation (Fig.72 **a** and **b** respectively) were higher in 1/2Nx+1.2% P rats as compared with Sham+1.2% P. Additionally, the trabecular number was reduced in the 1/2Nx+1.2% P group (Fig.72 **c**). No differences were observed in osteoid thickness (Fig.72 **d**) Altogether indicate an association between high levels of FGF23 and changes in bone microstructure. Representative pictures of Goldner's staining are shown in Fig.72 **e** and **f**.

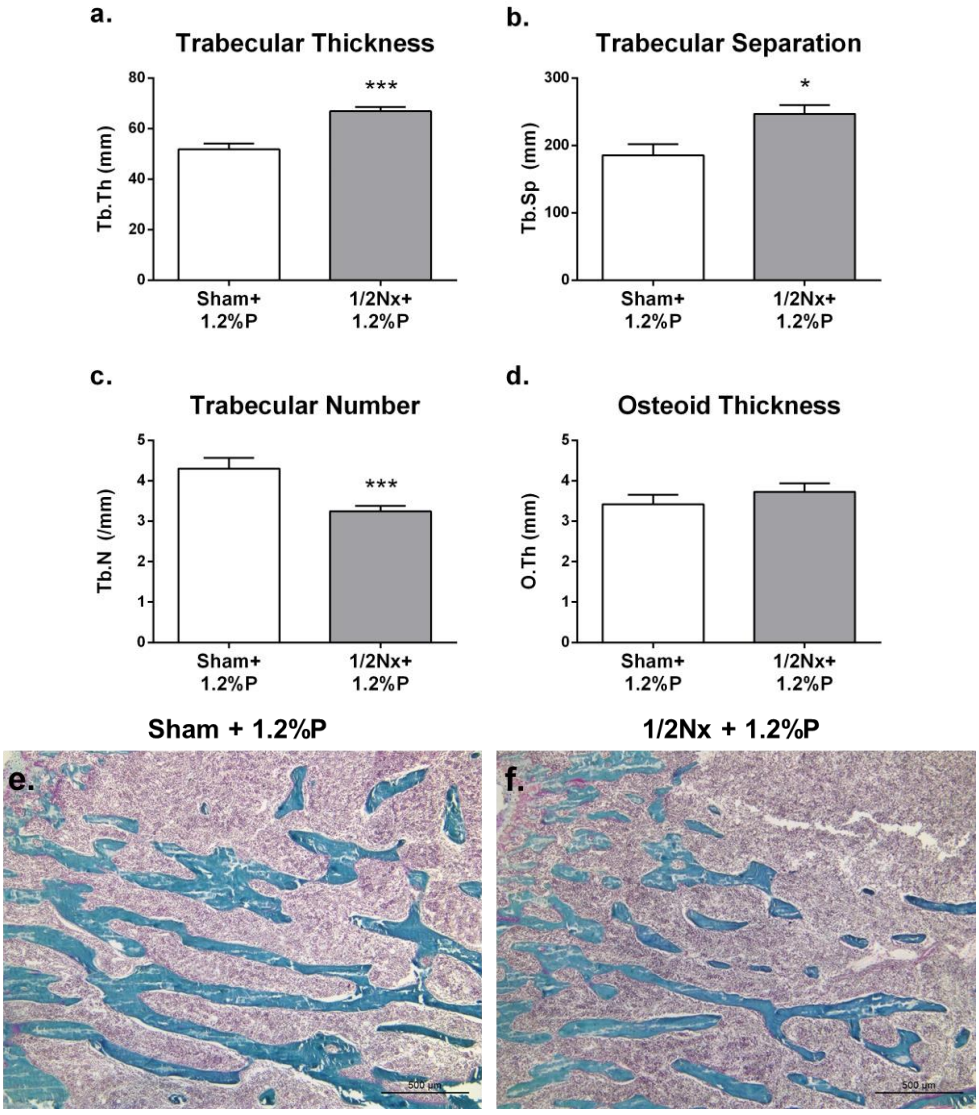

Figure 72. Early increase in plasma FGF23 induces changes in trabecular bone. Goldner's staining showed changes in bone microstructure in 1/2Nx+1.2% P rats (**f**) as compared with Sham+1.2% P (**e**). Bars are mean±SEM. t-test analysis * $p<0.05$; ** $p<0.01$; *** $p<0.001$. Augmentation: 40x. Scale bar: 500 µm.

4.1.3. Osteogenic gene expression in the bone of 1/2Nx rats

To evaluate osteoblast maturation, total mRNA was isolated from the proximal tibias and the expression of osteogenic marker genes was analyzed. *Runx2*, *Osterix* and *DMP1* mRNA expressions were down-regulated in the bone of 1/2Nx+1.2%P rats as compared with Sham (Fig. 73 **a**, **b** and **c**). Of note, *SOST* mRNA expression in the bones of the 1/2Nx+1.2%P rats was higher than in the Sham+1.2%P group (Fig.73 **d**), consistent with the plasma levels of sclerostin (previously shown in Table 15).

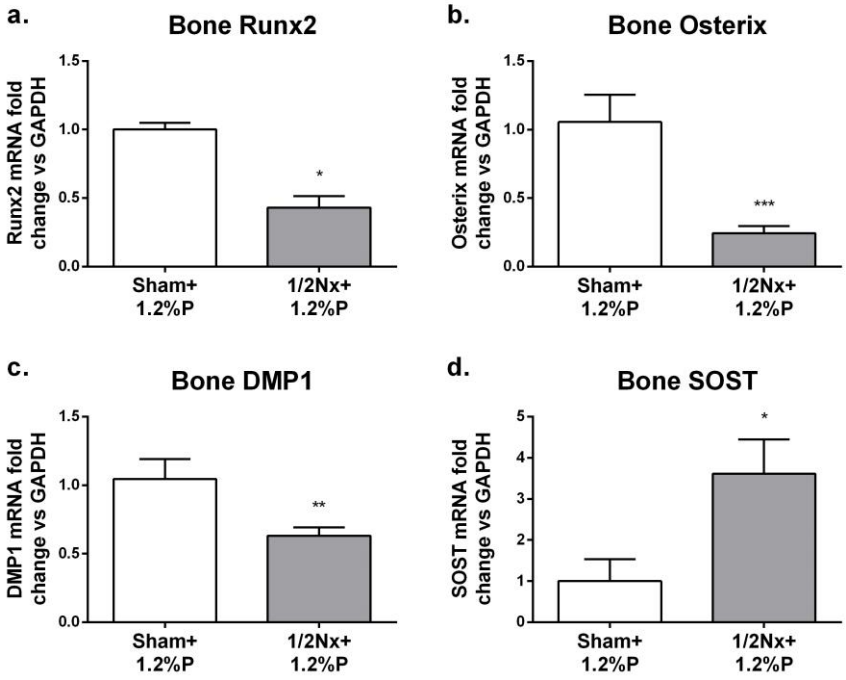

Figure 73. Gene expression of osteogenic genes was down-regulated in bone lysates of 1/2Nx+1.2%P rats except to sclerostin expression that was increased. T-test. *p<0.05 vs Sham+1.2%P **p<0.01 vs Sham+1.2%P; ***p<0.001 vs Sham+1.2%P.

4.2. *IN VITRO STUDY OF THE EFFECTS OF FGF23 ON OSTEOGENESIS*

The direct actions of FGF23 were studied in osteoblastic differentiation. To prevent FGF23 degradation, we used a rat recombinant FGF23 with arginine 176 replaced by glutamine (R176Q). Rat recombinant intact FGF23 (R176Q) (from here abbreviated rFGF23) was added at a high concentration similar to that found in the plasma of experimental rat models with renal insufficiency.

4.2.1. Evaluation of MSC differentiation into osteoblasts

To confirm *in vitro,* the effects of FGF23 in bone cells we investigated whether the treatment with rFGF23 exerts direct effects on the osteogenesis of bone marrow MSC. First, we examined the differentiation of the MSC after 21 days of osteogenic stimulus. Mineralization assessed by alizarin red staining showed an intense red color in MSC differentiated into osteoblasts (OB) respect to undifferentiated MSC (UC) that were not stained (Fig.74 **a**). Osteogenic stimulus promoted also the cell recruitment and formation of calcification nodules observed in the bright-field microphotographs (Fig.74 **b** and **c**).

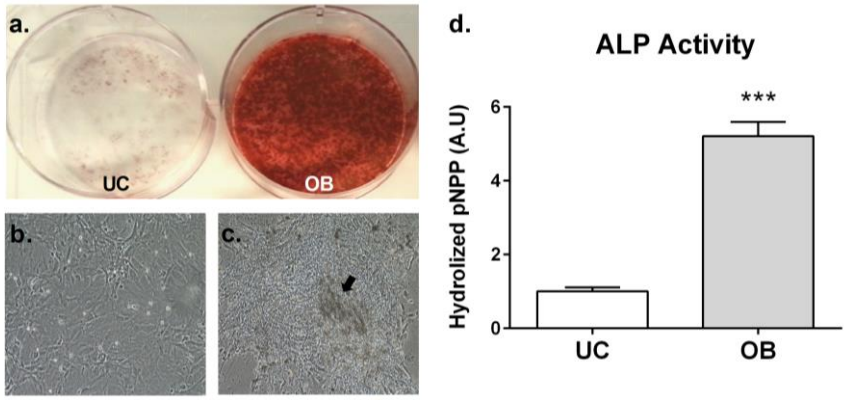

Figure 74. Mineralization of MSC differentiated into osteoblasts. Osteogenic stimuli increased mineralization assessed by alizarin red staining (**a**). Representative microphotograph of undifferentiated MSC (**b**) and MSC differentiated into osteoblasts (**c**). ALP activity was increased in MSC differentiated into osteoblasts (**d**). Arrow: calcification nodule. UC: undifferentiated control. OB: Ostegenic medium 21 days. Magnification: 100x.

Additionally, to evaluate the degree of osteoblastic differentiation, the expression of well-known osteogenic marker genes was analyzed. The gene expression of *Runx2* (Fig.75 **a**), *Osterix* (Fig.75 **b**) and *Osteocalcin* (Fig.75 **c**) were increased, indicating osteogenic differentiation. Of note, MSC differentiated into osteoblasts after 21 days also increased the expression of the *DMP1*, an osteocyte marker gene (Fig.75 **d**).

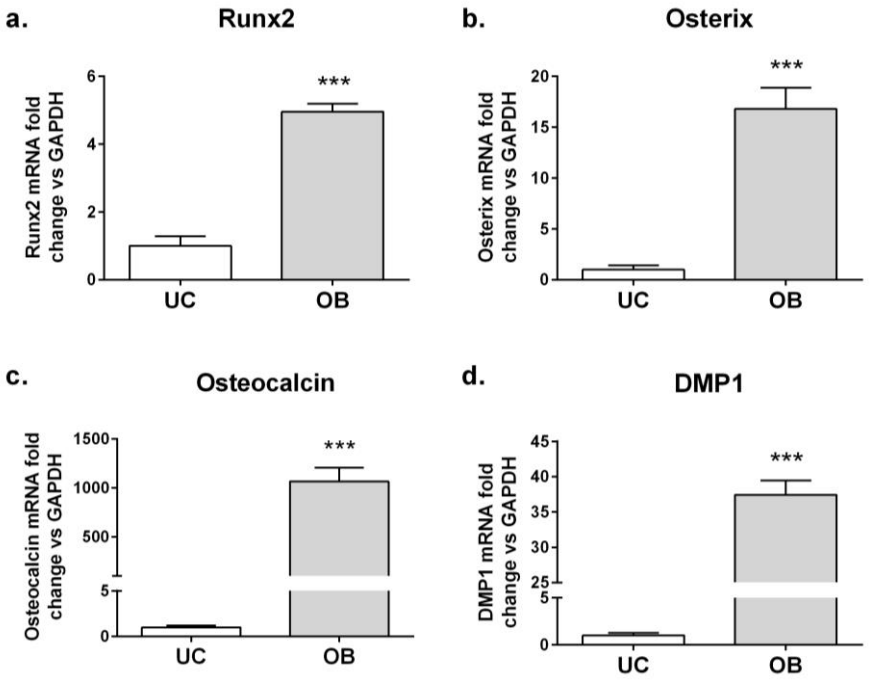

Figure 75. Osteogenic stimuli during 21 days up-regulated the expression of mature osteoblast and osteocytes marker genes. Bars are mean±SEM. t-test ***p<0.001 vs UC. UC=Undifferentiated cells; OB= Osteoblast cells.

4.2.2. In vitro effects of high levels of FGF23 during MSC osteogenesis

No significant differences were found in matrix mineralization (Fig.76 **a**) or calcium content (Fig.76 **b**) after the addition of rFGF23 at 15ng/ml to the MSC with osteogenic stimulus. However, rFGF23 addition throughout osteogenic differentiation decreased the ALP activity (Fig.76 **c**) and reduced the expression of

Runx2 (Fig.76 **c**), *Osterix* (Fig.76 **d**) and *Osteocalcin* (Fig.76 **e**) as compared with OB Vehicle.

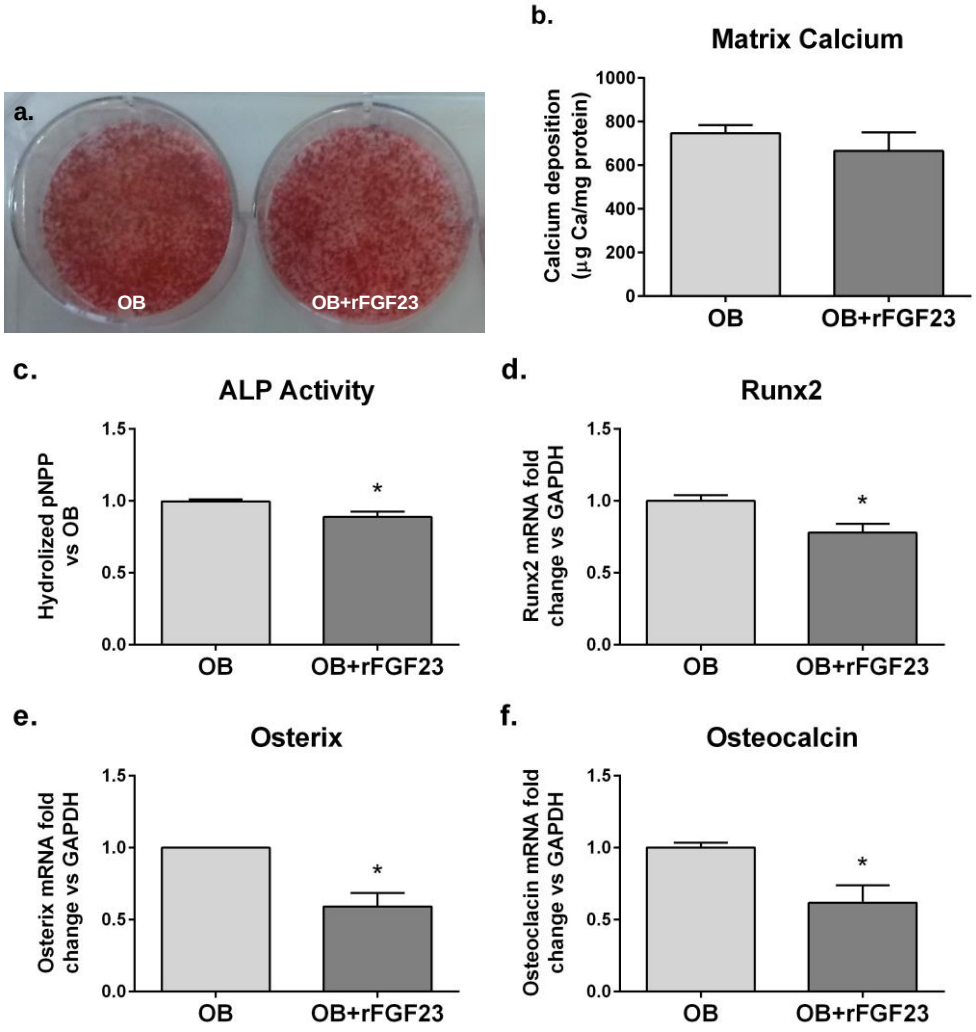

Figure 76. Rat recombinant FGF23 addition throughout osteogenic differentiation (21 days) decreases osteogenesis but not mineralization. Alizarin red staining showed similar mineralization in rFGF23-treated OB cells as compared with control OB (**a**). Quantification of eluted calcium from the mineralized matrix showed a tendency to decrease calcium content with rFGF23 treatment (**b**), consistent with a decrease in alkaline phosphatase activity (**c**). In addition, rFGF23 added throughout osteogenic differentiation down-regulated the expression of *Runx2* (**d**), *Osterix* (**e**) and *Osteocalcin* (**f**). T-test. *p<0.05 vs OB.

4.2.3. Effect of high FGF23 in osteocyte-like MSC

Furthermore, we considered of interest to evaluate the effects of high intact FGF23 in mature osteoblasts and osteocytes derived from MSC. Therefore, MSC were cultured with osteogenic medium during 20 days to generate mature osteoblasts similar to osteocytes. Once maturated, rFGF23 was added at 15 ng/ml for 24h to evaluate an acute effect. After 24 h, rFGF23 addition to generated osteocytes significantly decreased the expression of gene expression of *Osterix* (Fig.77 **a**), *Osteocalcin* (Fig.77 **b**), *DMP1* (Fig.77 **c**) and *RANKL* (Fig.77 **d**) while *OPG* remained similar (Fig.77 **e**). In this respect the ratio RANKL/OPG was decreased by rFGF23 in mature osteoblasts and osteocytes (Fig.77 **f**).

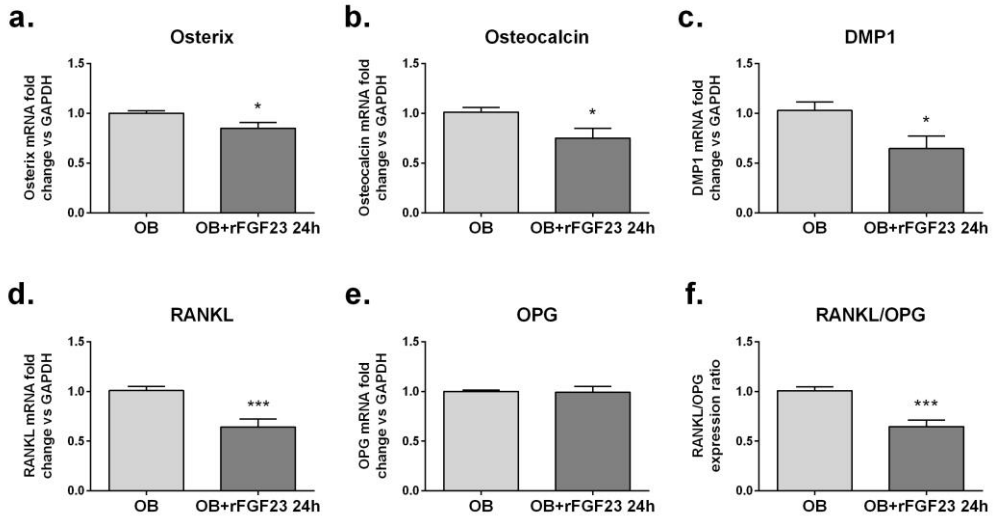

Figure 77. Effects of high rFGF23 addition in differentiated osteocytes after 24h of treatment. T-test. Treatment with high rFGF23 decreased the expression of the osteogenic genes *Osterix* (**a**), *Osterix* (**b**) and *Osteocalcin* (**c**) in MSC differentiated into osteocytes after 24 hours. In addition, high dose of rFGF23 decreased *RANKL* expression (**d**), whereas did not affect OPG expression (**e**), decreasing the ratio *RANKL*/*OPG*. *p<0.05 vs OB; ***p<0.001 vs OB.

4.2.4. Effects of high FGF23 on β-catenin nuclear translocation

Consistent with the down-regulation of the osteogenic marker genes, rFGF23 addition to mature osteoblasts inhibited nuclear translocation of β-catenin pathway after 24h of treatment, as it was assessed by confocal microscopy (Fig.78 **a** and **b**).

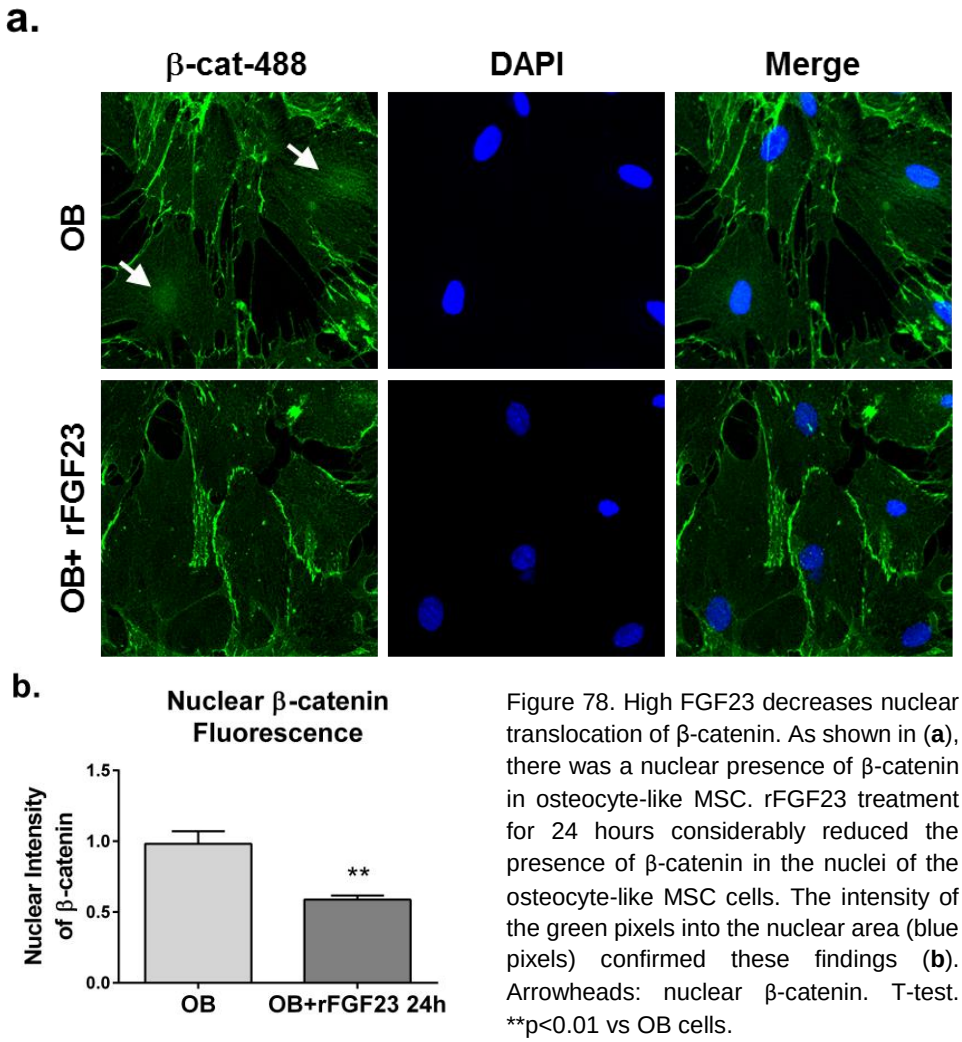

Figure 78. High FGF23 decreases nuclear translocation of β-catenin. As shown in (**a**), there was a nuclear presence of β-catenin in osteocyte-like MSC. rFGF23 treatment for 24 hours considerably reduced the presence of β-catenin in the nuclei of the osteocyte-like MSC cells. The intensity of the green pixels into the nuclear area (blue pixels) confirmed these findings (**b**). Arrowheads: nuclear β-catenin. T-test. **p<0.01 vs OB cells.

4.3. *EFFECTS OF FGF23 ON OSTEOCLASTOGENESIS IN VITRO*

The effects of a high dose of intact FGF23 were also analyzed in an *in vitro* model of osteoclastic differentiation from rat bone marrow hematopoietic stem cells

4.3.1. Effects of high FGF23 on osteoclast differentiation

To evaluate the effects of FGF23 on osteoclasts differentiation, rat recombinant intact FGF23 (R176Q) was added throughout differentiation at 0.1 and 10ng/ml. rFGF23 addition increased the number of TRAP-positive multinucleated cells (Fig.79 **a**, **b** and **c**) and *CTSK* expression (Fig.79 **d**).

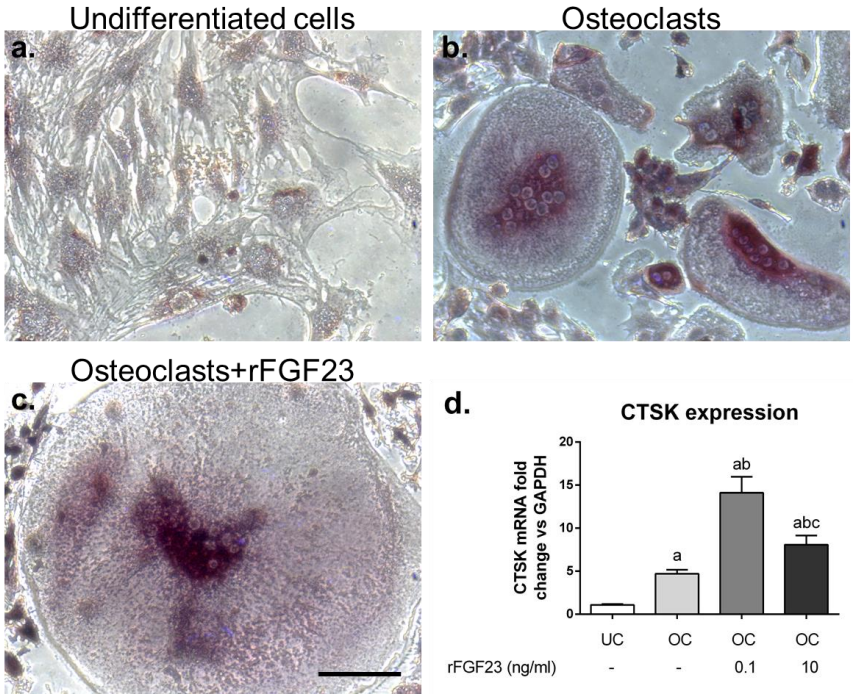

Figure 79. rFGF23 addition increases osteoclastogenesis of hematopoietic cells. Bright field representative microphotographs of positive-TRAP multinucleated cells obtained after 5 days of osteoclastic stimuli (**b**). High rFGF23 produced larger positive-TRAP multinucleated cells (**c**). rFGF23 treatment also increased *CTSK* expression osteoclast-like hematopoietic cells (**d**). ANOVA with Tukey test. a: $p<0.001$ vs undifferentiated cells; b: $p<0.001$ vs Osteoclasts; c: $p<0.01$ vs Osteoclasts+rFGF23 0.1 ng/ml. UC: undifferentiated control. OC: Osteoclasts.

Moreover, rFGF23 increased the number of the osteoclast-like cells respect to OC cells (Fig.80 **a**, [b] p<0.001). High rFGF23 supplementation significantly reduced the number of nuclei per osteoclast (Fig.80 **b**). Of note, the treatment with high rFGF23 increased the size of the osteoclast-like cells as assessed by the significantly higher length of the cellular axes (Fig.80 **c** and **d**).

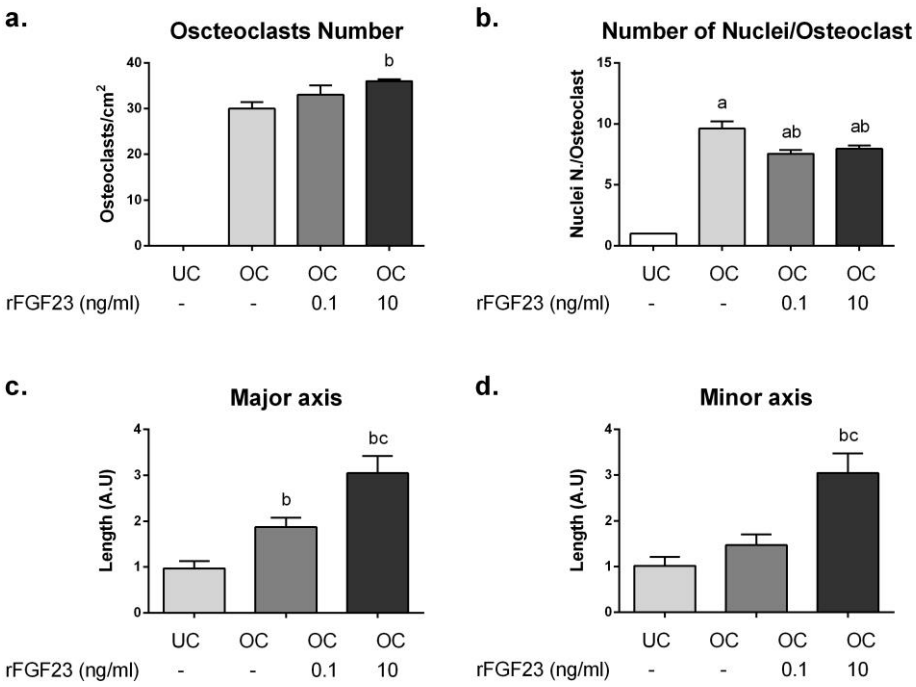

Figure 80. High rFGF23 modified osteoclastogenesis of hematopoietic cells. rFGF23 added throughout osteoclastogenesis produced an increase in the number of the differentiated osteoclasts (**a**) and reduced the number of nuclei per osteoclast (**b**). Osteoclast size was also significantly greater in the osteoclasts treated with high rFGF23 (**c** and **d**). ANOVA with Tukey test. a: p<0.001 vs undifferentiated cells; b: p<0.001 vs Osteoclasts; c: p<0.01 vs Osteoclasts+rFGF23 0.1 ng/ml. A.U: Arbitrary units.

DISCUSSION

In this thesis we investigated the potential role of calcitriol, calcimimetic, magnesium and FGF23 in renal osteodystrophy. Firstly, each element will be discussed separately in an uremic context and subsequently all these parameters altered during CKD will be related.

With respect to calcitriol, we investigated its bone effects independently of the actions on PTH secretion. We performed an animal model of renal insufficiency (5/6Nx rats) that underwent total parathyroidectomy and constant infusion of PTHx6 (1-34 length). The recommended dose of calcitriol to treat SHPT varies between 0.5-3 µg every 3 days[186] (equivalent to 7.7-46.2 ng/kg per dose considering a total body weight of 65 kg), therefore our *in vivo* experiment with 20, 40 and 60 ng/kg weight ranged between medium to high dose of calcitriol.

In these animals, the administration of calcitriol dose-dependently increased plasma Ca and P, according to the expected effects of calcitriol. It is important to note that in our model of 5/6Nx rats with clamped PTH, hypercalcemia could not affect PTH levels, which remained constant in these groups. In the group of rats treated with the highest dose of calcitriol an increase in plasma creatinine was observed. This fact could be explained by the exacerbation of the renal injury due to the hyperphosphatemia and hypercalcemia[187]. Plasma intact FGF23 levels increased according to the dose of calcitriol administered despite of the fact that PTH levels were clamped. The stimulation of FGF23 production and secretion by calcitriol have been widely described previously. In normal mice, administration of calcitriol significantly increased plasma FGF23 as early as 4 hours and this increase was associated with a higher FGF23 mRNA expression in bone. Furthermore calcitriol also increased FGF23 production in UMR cells dose and time dependently, and the treatment with actinomyzin D, an inhibitor of the RNA synthesis, prevented this effects indicating that calcitriol may trigger its actions at transcriptional level[188]. Of note, Nguyen-Yamamoto et al have reported that the local production of calcitriol by bone cells, which express 1-α hydroxylase, also increase FGF23[189].

With respect to bone histology, in the 5/6Nx-PTx-PTH group treated with CTR 60 ng/kg, a fall in the trabecular bone volume was observed, although osteoblast activity was not reduced. This fact might be explained by the high concentration of calcium

in plasma. In this way, the activation of the CaSR in osteoblasts by this extracellular calcium might lead to increased bone cell activity (discussed below). Additionally, plasma sclerostin levels increased significantly in the 5/6Nx-PTx-PTH treated with CTR 60 ng/kg as compared with the other 5/6Nx-PTx-PTH groups. Sclerostin is a well-known inhibitor of the Wnt/β-catenin pathway and bone formation contributing to the reduction of bone volume. The higher osteoblast activity was not accompanied by increased bone volume in the 5/6Nx-PTx-PTH treated with CTR 60 ng/kg, this fact may be due to the coexistence of bone anabolic and catabolic factors and additional studies are needed in order to clarify this controversial scenario.

It has been reported that bone sclerostin synthesis is mediated by PTH signaling *in vivo* and *in vitro*[190], however in our study we found that plasma sclerostin increased with clamped PTH, suggesting a sclerostin regulation independent of PTH changes. It is interesting to note that, despite its anti-anabolic actions in bone, sclerostin is involved in vitamin D metabolism since SOST-KO mice showed an increase of calcitriol and decreased levels of FGF23 while calcium and PTH remained similar to control[191]. Of note, plasma FGF23 concentration in this group was extremely high. In this respect, the negative effects of FGF23 on bone mineralization have been previously described[192] and they will be discussed below.

Respect to bone histomorphometry analysis, we observed that calcitriol administration by 20 and 40 ng/kg decreased the amount of osteoid, consistent with a tendency to decrease the mineralization lag time. We consider that these effects should be mainly influenced by the normalization in plasma phosphate and calcium levels. Previous studies have reported that knockout animal models for 1-α-hydroxylase or VDR recovered mineralization abnormalities when they were fed on a rescue diet[193–195].

However, the administration of the highest dose of calcitriol induced an increase in the osteoid thickness consistent with a tendency to increase the mineralization lag time. Contrary to some previous authors that reported a pro-osteoclastogenic effect[196], in our *in vivo* study (Nx5/6 and clamped PTH), calcitriol administration did not affect the bone surface covered by osteoclasts or the eroded surface suggesting an uncoupling of bone turnover.

The negative effects of excessive calcitriol on bone mineralization has been previously reported. Thus, knockout mice lacking the 24-hydroxylase shown increased levels of calcitriol, hypercalcemia and defective mineralization. Similarly, offspring from the crossing between 24-hydroxylase-KO and VDR-KO mice showed improved mineralization and changes in mineral parameters[197]. In 2012, Lieben et al reported that specific ablation of VDR in the gut conducted by the promoter of the villin gene produces an increase in plasma calcitriol with the subsequent maintenance of plasma calcium and phosphate levels, although these gut specific $VDR^{-/-}$ mice showed defective mineralization. In normal mice, administration of a high dose of calcitriol (0.5 µg/kg/day) produced the accumulation of osteoid and increased secretion of osteopontin, a mineralization inhibitor, and ANK, other well-known calcification inhibitor involved in pyrophosphate transport. Of note, specific ablation of VDR in osteocytes, conducted by the promotor of DMP1, prevented the defective mineralization triggered by the treatment with high calcitriol[198]. These studies support our results that suggest an inhibitory effect of calcitriol on bone mineralization.

Moreover, we observed *in vitro* a hormetic dose-response of calcitriol on osteogenic differentiation. At the lowest doses of calcitriol we observed that calcitriol stimulated differentiation and mineralization, while at the highest concentrations calcitriol administration arrested osteoblastic differentiation and mineralization. The doses we used for the *in vitro* experiments varies between 10^{-8} to 10^{-12} M, while *in vivo* the dose we administered may induce a change in plasma calcitriol from $0.8x10^{-9}$ to $2.4x10^{-9}$ M (considering a total blood volume of 15 ml per rat and a mean of 250 grs of total body weight). In this way, the doses assayed *in vitro* comprised a more extensive spectrum than those used *in vivo*.

Calcitriol administration at 10^{-12} M increased the osteogenic gene expressions and did not affect matrix calcification, while concentrations at 10^{-10} M or higher blocked the osteogenic differentiation and mineralization of MSC. These effects are mediated at least partially by the inhibition of the Wnt/β-catenin pathway. In this respect, it has been reported that the inhibition of the Wnt/β-catenin pathway in osteocytes occurs in a murine model of progressive renal disease and also in CKD patients and was associated with increased expression of sclerostin and decreased bone volume[57].

We also observed that supraphysiological doses of CTR increased the plasma levels of sclerostin in uremic rats with clamped PTH, which may lead to decreased bone volume. Furthermore, *in vitro* high CTR levels inhibited Wnt/β-catenin pathway and osteogenic gene expression. Altogether suggests a direct inhibitory effect of high calcitriol on osteogenesis.

Of note, we also found that increased calcitriol down-regulated the expression of the VDR in MSC differentiated into osteoblasts. This fact may be due to a negative feedback produced by the chronic exposure to excessive calcitriol concentration to reduce the cellular sensitivity, as it occurs with the insulin receptor[199].

We also found that calcitriol administration increased the number of osteoclasts and the expression of *CTSK*. In this respect, the pro-osteoclastogenic effects of calcitriol *in vitro* have been already largely studied[200–202]. It has been reported that the effects of calcitriol on osteoclastogenesis are widely influenced by extracellular calcium, thus hypocalcemia is associated with an increase in the osteoclastic function in order to normalize plasma calcium levels[198,203]. However, in our animal model we did not observe differences in the bone surface covered by osteoclasts or the eroded surface, suggesting that others molecules must be involved in the regulation of osteoclast activity *in vivo*.

In CKD patients, calcitriol is used to restore the calcitriol deficit, increase plasma calcium levels and treat SHPT. Healy MD et al, studied the bone effects of calcitriol treatment during six months in three patients with renal disease. They performed an iliac crest biopsy at the beginning of the study that revealed increased bone resorption and osteoid thickness. After treatment, osteoid accumulation and eroded surface were reduced, consistent with a reduction in plasma PTH levels[204]. Then, it was demonstrated that intermittent treatment with calcitriol for 12 months reduced bone turnover and reversed osteitis fibrosa in young patients undergoing hemodialysis and these results were largely attributed to the reduction in plasma of PTH concentration. Low PTH levels developed adynamic bone disease, however some patients with high PTH levels shown decreased bone formation, indicating that calcitriol may decrease osteoblast activity[205]. Additionally, a case report by Pahl M. et al showed that calcitriol treatment may decrease bone turnover in a patient

undergoing hemodialysis without affecting PTH levels[206]. Furthermore, this interpretation was also suggested by Ureña P. et al that reported a decrease in plasma bone specific alkaline phosphatase after treatment with calcitriol that was not accompanied by a decrease in plasma PTH in a hemodialysis patients. However, the suppressive effects of calcitriol on bone turnover were not observed in other hemodialysis patients, highlighting the complexity of the renal osteodystrophy[207]. Our results agree with those previous clinical studies that reported a direct suppressive effect of calcitriol on osteoblast activity. The principal findings in the study of the effects of CTR on bone are summarized in Figure 81.

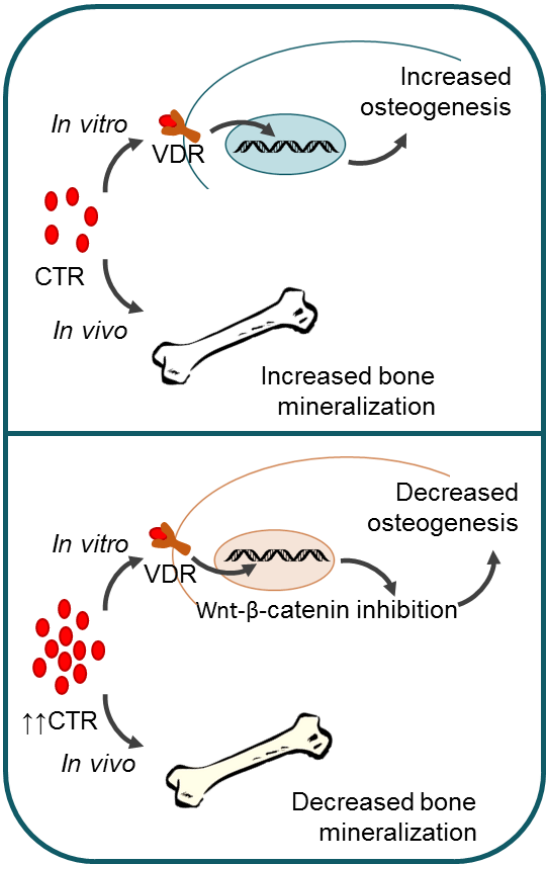

Figure 81. Summary figure of the bone effects of calcitriol. Moderate doses of calcitriol increase bone mineralization and osteogenesis. However, high doses of calcitriol promote the accumulation of osteoid and increase the time of mineralization. *In vitro*, high doses of calcitriol block osteogenic differentiation. At least partially, these actions are mediated by inhibition of the canonical Wnt-β-catenin pathway.

As abovementioned, calcitriol administration increases plasma calcium, and the effects of calcium through the CaSR might also influence bone turnover. Another

part of this thesis was focused on the study of the *in vivo* and *in vitro* effects of the CaSR activation by calcimimetic in bone cells.

In our *in vivo* experiments, calcimimetic administration to 5/6Nx rats produced the expected decrease in plasma intact PTH concentration. Despite this decrease in PTH, bone histomorphometry analysis showed that the bone surface covered by osteoblasts and osteoclasts remained similar between 5/6Nx and 5/6Nx+CM rats, suggesting that CaSR activation might exerts additional effects on bone. Recent studies using a murine model of reduced renal function by subtotal nephrectomy, have reported similar osteoblast and osteoclast activity in rats treated or not with the calcimimetic AMG416 (Parsabiv/Etelcalcetide) in spite of the differences in plasma PTH levels[148]. Wada et al reported that calcimimetic R-568 reduced PTH levels and ameliorated osteitis fibrosa in uremic rats. However, in this study bone cells activity was not different to that found in rats receiving vehicle[208]. In hemodialysis patients, Cozzolino M et al observed that the serum bone specific alkaline phosphatase activity increased in the subjects treated with cinacalcet as compared with those treated with paricalcitol after 28 days. These differences were explained by a lower PTH levels in treated patients with paricalcitol than with cinacalcet[209]; however these results would also agree with our hypothesis suggesting a direct effect of cinacalcet in bone cells.

To separate the actions of calcimimetic in the parathyroid glands from those in bone, we performed the experiment in 5/6Nx rats with parathyroidectomy receiving a constant infusion of PTH 1-34 (moderate PTH6x or high concentration PTH9x). PTH infusion by 6-fold the necessary dose to maintain plasma calcium in a PTx rat with normal renal function maintained plasma calcium and phosphate concentration similar to those observed in 5/6Nx animals. However, plasma intact FGF23 levels were lower in the parathyroidectomized 5/6Nx rats with PTH replacement by 6x than in the 5/6Nx group treated with vehicle. Despite the fact that the infusion of PTHx6 maintained the plasma mineral parameters, the bone cell activity was lower than that observed in the 5/6Nx group, suggesting that the amount of PTH 1-34 was insufficient. Actually, plasma PTH 1-34 levels were significantly lower in 5/6Nx-PTx-PTH6x than in 5/6Nx group. Furthermore, it is known that circadian rhythms regulate

PTH[210], which could not be mimicked in our animal model of clamped PTH. This aspect might also contribute to the differences between 5/6Nx and 5/6Nx-PTx-PTH6x, since intermittent PTH pulses induce bone anabolic effects while continuous administration does not achieve to increase bone mass[211]. Other issue that complicates the explanation of the differences between both, 5/6Nx and 5/6Nx-PTx-PTH groups is the existence of other biologically active fragments of PTH. It is assumed that the main biological activity of the PTH resides in the 1-34 fragment[212]. However, other fragments such as 7-84-PTH have demonstrated to inhibit the action of the intact (1-84) PTH[213,214]. In this way, the complexity of the actions and the presence of the several PTH fragments make difficult the comparison of an animal model with clamped PTH to animals with intact parathyroid glands.

Despite the differences between both 5/6Nx and 5/6Nx-PTx-PTH6x, the model of parathyroidectomized 5/6Nx rats with PTH replacement was useful to separate the bone effects of calcimimetics from those dependent of the concomitant reduction of PTH levels. Interestingly, we found that 5/6Nx-PTx-PTH6x rats treated with calcimimetic increased bone turnover with respect to those treated with vehicle, even with similar biochemical parameters between them. These effects might be explained by the activation of the CaSR in bone cells by calcimimetic.

Moreover, two additional groups of parathyroidectomized 5/6Nx rats receiving constant infusion of PTH 1-34 by 9-fold the necessary dose to maintain plasma calcium in a PTx rat with normal renal function were included, one of them receiving calcimimetic and the other one receiving vehicle. As expected, these animals showed increased osteoblast and osteoclast activity as compared with 5/6Nx rats and 5/6Nx-PTx-PTH6x rats. In these conditions of high PTH infusion, calcimimetic administration did not further increase bone turnover. As consequence of the elevated PTH infusion, these animals also increased plasma calcium levels; therefore, we consider that the bone effects of CaSR activation by calcimimetics in conditions of high plasma PTH and calcium are redundant being difficult to separate the effects of the high calcium on CaSR from those of calcimimetic.

The relevance of CaSR activity on bone health was already evaluated by Xue Y. et al in rodents null for PTH and CaSR. In this sense, the anabolic effects of PTH were

reduced in PTH-/- CaSR-/- mice as compared with PTH-/- mice[215]. Likewise, another study showed that high dietary Ca increased bone formation in both wild type and PTH-/- mice, but these effects were absent in PTH-/- CaSR-/- double knockout mice[216]. Similarly, osteoblast specific ablation of CaSR attenuated the anabolic action of PTH[217]. These studies agree with our results that support a critical role of CaSR in bone cell activity.

To confirm that the effects of calcimimetic were triggered directly in bone cells, we performed *in vitro* experiments. In this respect, firstly we checked that CaSR was expressed in the murine osteoblastic cell line UMR 106 and also in human bone marrow MSC. Furthermore, CaSR was functional, since Erk1/2 phosphorylation was modulated by calcimimetic and calcilytic addition. Yamaguchi et al reported that CaSR activation by calcium or its agonists, gadolinium or neomycin, increased osteoblast chemotaxis and proliferation as assessed by DNA synthesis[129]. In the same way, Chattopadhyay N. et al showed that high calcium led to an increased expression of Cyclin D1 in a primary culture of rat calvarial osteoblasts, and this effect was abolished after the expression of a dominant negative form of the CaSR[218].

At contrary, the administration of the calcilytic Calhex 231 inhibited the CaSR downstream signaling in UMR cells, as assessed by the decrease in ERK1/2 phosphorylation. This inhibition of the CaSR signaling was accompanied by a reduction in the expression of osteoblastic genes, demonstrating the critical role of the CaSR on osteogenesis. It has been reported that activation of the CaSR by the calcimimetic R-568 or calcium increases the osteogenic differentiation of human mesenchymal stem cells from amniotic fluid and these effects were abolished by the treatment with the calcilytics Calhex-231 or NPS-2143[219]. This study supports our results that CaSR modulation potentially regulates osteogenesis.

With respect to in vitro osteoclastogenesis our results showed that calcimimetic addition increases *CTSK* expression. Similarly, low calcium concentration used in this experiment generated osteoclast-like cells with a lesser number of nuclei (3-4), suggesting that CaSR activation might also participate in osteoclastogenesis. As described above, RANKL is a potent activator of osteoclastogenesis[220]. The actions

of RANKL are mediated via NFAT transcription factor activation[221–223]. NFAT2 (NFATc1) pathway activation is regulated by the calcium/calmodulin signaling, which in turn leads to the activation of the phosphatase calcineurin and the subsequent dephosphorylation of NFAT2 leading to its nuclear translocation and the transcription of the NFAT2 target genes[224]. In this respect, the reduction in the calcium levels may also inhibit the Calcium/Calcineurin/NFAT signaling that might modulate osteoclastogenesis. However, more studies using calcimimetic at different calcium concentrations are needed to clarify the role of the CaSR on osteoclastogenesis and the signaling pathways involved in this process.

The principal findings in these experiments are summarized in Figure 82.

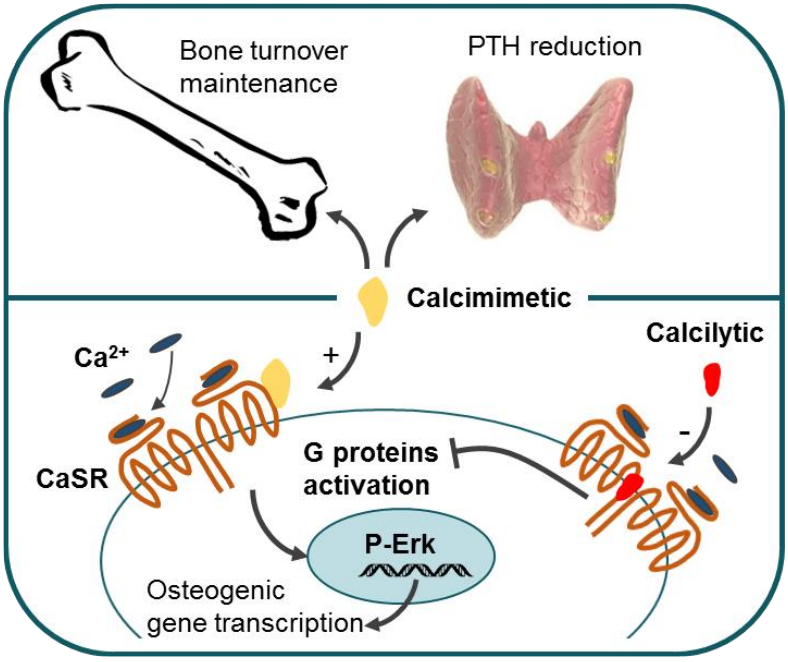

Figure 82. Summary figure shown the bone effects of calcimimetic. Activation of CaSR by calcimimetic decreases PTH production and secretion in the parathyroid glands while it maintains bone turnover. The bone actions of the calcimimetic are mediated through ERK1/2 signaling activation in osteoblasts that lead to increased osteogenic differentiation. Calcilytic administration reduces ERK1/2 phosphorylation and subsequently decreases the transcription of osteogenic genes.

In this thesis we also investigated the bone effects of Mg supplementation in the context of CKD using an animal model of vascular calcification. Mg salts are used in nephrology as phosphate binder, contributing to decrease hyperphosphatemia and vascular calcification[157,160]. *In vitro*, the beneficial effects of Mg on the prevention of phosphate-induced vascular smooth muscle cells calcification have been previously reported[61,225–227]. However, whether Mg supplementation promotes bone effects is unknown; similarly the role of Mg supplementation during the differentiation of bone cells is also unclear. In this respect, we investigated the bone effects of dietary Mg supplementation in an animal model of CKD-associated vascular calcification and our results showed that dietary Mg supplementation dose-dependently decreased plasma phosphate, FGF23 and PTH levels, increased plasma ionized calcium concentration and also prevented renal damage as assessed by the decrease in plasma creatinine levels.

The normalization of plasma calcium and phosphate levels with the prevention of the renal damage in the 5/6Nx rats fed on dietary Mg supplementation decidedly intervene in the progression of SHPT. Furthermore, it has also reported that ionized Mg can bind the CaSR in parathyroid glands and reduce serum PTH production and secretion[228]. Therefore direct actions of Mg on parathyroid glands might also participate in the reduction of PTH levels.

Of note, in spite of the reduced serum PTH levels in the 5/6Nx rats on dietary Mg supplementation, the bone surface covered by osteoblasts was similar among all 5/6Nx groups. Additionally, the bone surface covered by osteoclasts was reduced in the group with higher content of Mg in the diet (5/6Nx+0.6% Mg) as compared with moderate doses of Mg in the diet (5/6Nx+0.1% Mg and 5/6Nx+0.3% Mg groups), consistent with a prevention of the loss of trabecular bone volume. The effects of the high PTH concentration on osteoclast activity are well-known[229]. Furthermore, PTH knockout mice displays a decrease in bone turnover accompanied by an increase in bone volume[127]. Several studies in animals have reported a deleterious effect of Mg deficiency on bone. Rude et al reported that Mg depletion in the diet by the 50% increased the number of osteoclasts in rats[164], at least partially due to an increase in inflammation[230]. Furthermore, it has been reported recently that mild

hypermagnesemia is associated with a lower risk of hip fracture among patients undergoing hemodialysis[231]. This beneficial effects of Mg in bone may be derived, at least in part, by its direct actions on osteoblast activity. In this respect, our study is the first showing that dietary Mg supplementation decreases PTH levels while maintains osteoblast activity.

In addition, the 5/6Nx+0.6%Mg group showed an increase in the osteoid thickness, suggesting that high Mg content in the diet may induce defective mineralization in CKD. In 1988, Moriniere et al showed no significant changes in any bone histomorphometric parameters after 8 or 20 months of treatment with $Mg(OH)_2$, however showed clear tendencies to increase osteoid and decrease the resorption surface[232]. A coetaneous study by Gonella et al. showed that osteomalacia was prevented by decreasing Mg concentration in the dialyzed fluid[233]. These results highlight the importance of Mg levels on bone mineralization in CKD patients.

To confirm whether the Mg effects are triggered directly in osteoblastic cells, we evaluated the effects of increasing doses of $MgCl_2$ on the differentiation of bone marrow MSC into osteoblasts. We found that Mg supplementation in the culture medium increased matrix mineralization and expression of osteogenic master genes. These data support a direct effect of Mg on osteoblast differentiation. Furthermore, the addition of 2-APB, which blocks the Mg channel TRPM7[234,235], led to the contrary effects, indicating that the effects of Mg are triggered intracellularly. Other authors have demonstrated the requirement of TRPM7 for growth and skeletogenesis[236].

We found that Mg supplementation activated the Notch signaling pathway, as assessed by the increased amount of NICD into nuclei of MSC differentiated toward osteoblasts. It has been reported that the activation of Notch signaling is differentially involved in bone development at different stages of osteoblast differentiation. On the one hand, Hilton et al demonstrated that Notch signaling preserves the MSC pool by suppressing osteoblast differentiation[37]. Similarly, Zanotti et al reported that specific overexpression of NICD in osteoblasts inhibits bone formation[237]. Nevertheless, the same authors reported that Notch activation in osteocytes increases trabecular bone formation *in vivo*[38,40]. Notch signaling activation has been also demonstrated in

osteocytes and its conditional activation in these cells promoted bone formation mainly by increasing bone mineralization. On the contrary, loss of function of the prenisilin γ-secretase by haploinsufficiency blocked osteoblast differentiation[39]. Recently, the potential role of Notch signaling in the process of fracture healing has been also elucidated, since the conditional ablation of Notch signaling in mesenchymal progenitor cells leads to inability for fracture union[238]. Altogether, these results highlight the importance of Notch in bone development. We observed *in vitro*, that the activation of the Notch signaling was presumably in the progenitor cells, due to the fact that differentiated osteocyte substantially decreased the protein amount of nuclear NICD, indicating that the pro-osteogenic effects of Mg supplementation may be triggered due to increased proliferation of the progenitor cell pool during differentiation. Taken together, our results suggest that Mg activates NICD nuclear translocation mainly in undifferentiated MSC but not in differentiated osteoblasts, maintaining the stemness and the pool for a more abundant osteogenesis.

The finding of the differential effects of Mg on mineralization *in vitro* and *in vivo* might be due to differences in Mg concentration.

In addition, we performed *in vitro* experiments to investigate whether Mg participates in the colonization and osteoblastic differentiation of MSC in bone scaffolds. We observed that bone scaffolds cultured into Mg-supplemented medium increased cellular proliferation and osteoblast were well-organized. Additionally, MSC differentiated into osteoblasts with Mg supplementation displayed an osteocyte-like shape, and even cytoplasmic processes of the osteocytes were identified by SEM. In this way the pro-osteogenic effects of Mg through Notch signaling activation may contribute, at least in part, to the colonization and osteogenic differentiation of MSC in osteoblasts.

With respect to *in vitro* osteoclastogenesis, we found that Mg supplementation did not exert significant effects without differences in number of nuclei or CTSK expression. However, other authors have reported a potential role of Mg on osteoclast differentiation. Wu L et al, using higher Mg concentrations than those we used, demonstrated that increased levels of Mg extracts promote

osteoblastogenesis while inhibit osteoclastogenesis[239]. On the other site of the spectrum, other *in vitro* studies have reported that Mg deprivation enhances osteoclast differentiation[240]. With respect to these studies, we consider that Mg supplementation may not significantly affect osteoclastogenesis at the doses we investigated (1.4 and 2.6 mM), which are close to the physiological and lower than those previously assayed by other authors.

The main results of the experiments of the effects of Mg on bone are highlighted in Figure 83.

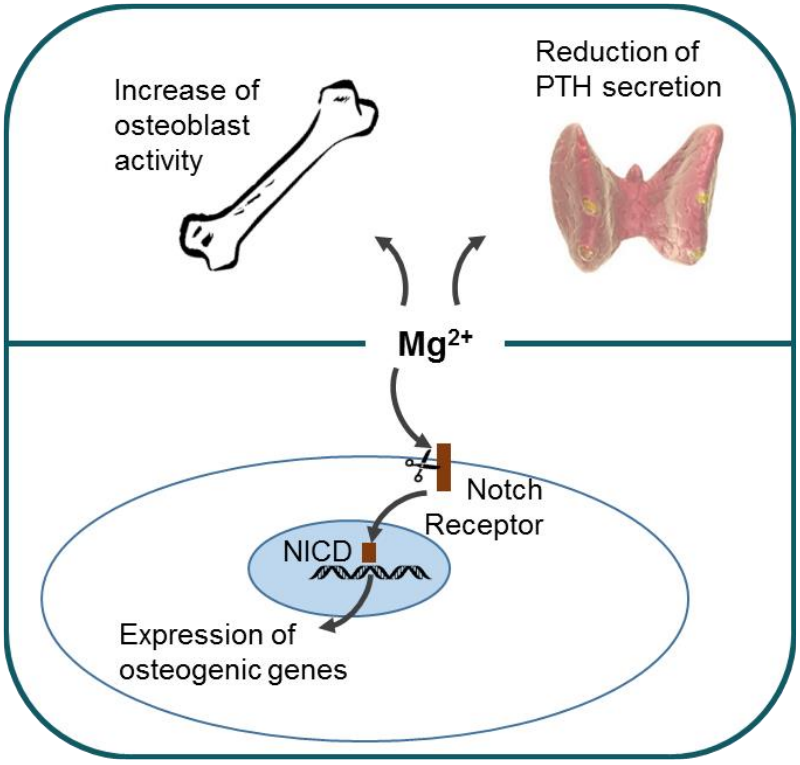

Figure 83. Summary figure of the bone effects of magnesium. In rats with renal insufficiency, Mg supplementation reduces plasma PTH levels while increases osteoblasts activity. *In vitro*, Mg addition increases the osteogenic differentiation of bone marrow mesenchymal stem cells by activation of the Notch signaling pathway.

Finally, the role of FGF23 on bone development was also studied in this thesis. We developed an animal model in rats by reducing the functional renal mass (50%) and

fed with a high phosphate diet that increased plasma intact FGF23 without significant changes in other important parameters of mineral metabolism such as calcium, PTH, serum phosphate or calcitriol. As previously reported, FGF23 increased this early stage of renal insufficiency, even before plasma phosphate, calcium, PTH or calcitriol alterations[84].

Bone histomorphometric analysis revealed that in hemi-nephrectomized animals with high phosphate in the diet and high FGF23 (1/2Nx+1.2%P) there was an increased bone turnover and a tendency to decrease trabecular bone volume as compared with those receiving Sham operation and fed on the same diet. The bone effects of FGF23 have been already suggested previously. Sitara D et al developed a FGF23 and NaPi-IIa double knockout murine model to separate the FGF23 bone effects from those derived from phosphaturia. In this animal model, hyperphosphatemia was prevented, yet defective bone mineralization remained existent, indicating that, at least partially, FGF23 decreases bone mineralization[241].

The bone effects of elevated FGF23 have been also evaluated in Hyp mice (from hypophosphatemia, gene symbol Hyp), a well-established murine model for X-linked hypophosphatemia that present high levels of plasma intact FGF23[242]. Murali SK et al found that in osteoblasts FGF23 binds the FGFR3 and impairs mineralization by suppression of the tissue non-specific alkaline phosphatase (TNAP) and subsequent accumulation of pyrophosphate, a potent inhibitor of calcification[243]. In addition, they reported that FGF23 also increases osteopontin expression, a secreted protein that binds Ca and inhibits hydroxyapatite crystal formation. In this regard, the FGF23-FGFR3 signaling in bone cells may directly impair mineralization in conditions of high FGF23[192].

In our study we found changes in bone turnover in the animals with higher plasma FGF23 levels, however we did not observed sign of defective mineralization. This difference with the previous studies may be due to the fact that the increase in the FGF23 levels in our animal model was not severe in order to avoid additional effects on mineral metabolism parameters such as plasma phosphate or ionized calcium.

Furthermore, we observed that 1/2Nx-1.2%P animals showed significant changes in trabecular bone microstructure, a critical event in the development of renal

osteodystrophy[244]. Thus, bone abnormalities occur in an early stage of CKD and FGF23 may participate in its development.

We also found that high plasma FGF23 levels were accompanied by high plasma sclerostin concentration. In this regard, increased sclerostin levels have been associated with decreased bone formation in long-term immobilized postmenopausal women[245], which may be mainly due to an inhibition of the canonical Wnt/β-catenin pathway[52,53].

It is interesting to note that despite the increased osteoblast activity, the expression of osteogenic genes was reduced in 1/2Nx-1.2%P rats as compared with Sham-1.2%P suggesting a delay in the maturation state of the osteocytes. This situation has been recently reported by others[246] who suggest a stalled maturation of the osteocytes in young dialysis (CKD 5) and predialysis (CKD 2-4) patients.

To further confirm the direct effects of FGF23 in osteoblasts, *in vitro* experiments were also performed. We observed that the addition of rat recombinant FGF23 during MSC osteogenic differentiation also decreased the expression of osteogenic genes. These results agree with others that reported similar effects of FGF23 on osteogenesis. In this way, *in vitro* studies with rat calvaria cells over-expressing FGF23 have shown that elevated FGF23 decreases matrix mineralization and down-regulates osteoblast marker genes. Furthermore, these effects were abrogated by administration of SU5402, a non-specific FGFR1 inhibitor[178], indicating that the effects of FGF23 may be triggered presumably through FGFR signaling.

Moreover, we observed that FGF23 administration to MSC differentiated into osteoblasts decreased the nuclear translocation of β-catenin after 24h, consistent with a decrease in the expression of osteogenic marker genes and an increase in SOST expression. These results are consistent with those observed in bone lysates of 1/2Nx-1.2%P rats, which also showed decreased osteogenic genes expression and increased SOST mRNA expression. It might suggest an involvement of FGF23 and Wnt/β-catenin pathway during the development of bone alterations in early CKD. In a murine model of renal insufficiency (7/8Nx rats), it has been reported that an increase in the expression of Wnt inhibitors occurs as renal impairment progresses time-dependently in animals fed on a high phosphate diet associated with a

reduction in tibial bone mineral density. Uremic serum from these animals or FGF23 plus α-klotho increased DKK, Secreted frizzled-related protein 1 (SFRP1) and the ratio phospho-β-catenin/total β-catenin[247].

On the other hand, we also investigated the effects of FGF23 on osteoclastogenesis by addition of rat recombinant FGF23 during *in vitro* osteoclastic differentiation of hematopoietic stem cells. Interestingly we found that FGF23 increased the number of osteoclasts, consistent with higher *CTSK* gene expression. The effects of FGF23 on osteoclastogenesis have not been previously described and this study is the first demonstrating an effect of FGF23 on osteoclasts. Nevertheless, additional studies are needed to clarify the effects of FGF23 on the bone resorptive capacity of the osteoclasts *in vitro*.

Of note, the osteoclasts treated with FGF23 became oversized and presented a lower number of nuclei as compared with control osteoclasts. In this respect, the increased enlargement of the osteoclasts in end stage renal disease has been previously reported by Kaye et al[248]. They found that osteoclasts increased the cell area in patients on dialysis, corresponding with a higher area of the lacuna[248]. It is important to note that FGF23 levels are extremely high in these patients and our results suggest that FGF23 may play a critical role in this process. In addition, the increased number of nuclei per osteoclast have been directly associated with the size of the resorption pit[249,250]. In this respect, our results indicate that FGF23 increase the osteoclast enlargement, which may lead to increased bone resorption, as we observed in the *in vivo* experiment. However, the treatment with FGF23 decreased the number of nuclei per osteoclasts that may also reduce the resorptive capability of the osteoclasts. Future experiments for evaluation of osteoclast resorption *in vitro* may help to clarify the role of FGF23 on osteoclast activity.

The main findings in the study of the bone effects of FGF23 are displayed in Figure 84.

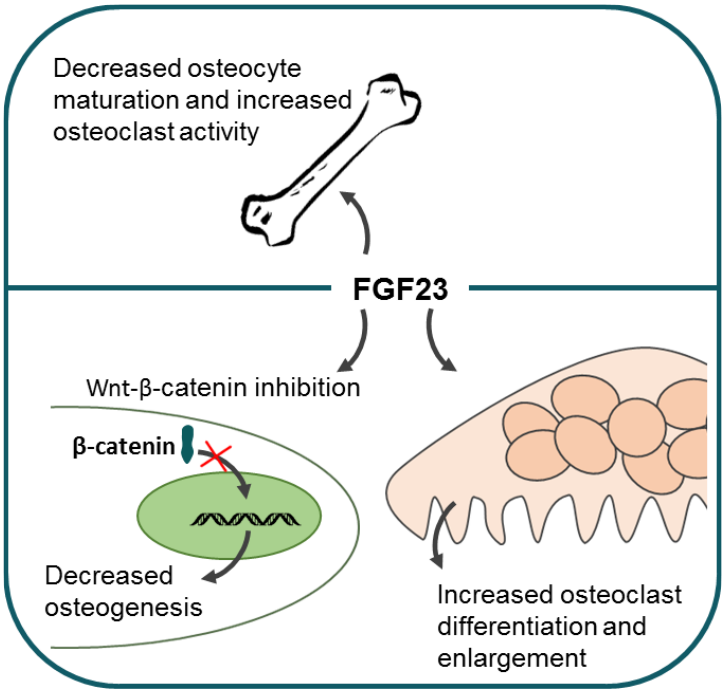

Figure 84. Summary figure shown the bone effects of FGF23. *In vivo*, high plasma intact FGF23 decreases osteoblast-osteocyte transition and increases osteoclast activity. *In vitro*, high FGF23 concentration decreased osteogenic differentiation of bone marrow mesenchymal stem cells and these effects are, at least in part, mediated by the inhibition of the canonical Wnt-pathway. Furthermore, high FGF23 concentration increases osteoclastogenesis and osteoclast enlargement.

Taken together, our studies shed some light on the complex scenario of CKD-MBD and suggest the development of clinical studies in the field of renal osteodystrophy that can lead to look for new therapeutical perspectives in the use of calcitriol, calcimimetic and Mg in the context of CKD and the consideration of FGF23 as an early biomarker of renal osteodystrophy.

Interactions among these molecules may occur *in vivo*. Our results demonstrate that calcitriol has a hormetic dose-response in bone (i.e. it supports mineralization at lower doses and decrease mineralization at higher doses) that is not dependent of the PTH action. However, calcitriol administration dose-dependently increased plasma FGF23 concentration, which may also influence bone mineralization.

Additionally, treatment with high doses of calcitriol produced hypercalcemia, and high calcium may also activate the CaSR in bone cells.

We highlighted a potential role of CaSR modulation on bone turnover. Physiologically, the gradual calcium concentration in the bone microenvironment may contribute to the coupling mechanism for bone resorption and bone formation. Thus, the increased calcium concentration in the area of resorption may participate in the activation and chemotaxis of osteoblasts, resulting in the classical situation of groups of bone-forming osteoblasts chasing bone-resorbing osteoclasts. This hypothesis agrees with previous studies that reported a role of the CaSR in osteoblast migration[129].

Mainly, positive allosteric modulation of the CaSR with calcimimetics is routinely used in hemodialysis patients in order to maintain plasma PTH levels within a non-pathological range. In this population, bone abnormalities are common and the side effects of calcimimetics in bone cells may be beneficial in scenarios of low bone turnover. In this respect, adynamic bone is the prevalent form of renal osteodystrophy in CKD patients[251,252], in which bone turnover is almost absent. Our results showed that calcimimetics maintain bone turnover despite the concomitant decrease in the plasma PTH levels in an animal model of renal insufficiency, and the treatment of SHPT with calcimimetic may prevent the development of adynamic bone. Clinical studies are needed to further clarify the actions of calcimimetics on bone turnover.

Of note, Zaidi et al reported that divalent cations, including Mg, may regulate osteoclast differentiation through, at that time still hypothetical, calcium receptor[253]. Thus, besides the pro-osteogenic effects of Mg mediated through the activation of the Notch pathway, the additional effects derived from the activation of the CaSR by Mg should not be excluded, resulting in synergistic effects. Nevertheless, in presence of calcium and phosphate, high Mg may produce whitlockite instead of hydroxyapatite, [162]. Whitlockite is the second most abundant mineral in bone[254], and it has been reported that whitlockite has higher osteogenic potential than hydroxyapatite[255]. Hydroxyapatite and whitlockite ratio is fine-tuned in bone, albeit,

increased Mg or decreased pH block hydroxyapatite crystal formation in favor of whitlockite biomineralization and this fact may impede stable bone mineralization[256]. Another key finding in this thesis is the implication of FGF23 in bone abnormalities in an animal model with a 50% reduction of renal mass.

Animals with higher intact FGF23 levels shown increased bone turnover and a trend to decrease trabecular bone volume was observed. These findings highlight the role of FGF23 in the early development of bone abnormalities. As indicated previously, a supraphysiological dose of CTR increase plasma FGF23 and sclerostin levels. In this respect, the extremely high FGF23 levels induced by the treatment with CTR may contribute at least partially to elevate plasma sclerostin, which in turn may lead to impaired mineralization and decreased bone volume.

It is interesting to note that *in vitro* experiments demonstrate an anti-osteogenic effect of FGF23, which may not agree with the increased bone turnover observed in the *in vivo* model. However, our data demonstrated that FGF23 impaired osteoblast maturation. In addition, FGF23 directly enhances osteoclast differentiation, which may explain the increased turnover due to the coupling between bone cells. In view of these results, FGF23 may play an important role in the development of renal osteodystrophy at early stages of renal disease. However, our model did not replicate a progressive renal damage as the observed in the CKD population and clinical studies are needed to further clarify the involvement of FGF23 in early bone alterations.

The results from the studies in this thesis indicate that bone is heterogeneously affected in CKD and this fact is clinically noticed since the spectrum of renal osteodystrophy is very broad in CKD patients. Historically, the most of the bone disorders associated with CKD have been related to the excessive plasma PTH levels, however other factors may also influence bone status. The administration of CTR to treat secondary hyperparathyroidism may also alter bone mineralization and osteogenesis, particularly if high doses are administered. Furthermore, excessive CTR elevates plasma FGF23 levels, which are very high in hemodialysis patients and also affects osteocyte maturation and osteoclastogenesis. On the other hand, patients that present hypomagnesemia may also develop low bone turnover

diseases or adynamic bone. Therefore, the maintenance of the plasma Mg levels within a narrow range or moderately elevated may be beneficial. Moreover, treatment with calcimimetic maintains bone turnover despite the concomitant decrease in plasma PTH by acting on the CaSR in osteoblasts. In this way, the treatment with calcimimetic may be useful to prevent adynamic bone disease in CKD patients.

Taken together, we hope that our results may contribute to the understanding of the complex scenario of the bone and mineral disorders found in the context of renal diseases and may be helpful for the establishment of future studies in the search of a better quality of life for renal disease patients.

CONCLUSIONS

1. In a rat model of renal insufficiency, Calcitriol administration at doses that do not promote hyperphosphatemia and hypercalcemia reduces the time of mineralization and osteoblast activity in a PTH-independent manner.
2. *In vitro*, calcitriol inhibits osteoblast differentiation and mineralization and promotes osteoclast differentiation.
3. In a murine model of renal insufficiency, treatment with calcimimetic maintains bone turnover despite the concomitant decrease in parathyroid hormone levels.
4. Calcium sensing receptor modulation by calcimimetic and calcilytic regulates osteoblast differentiation and mineralization and may promote osteoclast differentiation.
5. In a rat model of vascular calcification, dietary magnesium supplementation maintains osteoblast activity in bone and reduces the osteoclast activity in spite of the decrease in plasma parathyroid hormone concentration, however at high doses might promote defective mineralization.
6. *In vitro*, magnesium supplementation promotes osteoblast differentiation and mineralization and do not significantly affects osteoclast differentiation.
7. The increase in plasma FGF23 is associated with increased bone turnover and changes in trabecular bone microstructure in a murine model of early CKD.
8. High FGF23 concentration decreases osteogenic differentiation by inhibition of the Wnt/β-catenin pathway and increases osteoclast differentiation.

REFERENCES

1. Silva HC, Pinheiro MM, Genaro PS, et al. Higher prevalence of morphometric vertebral fractures in patients with recent coronary events independently of BMD measurements. *Bone*. 2013;52(2):562-567. doi:10.1016/j.bone.2012.11.004
2. Tsai C-H, Lin C-L, Hsu H-C, Chung W-S. Increased risk of coronary heart disease in patients with hip fracture: a nationwide cohort study. *Osteoporos Int J Establ Result Coop Eur Found Osteoporos Natl Osteoporos Found USA*. 2015;26(6):1849-1855. doi:10.1007/s00198-015-3097-y
3. Karsenty G, Ferron M. The contribution of bone to whole-organism physiology. *Nature*. 2012;481(7381):314-320. doi:10.1038/nature10763
4. D'Amelio P, Sassi F. Osteoimmunology: from mice to humans. *BoneKEy Rep*. 2016;5:802. doi:10.1038/bonekey.2016.29
5. Almeida M, Laurent MR, Dubois V, et al. Estrogens and Androgens in Skeletal Physiology and Pathophysiology. *Physiol Rev*. 2017;97(1):135-187. doi:10.1152/physrev.00033.2015
6. Mosialou I, Shikhel S, Liu J-M, et al. MC4R-dependent suppression of appetite by bone-derived lipocalin 2. *Nature*. 2017;543(7645):385-390. doi:10.1038/nature21697
7. Oury F, Khrimian L, Denny CA, et al. Maternal and offspring pools of osteocalcin influence brain development and functions. *Cell*. 2013;155(1):228-241. doi:10.1016/j.cell.2013.08.042
8. Gutiérrez OM, Januzzi JL, Isakova T, et al. Fibroblast growth factor 23 and left ventricular hypertrophy in chronic kidney disease. *Circulation*. 2009;119(19):2545-2552. doi:10.1161/CIRCULATIONAHA.108.844506
9. Faul C, Amaral AP, Oskouei B, et al. FGF23 induces left ventricular hypertrophy. *J Clin Invest*. 2011;121(11):4393-4408. doi:10.1172/JCI46122
10. Scialla JJ, Xie H, Rahman M, et al. Fibroblast Growth Factor-23 and Cardiovascular Events in CKD. *J Am Soc Nephrol*. 2014;25(2):349-360. doi:10.1681/ASN.2013050465
11. Murray J. Favus, David A. Bushinsky,, and Jacob Lemann Jr. *Regulation of Calcium, Magnisium, and Phsophate Metabolism. In: Favus ML Editor. Primer of the Metabolic Bone Disease and Disorders of Mineral Metabolism, 6th Edition.* 6th Edition. Rittenhouse Book Distributors; 2006.
12. Beresford JN. Osteogenic stem cells and the stromal system of bone and marrow. *Clin Orthop*. 1989;(240):270-280.
13. Beresford JN, Bennett JH, Devlin C, Leboy PS, Owen ME. Evidence for an inverse relationship between the differentiation of adipocytic and osteogenic cells in rat marrow stromal cell cultures. *J Cell Sci*. 1992;102 (Pt 2):341-351.
14. Chen Q, Shou P, Zheng C, et al. Fate decision of mesenchymal stem cells: adipocytes or osteoblasts? *Cell Death Differ*. 2016;23(7):1128-1139. doi:10.1038/cdd.2015.168
15. Kim M, Kim C, Choi YS, Kim M, Park C, Suh Y. Age-related alterations in mesenchymal stem cells related to shift in differentiation from osteogenic to adipogenic potential: implication to age-associated bone diseases and defects. *Mech Ageing Dev*. 2012;133(5):215-225. doi:10.1016/j.mad.2012.03.014
16. Fan Y, Hanai J-I, Le PT, et al. Parathyroid Hormone Directs Bone Marrow Mesenchymal Cell Fate. *Cell Metab*. 2017;25(3):661-672. doi:10.1016/j.cmet.2017.01.001

17. Kraenzlin ME, Meier C. Parathyroid hormone analogues in the treatment of osteoporosis. *Nat Rev Endocrinol*. 2011;7(11):647-656. doi:10.1038/nrendo.2011.108
18. Nakashima K, Zhou X, Kunkel G, et al. The novel zinc finger-containing transcription factor osterix is required for osteoblast differentiation and bone formation. *Cell*. 2002;108(1):17-29.
19. Wei J, Karsenty G. An overview of the metabolic functions of osteocalcin. *Rev Endocr Metab Disord*. 2015;16(2):93-98. doi:10.1007/s11154-014-9307-7
20. Franz-Odendaal TA, Hall BK, Witten PE. Buried alive: how osteoblasts become osteocytes. *Dev Dyn Off Publ Am Assoc Anat*. 2006;235(1):176-190. doi:10.1002/dvdy.20603
21. Dallas SL, Prideaux M, Bonewald LF. The Osteocyte: An Endocrine Cell … and More. *Endocr Rev*. 2013;34(5):658-690. doi:10.1210/er.2012-1026
22. Knothe Tate ML, Adamson JR, Tami AE, Bauer TW. The osteocyte. *Int J Biochem Cell Biol*. 2004;36(1):1-8. doi:10.1016/S1357-2725(03)00241-3
23. Pajevic PD. Regulation of bone resorption and mineral homeostasis by osteocytes. *IBMS BoneKEy Wash*. 2009;6:63-70. doi:http://dx.doi.org/10.1138/20090363
24. Udagawa N, Takahashi N, Akatsu T, et al. Origin of osteoclasts: mature monocytes and macrophages are capable of differentiating into osteoclasts under a suitable microenvironment prepared by bone marrow-derived stromal cells. *Proc Natl Acad Sci*. 1990;87(18):7260-7264. doi:10.1073/pnas.87.18.7260
25. Cole AA, Walters LM. Tartrate-resistant acid phosphatase in bone and cartilage following decalcification and cold-embedding in plastic. *J Histochem Cytochem Off J Histochem Soc*. 1987;35(2):203-206. doi:10.1177/35.2.3540104
26. Parfitt AM. Osteonal and hemi-osteonal remodeling: the spatial and temporal framework for signal traffic in adult human bone. *J Cell Biochem*. 1994;55(3):273-286. doi:10.1002/jcb.240550303
27. Hsu H, Lacey DL, Dunstan CR, et al. Tumor necrosis factor receptor family member RANK mediates osteoclast differentiation and activation induced by osteoprotegerin ligand. *Proc Natl Acad Sci U S A*. 1999;96(7):3540-3545.
28. Lacey DL, Timms E, Tan HL, et al. Osteoprotegerin ligand is a cytokine that regulates osteoclast differentiation and activation. *Cell*. 1998;93(2):165-176.
29. Udagawa N, Takahashi N, Yasuda H, et al. Osteoprotegerin produced by osteoblasts is an important regulator in osteoclast development and function. *Endocrinology*. 2000;141(9):3478-3484. doi:10.1210/endo.141.9.7634
30. Saftig P, Hunziker E, Wehmeyer O, et al. Impaired osteoclastic bone resorption leads to osteopetrosis in cathepsin-K-deficient mice. *Proc Natl Acad Sci U S A*. 1998;95(23):13453-13458.
31. Hayman AR, Jones SJ, Boyde A, et al. Mice lacking tartrate-resistant acid phosphatase (Acp 5) have disrupted endochondral ossification and mild osteopetrosis. *Dev Camb Engl*. 1996;122(10):3151-3162.
32. Artavanis-Tsakonas S, Rand MD, Lake RJ. Notch Signaling: Cell Fate Control and Signal Integration in Development. *Science*. 1999;284(5415):770-776. doi:10.1126/science.284.5415.770
33. Bray SJ. Notch signalling in context. *Nat Rev Mol Cell Biol*. 2016;17(11):722-735. doi:10.1038/nrm.2016.94

34. Tezuka K-I, Yasuda M, Watanabe N, et al. Stimulation of osteoblastic cell differentiation by Notch. *J Bone Miner Res Off J Am Soc Bone Miner Res*. 2002;17(2):231-239. doi:10.1359/jbmr.2002.17.2.231
35. Nobta M, Tsukazaki T, Shibata Y, et al. Critical regulation of bone morphogenetic protein-induced osteoblastic differentiation by Delta1/Jagged1-activated Notch1 signaling. *J Biol Chem*. 2005;280(16):15842-15848. doi:10.1074/jbc.M412891200
36. Engin F, Yao Z, Yang T, et al. Dimorphic effects of Notch signaling in bone homeostasis. *Nat Med*. 2008;14(3):299-305. doi:10.1038/nm1712
37. Hilton MJ, Tu X, Wu X, et al. Notch signaling maintains bone marrow mesenchymal progenitors by suppressing osteoblast differentiation. *Nat Med*. 2008;14(3):306-314. doi:10.1038/nm1716
38. Canalis E, Adams DJ, Boskey A, Parker K, Kranz L, Zanotti S. Notch signaling in osteocytes differentially regulates cancellous and cortical bone remodeling. *J Biol Chem*. 2013;288(35):25614-25625. doi:10.1074/jbc.M113.470492
39. Liu P, Ping Y, Ma M, et al. Anabolic actions of Notch on mature bone. *Proc Natl Acad Sci*. 2016;113(15):E2152-E2161. doi:10.1073/pnas.1603399113
40. Canalis E, Bridgewater D, Schilling L, Zanotti S. Canonical Notch activation in osteocytes causes osteopetrosis. *Am J Physiol Endocrinol Metab*. 2016;310(2):E171-182. doi:10.1152/ajpendo.00395.2015
41. Ji Y, Ke Y, Gao S. Intermittent activation of notch signaling promotes bone formation. *Am J Transl Res*. 2017;9(6):2933-2944.
42. Niehrs C. The complex world of WNT receptor signalling. *Nat Rev Mol Cell Biol*. 2012;13(12):767-779. doi:10.1038/nrm3470
43. Boyden LM, Mao J, Belsky J, et al. High bone density due to a mutation in LDL-receptor-related protein 5. *N Engl J Med*. 2002;346(20):1513-1521. doi:10.1056/NEJMoa013444
44. Gong Y, Slee RB, Fukai N, et al. LDL receptor-related protein 5 (LRP5) affects bone accrual and eye development. *Cell*. 2001;107(4):513-523.
45. Krishnan V, Bryant HU, Macdougald OA. Regulation of bone mass by Wnt signaling. *J Clin Invest*. 2006;116(5):1202-1209. doi:10.1172/JCI28551
46. Bafico A, Gazit A, Pramila T, Finch PW, Yaniv A, Aaronson SA. Interaction of frizzled related protein (FRP) with Wnt ligands and the frizzled receptor suggests alternative mechanisms for FRP inhibition of Wnt signaling. *J Biol Chem*. 1999;274(23):16180-16187.
47. Dann CE, Hsieh JC, Rattner A, Sharma D, Nathans J, Leahy DJ. Insights into Wnt binding and signalling from the structures of two Frizzled cysteine-rich domains. *Nature*. 2001;412(6842):86-90. doi:10.1038/35083601
48. Semënov M, Tamai K, He X. SOST is a ligand for LRP5/LRP6 and a Wnt signaling inhibitor. *J Biol Chem*. 2005;280(29):26770-26775. doi:10.1074/jbc.M504308200
49. Li X, Zhang Y, Kang H, et al. Sclerostin binds to LRP5/6 and antagonizes canonical Wnt signaling. *J Biol Chem*. 2005;280(20):19883-19887. doi:10.1074/jbc.M413274200
50. Mao B, Wu W, Li Y, et al. LDL-receptor-related protein 6 is a receptor for Dickkopf proteins. *Nature*. 2001;411(6835):321-325. doi:10.1038/35077108

51. Van Buchem FS, Hadders HN, Ubbens R. An uncommon familial systemic disease of the skeleton: hyperostosis corticalis generalisata familiaris. *Acta Radiol*. 1955;44(2):109-120.
52. Balemans W, Ebeling M, Patel N, et al. Increased bone density in sclerosteosis is due to the deficiency of a novel secreted protein (SOST). *Hum Mol Genet*. 2001;10(5):537-543.
53. Brunkow ME, Gardner JC, Van Ness J, et al. Bone dysplasia sclerosteosis results from loss of the SOST gene product, a novel cystine knot-containing protein. *Am J Hum Genet*. 2001;68(3):577-589.
54. Evenepoel P, D'Haese P, Brandenburg V. Sclerostin and DKK1: new players in renal bone and vascular disease. *Kidney Int*. 2015;88(2):235-240. doi:10.1038/ki.2015.156
55. Cejka D, Herberth J, Branscum AJ, et al. Sclerostin and Dickkopf-1 in renal osteodystrophy. *Clin J Am Soc Nephrol CJASN*. 2011;6(4):877-882. doi:10.2215/CJN.06550810
56. Behets GJ, Viaene L, Meijers B, et al. Circulating levels of sclerostin but not DKK1 associate with laboratory parameters of CKD-MBD. *PloS One*. 2017;12(5):e0176411. doi:10.1371/journal.pone.0176411
57. Sabbagh Y, Graciolli FG, O'Brien S, et al. Repression of osteocyte Wnt/β-catenin signaling is an early event in the progression of renal osteodystrophy. *J Bone Miner Res Off J Am Soc Bone Miner Res*. 2012;27(8):1757-1772. doi:10.1002/jbmr.1630
58. Pelletier S, Dubourg L, Carlier M-C, Hadj-Aissa A, Fouque D. The relation between renal function and serum sclerostin in adult patients with CKD. *Clin J Am Soc Nephrol CJASN*. 2013;8(5):819-823. doi:10.2215/CJN.07670712
59. Cejka D, Jäger-Lansky A, Kieweg H, et al. Sclerostin serum levels correlate positively with bone mineral density and microarchitecture in haemodialysis patients. *Nephrol Dial Transplant Off Publ Eur Dial Transpl Assoc - Eur Ren Assoc*. 2012;27(1):226-230. doi:10.1093/ndt/gfr270
60. Moe SM, Chen NX, Newman CL, et al. Anti-sclerostin antibody treatment in a rat model of progressive renal osteodystrophy. *J Bone Miner Res Off J Am Soc Bone Miner Res*. 2015;30(3):499-509. doi:10.1002/jbmr.2372
61. Montes de Oca A, Guerrero F, Martinez-Moreno JM, et al. Magnesium inhibits Wnt/β-catenin activity and reverses the osteogenic transformation of vascular smooth muscle cells. *PloS One*. 2014;9(2):e89525. doi:10.1371/journal.pone.0089525
62. Muñoz-Castañeda JR, Herencia C, Pendón-Ruiz de Mier MV, et al. Differential regulation of renal Klotho and FGFR1 in normal and uremic rats. *FASEB J Off Publ Fed Am Soc Exp Biol*. 2017;31(9):3858-3867. doi:10.1096/fj.201700006R
63. Brown EM, Gamba G, Riccardi D, et al. Cloning and characterization of an extracellular Ca(2+)-sensing receptor from bovine parathyroid. *Nature*. 1993;366(6455):575-580. doi:10.1038/366575a0
64. de Groot T, Lee K, Langeslag M, et al. Parathyroid hormone activates TRPV5 via PKA-dependent phosphorylation. *J Am Soc Nephrol JASN*. 2009;20(8):1693-1704. doi:10.1681/ASN.2008080873
65. Christakos S, Lieben L, Masuyama R, Carmeliet G. Vitamin D endocrine system and the intestine. *BoneKEy Rep*. 2014;3. doi:10.1038/bonekey.2013.230

66. Huang JC, Sakata T, Pfleger LL, et al. PTH differentially regulates expression of RANKL and OPG. *J Bone Miner Res Off J Am Soc Bone Miner Res*. 2004;19(2):235-244. doi:10.1359/JBMR.0301226
67. Blair HC, Larrouture QC, Li Y, et al. Osteoblast Differentiation and Bone Matrix Formation In Vivo and In Vitro. *Tissue Eng Part B Rev*. 2016;23(3):268-280. doi:10.1089/ten.teb.2016.0454
68. Boskey AL, Coleman R. Aging and bone. *J Dent Res*. 2010;89(12):1333-1348. doi:10.1177/0022034510377791
69. Bacic D, Lehir M, Biber J, Kaissling B, Murer H, Wagner CA. The renal Na+/phosphate cotransporter NaPi-IIa is internalized via the receptor-mediated endocytic route in response to parathyroid hormone. *Kidney Int*. 2006;69(3):495-503. doi:10.1038/sj.ki.5000148
70. Slatopolsky E, Finch J, Denda M, et al. Phosphorus restriction prevents parathyroid gland growth. High phosphorus directly stimulates PTH secretion in vitro. *J Clin Invest*. 1996;97(11):2534-2540. doi:10.1172/JCI118701
71. Almaden Y, Canalejo A, Hernandez A, et al. Direct effect of phosphorus on PTH secretion from whole rat parathyroid glands in vitro. *J Bone Miner Res Off J Am Soc Bone Miner Res*. 1996;11(7):970-976. doi:10.1002/jbmr.5650110714
72. Shimada T, Mizutani S, Muto T, et al. Cloning and characterization of FGF23 as a causative factor of tumor-induced osteomalacia. *Proc Natl Acad Sci U S A*. 2001;98(11):6500-6505. doi:10.1073/pnas.101545198
73. Lavi-Moshayoff V, Wasserman G, Meir T, Silver J, Naveh-Many T. PTH increases FGF23 gene expression and mediates the high-FGF23 levels of experimental kidney failure: a bone parathyroid feedback loop. *Am J Physiol Renal Physiol*. 2010;299(4):F882-889. doi:10.1152/ajprenal.00360.2010
74. Lamb KE, Lodhi S, Meier-Kriesche H-U. Long-term renal allograft survival in the United States: a critical reappraisal. *Am J Transplant Off J Am Soc Transplant Am Soc Transpl Surg*. 2011;11(3):450-462. doi:10.1111/j.1600-6143.2010.03283.x
75. Brück K, Stel VS, Gambaro G, et al. CKD Prevalence Varies across the European General Population. *J Am Soc Nephrol JASN*. 2016;27(7):2135-2147. doi:10.1681/ASN.2015050542
76. Otero A, de Francisco A, Gayoso P, García F, EPIRCE Study Group. Prevalence of chronic renal disease in Spain: results of the EPIRCE study. *Nefrol Publicacion Of Soc Espanola Nefrol*. 2010;30(1):78-86. doi:10.3265/Nefrologia.pre2009.Dic.5732
77. GBD 2016 Causes of Death Collaborators. Global, regional, and national age-sex specific mortality for 264 causes of death, 1980-2016: a systematic analysis for the Global Burden of Disease Study 2016. *Lancet Lond Engl*. 2017;390(10100):1151-1210. doi:10.1016/S0140-6736(17)32152-9
78. Go AS, Chertow GM, Fan D, McCulloch CE, Hsu C. Chronic kidney disease and the risks of death, cardiovascular events, and hospitalization. *N Engl J Med*. 2004;351(13):1296-1305. doi:10.1056/NEJMoa041031
79. Vervloet MG, Massy ZA, Brandenburg VM, et al. Bone: a new endocrine organ at the heart of chronic kidney disease and mineral and bone disorders. *Lancet Diabetes Endocrinol*. 2014;2(5):427-436. doi:10.1016/S2213-8587(14)70059-2

80. Drüeke TB, Massy ZA. Circulating Klotho levels: clinical relevance and relationship with tissue Klotho expression. *Kidney Int*. 2013;83(1):13-15. doi:10.1038/ki.2012.370
81. John GB, Cheng C-Y, Kuro-o M. Role of Klotho in aging, phosphate metabolism, and CKD. *Am J Kidney Dis Off J Natl Kidney Found*. 2011;58(1):127-134. doi:10.1053/j.ajkd.2010.12.027
82. Drüeke TB, Massy ZA. Changing bone patterns with progression of chronic kidney disease. *Kidney Int*. 2016;89(2):289-302. doi:10.1016/j.kint.2015.12.004
83. Shimada T, Kakitani M, Yamazaki Y, et al. Targeted ablation of Fgf23 demonstrates an essential physiological role of FGF23 in phosphate and vitamin D metabolism. *J Clin Invest*. 2004;113(4):561-568. doi:10.1172/JCI19081
84. Isakova T, Wahl P, Vargas GS, et al. Fibroblast growth factor 23 is elevated before parathyroid hormone and phosphate in chronic kidney disease. *Kidney Int*. 2011;79(12):1370-1378. doi:10.1038/ki.2011.47
85. Canalejo R, Canalejo A, Martinez-Moreno JM, et al. FGF23 fails to inhibit uremic parathyroid glands. *J Am Soc Nephrol JASN*. 2010;21(7):1125-1135. doi:10.1681/ASN.2009040427
86. Fukagawa M, Kazama JJ, Kurokawa K. Renal osteodystrophy and secondary hyperparathyroidism. *Nephrol Dial Transplant Off Publ Eur Dial Transpl Assoc - Eur Ren Assoc*. 2002;17 Suppl 10:2-5.
87. Moe S, Drüeke T, Cunningham J, et al. Definition, evaluation, and classification of renal osteodystrophy: a position statement from Kidney Disease: Improving Global Outcomes (KDIGO). *Kidney Int*. 2006;69(11):1945-1953. doi:10.1038/sj.ki.5000414
88. Clement Lucas R. ON A FORM OF LATE RICKETS ASSOCIATED WITH ALBUMINURIA, RICKETS OF ADOLESCENTS. *The Lancet*. 1883;121(3119):993-994. doi:10.1016/S0140-6736(02)37965-0
89. Pendras JP, Erickson RV. Hemodialysis: a successful therapy for chronic uremia. *Ann Intern Med*. 1966;64(2):293-311.
90. Martin KJ, González EA. Metabolic Bone Disease in Chronic Kidney Disease. *J Am Soc Nephrol*. 2007;18(3):875-885. doi:10.1681/ASN.2006070771
91. Lotinun S, Sibonga JD, Turner RT. Evidence that the cells responsible for marrow fibrosis in a rat model for hyperparathyroidism are preosteoblasts. *Endocrinology*. 2005;146(9):4074-4081. doi:10.1210/en.2005-0480
92. Massy Z, Drueke T. Adynamic bone disease is a predominant bone pattern in early stages of chronic kidney disease. *J Nephrol*. 2017;30(5):629-634. doi:10.1007/s40620-017-0397-7
93. Cannata-Andía JB, Rodriguez García M, Gómez Alonso C. Osteoporosis and adynamic bone in chronic kidney disease. *J Nephrol*. 2013;26(1):73-80. doi:10.5301/jn.5000212
94. Picton ML, Moore PR, Mawer EB, et al. Down-regulation of human osteoblast PTH/PTHrP receptor mRNA in end-stage renal failure. *Kidney Int*. 2000;58(4):1440-1449. doi:10.1046/j.1523-1755.2000.00306.x
95. Alem AM, Sherrard DJ, Gillen DL, et al. Increased risk of hip fracture among patients with end-stage renal disease. *Kidney Int*. 2000;58(1):396-399. doi:10.1046/j.1523-1755.2000.00178.x

96. Rodríguez-García M, Gómez-Alonso C, Naves-Díaz M, et al. Vascular calcifications, vertebral fractures and mortality in haemodialysis patients. *Nephrol Dial Transplant Off Publ Eur Dial Transpl Assoc - Eur Ren Assoc*. 2009;24(1):239-246. doi:10.1093/ndt/gfn466
97. Moe SM, Nickolas TL. Fractures in Patients with CKD: Time for Action. *Clin J Am Soc Nephrol CJASN*. 2016;11(11):1929-1931. doi:10.2215/CJN.09500916
98. Wagner J, Jhaveri KD, Rosen L, Sunday S, Mathew AT, Fishbane S. Increased bone fractures among elderly United States hemodialysis patients. *Nephrol Dial Transplant Off Publ Eur Dial Transpl Assoc - Eur Ren Assoc*. 2014;29(1):146-151. doi:10.1093/ndt/gft352
99. Nickolas TL, McMahon DJ, Shane E. Relationship between moderate to severe kidney disease and hip fracture in the United States. *J Am Soc Nephrol JASN*. 2006;17(11):3223-3232. doi:10.1681/ASN.2005111194
100. Denburg MR, Kumar J, Jemielita T, et al. Fracture Burden and Risk Factors in Childhood CKD: Results from the CKiD Cohort Study. *J Am Soc Nephrol JASN*. 2016;27(2):543-550. doi:10.1681/ASN.2015020152
101. Al Helal B, Su WS, Churchill DN, Gangji AS. Relative hypoparathyroidism and hypoalbuminemia are associated with hip fracture in hemodialysis patients. *Clin Nephrol*. 2010;73(2):88-93.
102. Center JR, Nguyen TV, Schneider D, Sambrook PN, Eisman JA. Mortality after all major types of osteoporotic fracture in men and women: an observational study. *Lancet Lond Engl*. 1999;353(9156):878-882. doi:10.1016/S0140-6736(98)09075-8
103. Abrahamsen B, van Staa T, Ariely R, Olson M, Cooper C. Excess mortality following hip fracture: a systematic epidemiological review. *Osteoporos Int J Establ Result Coop Eur Found Osteoporos Natl Osteoporos Found USA*. 2009;20(10):1633-1650. doi:10.1007/s00198-009-0920-3
104. Forsén L, Sogaard AJ, Meyer HE, Edna T, Kopjar B. Survival after hip fracture: short- and long-term excess mortality according to age and gender. *Osteoporos Int J Establ Result Coop Eur Found Osteoporos Natl Osteoporos Found USA*. 1999;10(1):73-78.
105. Carnevale V, Fontana A, Scillitani A, Sinisi R, Romagnoli E, Copetti M. Incidence and all-cause mortality for hip fracture in comparison to stroke, and myocardial infarction: a fifteen years population-based longitudinal study. *Endocrine*. September 2017. doi:10.1007/s12020-017-1423-1
106. Ketteler M, Block GA, Evenepoel P, et al. Executive summary of the 2017 KDIGO Chronic Kidney Disease-Mineral and Bone Disorder (CKD-MBD) Guideline Update: what's changed and why it matters. *Kidney Int*. 2017;92(1):26-36. doi:10.1016/j.kint.2017.04.006
107. Parfitt AM, Drezner MK, Glorieux FH, et al. Bone histomorphometry: standardization of nomenclature, symbols, and units. Report of the ASBMR Histomorphometry Nomenclature Committee. *J Bone Miner Res Off J Am Soc Bone Miner Res*. 1987;2(6):595-610. doi:10.1002/jbmr.5650020617
108. Dempster DW, Compston JE, Drezner MK, et al. Standardized nomenclature, symbols, and units for bone histomorphometry: a 2012 update of the report of the ASBMR Histomorphometry Nomenclature Committee. *J Bone Miner Res Off J Am Soc Bone Miner Res*. 2013;28(1):2-17. doi:10.1002/jbmr.1805

109. Fraser DR, Kodicek E. Unique Biosynthesis by Kidney of a Biologically Active Vitamin D Metabolite. *Nature*. 1970;228(5273):764-766. doi:10.1038/228764a0
110. Brickman AS, Sherrard DJ, Jowsey J, et al. 1,25-dihydroxycholecalciferol. Effect on skeletal lesions and plasma parathyroid hormone levels in uremic osteodystrophy. *Arch Intern Med*. 1974;134(5):883-888.
111. Rutherford WE, Bordier P, Marie P, et al. Phosphate control and 25-hydroxycholecalciferol administration in preventing experimental renal osteodystrophy in the dog. *J Clin Invest*. 1977;60(2):332-341. doi:10.1172/JCI108781
112. Slatopolsky E, Weerts C, Thielan J, Horst R, Harter H, Martin KJ. Marked suppression of secondary hyperparathyroidism by intravenous administration of 1,25-dihydroxy-cholecalciferol in uremic patients. *J Clin Invest*. 1984;74(6):2136-2143. doi:10.1172/JCI111639
113. Howard GA, Turner RT, Sherrard DJ, Baylink DJ. Human bone cells in culture metabolize 25-hydroxyvitamin D3 to 1,25-dihydroxyvitamin D3 and 24,25-dihydroxyvitamin D3. *J Biol Chem*. 1981;256(15):7738-7740.
114. Raisz LG, Trummel CL, Holick MF, DeLuca HF. 1,25-dihydroxycholecalciferol: a potent stimulator of bone resorption in tissue culture. *Science*. 1972;175(4023):768-769.
115. Moorthy AV, Harrington AR, Mazess RB, Simpson DP. Long-term therapy of uremic osteodystrophy in adults with calcitriol. *Clin Nephrol*. 1981;16(2):93-100.
116. Peppone LJ, Hebl S, Purnell JQ, et al. The efficacy of calcitriol therapy in the management of bone loss and fractures: a qualitative review. *Osteoporos Int J Establ Result Coop Eur Found Osteoporos Natl Osteoporos Found USA*. 2010;21(7):1133-1149. doi:10.1007/s00198-009-1136-2
117. Reid IR, Bolland MJ, Grey A. Effects of vitamin D supplements on bone mineral density: a systematic review and meta-analysis. *Lancet Lond Engl*. 2014;383(9912):146-155. doi:10.1016/S0140-6736(13)61647-5
118. Idelevich A, Kerschnitzki M, Shahar R, Monsonego-Ornan E. 1,25(OH)2D3 alters growth plate maturation and bone architecture in young rats with normal renal function. *PloS One*. 2011;6(6):e20772. doi:10.1371/journal.pone.0020772
119. Myrtle JF, Norman AW. Vitamin D: A cholecalciferol metabolite highly active in promoting intestinal calcium transport. *Science*. 1971;171(3966):79-82.
120. Silverberg SJ, Bone HG, Marriott TB, et al. Short-term inhibition of parathyroid hormone secretion by a calcium-receptor agonist in patients with primary hyperparathyroidism. *N Engl J Med*. 1997;337(21):1506-1510. doi:10.1056/NEJM199711203372104
121. Goodman WG, Frazao JM, Goodkin DA, Turner SA, Liu W, Coburn JW. A calcimimetic agent lowers plasma parathyroid hormone levels in patients with secondary hyperparathyroidism. *Kidney Int*. 2000;58(1):436-445. doi:10.1046/j.1523-1755.2000.00183.x
122. Block GA, Martin KJ, de Francisco ALM, et al. Cinacalcet for secondary hyperparathyroidism in patients receiving hemodialysis. *N Engl J Med*. 2004;350(15):1516-1525. doi:10.1056/NEJMoa031633
123. Riccardi D, Valenti G. Localization and function of the renal calcium-sensing receptor. *Nat Rev Nephrol*. 2016;12(7):414-425. doi:10.1038/nrneph.2016.59

124. Brown EM, Thatcher JG, Watson EJ, Leombruno R. Extracellular calcium potentiates the inhibitory effects of magnesium on parathyroid function in dispersed bovine parathyroid cells. *Metabolism*. 1984;33(2):171-176.
125. Kifor O, MacLeod RJ, Diaz R, et al. Regulation of MAP kinase by calcium-sensing receptor in bovine parathyroid and CaR-transfected HEK293 cells. *Am J Physiol Renal Physiol*. 2001;280(2):F291-302. doi:10.1152/ajprenal.2001.280.2.F291
126. Gorvin CM, Babinsky VN, Malinauskas T, et al. A calcium-sensing receptor mutation causing hypocalcemia disrupts a transmembrane salt bridge to activate β-arrestin-biased signaling. *Sci Signal*. 2018;11(518). doi:10.1126/scisignal.aan3714
127. Miao D, He B, Lanske B, et al. Skeletal abnormalities in Pth-null mice are influenced by dietary calcium. *Endocrinology*. 2004;145(4):2046-2053. doi:10.1210/en.2003-1097
128. Yamaguchi T, Olozak I, Chattopadhyay N, et al. Expression of extracellular calcium (Ca2+o)-sensing receptor in human peripheral blood monocytes. *Biochem Biophys Res Commun*. 1998;246(2):501-506. doi:10.1006/bbrc.1998.8648
129. Yamaguchi T, Chattopadhyay N, Kifor O, Butters RR, Sugimoto T, Brown EM. Mouse osteoblastic cell line (MC3T3-E1) expresses extracellular calcium (Ca2+o)-sensing receptor and its agonists stimulate chemotaxis and proliferation of MC3T3-E1 cells. *J Bone Miner Res Off J Am Soc Bone Miner Res*. 1998;13(10):1530-1538. doi:10.1359/jbmr.1998.13.10.1530
130. Dvorak MM, Siddiqua A, Ward DT, et al. Physiological changes in extracellular calcium concentration directly control osteoblast function in the absence of calciotropic hormones. *Proc Natl Acad Sci U S A*. 2004;101(14):5140-5145. doi:10.1073/pnas.0306141101
131. Dvorak-Ewell MM, Chen T-H, Liang N, et al. Osteoblast extracellular Ca2+ -sensing receptor regulates bone development, mineralization, and turnover. *J Bone Miner Res Off J Am Soc Bone Miner Res*. 2011;26(12):2935-2947. doi:10.1002/jbmr.520
132. Chang W, Tu C, Chen T-H, Bikle D, Shoback D. The extracellular calcium-sensing receptor (CaSR) is a critical modulator of skeletal development. *Sci Signal*. 2008;1(35):ra1. doi:10.1126/scisignal.1159945
133. Wada M, Furuya Y, Sakiyama J, et al. The calcimimetic compound NPS R-568 suppresses parathyroid cell proliferation in rats with renal insufficiency. Control of parathyroid cell growth via a calcium receptor. *J Clin Invest*. 1997;100(12):2977-2983. doi:10.1172/JCI119851
134. Chin J, Miller SC, Wada M, Nagano N, Nemeth EF, Fox J. Activation of the calcium receptor by a calcimimetic compound halts the progression of secondary hyperparathyroidism in uremic rats. *J Am Soc Nephrol JASN*. 2000;11(5):903-911.
135. Nemeth EF, Van Wagenen BC, Balandrin MF. Discovery and Development of Calcimimetic and Calcilytic Compounds. *Prog Med Chem*. 2018;57(1):1-86. doi:10.1016/bs.pmch.2017.12.001
136. Goodman WG, Hladik GA, Turner SA, et al. The Calcimimetic agent AMG 073 lowers plasma parathyroid hormone levels in hemodialysis patients with secondary hyperparathyroidism. *J Am Soc Nephrol JASN*. 2002;13(4):1017-1024.

137. Quarles LD, Sherrard DJ, Adler S, et al. The calcimimetic AMG 073 as a potential treatment for secondary hyperparathyroidism of end-stage renal disease. *J Am Soc Nephrol JASN*. 2003;14(3):575-583.
138. Behets GJ, Spasovski G, Sterling LR, et al. Bone histomorphometry before and after long-term treatment with cinacalcet in dialysis patients with secondary hyperparathyroidism. *Kidney Int*. 2015;87(4):846-856. doi:10.1038/ki.2014.349
139. Tennakoon S, Aggarwal A, Kállay E. The calcium-sensing receptor and the hallmarks of cancer. *Biochim Biophys Acta*. 2016;1863(6 Pt B):1398-1407. doi:10.1016/j.bbamcr.2015.11.017
140. Kim W, Takyar FM, Swan K, et al. Calcium-Sensing Receptor Promotes Breast Cancer by Stimulating Intracrine Actions of Parathyroid Hormone-Related Protein. *Cancer Res*. 2016;76(18):5348-5360. doi:10.1158/0008-5472.CAN-15-2614
141. Rodríguez-Hernández CJ, Mateo-Lozano S, García M, et al. Cinacalcet inhibits neuroblastoma tumor growth and upregulates cancer-testis antigens. *Oncotarget*. 2016;7(13):16112-16129. doi:10.18632/oncotarget.7448
142. Yamamura A, Guo Q, Yamamura H, et al. Enhanced Ca(2+)-sensing receptor function in idiopathic pulmonary arterial hypertension. *Circ Res*. 2012;111(4):469-481. doi:10.1161/CIRCRESAHA.112.266361
143. Yamamura A, Yamamura H, Guo Q, et al. Dihydropyridine Ca(2+) channel blockers increase cytosolic [Ca(2+)] by activating Ca(2+)-sensing receptors in pulmonary arterial smooth muscle cells. *Circ Res*. 2013;112(4):640-650. doi:10.1161/CIRCRESAHA.113.300897
144. Yarova PL, Stewart AL, Sathish V, et al. Calcium-sensing receptor antagonists abrogate airway hyperresponsiveness and inflammation in allergic asthma. *Sci Transl Med*. 2015;7(284):284ra60. doi:10.1126/scitranslmed.aaa0282
145. Lee J-W, Park HA, Kwon O-K, et al. NPS 2143, a selective calcium-sensing receptor antagonist inhibits lipopolysaccharide-induced pulmonary inflammation. *Mol Immunol*. 2017;90:150-157. doi:10.1016/j.molimm.2017.07.012
146. Yajima A, Akizawa T, Tsukamoto Y, Kurihara S, Ito A, K Study Group. Impact of cinacalcet hydrochloride on bone histology in patients with secondary hyperparathyroidism. *Ther Apher Dial Off Peer-Rev J Int Soc Apher Jpn Soc Apher Jpn Soc Dial Ther*. 2008;12 Suppl 1:S38-43. doi:10.1111/j.1744-9987.2008.00630.x
147. Moe SM, Abdalla S, Chertow GM, et al. Effects of Cinacalcet on Fracture Events in Patients Receiving Hemodialysis: The EVOLVE Trial. *J Am Soc Nephrol JASN*. 2015;26(6):1466-1475. doi:10.1681/ASN.2014040414
148. Li X, Yu L, Asuncion F, et al. Etelcalcetide (AMG 416), a peptide agonist of the calcium-sensing receptor, preserved cortical bone structure and bone strength in subtotal nephrectomized rats with established secondary hyperparathyroidism. *Bone*. 2017;105:163-172. doi:10.1016/j.bone.2017.08.026
149. Hutchison AJ, Smith CP, Brenchley PEC. Pharmacology, efficacy and safety of oral phosphate binders. *Nat Rev Nephrol*. 2011;7(10):578-589. doi:10.1038/nrneph.2011.112
150. Sullivan C, Sayre SS, Leon JB, et al. Effect of food additives on hyperphosphatemia among patients with end-stage renal disease: a randomized controlled trial. *JAMA*. 2009;301(6):629-635. doi:10.1001/jama.2009.96

151. Shutto Y, Shimada M, Kitajima M, et al. Inadequate awareness among chronic kidney disease patients regarding food and drinks containing artificially added phosphate. *PloS One*. 2013;8(11):e78660. doi:10.1371/journal.pone.0078660
152. Tonelli M, Sacks F, Pfeffer M, Gao Z, Curhan G, Cholesterol And Recurrent Events Trial Investigators. Relation between serum phosphate level and cardiovascular event rate in people with coronary disease. *Circulation*. 2005;112(17):2627-2633. doi:10.1161/CIRCULATIONAHA.105.553198
153. Block GA, Klassen PS, Lazarus JM, Ofsthun N, Lowrie EG, Chertow GM. Mineral metabolism, mortality, and morbidity in maintenance hemodialysis. *J Am Soc Nephrol JASN*. 2004;15(8):2208-2218. doi:10.1097/01.ASN.0000133041.27682.A2
154. Kalantar-Zadeh K, Gutekunst L, Mehrotra R, et al. Understanding sources of dietary phosphorus in the treatment of patients with chronic kidney disease. *Clin J Am Soc Nephrol CJASN*. 2010;5(3):519-530. doi:10.2215/CJN.06080809
155. Slatopolsky E, Bricker NS. The role of phosphorus restriction in the prevention of secondary hyperparathyroidism in chronic renal disease. *Kidney Int*. 1973;4(2):141-145.
156. Alfrey AC, LeGendre GR, Kaehny WD. The dialysis encephalopathy syndrome. Possible aluminum intoxication. *N Engl J Med*. 1976;294(4):184-188. doi:10.1056/NEJM197601222940402
157. O'Donovan R, Baldwin D, Hammer M, Moniz C, Parsons V. Substitution of aluminium salts by magnesium salts in control of dialysis hyperphosphataemia. *Lancet Lond Engl*. 1986;1(8486):880-882.
158. Oe PL, Lips P, van der Meulen J, de Vries PM, van Bronswijk H, Donker AJ. Long-term use of magnesium hydroxide as a phosphate binder in patients on hemodialysis. *Clin Nephrol*. 1987;28(4):180-185.
159. Slatopolsky E, Weerts C, Lopez-Hilker S, et al. Calcium carbonate as a phosphate binder in patients with chronic renal failure undergoing dialysis. *N Engl J Med*. 1986;315(3):157-161. doi:10.1056/NEJM198607173150304
160. Spiegel DM, Farmer B, Smits G, Chonchol M. Magnesium carbonate is an effective phosphate binder for chronic hemodialysis patients: a pilot study. *J Ren Nutr Off J Counc Ren Nutr Natl Kidney Found*. 2007;17(6):416-422. doi:10.1053/j.jrn.2007.08.005
161. Alfrey AC, Miller NL. Bone magnesium pools in uremia. *J Clin Invest*. 1973;52(12):3019-3027. doi:10.1172/JCI107500
162. Ennever J, Vogel JJ. Magnesium inhibition of apatite nucleation by proteolipid. *J Dent Res*. 1981;60(4):838-841. doi:10.1177/00220345810600041301
163. Covic A, Passlick-Deetjen J, Kroczak M, et al. A comparison of calcium acetate/magnesium carbonate and sevelamer-hydrochloride effects on fibroblast growth factor-23 and bone markers: post hoc evaluation from a controlled, randomized study. *Nephrol Dial Transplant Off Publ Eur Dial Transpl Assoc - Eur Ren Assoc*. 2013;28(9):2383-2392. doi:10.1093/ndt/gft203
164. Rude RK, Gruber HE, Norton HJ, Wei LY, Frausto A, Kilburn J. Reduction of dietary magnesium by only 50% in the rat disrupts bone and mineral metabolism. *Osteoporos Int J Establ Result Coop Eur Found Osteoporos Natl Osteoporos Found USA*. 2006;17(7):1022-1032. doi:10.1007/s00198-006-0104-3

165. Tucker KL, Hannan MT, Chen H, Cupples LA, Wilson PW, Kiel DP. Potassium, magnesium, and fruit and vegetable intakes are associated with greater bone mineral density in elderly men and women. *Am J Clin Nutr*. 1999;69(4):727-736. doi:10.1093/ajcn/69.4.727
166. Cai Q, Hodgson SF, Kao PC, et al. Brief report: inhibition of renal phosphate transport by a tumor product in a patient with oncogenic osteomalacia. *N Engl J Med*. 1994;330(23):1645-1649. doi:10.1056/NEJM199406093302304
167. Ben-Dov IZ, Galitzer H, Lavi-Moshayoff V, et al. The parathyroid is a target organ for FGF23 in rats. *J Clin Invest*. 2007;117(12):4003-4008. doi:10.1172/JCI32409
168. Andrukhova O, Smorodchenko A, Egerbacher M, et al. FGF23 promotes renal calcium reabsorption through the TRPV5 channel. *EMBO J*. 2014;33(3):229-246. doi:10.1002/embj.201284188
169. Francis F, Hennig S, Korn B, et al. A gene (PEX) with homologies to endopeptidases is mutated in patients with X–linked hypophosphatemic rickets. *Nat Genet*. 1995;11(2):130-136. doi:10.1038/ng1095-130
170. ADHR Consortium. Autosomal dominant hypophosphataemic rickets is associated with mutations in FGF23. *Nat Genet*. 2000;26(3):345-348. doi:10.1038/81664
171. Topaz O, Shurman DL, Bergman R, et al. Mutations in GALNT3, encoding a protein involved in O-linked glycosylation, cause familial tumoral calcinosis. *Nat Genet*. 2004;36(6):579-581. doi:10.1038/ng1358
172. Bowe AE, Finnegan R, Jan de Beur SM, et al. FGF-23 inhibits renal tubular phosphate transport and is a PHEX substrate. *Biochem Biophys Res Commun*. 2001;284(4):977-981. doi:10.1006/bbrc.2001.5084
173. Fuente R, Gil-Peña H, Claramunt-Taberner D, et al. X-linked hypophosphatemia and growth. *Rev Endocr Metab Disord*. 2017;18(1):107-115. doi:10.1007/s11154-017-9408-1
174. White KE, Carn G, Lorenz-Depiereux B, Benet-Pages A, Strom TM, Econs MJ. Autosomal-dominant hypophosphatemic rickets (ADHR) mutations stabilize FGF-23. *Kidney Int*. 2001;60(6):2079-2086. doi:10.1046/j.1523-1755.2001.00064.x
175. Kato K, Jeanneau C, Tarp MA, et al. Polypeptide GalNAc-transferase T3 and Familial Tumoral Calcinosis: Secretion of fibroblast growth factor 23 requires O-glycosylation. *J Biol Chem*. 2006;281(27):18370-18377. doi:10.1074/jbc.M602469200
176. Tagliabracci VS, Engel JL, Wiley SE, et al. Dynamic regulation of FGF23 by Fam20C phosphorylation, GalNAc-T3 glycosylation, and furin proteolysis. *Proc Natl Acad Sci U S A*. 2014;111(15):5520-5525. doi:10.1073/pnas.1402218111
177. Lane NE, Parimi N, Corr M, et al. Association of serum fibroblast growth factor 23 (FGF23) and incident fractures in older men: the Osteoporotic Fractures in Men (MrOS) study. *J Bone Miner Res Off J Am Soc Bone Miner Res*. 2013;28(11):2325-2332. doi:10.1002/jbmr.1985
178. Wang H, Yoshiko Y, Yamamoto R, et al. Overexpression of fibroblast growth factor 23 suppresses osteoblast differentiation and matrix mineralization in vitro. *J Bone Miner Res Off J Am Soc Bone Miner Res*. 2008;23(6):939-948. doi:10.1359/jbmr.080220
179. Lopez I, Aguilera-Tejero E, Mendoza FJ, et al. Calcimimetic R-568 Decreases Extraosseous Calcifications in Uremic Rats Treated with Calcitriol. *J Am Soc Nephrol*. 2006;17(3):795-804. doi:10.1681/ASN.2005040342

180. Rodriguez M, Lorenzo V, Felsenfeld AJ, Llach F. Effect of parathyroidectomy on aluminum toxicity and azotemic bone disease in the rat. *J Bone Miner Res Off J Am Soc Bone Miner Res*. 1990;5(4):379-386. doi:10.1002/jbmr.5650050411
181. Berdud I, Martin-Malo A, Almaden Y, Aljama P, Rodriguez M, Felsenfeld AJ. The PTH-calcium relationship during a range of infused PTH doses in the parathyroidectomized rat. *Calcif Tissue Int*. 1998;62(5):457-461.
182. Villanueva AR. A New Goldner's One-Step Trichrome Stain for Identification of Osteoid Seams, Bone and Cells in Undecalcified, Plastic Embedded Sections of Bone. *J Histotechnol*. 1988;11(4):249-251. doi:10.1179/his.1988.11.4.249
183. Erben RG, Glösmann M. Histomorphometry in rodents. *Methods Mol Biol Clifton NJ*. 2012;816:279-303. doi:10.1007/978-1-61779-415-5_19
184. Lopez I, Mendoza FJ, Aguilera-Tejero E, et al. The effect of calcitriol, paricalcitol, and a calcimimetic on extraosseous calcifications in uremic rats. *Kidney Int*. 2008;73(3):300-307. doi:10.1038/sj.ki.5002675
185. Shahabipour F, Mahdavi-Shahri N, Matin MM, Tavassoli A, Zebarjad SM. Scaffolds derived from cancellous bovine bone support mesenchymal stem cells' maintenance and growth. *In Vitro Cell Dev Biol Anim*. 2013;49(6):440-448. doi:10.1007/s11626-013-9591-7
186. Rodríguez García M, Fernández Martín JL, Ruiz de Castañeda J, Hervás Sánchez J, Cannata Andía JB, Grupo de Estudio Caldial. [Calcitriol dose optimization in the treatment of secondary hyperparathyroidism during dialysis. Results at 6 months]. *Nefrol Publicacion Of Soc Espanola Nefrol*. 2002;22(4):370-376.
187. Sayer JA, Carr G, Simmons NL. Nephrocalcinosis: molecular insights into calcium precipitation within the kidney. *Clin Sci Lond Engl 1979*. 2004;106(6):549-561. doi:10.1042/CS20040048
188. Kolek OI, Hines ER, Jones MD, et al. 1alpha,25-Dihydroxyvitamin D3 upregulates FGF23 gene expression in bone: the final link in a renal-gastrointestinal-skeletal axis that controls phosphate transport. *Am J Physiol Gastrointest Liver Physiol*. 2005;289(6):G1036-1042. doi:10.1152/ajpgi.00243.2005
189. Nguyen-Yamamoto L, Karaplis AC, St-Arnaud R, Goltzman D. Fibroblast Growth Factor 23 Regulation by Systemic and Local Osteoblast-Synthesized 1,25-Dihydroxyvitamin D. *J Am Soc Nephrol JASN*. 2017;28(2):586-597. doi:10.1681/ASN.2016010066
190. Keller H, Kneissel M. SOST is a target gene for PTH in bone. *Bone*. 2005;37(2):148-158. doi:10.1016/j.bone.2005.03.018
191. Ryan ZC, Ketha H, McNulty MS, et al. Sclerostin alters serum vitamin D metabolite and fibroblast growth factor 23 concentrations and the urinary excretion of calcium. *Proc Natl Acad Sci U S A*. 2013;110(15):6199-6204. doi:10.1073/pnas.1221255110
192. Murali SK, Roschger P, Zeitz U, Klaushofer K, Andrukhova O, Erben RG. FGF23 Regulates Bone Mineralization in a 1,25(OH)2 D3 and Klotho-Independent Manner. *J Bone Miner Res Off J Am Soc Bone Miner Res*. 2016;31(1):129-142. doi:10.1002/jbmr.2606
193. Amling M, Priemel M, Holzmann T, et al. Rescue of the skeletal phenotype of vitamin D receptor-ablated mice in the setting of normal mineral ion homeostasis: formal

histomorphometric and biomechanical analyses. *Endocrinology*. 1999;140(11):4982-4987. doi:10.1210/endo.140.11.7110

194. Dardenne O, Prud'homme J, Arabian A, Glorieux FH, St-Arnaud R. Targeted inactivation of the 25-hydroxyvitamin D(3)-1(alpha)-hydroxylase gene (CYP27B1) creates an animal model of pseudovitamin D-deficiency rickets. *Endocrinology*. 2001;142(7):3135-3141. doi:10.1210/endo.142.7.8281
195. Panda DK, Miao D, Bolivar I, et al. Inactivation of the 25-hydroxyvitamin D 1alpha-hydroxylase and vitamin D receptor demonstrates independent and interdependent effects of calcium and vitamin D on skeletal and mineral homeostasis. *J Biol Chem*. 2004;279(16):16754-16766. doi:10.1074/jbc.M310271200
196. Kitazawa R, Mori K, Yamaguchi A, Kondo T, Kitazawa S. Modulation of mouse RANKL gene expression by Runx2 and vitamin D3. *J Cell Biochem*. 2008;105(5):1289-1297. doi:10.1002/jcb.21929
197. St-Arnaud R, Arabian A, Travers R, et al. Deficient mineralization of intramembranous bone in vitamin D-24-hydroxylase-ablated mice is due to elevated 1,25-dihydroxyvitamin D and not to the absence of 24,25-dihydroxyvitamin D. *Endocrinology*. 2000;141(7):2658-2666. doi:10.1210/endo.141.7.7579
198. Lieben L, Masuyama R, Torrekens S, et al. Normocalcemia is maintained in mice under conditions of calcium malabsorption by vitamin D-induced inhibition of bone mineralization. *J Clin Invest*. 2012;122(5):1803-1815. doi:10.1172/JCI45890
199. Krupp M, Lane MD. On the mechanism of ligand-induced down-regulation of insulin receptor level in the liver cell. *J Biol Chem*. 1981;256(4):1689-1694.
200. Thavarajah M, Evans DB, Kanis JA. 1,25(OH)2D3 induces differentiation of osteoclast-like cells from human bone marrow cultures. *Biochem Biophys Res Commun*. 1991;176(3):1189-1195.
201. Roodman GD, Ibbotson KJ, MacDonald BR, Kuehl TJ, Mundy GR. 1,25-Dihydroxyvitamin D3 causes formation of multinucleated cells with several osteoclast characteristics in cultures of primate marrow. *Proc Natl Acad Sci U S A*. 1985;82(23):8213-8217.
202. Bar-Shavit Z, Teitelbaum SL, Reitsma P, et al. Induction of monocytic differentiation and bone resorption by 1,25-dihydroxyvitamin D3. *Proc Natl Acad Sci U S A*. 1983;80(19):5907-5911.
203. Kanatani M, Sugimoto T, Kanzawa M, Yano S, Chihara K. High extracellular calcium inhibits osteoclast-like cell formation by directly acting on the calcium-sensing receptor existing in osteoclast precursor cells. *Biochem Biophys Res Commun*. 1999;261(1):144-148. doi:10.1006/bbrc.1999.0932
204. Healy MD, Malluche HH, Goldstein DA, Singer FR, Massry SG. Effects of Long-term Therapy With Calcitriol in Patients With Moderate Renal Failure. *Arch Intern Med*. 1980;140(8):1030-1033. doi:10.1001/archinte.1980.00330190042017
205. Goodman WG, Ramirez JA, Belin TR, et al. Development of adynamic bone in patients with secondary hyperparathyroidism after intermittent calcitriol therapy. *Kidney Int*. 1994;46(4):1160-1166.
206. Pahl M, Jara A, Bover J, Felsenfeld AJ. Studies in a hemodialysis patient indicating that calcitriol may have a direct suppressive effect on bone. *Nephron*. 1995;71(2):218-223.

207. Ureña P, Prieur P, Pétrover M. Calcitriol may directly suppress bone turnover. *Nephron*. 1997;75(1):116-117. doi:10.1159/000189517
208. Wada M, Ishii H, Furuya Y, Fox J, Nemeth EF, Nagano N. NPS R-568 halts or reverses osteitis fibrosa in uremic rats. *Kidney Int*. 1998;53(2):448-453. doi:10.1046/j.1523-1755.1998.00782.x
209. Cozzolino M, Ketteler M, Martin KJ, Sharma A, Goldsmith D, Khan S. Paricalcitol- or cinacalcet-centred therapy affects markers of bone mineral disease in patients with secondary hyperparathyroidism receiving haemodialysis: results of the IMPACT-SHPT study. *Nephrol Dial Transplant Off Publ Eur Dial Transpl Assoc - Eur Ren Assoc*. 2014;29(4):899-905. doi:10.1093/ndt/gfu011
210. Jubiz W, Canterbury JM, Reiss E, Tyler FH. Circadian rhythm in serum parathyroid hormone concentration in human subjects: correlation with serum calcium, phosphate, albumin, and growth hormone levels. *J Clin Invest*. 1972;51(8):2040-2046.
211. Hock JM, Gera I. Effects of continuous and intermittent administration and inhibition of resorption on the anabolic response of bone to parathyroid hormone. *J Bone Miner Res Off J Am Soc Bone Miner Res*. 1992;7(1):65-72. doi:10.1002/jbmr.5650070110
212. Potts JT, Tregear GW, Keutmann HT, et al. Synthesis of a Biologically Active N-Terminal Tetratriacontapeptide of Parathyroid Hormone. *Proc Natl Acad Sci*. 1971;68(1):63-67. doi:10.1073/pnas.68.1.63
213. Slatopolsky E, Finch J, Clay P, et al. A novel mechanism for skeletal resistance in uremia. *Kidney Int*. 2000;58(2):753-761. doi:10.1046/j.1523-1755.2000.00222.x
214. Huan J, Olgaard K, Nielsen LB, Lewin E. Parathyroid hormone 7-84 induces hypocalcemia and inhibits the parathyroid hormone 1-84 secretory response to hypocalcemia in rats with intact parathyroid glands. *J Am Soc Nephrol JASN*. 2006;17(7):1923-1930. doi:10.1681/ASN.2005101136
215. Xue Y, Xiao Y, Liu J, et al. The calcium-sensing receptor complements parathyroid hormone-induced bone turnover in discrete skeletal compartments in mice. *Am J Physiol Endocrinol Metab*. 2012;302(7):E841-851. doi:10.1152/ajpendo.00599.2011
216. Shu L, Ji J, Zhu Q, et al. The calcium-sensing receptor mediates bone turnover induced by dietary calcium and parathyroid hormone in neonates. *J Bone Miner Res Off J Am Soc Bone Miner Res*. 2011;26(5):1057-1071. doi:10.1002/jbmr.300
217. Al-Dujaili SA, Koh AJ, Dang M, et al. Calcium Sensing Receptor Function Supports Osteoblast Survival and Acts as a Co-Factor in PTH Anabolic Actions in Bone. *J Cell Biochem*. 2016;117(7):1556-1567. doi:10.1002/jcb.25447
218. Chattopadhyay N, Yano S, Tfelt-Hansen J, et al. Mitogenic action of calcium-sensing receptor on rat calvarial osteoblasts. *Endocrinology*. 2004;145(7):3451-3462. doi:10.1210/en.2003-1127
219. Pipino C, Di Tomo P, Mandatori D, et al. Calcium sensing receptor activation by calcimimetic R-568 in human amniotic fluid mesenchymal stem cells: correlation with osteogenic differentiation. *Stem Cells Dev*. 2014;23(24):2959-2971. doi:10.1089/scd.2013.0627
220. Yasuda H, Shima N, Nakagawa N, et al. Osteoclast differentiation factor is a ligand for osteoprotegerin/osteoclastogenesis-inhibitory factor and is identical to TRANCE/RANKL. *Proc Natl Acad Sci U S A*. 1998;95(7):3597-3602.

221. Takayanagi H, Kim S, Koga T, et al. Induction and activation of the transcription factor NFATc1 (NFAT2) integrate RANKL signaling in terminal differentiation of osteoclasts. *Dev Cell*. 2002;3(6):889-901.
222. Hirotani H, Tuohy NA, Woo J-T, Stern PH, Clipstone NA. The calcineurin/nuclear factor of activated T cells signaling pathway regulates osteoclastogenesis in RAW264.7 cells. *J Biol Chem*. 2004;279(14):13984-13992. doi:10.1074/jbc.M213067200
223. Ikeda F, Nishimura R, Matsubara T, et al. Critical roles of c-Jun signaling in regulation of NFAT family and RANKL-regulated osteoclast differentiation. *J Clin Invest*. 2004;114(4):475-484. doi:10.1172/JCI19657
224. Hogan PG, Chen L, Nardone J, Rao A. Transcriptional regulation by calcium, calcineurin, and NFAT. *Genes Dev*. 2003;17(18):2205-2232. doi:10.1101/gad.1102703
225. Montezano AC, Zimmerman D, Yusuf H, et al. Vascular smooth muscle cell differentiation to an osteogenic phenotype involves TRPM7 modulation by magnesium. *Hypertens Dallas Tex 1979*. 2010;56(3):453-462. doi:10.1161/HYPERTENSIONAHA.110.152058
226. Kircelli F, Peter ME, Sevinc Ok E, et al. Magnesium reduces calcification in bovine vascular smooth muscle cells in a dose-dependent manner. *Nephrol Dial Transplant Off Publ Eur Dial Transpl Assoc - Eur Ren Assoc*. 2012;27(2):514-521. doi:10.1093/ndt/gfr321
227. Louvet L, Büchel J, Steppan S, Passlick-Deetjen J, Massy ZA. Magnesium prevents phosphate-induced calcification in human aortic vascular smooth muscle cells. *Nephrol Dial Transplant Off Publ Eur Dial Transpl Assoc - Eur Ren Assoc*. 2013;28(4):869-878. doi:10.1093/ndt/gfs520
228. McLarnon SJ, Riccardi D. Physiological and pharmacological agonists of the extracellular Ca2+-sensing receptor. *Eur J Pharmacol*. 2002;447(2-3):271-278.
229. McSheehy PM, Chambers TJ. Osteoblastic cells mediate osteoclastic responsiveness to parathyroid hormone. *Endocrinology*. 1986;118(2):824-828. doi:10.1210/endo-118-2-824
230. Rude RK, Gruber HE, Norton HJ, Wei LY, Frausto A, Mills BG. Bone loss induced by dietary magnesium reduction to 10% of the nutrient requirement in rats is associated with increased release of substance P and tumor necrosis factor-alpha. *J Nutr*. 2004;134(1):79-85. doi:10.1093/jn/134.1.79
231. Sakaguchi Y, Hamano T, Wada A, Hoshino J, Masakane I. Magnesium and Risk of Hip Fracture among Patients Undergoing Hemodialysis. *J Am Soc Nephrol JASN*. 2018;29(3):991-999. doi:10.1681/ASN.2017080849
232. Morinière P, Vinatier I, Westeel PF, et al. Magnesium hydroxide as a complementary aluminium-free phosphate binder to moderate doses of oral calcium in uraemic patients on chronic haemodialysis: lack of deleterious effect on bone mineralisation. *Nephrol Dial Transplant Off Publ Eur Dial Transpl Assoc - Eur Ren Assoc*. 1988;3(5):651-656.
233. Gonella M, Ballanti P, Della Rocca C, et al. Improved bone morphology by normalizing serum magnesium in chronically hemodialyzed patients. *Miner Electrolyte Metab*. 1988;14(4):240-245.

234. Callera GE, He Y, Yogi A, et al. Regulation of the novel Mg2+ transporter transient receptor potential melastatin 7 (TRPM7) cation channel by bradykinin in vascular smooth muscle cells. *J Hypertens*. 2009;27(1):155-166.
235. Hamaguchi Y, Matsubara T, Amano T, et al. Na(+)-independent Mg(2+) transport sensitive to 2-aminoethoxydiphenyl borate (2-APB) in vascular smooth muscle cells: involvement of TRPM-like channels. *J Cell Mol Med*. 2008;12(3):962-974. doi:10.1111/j.1582-4934.2008.00157.x
236. Elizondo MR, Arduini BL, Paulsen J, et al. Defective skeletogenesis with kidney stone formation in dwarf zebrafish mutant for trpm7. *Curr Biol CB*. 2005;15(7):667-671. doi:10.1016/j.cub.2005.02.050
237. Zanotti S, Smerdel-Ramoya A, Stadmeyer L, Durant D, Radtke F, Canalis E. Notch inhibits osteoblast differentiation and causes osteopenia. *Endocrinology*. 2008;149(8):3890-3899. doi:10.1210/en.2008-0140
238. Wang C, Inzana JA, Mirando AJ, et al. NOTCH signaling in skeletal progenitors is critical for fracture repair. *J Clin Invest*. 2016;126(4):1471-1481. doi:10.1172/JCI80672
239. Wu L, Feyerabend F, Schilling AF, Willumeit-Römer R, Luthringer BJC. Effects of extracellular magnesium extract on the proliferation and differentiation of human osteoblasts and osteoclasts in coculture. *Acta Biomater*. 2015;27:294-304. doi:10.1016/j.actbio.2015.08.042
240. Belluci MM, Schoenmaker T, Rossa-Junior C, Orrico SR, de Vries TJ, Everts V. Magnesium deficiency results in an increased formation of osteoclasts. *J Nutr Biochem*. 2013;24(8):1488-1498. doi:10.1016/j.jnutbio.2012.12.008
241. Sitara D, Kim S, Razzaque MS, et al. Genetic evidence of serum phosphate-independent functions of FGF-23 on bone. *PLoS Genet*. 2008;4(8):e1000154. doi:10.1371/journal.pgen.1000154
242. Eicher EM, Southard JL, Scriver CR, Glorieux FH. Hypophosphatemia: mouse model for human familial hypophosphatemic (vitamin D-resistant) rickets. *Proc Natl Acad Sci U S A*. 1976;73(12):4667-4671.
243. Murali SK, Andrukhova O, Clinkenbeard EL, White KE, Erben RG. Excessive Osteocytic Fgf23 Secretion Contributes to Pyrophosphate Accumulation and Mineralization Defect in Hyp Mice. *PLoS Biol*. 2016;14(4):e1002427. doi:10.1371/journal.pbio.1002427
244. Hopper TAJ, Wehrli FW, Saha PK, et al. Quantitative microcomputed tomography assessment of intratrabecular, intertrabecular, and cortical bone architecture in a rat model of severe renal osteodystrophy. *J Comput Assist Tomogr*. 2007;31(2):320-328. doi:10.1097/01.rct.0000238007.19258.3d
245. Gaudio A, Pennisi P, Bratengeier C, et al. Increased sclerostin serum levels associated with bone formation and resorption markers in patients with immobilization-induced bone loss. *J Clin Endocrinol Metab*. 2010;95(5):2248-2253. doi:10.1210/jc.2010-0067
246. Pereira RC, Salusky IB, Roschger P, et al. Impaired osteocyte maturation in the pathogenesis of renal osteodystrophy. *Kidney Int*. 2018;94(5):1002-1012. doi:10.1016/j.kint.2018.08.011

247. Carrillo-López N, Panizo S, Alonso-Montes C, et al. Direct inhibition of osteoblastic Wnt pathway by fibroblast growth factor 23 contributes to bone loss in chronic kidney disease. *Kidney Int*. 2016;90(1):77-89. doi:10.1016/j.kint.2016.01.024
248. Kaye M, Zucker SW, Leclerc YG, Prichard S, Hodsman AB, Barré PE. Osteoclast enlargement in endstage renal disease. *Kidney Int*. 1985;27(3):574-581.
249. Makris GP, Saffar JL. Quantitative relationship between osteoclasts, osteoclast nuclei and the extent of the resorbing surface in hamster periodontal disease. *Arch Oral Biol*. 1982;27(11):965-969.
250. Piper K, Boyde A, Jones SJ. The relationship between the number of nuclei of an osteoclast and its resorptive capability in vitro. *Anat Embryol (Berl)*. 1992;186(4):291-299.
251. Spasovski GB, Bervoets ARJ, Behets GJS, et al. Spectrum of renal bone disease in end-stage renal failure patients not yet on dialysis. *Nephrol Dial Transplant Off Publ Eur Dial Transpl Assoc - Eur Ren Assoc*. 2003;18(6):1159-1166.
252. Malluche HH, Mawad HW, Monier-Faugere M-C. Renal osteodystrophy in the first decade of the new millennium: analysis of 630 bone biopsies in black and white patients. *J Bone Miner Res Off J Am Soc Bone Miner Res*. 2011;26(6):1368-1376. doi:10.1002/jbmr.309
253. Zaidi M, Kerby J, Huang CL, et al. Divalent cations mimic the inhibitory effect of extracellular ionised calcium on bone resorption by isolated rat osteoclasts: further evidence for a “calcium receptor.” *J Cell Physiol*. 1991;149(3):422-427. doi:10.1002/jcp.1041490310
254. Driessens FCM, Verbeeck RK. *Biominerals*. CRC Press; 1990.
255. Kim HD, Jang HL, Ahn H-Y, et al. Biomimetic whitlockite inorganic nanoparticles-mediated in situ remodeling and rapid bone regeneration. *Biomaterials*. 2017;112:31-43. doi:10.1016/j.biomaterials.2016.10.009
256. Jang HL, Lee HK, Jin K, Ahn H-Y, Lee H-E, Nam KT. Phase transformation from hydroxyapatite to the secondary bone mineral, whitlockite. *J Mater Chem B*. 2015;3(7):1342-1349. doi:10.1039/C4TB01793E

ARTICLES

SCIENTIFIC REPORTS

OPEN

Magnesium Chloride promotes Osteogenesis through Notch signaling activation and expansion of Mesenchymal Stem Cells

Received: 18 October 2016
Accepted: 10 July 2017
Published online: 10 August 2017

Juan M. Díaz-Tocados[1,2,3,4], Carmen Herencia[1,2,3], Julio M. Martínez-Moreno[1,2,3], Addy Montes de Oca[1,2,3], Maria E. Rodríguez-Ortiz[4,5], Noemi Vergara[1,2,3], Alfonso Blanco[6], Sonja Steppan[7], Yolanda Almadén[1,3,8,9], Mariano Rodríguez[1,2,3,4] & Juan R. Muñoz-Castañeda[1,2,3,4]

Mesenchymal stem cells (MSC) are osteoblasts progenitors and a variety of studies suggest that they may play an important role for the health in the field of bone regeneration. Magnesium supplementation is gaining importance as adjuvant treatment to improve osteogenesis, although the mechanisms involving this process are not well understood. The objective of this study was to investigate the effects of magnesium on MSC differentiation. Here we show that in rat bone marrow MSC, magnesium chloride increases MSC proliferation in a dose-dependent manner promoting osteogenic differentiation and mineralization. These effects are reduced by 2-APB administration, an inhibitor of magnesium channel TRPM7. Of note, magnesium supplementation did not increase the canonical Wnt/β-catenin pathway, although it promoted the activation of Notch1 signaling, which was also decreased by addition of 2-APB. Electron microscopy showed higher proliferation, organization and maturation of osteoblasts in bone decellularized scaffolds after magnesium addition. In summary, our results demonstrate that magnesium chloride enhances MSC proliferation by Notch1 signaling activation and induces osteogenic differentiation, shedding light on the understanding of the role of magnesium during bone regeneration.

Bone growth is a process required in a wide variety of conditions in which functional restoration of damaged bone is needed. There are pathological conditions such as polytraumatism, bone tumors, degenerative diseases, orthopedic surgeries, osteonecrosis, osteotomy or non-union fractures where a combination of prosthesis implantation and enhanced osteogenesis is necessary[1,2]. The standard treatment in some of these conditions require autologous or allogenic cancellous bone transplantation, supplemented with growth factors and/or progenitor cells. These alternatives have limitations such as surgical complications, elevated cost and/or immunogenic rejection[3–5]. Therefore, the search for new strategies to improve bone grafts has risen widely over the last years. An optimal biomaterial should be simple, biologically safe, biocompatible and with a high degree of interaction with the patient's bone tissue to favor proliferation and differentiation of progenitor cells into an osteogenic phenotype.

Nowadays, there are many types of scaffolds such as calcium phosphate-based materials (extensively studied as bone scaffold for tissue engineering), polymeric (collagen, fibrin, alginate, silk, hyaluronic acid, or chitosan), composite (two or more distinct materials), metallic (magnesium or titanium) or third generation scaffolds that combine the aforementioned materials with stem cells, growth factors, cytokines, etc[1].

[1]Maimonides Institute for Biomedical Research (IMIBIC), 14004, Cordoba, Spain. [2]Nephrology Service, Reina Sofia University Hospital, 14004, Cordoba, Spain. [3]University of Cordoba, 14004, Cordoba, Spain. [4]Spanish Renal Research Network (REDinREN), Institute of Health Carlos III, 28029, Madrid, Spain. [5]Laboratory of Nephrology, Health Research Institute-Jiménez Diaz Foundation, 28220, Madrid, Spain. [6]Dept. of Anatomy and Comparative Pathology and Anatomy, University of Cordoba, 14014, Cordoba, Spain. [7]Fresenius Medical Care Deutschland GmbH, 61352, Bad Homburg, Germany. [8]Internal Medicine Service, Reina Sofia University Hospital, 14004, Cordoba, Spain. [9]Biomedical Research Center Network on Physiopathology of Obesity and Nutrition (CIBERobn), Institute of Health Carlos III, 28029, Madrid, Spain. Juan M. Díaz-Tocados and Carmen Herencia contributed equally to this work. Mariano Rodríguez and Juan R. Muñoz-Castañeda jointly supervised this work. Correspondence and requests for materials should be addressed to Y.A. (email: yolandaalmaden@yahoo.es)

Magnesium (Mg^{2+}) is particularly interesting because of its abundance in the organism, where it participates in numerous biological processes, like osteogenesis of progenitor cells. In addition, low Mg^{2+} concentrations have been associated with osteoporosis or osteopenia[6]. In biomaterial engineering, Mg-based implants have been used to enhance bone formation "*in vivo*"[7–10]. Due to corrosion resistance of Mg^{2+} alloys[11], new formulas based on Mg^{2+} are being investigated. Currently, Mg^{2+} is used in combination with other materials as calcium and phosphate, or as Mg-coated structures to enhance osteogenesis. However, little is known about the mechanisms whereby Mg^{2+} salts affect osteogenesis and bone formation. It is known that Wnt/β-pathway and Notch signaling are involved in bone marrow mesenchymal stem cells (MSC) osteogenesis[12,13]. Although other works show that Notch signaling activation is also related to the maintenance of stemness[14] even with the inhibition of osteogenesis[15].

The characterization of the pro-osteogenic effects of Mg^{2+} will add knowledge on the biology of bone cells; thus, new or improved strategies can be developed aiming to enhance osteogenesis, and osseointegration of bone prosthesis.

The present study evaluates the effects of magnesium chloride on osteogenesis of bone marrow MSC and its capability to repopulate decellularized bone scaffolds. Moreover, the mechanisms whereby magnesium chloride triggers its pro-osteogenic effect are also investigated.

Results

Moderately high concentrations of Mg^{2+} increase osteogenesis and mineralization of rat MSC. Increasing Mg^{2+} concentrations (0.8, 1.2, and 1.8 mM) enhanced MSC osteogenesis (Fig. 1). In MSC differentiated into osteoblasts with 1.2 mM of $MgCl_2$, alkaline phosphatase activity (ALP) increased by 4.2-fold (vs 0.8 mM) and by 6-fold with 1.8 mM of $MgCl_2$, (Fig. 1a). Likewise, matrix mineralization, verified by Alizarin Red S, was more abundant in cells cultured with high Mg^{2+} concentrations (Fig. 1b).

The enhancement of mineralization was accompanied by a significant increase in the expression of osteogenic master genes such as *RUNX2* (Fig. 1c), regulator of the early osteoblast differentiation, *OSTERIX* (Fig. 1d), transcription factor required for the transition of pre-osteoblasts to osteoblasts, and *OSTEOCALCIN* (Fig. 1e), produced by mature osteoblasts. The addition of $MgCl_2$ increased the expression of these genes in a concentration-dependent manner. As FGF23 is released by mature osteoblasts and osteocytes, the amount of FGF23 in the supernatant demonstrates the presence of mature osteoblasts. FGF23 production during 24 h was measured at 21 days of osteogenic differentiation. Undifferentiated cells did not produce FGF23 while in MSC differentiated into osteoblasts with 1.8 mM of $MgCl_2$ FGF23 levels were 31-fold increased as compared with 0.8 mM (Fig. 1f).

The inhibition of the Mg^{2+} transporter TRPM7 by 2-APB produced a decrease in ALP activity (Fig. 2a) as well as in matrix calcification (Fig. 2b). It also resulted in a significant down-regulation of the osteogenic marker genes *RUNX2*, *OSTERIX* and *OSTEOCALCIN* (Fig. 2c–e, respectively). Moreover, 2-APB treatment reduced FGF23 secretion (Fig. 2f).

Protein levels of Cyclin D1 and PCNA, markers of cellular proliferation, were analyzed by Western blot. The expression of both proteins was increased in osteoblasts as compared with undifferentiated controls. The addition of Mg^{2+} to the medium induced a dose dependent increase in both PCNA and Cyclin D1 (Fig. 2g and h). Notably, the inhibition of the Mg^{2+} channel TRPM7 with 2-APB significantly reduced Cyclin D1 and PCNA protein expression.

Magnesium increases osteogenic differentiation through activation of Notch1 signaling in MSC. The Wnt/β-catenin and Notch signaling are pathways closely involved in bone development. The effect of Mg^{2+} on both pathways was explored. Immunofluorescence analyses revealed that osteogenic differentiation is associated with nuclear translocation of β-catenin. However, increasing $MgCl_2$ concentrations in the culture medium did not produce a further increase the nuclear translocation of β-catenin (Fig. 3a and b).

Confocal microscopy analysis of Notch1 intracellular domain (NICD) showed that Mg^{2+} supplementation produced an increase in nuclear translocation of NICD (Fig. 4a). Osteogenic differentiation decreased the nuclear NICD as compared with UC while Mg^{2+} supplementation increased the presence of nuclear NICD. In OB cells treated with 2-APB the DAPI-NICD co-localization was almost inexistent. As it is observed in the last column of Fig. 4a as compared to 0.8 mM, after Mg addition there was an increase of green pixels (NICD) matching with blue pixels (DAPI), demonstrating nuclear colocalization of NICD protein. Similarly, Fig. 4b shows that a moderate increase of Mg^{2+} in the osteogenic medium upregulated the mRNA expression of HEY2, one of the classic Notch target genes. The opposite effect was observed by the inhibition of the Mg^{2+} transporter TRPM7 with 2-APB, which reduced the nuclear translocation of NICD (Fig. 4a) and Notch activation (Fig. 4b). To examine a likely direct effect of $MgCl_2$, the nuclear expression of NICD was evaluated after 24 h of Mg supplementation on MSC or MSC plus osteogenic stimulus. The addition of $MgCl_2$ for 24 h increased the nuclear protein expression of NICD as it was confirmed by western blotting (Fig. 4c). However, when $MgCl_2$ was administrated for 24 hours in presence of an osteogenic stimulus the levels of nuclear NICD expression were similar to those found with basal Mg^{2+} content (Fig. 4d). The administration of $MgCl_2$ for 24 h to differentiated osteoblasts or 2-APB treated cells for 21 days did not modify the nuclear NICD protein expression (Fig. 4e). A high NICD protein expression was also detected by immunoblotting of nuclear protein extracts from MSC and differentiated osteoblasts with Mg^{2+} supplementation after 21 days (Supplementary Figure S1). However, NICD expression was again highly induced in undifferentiated MSC. Taken together, these data suggest that Mg^{2+} activates NICD nuclear translocation on undifferentiated MSC but not in differentiated osteoblasts.

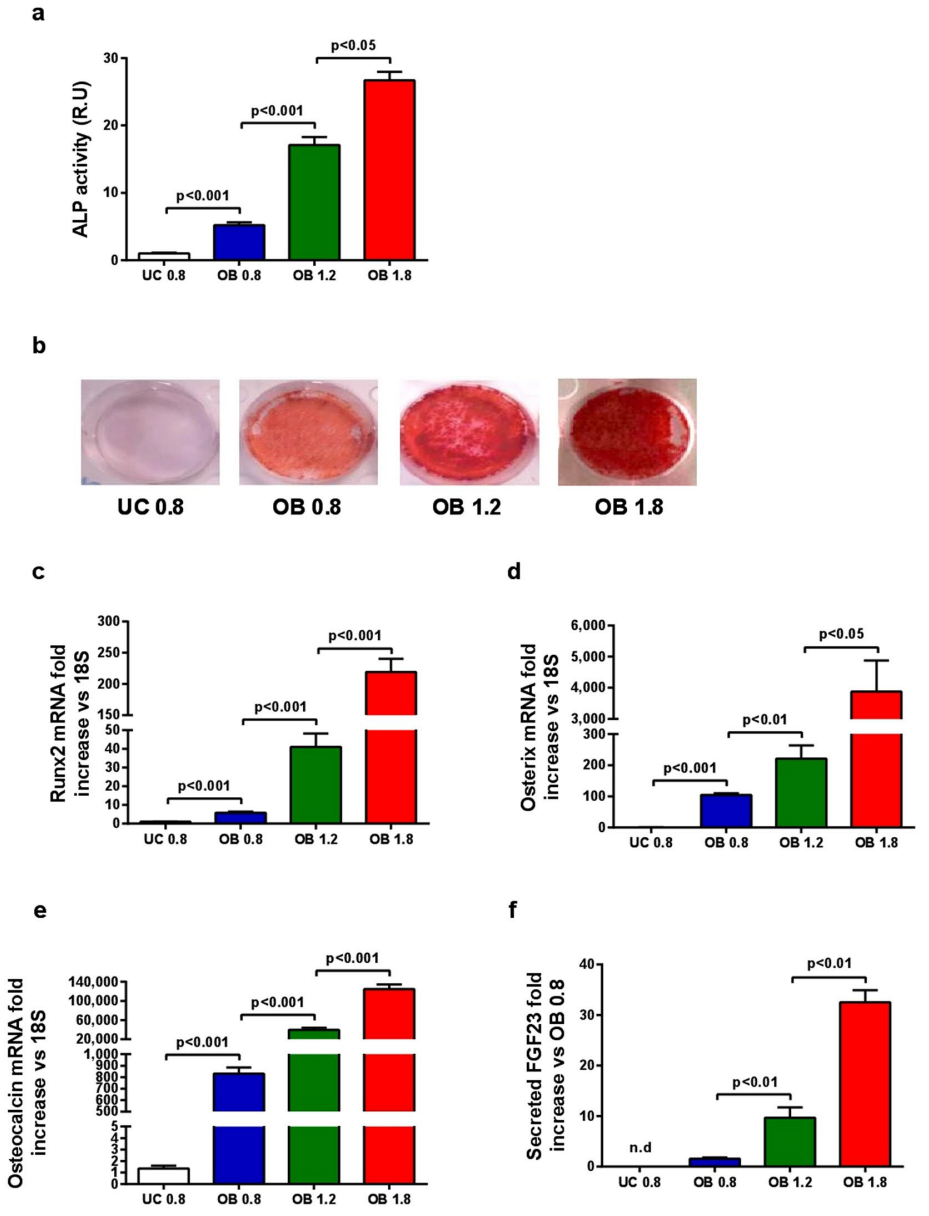

Figure 1. Effects of $MgCl_2$ supplementation on osteogenesis and mineralization of rat MSC. (**a**) ALP activity was significantly and dose-dependently increased by Mg^{2+} concentration. (**b**) Matrix mineralization verified by Alizarin Red S staining was higher according to Mg^{2+} levels. (**c**) Osteogenic marker genes Runx2, (**d**) Osterix and (**e**) Osteocalcin expression was up-regulated according to the increase in Mg^{2+} concentrations. (**f**) Intact FGF23 in the liquid supernatant was increased according to Mg^{2+} concentrations. FGF23 was not detected in liquid supernatant of UC. UC - undifferentiated cells, OB - osteoblasts. Bars show mean ± SEM. n = 4.

Magnesium promotes maturation and distribution of osteoblast into decellularized scaffolds. *Scanning Electron Microscopy (SEM).* In decellularized scaffolds (Fig. 5a), osseous matrix was observed as series of uniform and regular depressions corresponding to ducts osteons (Fig. 5b). Whole bone surface and cavities were covered with a thin membrane with scarce cells. In the scaffolds recellularized with MSC and treated with basal levels of Mg^{2+} (0.8 mM) (Fig. 5c), bone matrix was covered with an irregular membrane with abundant cells following an unspecific distribution and presenting a stellate morphology. After Mg^{2+} supplementation (1.2 mM), MSC formed a uniformly organized layer over the bone surface, of smooth aspect and with abundant

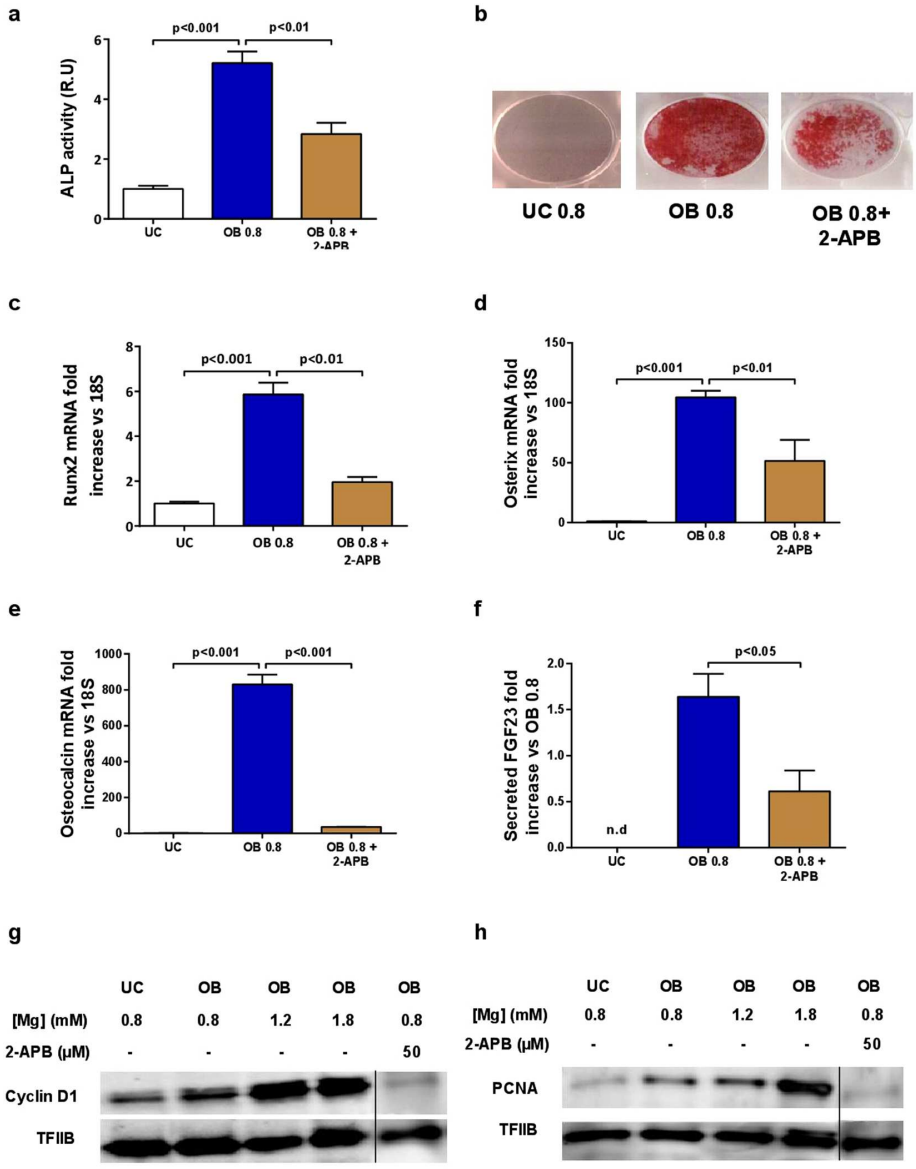

Figure 2. Decrease in intracellular Mg^{2+} reduces osteogenesis, mineralization and proliferation during differentiation of rat MSC into osteoblasts. Inhibition of Mg^{2+} entry by blocking TRPM7 with 2-APB (50 μM) significantly decreased (**a**) ALP activity and (**b**) matrix mineralization as assessed by Alizarin Red S staining. Specific osteogenic marker genes (**c**) *RUNX2*, (**d**) *OSTERIX* and (**e**) *OSTEOCALCIN* were down-regulated by inhibition of Mg^{2+} entry with 2-APB. (**f**) FGF23 production was decreased by inhibition of the Mg^{2+} transporter TRPM7 with 2-APB. (**g**) Western blots show an increased stimulation of Cyclin D1 and (**h**) PCNA according to Mg^{2+} concentrations at 21 days of osteogenic differentiation. TFIIB was used as a loading control, UC - undifferentiated cells, OB - osteoblasts. Bars show mean ± SEM. n = 4. Vertical black line separates results from different gels using the same exposure and protein load (see Supplementary Figures S3–S4).

cellular proliferation filling the osteon canals (Fig. 5d). In the scaffolds treated with 1.8 mM Mg^{2+}, a continuous and regular layer of germinal bone tissue that fully occupied the scaffolds, was observed (Fig. 5e).

Transmission Electron Microscopy (TEM). Cellular layers on decellularized bone scaffolds were analyzed with TEM. During the osteoinduction of MSC with basal Mg^{2+} levels (0.8 mM), collagen-producing blastic cells were poorly organized and with immature matrix (Fig. 6a). After Mg^{2+} supplementation (1.2 mM), the number of

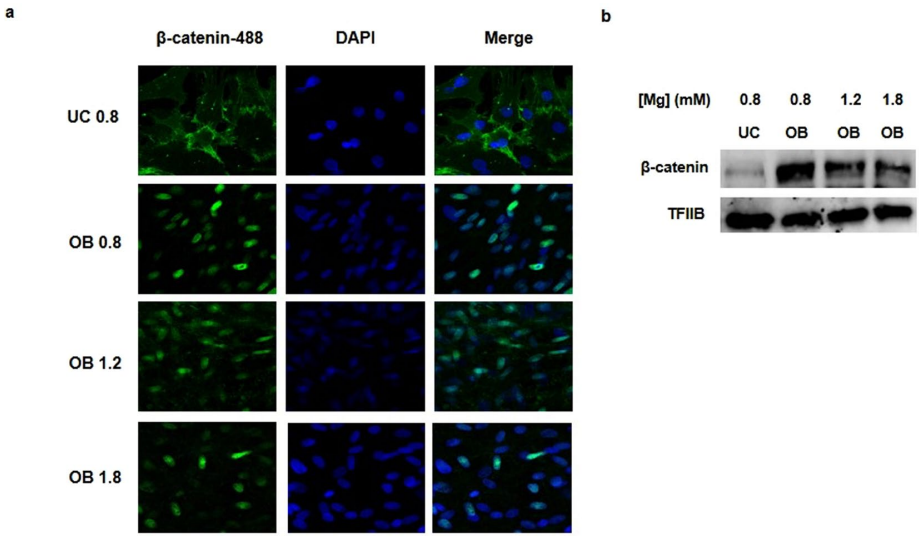

Figure 3. Mg^{2+} supplementation does not induce nuclear translocation of β-catenin. (**a**) Confocal microscopy showed translocation of β-catenin (green) to the nuclei in rat MSC cultured in osteogenic medium, but no significant differences were observed in groups with higher Mg^{2+} levels. (**b**) Western blot analysis of β-catenin for nuclear protein extracts. TFIIB was used as loading control. UC - undifferentiated cells, OB - osteoblasts. Original magnification: 400x.

osteoblasts increased and they were organized in layers, similar to appositional growth of bone, and more mature osteoblasts (osteocytes) were observed. These osteocytes showed bone canaliculi prolongation and a more organized collagen matrix (Fig. 6b). The highest concentration of $MgCl_2$ (1.8 mM) produced a further increase in the number of osteoblast layers (appositional growth), with more mature osteocytes, large bone canaliculi and an organized deposition of collagen (osteoid matrix) (Fig. 6c).

Discussion

In the present study, we have investigated the potential effects of $MgCl_2$ in bone marrow MSC during osteogenic differentiation including its effect on anchorage, cellular attachment and differentiation when they are cultured on decellularized bone scaffolds. As it is illustrated in Fig. 7, high concentrations of $MgCl_2$ (1.2 mM or 1.8 mM) enhanced proliferation of rat bone marrow MSC in a dose-dependent manner, and increased the subsequent osteogenesis. These effects were not observed after inhibition of the Mg^{2+} channel TRPM7 by 2-APB, which confirmed the key role of intracellular Mg^{2+} in the osteogenesis of MSC. We evaluated the intracellular pathways whereby Mg^{2+} promotes osteogenesis of MSC, finding that $MgCl_2$ addition did not increase canonical Wnt/β-catenin pathway activation, although this pathway was activated under osteogenic stimuli. It was interesting to observe that $MgCl_2$ supplementation induced the nuclear translocation of NICD and *HEY2* expression. Our results show a direct effect of Mg^{2+} on Notch activation in MSC rather on differentiated osteoblasts from MSC (Fig. 4), suggesting a specific role of Mg^{2+} on the maintenance of stemness of MSC rather on osteogenic process. Furthermore, moderate concentrations of $MgCl_2$ considerably promoted osteocyte maturation and enhanced cell attachment to the decellularized bone surface. Note that $MgCl_2$ increased the effects of the osteogenic stimuli while conditioned medium with basal levels of Mg^{2+} only produced blastic cells, poorly organized, and without osteocytic phenotype.

The beneficial effects of several Mg^{2+} alloys on bone formation have been widely reported. The balanced combination of Mg^{2+} with different elements such as calcium and phosphate or in Mg-coating prosthesis has demonstrated osteoinductive effects[7,16]. These effects are supported by the formation of a better structure. The structure and surface characteristic of the biomaterials/scaffolds are key for the attachment and function of the cells and, it may affect the absorption and/or integration of proteins; and in turn, the quality of the anchorage, influences the subsequent cellular responses and tissue regeneration. Minardi *et al*. suggested that Mg^{2+} provides the scaffolds with structural characteristics similar to those of bone, allowing anchorage and proliferation of progenitor cells[9]. Few studies have investigated the active effects of Mg^{2+} on osteogenesis. Recently, Zhang *et al*. have demonstrated that cement formed by a combination of calcium, phosphate and Mg^{2+} increased osteogenesis through a specific interaction between fibronectin and integrin α5β1[17]. Of interest, the authors observed a significant increase in Mg^{2+} concentration (approx. 2.5 mM) after soaking these scaffolds with culture medium; this study support our results demonstrating that Mg^{2+} salts may enhance osteogenesis of progenitor cells. Yoshizawa *et al*. observed that supra-physiological concentrations of Mg_2SO_4 (10 mM) also promoted the expression of transcription factors related to *COL10A1* expression[18]. Therefore, these findings suggest that Mg^{2+} salts promote bone formation *in*

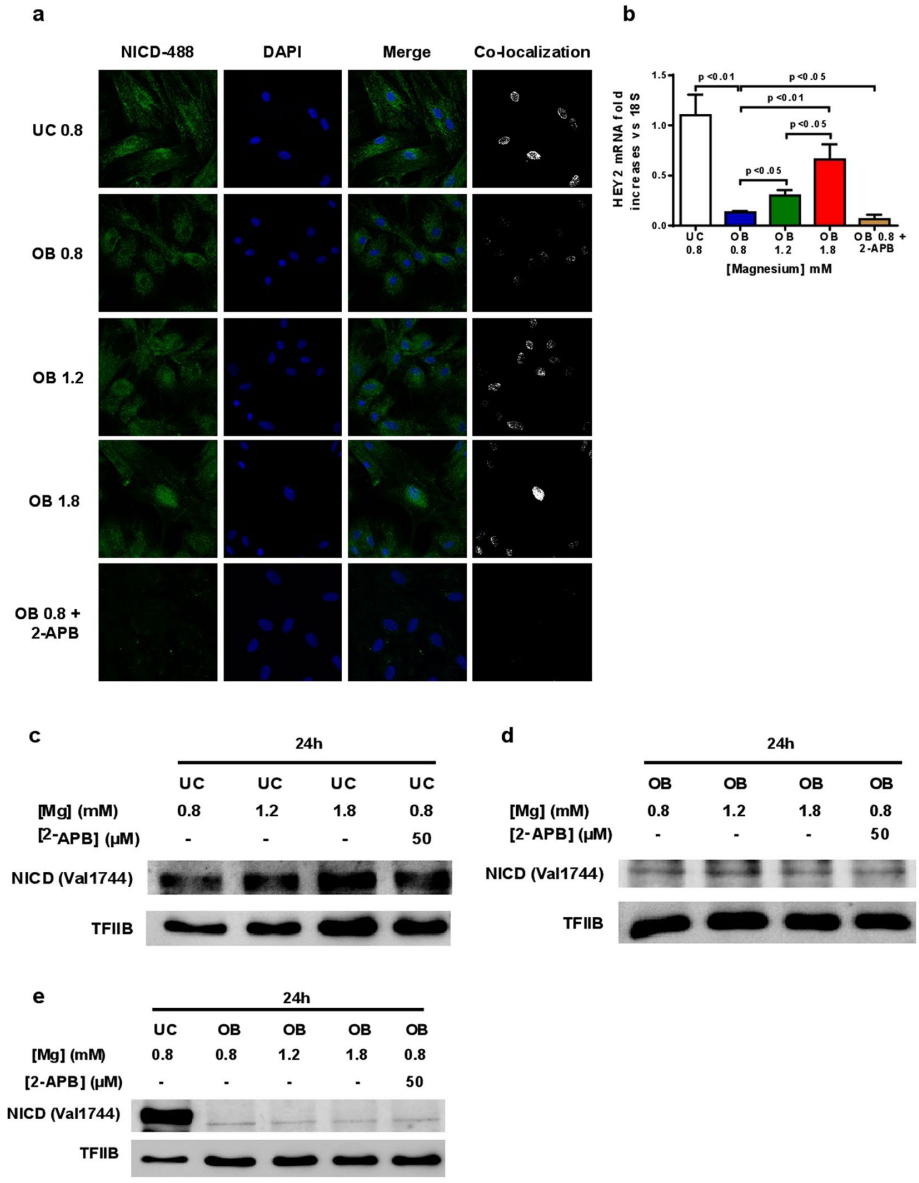

Figure 4. Moderately high Mg^{2+} levels induce Notch signaling activation. (**a**) Confocal microscopy of NICD protein in undifferentiated MSC (UC 0.8 mM), differentiated osteoblasts with basal levels of Mg (OB 0.8) or plus Mg supplementation at 1.2 mM (OB 1.2) or 1.8 mM (OB 1.8 mM) and osteoblasts with Mg channel block (OB 0.8 + 2-APB). First column represents NICD immunostaining in green color; second column corresponds with nuclei staining with DAPI; the third column is a merge composition of green and blue staining while the last column shows green pixels that matches with blue pixels. (**b**) Gene expression of the Notch target gene HEY2. (**c**) Western blot for nuclear NICD in undifferentiated MSC after 24 h of stimulus with Mg^{2+}. (**d**) Nuclear protein levels of NICD after 24 h of osteogenic stimulus with Mg^{2+} or 2APB. (**e**) NICD expression in MSC and differentiated osteoblast from MSC plus 24 h of Mg^{2+} stimulus after 21 days of treatment.

vitro. In fact, Mg^{2+} is abundant in the skeleton and it is an essential ion in bone development allowing physiological, mineralization and osteogenesis of MSC[19].

The Mg^{2+} channel TRPM7 is ubiquitously expressed and it is implicated in cellular Mg^{2+} homeostasis[20]. Expression and activity of TRPM7 are modulated by the availability of Mg^{2+} and Ca^{2+}. High influx of Mg^{2+}

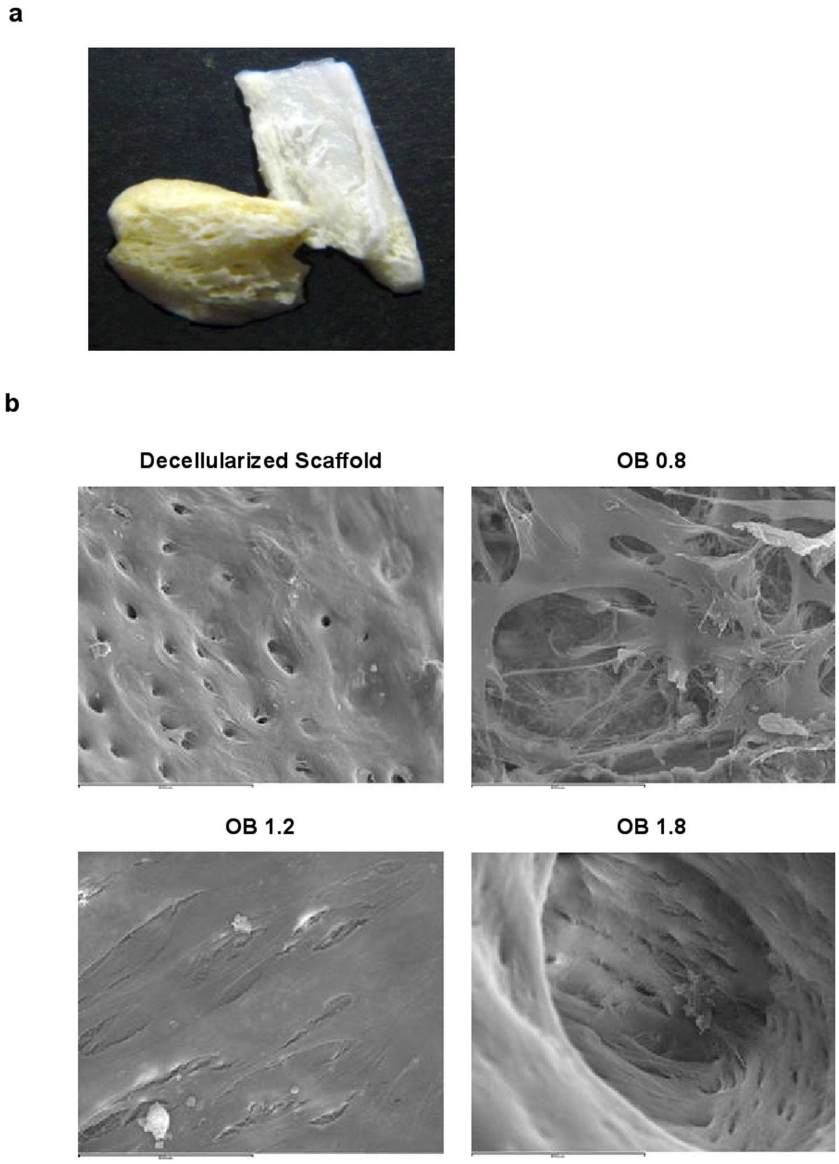

Figure 5. $MgCl_2$ supplementation promotes attachment and osteogenesis of MSC on decellularized bone scaffolds. (**a**) Macroscopic picture of rat decellularized bone scaffolds used in this study. Pictures show SEM images of (**b**) decellularized bone scaffold, (**c**) re-cellularized scaffolds after 21 days of osteogenic differentiation with basal Mg^{2+} (0.8 mM), where spindle-shaped cells attached to the scaffold were observed. Mineralization, cell attachment and proliferation were enhanced dose-dependently as it is showed in (**d**) Mg^{2+} 1.2 mM and (**e**) Mg^{2+} 1.8 mM. Scale bar 800 μm.

stimulates gene expression of TRPM7 channel and promotes osteoblasts proliferation[21]. Other authors have demonstrated the requirement of TRPM7 for growth and skeletogenesis[22]. The results of these studies are in line with our findings, where TRPM7 inactivation by 2-APB inhibited osteogenesis of bone marrow MSC and significantly reduced Notch1 signaling. The contrary effect was observed with the addition of moderate concentrations of $MgCl_2$, which promoted Notch1 signaling activation and increased osteogenesis of the MSC. The central role of this pathway during osteogenesis has been described already[13,23], although other works highlights too an inhibition of this pathway during osteogenesis[15]. The interrelationship among Notch1 signaling pathway, Mg^{2+} and osteogenesis is unknown; taken together, our *in vitro* and *in vivo* results suggest that Mg^{2+} supplementation

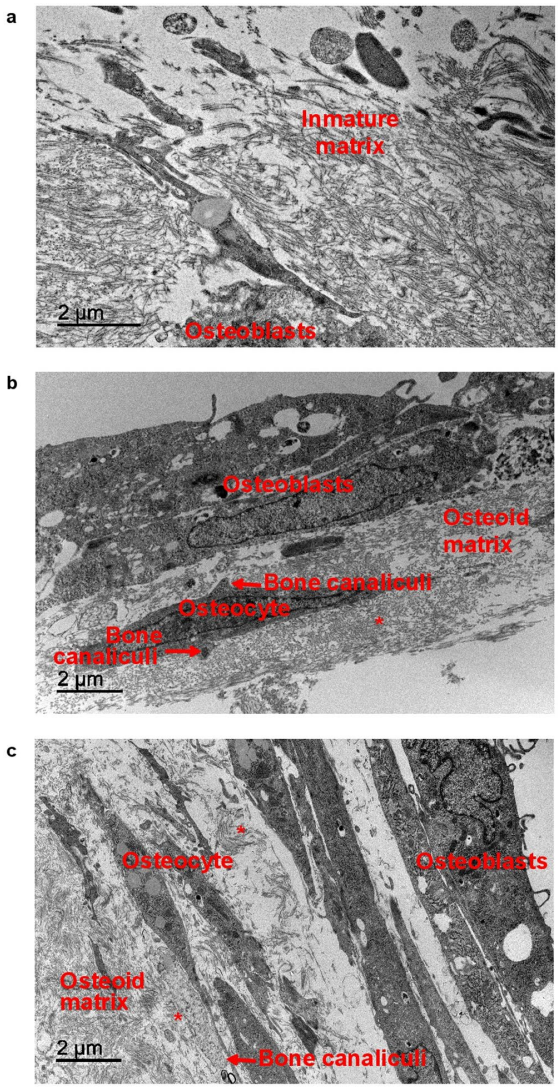

Figure 6. Rat bone marrow MSC differentiated into osteoblasts displayed phenotypic characteristics of osteocyte with $MgCl_2$ supplementation. Pictures show TEM images of a MSC after 21 days of osteogenic stimuli with Mg^{2+} 0.8 mM, b 1.2 mM and c 1.8 mM. Scale bar 5 µm. *Collagen fibers; Arrows: Bone Canaliculi.

promotes Notch activation tissue-specifically in MSC increasing the pool of osteoprogenitor cells susceptible to be differentiated into osteoblasts in the presence of osteogenic stimuli.

In a recent study, it is demonstrated that the inhibition of Notch pathway in MSC leads to a lesser proliferation and osteogenic capability avoiding fracture healing[24]. Zanotti *et al*. have observed that Notch effects in the skeleton are cell-context-dependent finding different effects on immature osteoblasts or osteocytes[25]. These and other works highlight the potential dimorphic effects of Notch signaling in bone homeostasis[26].

Finally, and with respect to Mg^{2+} supplementation more studies, considering other important parameters for bone turnover such as PTH or vitamin D, should be led to evaluate with precision the *in vivo* effects of Mg^{2+} supplementation on the mineralization or the osteoid production in the bone.

In addition, we studied the effect of Mg^{2+} on cell organization and osseointegration of progenitor cells on rat decellularized bone. Our results reveal that the supplementation with Mg^{2+} improves cell attachment and increases osteogenic differentiation of MSC cultured on decellularized bone. Transmission electron microscopy analysis showed that Mg^{2+} supplementation increased proliferation and maturation of MSC differentiated into osteocytes with the presence of cytoplasmic prolongations between osteocytes (bone canaliculi) and a well-organized osteoid matrix with a large number of layers similar to the appositional growth observed in bones.

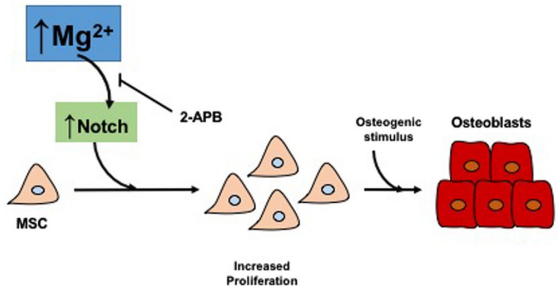

Figure 7. Summary figure. Magnesium supplementation enhances proliferation of MSC. Mechanistically, magnesium ions enter into MSC through TRPM7 channel, increasing Notch Intracellular Domain (NICD) nuclear translocation. Proliferation of MSC contributes to a subsequent osteogenesis. Inhibition of TRPM7 channels by 2-APB decreases the osteogenic potential of magnesium.

Similarly, using scanning electron microscopy analysis, it was shown that Mg^{2+} induced proliferation, differentiation and a more organized distribution of the osteocytes coating the surface of decellularized bone, allowing mineralization and formation of new bone. These data indicate that the bone tissue formed on decellularized rat bone after Mg^{2+} supplementation has a better internal distribution with highly organized structures. Several studies have shown that Mg^{2+} ions may enhance cell attachment and promote bone formation. Moreover, previous studies have demonstrated that Mg^{2+} ions support the initial cell adhesion of MSC and increase proliferation and activation of integrins[27]. Recently, Galli *et al.* also showed that the immersion of threaded screws in a solution of $MgCl_2$ (10 mg/ml) leads to enhanced osteogenesis and improves osseointegration[28].

The data reported in this study could represent a new, feasible and economic strategy to improve bone formation in different types of scaffolds. In addition, these results also suggest that local administration of moderately high levels of Mg^{2+} could be suitable to promote osteogenesis in pathologies in which bone formation is necessary.

This approach would significantly impact the orthopaedic field, and further provides new targets to improve the quality of the materials currently available.

Methods

Isolation of rat bone marrow MSC. All experimental protocols were reviewed and approved by the Ethics Committee for Animal Research of IMIBIC in accordance with the ethical guidelines of the Institution and the EC Directive 86/609/EEC for animal experimentation. Twenty male Wistar rats were euthanized by aortic puncture under general anesthesia with pentobarbital sodium (50 mg/kg) and midazolam (4 mg/kg/i.p). Tibiae and femurs were cut at the epiphyses and subsequently perfused with alpha minimal essential medium (αMEM; Sigma-Aldrich CO, St. Louis, MO, USA) containing FBS (15%; Lonza Inc., Walkersville, MD, USA), ultraglutamine (1%; Lonza), penicillin (100 U/mL) and streptomycin (100 µg/mL). Single-cell suspension was generated by filtration through 70 µm cell strainer (BD Biosciences, San Jose, CA, USA). MSC were isolated according to their plastic adherence properties. Following centrifugation and washing with αMEM, bone marrow cells were cultured in 25 cm^2 flasks (NUNC A/S, Roskilde, DE, USA) with αMEM containing FBS (15%), ultraglutamine (1%), penicillin (100 U/mL), streptomycin (100 mg/mL) and basic fibroblast growth factor (bFGF; 1 ng/mL; PeproTech EC Ltd., London, UK) in a humidified atmosphere with 5% CO_2 at 37 °C. Fresh α-MEM with FBS (10%), ultraglutamine (1%), penicillin (100 U/mL), streptomycin (100 µg/mL) and bFGF (1 ng/mL) was added after 24 h and changed every 3 days. Once 85–90% confluence was reached, cells were collected using Trypsin-EDTA (Lonza) and seeded in 6-well plates (NUNC) at 13000 cells/cm^2. Treatments were started as described below when cells reached 90% confluence.

Osteogenic differentiation of MSC and treatments. MSC were cultured for 21 days in αMEM with FBS (10%), ultraglutamine (1%), penicillin (100 U/mL), streptomycin (100 µg/ml) and osteogenic stimuli based on dexamethasone (1 µM; Sigma-Aldrich), β-glycerol phosphate (10 mM; Sigma-Aldrich) and ascorbic acid (0.2 mM; BAYER, Barcelona, Spain). Basal Mg^{2+} concentration in the medium was 0.8 mM. In order to increase the Mg^{2+} content in the pro-osteogenic medium, $MgCl_2$ (Carlo ErbaReagentiSpA, Milano, Italy) was added to achieve final Mg^{2+} concentrations of 1.2 mM and 1.8 mM during the osteogenic stimulus. Fresh medium alone or osteogenic medium supplemented with $MgCl_2$ was replaced every 3 days. Furthermore, 2-APB (50 µM; Tocris Bioscience, Bristol, UK) was added to the osteogenic medium containing 0.8 mM of Mg^{2+} during differentiation to determine the effects of inhibiting the Mg^{2+} channel TRPM7. To examine a direct effect of Mg^{2+} supplementation (1.2 and 1.8 m, or 2-APB) for 24 hours on undifferentiated MSC or at the different stages of differentiation (early or mature osteoblasts obtained from MSC) the NICD expression was also analyzed by western blot. All experiments were repeated at least three times.

RNA isolation and quantitative RT-PCR. Total RNA was extracted with TRI reagent (1 mL; Sigma-Aldrich) and quantified by spectrophotometry (ND-1000, Nanodrop Technologies, Wilmington, DE, USA). cDNA was synthesized from 1 µg of total RNA with a first strand cDNA synthesis kit (Qiagen,

Hilden, Germany) in the presence of random hexamers in a final volume of 20 µl at 25 °C for 10 min, followed by 42 °C for 15 min and 95 °C for 3 min. PCR SYBR Green kit (Qiagen N.V., Hilden, Germany) was used to quantify mRNA expression levels. Primers for PCR were synthesized with Oligo software. *RUNX2* (Forward 5′CGG-GAA-TGA-TGA-GAA-CTA-CTC3′ Reverse 5′CGG-TCA-GAG-AAC-AAA-CTA-GGT3′), *OSTERIX* (Forward 5′GTA-CGG-CAA-GGC-TTC-GCA-TCT-GA3′ Reverse 5′TCA-AGT-GGT-CGC -TTC-GGG-TAA-AG3′), *OSTEOCALCIN* (Forward 5′TCT-GAG-TCT-GAC-AAA-GCC-TTC-ATG3′ Reverse 5′TGG-GTA-GGG-GGC-T GG-GGC-TCC3′), and *18-S* (Forward 5′GTA-ACC-CGT-TGA-ACC-CCA-TT3 ′Reverse 5′CCA-TCC-AAT-CGG-TAG-TAG-CG3′). Primers for *HEY2* (Forward: 5′TCC-AAT-GCT -CAT-AAA-GTC-CGT3′ and Reverse: 5′ TCT-GCA-AAT-GAC-AGT-GGA-TCA3′) were purchased from IDT Integrated DNA Technologies (Leuven, Belgium). The expression level of these genes was evaluated by quantitative RT-PCR (Light cycler, Roche Diagnostics, Basel, Switzerland) with the $2^{-\Delta\Delta}C_t$ method, using ribosomal 18 S RNA as housekeeping control.

Protein extraction and Western blot analysis. Cytosolic protein was isolated from cells in lysis buffer A, containing Hepes (10 mM), KCl (10 mM), EDTA (0.1 mM), EGTA (0.1 mM), DTT (1 mM), PMSF (0.5 mM), Protease Inhibitor Cocktail (15 µL/mL; Sigma-Aldrich), Igepal CA-630 (0.5%; Sigma-Aldrich), pH 7.9. The suspension was centrifuged, and the supernatant (cytosolic extract) was stored. Nuclear extracts were obtained by incubating the pellet obtained from the cytosolic extract in lysis buffer B, containing HEPES (20 mM), NaCl (0.4 M), EDTA (1 mM), EGTA (1 mM), DTT (1 mM), PMSF (0.5 mM), Protease Inhibitor Cocktail (15 µL/mL), pH 7.9. Protein concentration was determined by Bradford assay (Bio-Rad Laboratories, Hercules, CA, USA). To determine specific protein contents, 20 µg of nuclear cell lysates were analyzed by immunoblotting using antibodies against proliferating cell nuclear antigen (PCNA; 1:100; Santa Cruz Biotechnology INC, Dallas, TX, USA), Cyclin D1 (1:500; Cell Signaling Technology Inc., Danvers, MA, USA) and cleaved Notch 1 (Val1744) (1:200; Cell Signaling Technology) as primary antibodies, and horseradish peroxidase-conjugated goat anti-mouse (1:10000; Santa Cruz Biotechnology) and goat anti-rabbit (1:10000; Santa Cruz Biotechnology) as secondary antibodies. Transcription factor II B (TFIIB; 1:1000; Cell Signaling Technology) was used as loading control.

Alkaline phosphatase activity quantification. 2 µg of cytoplasmic cell lysates were incubated in p-nitrophenol phosphate (2 mM; Sigma-Aldrich) for 30 min at 37 °C. The reaction was stopped by adding NaOH (3 M), and alkaline phosphatase (ALP) activity was measured by quantifying absorption at 405 nm. ALP activity was expressed as µmol of hydrolyzed p-nitrophenol phosphate per min and per mg of protein versus undifferentiated control cells.

Alizarin red S staining. Matrix mineralization was detected by alizarin red S staining. Cells were washed twice with PBS, fixed with para-formaldehyde (2%) and sucrose (1%) for 15 min and subsequently washed 3 times with PBS. Then, cells were stained with alizarin red S pH 4.1 (40 mM; Sigma-Aldrich) for 20 min, and washed 4 times for 5 min with water at pH 7. Finally, water was removed and samples were dried at room temperature. Plates were scanned in a WIFI OKI Scanner (Madrid, Spain).

Immunofluorescence analysis. For immunofluorescence analysis cells were cultured upon glass coverslips in 6-well plates. After 14 days of treatment, cells were fixed with cold methanol for 20 min and subsequently washed with PBS. Fixed cells were incubated with the antibodies diluted in BSA (1%; Sigma-Aldrich) in PBS. Primary antibodies against cleaved Notch 1 (Val1744) (1:50) and β-catenin (1:75; BD Biosciences, San Jose, CA, USA) were incubated for 1 h at 4 °C. Subsequently, cells were washed with PBS and incubated with Alexa Fluor 488 anti-mouse (1:500; Invitrogen Ltd., Paisley, UK) diluted in BSA (1%) in PBS. Cell nuclei were visualized with the nuclear dye 4′,6-diamino-2-phenylindole dihydrochloride (DAPI) (Invitrogen). Pictures were obtained at 40X in Axio Observer Z1 Inverted Confocal microscope (LSM5 Exciter Zeiss, Jena, Germany). ImageJ software (National Institutes of Health, Bethesda, MD, USA) was used to analyze the confocal images.

FGF23 secretion quantification. Supernatants from cultures were collected and pooled, and intact fibroblast growth factor 23 (FGF23) secretion was determined by using a specific ELISA kit (Kainos Laboratories, Tokyo, Japan).

Rat femurs decellularization and scaffolds preparation. Bone scaffolds were obtained as it has been previously reported by Shahabipour[29]. Briefly, rat femurs and tibiae were cut longitudinally in 5 mm pieces. Subsequently, bone pieces were boiled 4 times for 5 minutes to remove fat tissues. Pieces were stored overnight at −20 °C before decellularization. Bone specimens were thawed at room temperature, washed with PBS and placed in liquid nitrogen for 2 minutes. Then, pieces were maintained in distilled water at room temperature and washed with PBS. The freeze-thaw process was repeated five times to lysate the cells. Bone scaffolds were decellularized in SDS (2.5%) for 24 hours at 37 °C with gentle shaking. Then, bone specimens were washed with PBS twice for 15 minutes to remove SDS, washed in ethanol (70%) and maintained in PBS for 30 minutes with shaking at room temperature.

Scanning Electron Microscope (SEM). Decellularized bone fragments were cut in small pieces and washed in buffer solution for 15 minutes to remove debris. Then samples were kept in glutaraldehyde (2.5%). Decellularized bones without addition of MSC were also analyzed to ensure the decellularization process. Bone scaffolds were mounted on the SEM specimen stubs with carbon tape and were carbon-coated. Samples were analyzed and photographed with a Hitachi S520 SEM (Tokyo, Japan).

Transmission Electron Microscope (TEM). Bone marrow MSC were cultured in the presence of different concentrations of $MgCl_2$ (0.8, 1.2 and 1.8 mM) on rat femur scaffolds. After 21 days of culture, the cellular layer was removed from the surface of the bone scaffolds and they were analyzed by electronic microscopy. For the ultrastructural study, randomly selected samples of decellularized bone scaffolds were primarily fixed in a glutaraldehyde (2%) solution in phosphate buffer (0.1 M) pH 7.4 overnight at 4 °C and then re-fixed in osmium tetroxide (1%) in phosphate buffer (0.1 M) pH 7.4 for 30 minutes. After dehydration in graded ethanol series and embedding in araldite, semi-thin and ultra-thin sections were cut with a LKB ultramicrotome. Ultra-thin sections were viewed and photographed in a Philips CM10 transmission electron microscope.

Statistical analysis. Differences between means for three or more groups were assessed by T-test. A P-value < 0.05 was considered significant. Statistical analyses were performed with the assistance of GraphPad Prism version 6.1 software (GraphPad Software, Inc., La Jolla, CA, USA).

References

1. Oryan, A., Alidadi, S., Moshiri, A. & Maffulli, N. Bone regenerative medicine: classic options, novel strategies, and future directions. *J. Orthop. Surg. Res.* **9**, 18 (2014).
2. Garcia-Gareta, E., Coathup, M. J. & Blunn, G. W. Osteoinduction of bone grafting materials for bone repair and regeneration. *Bone* **81**, 112–121 (2015).
3. Bucholz, R. W. Nonallograft osteoconductive bone graft substitutes. *ClinOrthopRelat Res* 44–52 (2002).
4. Giannoudis, P. V., Dinopoulos, H. & Tsiridis, E. Bone substitutes: an update. *Injury* **36**(Suppl 3), S20–S27 (2005).
5. Silber, J. S. *et al*. Donor site morbidity after anterior iliac crest bone harvest for single-level anterior cervical discectomy and fusion. *Spine Phila Pa 1976* **28**, 134–139 (2003).
6. Kanazawa, I. *et al*. A case of magnesium deficiency associated with insufficient parathyroid hormone action and severe osteoporosis. *Endocr J.* **54**, 935–940 (2007).
7. Farraro, K. F., Kim, K. E., Woo, S. L., Flowers, J. R. & McCullough, M. B. Revolutionizing orthopaedic biomaterials: The potential of biodegradable and bioresorbable magnesium-based materials for functional tissue engineering. *J. Biomech.* **47**, 1979–1986 (2014).
8. Kraus, T. *et al*. Magnesium alloys for temporary implants in osteosynthesis: *in vivo* studies of their degradation and interaction with bone. *Acta Biomater* **8**, 1230–1238 (2012).
9. Minardi, S. *et al*. Evaluation of the osteoinductive potential of a bio-inspired scaffold mimicking the osteogenic niche for bone augmentation. *Biomaterials* **62**, 128–137 (2015).
10. Witte, F. *et al*. *In vivo* corrosion of four magnesium alloys and the associated bone response. *Biomaterials* **26**, 3557–3563 (2005).
11. Han, P. *et al*. *In vitro* and *in vivo* studies on the degradation of high-purity Mg (99.99wt.%) screw with femoral intracondylar fractured rabbit model. *Biomaterials* **64**, 57–69 (2015).
12. Abdallah, B. M., Jafari, A., Zaher, W., Qiu, W. & Kassem, M. Skeletal (stromal) stem cells: an update on intracellular signaling pathways controlling osteoblast differentiation. *Bone* **70**, 28–36 (2015).
13. Lin, G. & Hankenson, K. D. Integration of BMP, Wnt, and Notch signaling pathways in osteoblast differentiation. *J. Cell. Biochem.* **112**, 3491–3501 (2011).
14. Engin, F. & Lee, B. NOTCHing the bone: insights into multi-functionality. *Bone* **46**, 274–280 (2010).
15. Hilton, M. J. *et al*. Notch signaling maintains bone marrow mesenchymal progenitors by suppressing osteoblast differentiation. *Nat. Med.* **14**, 306–314 (2008).
16. Staiger, M. P., Pietak, A. M., Huadmai, J. & Dias, G. Magnesium and its alloys as orthopedic biomaterials: a review. *Biomaterials* **27**, 1728–1734 (2006).
17. Zhang, J. *et al*. Magnesium modification of a calcium phosphate cement alters bone marrow stromal cell behavior via an integrin-mediated mechanism. *Biomaterials* **53**, 251–264 (2015).
18. Yoshizawa, S., Brown, A., Barchowsky, A. & Sfeir, C. Magnesium ion stimulation of bone marrow stromal cells enhances osteogenic activity, simulating the effect of magnesium alloy degradation. *Acta Biomater* **10**, 2834–2842 (2014).
19. Rude, R. K. & Gruber, H. E. Magnesium deficiency and osteoporosis: animal and human observations. *J.Nutr. Biochem.* **15**, 710–716 (2004).
20. Hoenderop, J. G. & Bindels, R. J. Epithelial Ca2+ and Mg2+ channels in health and disease. *J. Am. Soc. Nephrol.* **16**, 15–26 (2005).
21. Abed, E. & Moreau, R. Importance of melastatin-like transient receptor potential 7 and magnesium in the stimulation of osteoblast proliferation and migration by platelet-derived growth factor. *AmJPhysiol Cell Physiol* **297**, C360–C368 (2009).
22. Elizondo, M. R. *et al*. Defective skeletogenesis with kidney stone formation in dwarf zebrafish mutant for trpm7. *Curr. Biol.* **15**, 667–671 (2005).
23. Long, F. Building strong bones: molecular regulation of the osteoblast lineage. *Nat. Rev. Mol. Cell. Biol* **13**, 27–38 (2012).
24. Wang, C. *et al*. NOTCH signaling in skeletal progenitors is critical for fracture repair. *J. Clin. Invest.* **126**, 1471–1481 (2016).
25. Zanotti, S. *et al*. Notch inhibits osteoblast differentiation and causes osteopenia. *Endocrinology* **149**, 3890–3899 (2008).
26. Engin, F. *et al*. Dimorphic effects of Notch signaling in bone homeostasis. *Nat. Med* **14**, 299–305 (2008).
27. Kim, B. S., Kim, J. S., Park, Y. M., Choi, B. Y. & Lee, J. Mg ion implantation on SLA-treated titanium surface and its effects on the behavior of mesenchymal stem cell. *Mater. Sci. Eng. CMater. Biol. Appl* **33**, 1554–1560 (2013).
28. Galli, S. *et al*. Local release of magnesium from mesoporous TiO2 coatings stimulates the peri-implant expression of osteogenic markers and improves osteoconductivity *in vivo*. *Acta Biomater* **10**, 5193–5201 (2014).
29. Shahabipour, F., Mahdavi-Shahri, N., Matin, M. M., Tavassoli, A. & Zebarjad, S. M. Scaffolds derived from cancellous bovine bone support mesenchymal stem cells' maintenance and growth. *Vitro Cell DevBiolAnim* **49**, 440–448 (2013).

Acknowledgements

We acknowledge the technical support provided by Esther Peralbo in performing the studies with Confocal Microscopy (IMIBIC). N Vergara and JM Díaz-Tocados are supported by Consejería de Economía, Innovación, Ciencia y Empleo from Junta de Andalucía (CVI-7925). ME Rodriguez-Ortiz is recipient of a "Sara Borrell" research contract from the National Institute of Health Carlos III. Y. Almaden and JR. Muñoz-Castañeda are senior researchers supported by Nicolás Monardes Programme, Consejeria de Salud-SAS (Junta de Andalucia).

Author Contributions

Conception and design: M.R., Y.A., and J.R.M.-C. Acquisition of data: J.M.D.-T., C.H., J.M.M.-M., M.E.R.-O., A.B., A.M.D.O., N.V. Analysis and interpretation of data: J.M.D.-T., Y.A., J.R.M.-C., A.B., S.S. Drafting, revision or important intellectual content: M.R., S.S., Y.A., J.R.M.-C. Final approbation: M.R., Y.A., J.R.M.-C. Total agreement with the manuscript: All authors. Responsibility for the integrity of the data analysis: M.R. and J.R.M.-C.

Additional Information

Supplementary information accompanies this paper at doi:10.1038/s41598-017-08379-y

Competing Interests: Mariano Rodriguez has received honorarium for lectures from Abbott, Amgen, Fresenius, Shire. Sonja Steppan is employee of Fresenius Medical Care Deutschland GmbH.

Publisher's note: Springer Nature remains neutral with regard to jurisdictional claims in published maps and institutional affiliations.

Dietary magnesium supplementation prevents and reverses vascular and soft tissue calcifications in uremic rats

see commentary on page 1034

Juan M. Diaz-Tocados[1,10], Alan Peralta-Ramirez[2,3,10], María E. Rodríguez-Ortiz[1], Ana I. Raya[2], Ignacio Lopez[2], Carmen Pineda[2], Carmen Herencia[1], Addy Montes de Oca[1], Noemi Vergara[1], Sonja Steppan[4], M. Victoria Pendon-Ruiz de Mier[1], Paula Buendía[5], Andrés Carmona[5], Julia Carracedo[5], Juan F. Alcalá-Díaz[6], Joao Frazao[7], Julio M. Martínez-Moreno[1], Antonio Canalejo[8], Arnold Felsenfeld[9], Mariano Rodriguez[1], Escolástico Aguilera-Tejero[2], Yolanda Almadén[6,11] and Juan R. Muñoz-Castañeda[1,11]

[1]Servicio de Nefrología (Red in Ren), GC13, Metabolismo del calcio, Calcificación Vascular, Instituto Maimónides de Investigación Biomédica de Córdoba/Hospital Universitario Reina Sofia/Universidad de Cordoba, Cordoba, Spain; [2]Department Medicina y Cirugía Animal, Universidad de Córdoba, Córdoba, Spain; [3]Escuela de Medicina Veterinaria, Universidad Nacional Autónoma de Nicaragua, (UNAN- 15 Leon), Leon, Nicaragua; [4]Fresenius Medical Care Deutschland GmbH, Bad Homburg, Germany; [5]Servicio de Nefrología (Red in Ren), GC-07, Nefrología. Daño celular en la inflamación crónica. Instituto Maimónides de Investigación Biomédica de Córdoba/Hospital Universitario Reina Sofia/Universidad de Cordoba, Cordoba, Spain; [6]Unidad de Lípidos y Aterosclerosis, IMIBIC/Hospital Universitario Reina Sofia/Universidad de Cordoba and CIBER Fisiopatologia Obesidad y Nutricion (CIBEROBN), Instituto de Salud Carlos III, Córdoba, Spain; [7]Departamento de Investigación y Desarrollo en Nefrologiay enfermedades infecciosas-unidad de histomorfometria, INEB-(I3S), Universidad de Oporto, Oporto, Portugal; [8]Department of Biologia Ambiental y Salud Publica, Universidad de Huelva, Huelva, Spain; and [9]Department of Medicine, Veterans Affairs Greater Los Angeles Healthcare System and the David Geffen School of Medicine, University of California, Los Angeles, California, USA

Although magnesium has been shown to prevent vascular calcification *in vitro*, controlled *in vivo* studies in uremic animal models are limited. To determine whether dietary magnesium supplementation protects against the development of vascular calcification, 5/6 nephrectomized Wistar rats were fed diets with different magnesium content increasing from 0.1 to 1.1%. In one study we analyzed bone specimens from rats fed 0.1%, 0.3%, and 0.6% magnesium diets, and in another study we evaluated the effect of intraperitoneal magnesium on vascular calcification in 5/6 nephrectomized rats. The effects of magnesium on established vascular calcification were also evaluated in uremic rats fed on diets with either normal (0.1%) or moderately increased magnesium (0.6%) content. The increase in dietary magnesium resulted in a marked reduction in vascular calcification, together with improved mineral metabolism and renal function. Moderately elevated dietary magnesium (0.3%), but not high dietary magnesium (0.6%), improved bone homeostasis as compared to basal dietary magnesium (0.1%). Results of our study also suggested that the protective effect of magnesium on vascular calcification was not limited to its action as an intestinal phosphate binder since magnesium administered intraperitoneally also decreased vascular calcification. Oral magnesium supplementation also reduced blood pressure in uremic rats, and in vitro medium magnesium decreased BMP-2 and p65–NF-κB in TNF-α–treated human umbilical vein endothelial cells. Finally, in uremic rats with established vascular calcification, increasing dietary magnesium from 0.1% magnesium to 0.6% reduced the mortality rate from 52% to 28%, which was associated with reduced vascular calcification. Thus, increasing dietary magnesium reduced both vascular calcification and mortality in uremic rats.

Kidney International (2017) **92,** 1084–1099; http://dx.doi.org/10.1016/j.kint.2017.04.011

KEYWORDS: dietary magnesium; hypertension; mineral metabolism; phosphate binder; vascular calcification

Correspondence: *Mariano Rodriguez, Servicio de Nefrología (Red in Ren), GC13, Metabolismo del calico, Calcificación Vascular, Instituto Maimónides de Investigación Biomédica de Córdoba/Hospital Universitario Reina Sofia/Universidad de Cordoba, Cordoba, Spain. E-mail: marianorodriguezportillo@gmail.com*

[10]These authors shared first authorship.

[11]These authors shared last authorship.

Received 24 August 2016; revised 21 March 2017; accepted 6 April 2017; published online 29 July 2017

The role of magnesium (Mg) in the prevention of cardiovascular disease (CVD) is a subject of growing interest. The American Medical Association has included recommendations on Mg intake to prevent CVD.[1] Epidemiologic, prospective, and recent meta-analysis studies have favorably associated Mg intake with a decreased risk of CVD.[2–6] Taking into account the pleiotropic effects of Mg, several plausible mechanisms have been proposed to explain its cardiometabolic benefits, including its effects on

inflammation, lipid metabolism, and endothelial function.[4] In animal studies, Mg deficiency accelerated atherosclerosis, while Mg supplementation suppressed its development.[7]

CVD, particularly the development of vascular calcification (VC), is a major cause of morbidity and mortality in patients with chronic kidney disease (CKD). Experimental and clinical studies have shown that high serum phosphate (P) is a critical factor in the development of VC[8] and CKD.[9,10] Phosphate binders are used to control serum P in uremic patients, and Mg-containing phosphate binders have been shown to be effective.[11,12]

Recent data show a clear association between low serum Mg levels and mortality in CKD patients.[13] Also, serum Mg concentrations have been inversely associated with cardiovascular events in CKD.[14] In nondiabetic hemodialysis patients, hypomagnesemia is associated with VC of hand arteries independently of the serum concentration of calcium (Ca) and P.[15] Mitral annular calcification and an increase in carotid intima-media thickness were strongly associated with low Mg values in hemodialysis patients.[16,17] Conversely, a moderate increase in serum Mg may have beneficial effects on VC and mortality rates in CKD patients. Long-term Mg supplementation has been reported to reduce carotid intima-media thickness and may retard progression of vascular disease.[18]

We and others have shown in *in vitro* studies that Mg reduces calcification of vascular smooth muscle cells (VSMCs) cultured in high-P medium[19–22] and also decreases hydroxyapatite crystal growth.[23] Inhibition of Mg transport into cells prevents the protective effect of Mg on VSMC calcification, indicating that Mg is taken up by the cells and exerts its beneficial effect through active intracellular processes. *In vivo*, Mg may also protect against VC by decreasing serum P.[16] Furthermore, Mg modulates metabolic derangements associated with uremia such as insulin resistance and oxidative stress, both of which have been shown to enhance VC in rats with renal failure.[24]

Controlled *in vivo* studies addressing the influence of dietary Mg on uremic VC are lacking. Moreover, changes in mineral metabolism parameters elicited by Mg supplementation have not been described in detail in the uremic setting. Our study was aimed at investigating the effect of different levels of dietary Mg intake on the prevention and treatment of VC in uremic rats. In addition, we analyzed bone effects of Mg supplementation and also evaluated whether the effects of Mg are dependent on its effect as a phosphate binder. To address these objectives, an experimental model of 5/6 nephrectomy in Wistar rats was used because it resembles the mineral abnormalities associated with uremia.

RESULTS

Experiment 1: effect of dietary Mg intake on the development of VC

Parameters of mineral metabolism. The first part of the study was designed to assess the effect of different dietary Mg intake on the prevention of VC in uremic rats (Figure 1). The

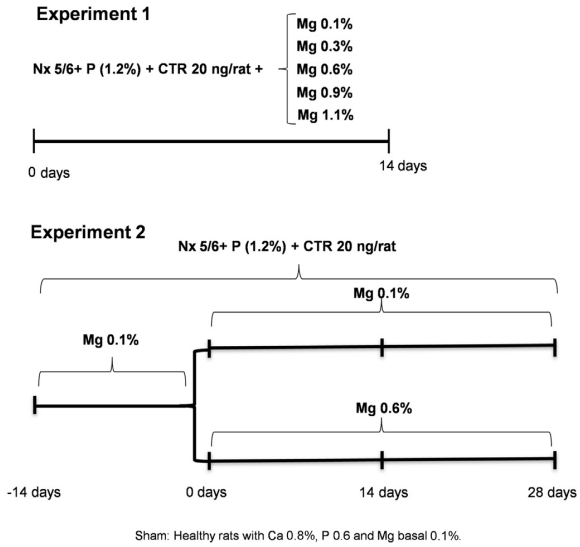

Figure 1 | Experimental design. (See text for details.) CTR, calcitriol; Mg, magnesium; Nx 5/6, 5/6 nephrectomy; P, phosphate.

body weights of all groups before 5/6 nephrectomy and sham operation were not different. At killing, body weight in the sham group was greater than that in the nephrectomy groups, but among nephrectomy groups body weight did not differ. The results of serum biochemistry in the study groups are shown in Table 1. As expected, the concentration of serum creatinine was increased in nephrectomized rats compared with sham-operated rats. Among nephrectomized rats, serum creatinine was greatest ($P < 0.05$) in rats ingesting the lowest (normal) Mg diet (0.1%). Nephrectomized rats fed Mg 0.1% had higher serum Mg levels than sham-operated rats fed Mg 0.1% ($P < 0.05$). Among nephrectomized rats, a progressive increase in serum Mg concentration was observed as dietary Mg was increased from 0.1% to 1.1%. Serum P was greater in nephrectomized than in sham-operated rats ($P < 0.05$). In nephrectomized rats, serum P was greatest in rats on the Mg 0.1% diet. As expected, nephrectomized rats showed a decrease in ionized calcium (iCa) concentration that was accentuated by the Mg 0.1% diet, which also had the highest value of serum P. In nephrectomized rats the elevated parathyroid hormone (PTH) values progressively decreased as dietary Mg was increased from 0.1% to 0.9%, at which point normal PTH values were observed. Serum calcitriol values were decreased in nephrectomized rats compared with sham-operated rats and were similar among nephrectomy groups with different intakes of Mg. Fibroblast growth factor 23 (FGF23) values were greater in nephrectomized than in sham-operated rats; however, among nephrectomized rats, the pattern of FGF23 increase as dietary Mg was increased was not uniform.

Urine Ca, P, and Mg concentrations were corrected for urine creatinine (Table 2). Creatinine clearance (CrCl) was greater in the 5/6 nephrectomy groups that received Mg

Table 1 | Experiment 1: effect of dietary magnesium on the development of aortic calcification (mean ± SEM)

Parameter	Sham + Mg 0.1% (n = 10)	Nx + Mg 0.1% (n = 14)	Nx + Mg 0.3% (n = 10)	Nx + Mg 0.6% (n = 10)	Nx + Mg 0.9% (n = 10)	Nx + Mg 1.1% (n = 10)
Body weight (g)	306 ± 34.9	235 ± 40.6[a]	242 ± 20.2[a]	236 ± 31.1[a]	233 ± 31.1[a]	226 ± 19.5[a]
Creatinine (mg/dl)	0.41 ± 0.06	1.71 ± 0.2[a]	1.11 ± 0.12[a,b]	1.10 ± 0.16[a,b]	1.04 ± 0.06[a,b]	1.20 ± 0.2[a,b]
Magnesium (mg/dl)	2.14 ± 0.09	2.97 ± 0.3[a]	2.98± 0.2[a,b]	3.31 ± 0.4[a,b]	4.43± 0.4[a,b]	4.58 ± 0.4[a,b]
Phosphate (mg/dl)	6.5 ± 0.3	10.7 ± 1.4[a]	8.0 ± 0.8[a,b]	7.9 ± 0.9[a,b]	7.9 ± 0.5[a,b]	7.8 ± 0.4[a,b]
Ionized calcium (mM)	1.20 ± 0.01	1.07 ± 0.03[a]	1.19 ± 0.02[b]	1.13 ± 0.03[a,b]	1.16 ± 0.02[a,b]	1.18 ± 0.02[b]
PTH (pg/ml)	21 ± 7	529 ± 171[a]	401 ± 170[a]	79 ± 46[a,b]	23 ± 17[b]	29 ± 7[b]
Calcitriol (pg/ml)	318 ± 29	110 ± 23[a]	120 ± 25[a]	89 ± 25[a]	125 ± 32[a]	143 ± 18[a]
FGF23 (pg/ml)	218 (147)	10,0311 (158105)[c]	783 (814)[c,d]	16,253 (9121)[c,e]	20,546 (5437)[c,e]	5740 (6001)[c,e]

FGF23, fibroblast growth factor 23; Mg, magnesium; Nx, nephrectomy; PTH, parathyroid hormone.
[a]$P < 0.05$ versus sham + Mg 0.1%.
[b]$P < 0.05$ versus Nx + Mg 0.1%.
[c]$P < 0.01$ versus sham plus Mg 0.1%.
[d]$P < 0.01$ versus Nx plus Mg 0.1%.
[e]$P < 0.05$ versus Nx plus Mg 0.1%.

supplementation compared with those that did not (Table 1). In rats fed Mg 0.6%, 0.9%, and 1.1%, CrCl was similar and significantly greater than 0.3%, which in turn was greater than in rats on Mg 0.1%. Urinary Ca was greater in the Mg 1.1% group than in the rest of the nephrectomized rats. Urine P and the fractional excretion of P were greatest in the nephrectomy plus Mg 0.1% and nephrectomy plus Mg 0.3% groups, which had the highest PTH values. The fractional excretion of P was also greater in the nephrectomy plus Mg groups than in the Mg 0.1% sham group. Urine Mg excretion was less in the nephrectomy plus Mg 0.1% group than in the sham plus Mg 0.1% group. Urine Mg excretion was increased in the nephrectomy plus 0.3%, 0.6%, and 0.9% Mg groups, which also had the highest serum Mg values.

Tissue Ca and P content. Tissue Ca and P were evaluated both by direct measurement and histology (Figure 2). The Ca content of the aorta in nephrectomized rats fed a Mg 0.1% diet (13.6 ± 2.2 mg/g tissue) was more than 80 times greater than in sham-operated rates fed a Mg 0.1% diet (Figure 2a). In nephrectomized rats, the change from 0.1% to Mg 0.3% was associated with a 15-fold reduction in the Ca content in the aorta (1.06 ± 0.31 mg/g tissue). The increase in aortic P content after nephrectomy was even greater, with values of 37.8 ± 6.8 mg/g tissue in nephrectomized rats on a Mg 0.1% diet compared with 0.04 ± 0.02 mg/g in sham-operated rats (Figure 2b). The decrease in aortic P content with an increase in Mg intake was similar to the reduction observed in Ca. Moreover, in the nephrectomy groups, an increase in dietary Mg intake from 0.3% to 0.6% reduced the aortic Ca and P content to levels similar to sham-operated rats. Histological staining for CaP showed widespread distribution of CaP in the aorta in the nephrectomy plus Mg 0.1% group. Increasing dietary Mg in the nephrectomy groups essentially prevented CaP deposition as assessed by histology (Figure 2c). The osteochondrogenic markers Runx2 (Figure 2d) and BMP-2 (Figure 2e) were significantly increased in the nephrectomy plus Mg 0.1% group compared with sham-operated animals. The expression of these markers decreased significantly after 14 days with 0.3% and 0.6% dietary Mg supplementation.

Calcification in the stomach was similar to that seen in the aorta. In nephrectomized rats on the Mg 0.1% diet, stomach Ca content was 2.3 ± 0.4 mg/g tissue, whereas on the Mg 0.3% diet, the Ca content was only 0.06 ± 0.01 mg/g tissue. Values for the stomach content of P paralleled those of Ca. An additional increase in dietary Mg intake did not further reduce Ca deposition in the stomach (Supplementary Figure S1).

With respect to bone status, Figure 3 shows that compared with sham-operated rats, uremic rats fed Mg 0.1% presented a decrease in bone volume and an increase in osteoid volume, osteoid surface, osteoid thickness, osteoblasts, and osteoclast surface. Increasing Mg supplementation to 0.3% significantly changed some bone parameters, reducing osteoid volume and osteoid surface compared with rats on the Mg 0.1% diet and

Table 2 | Experiment 1: effect of dietary magnesium on the development of aortic calcification, urine chemistry in the study groups (see text for details)

Parameter	Sham + Mg 0.1%	Nx + Mg 0.1%	Nx + Mg 0.3%	Nx + Mg 0.6%	Nx + Mg 0.9%	Nx + Mg 1.1%
Creat. clearance	3.25 ± 0.30	0.57 ± 0.11[a]	0.68± 0.14[a]	1.16 ± 0.21[a,b]	1.63 ± 0.22[a,b,c]	1.13 ± 0.13[a,b]
Ca-to-creat. ratio	0.05 ± 0.01	0.11 ± 0.07	0.18 ± 0.03	0.15 ± 0.04	0.15 ± 0.04	0.35 ± 0.12[a,b]
P-to-creat. ratio	0.68 ± 0.06	6.12 ± 0.83[a]	6.11 ± 0.70[a]	3.47 ± 0.44[b]	1.97 ± 0.30[b]	2.40 ± 0.64[b]
Mg-to-creat. ratio	1.04 ± 0.10	0.45 ± 0.06[a]	1.48 ± 0.16[a,b]	1.72 ± 0.25[a,b]	1.86 ±0.20[a,b]	N/A
Frac. excretion of P (%)	4.9 ± 0.80	95.0 ± 17.2[a]	86.5 ± 7.1[a]	44.8 ± 6.0 (ab)	21.7 ± 3.4[a,b]	36.4 ± 12.7[a,b]

Ca, calcium; creat., creatinine; frac., fractional; Mg, magnesium; N/A, not applicable; Nx, nephrectomy; P, phosphate.
[a]$P < 0.05$ versus sham plus Mg 0.1%.
[b]$P < 0.05$ versus Nx plus Mg 0.1%.
[c]$P < 0.05$ versus Nx plus Mg 0.3%.

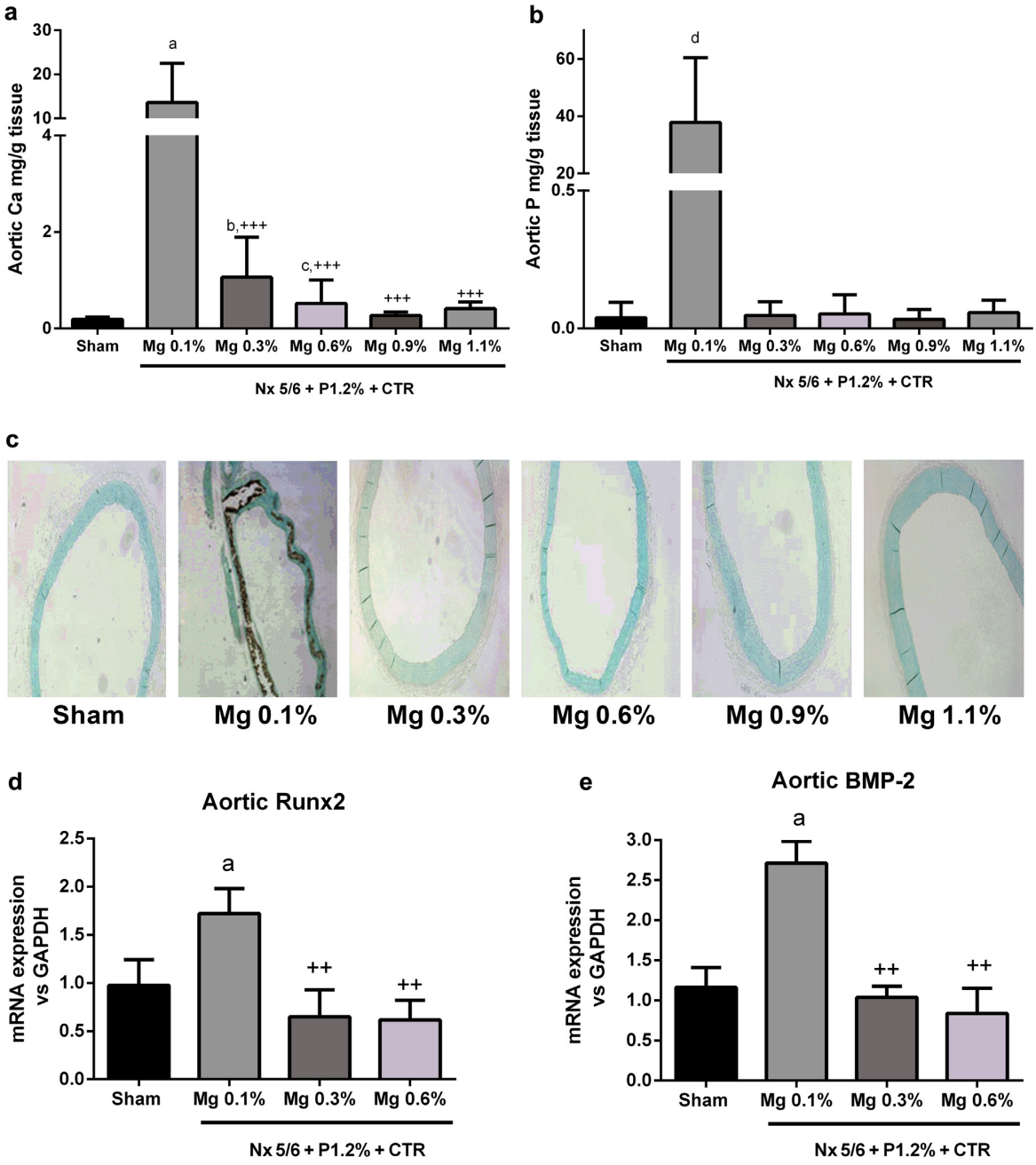

Figure 2 | Effect of dietary magnesium (Mg) intake on the development of aortic calcification. (**a**) Aortic calcium (Ca) content in the study groups. (**b**) Aortic phosphate (P) content in the study groups. (**c**) von Kossa–stained sections from the study groups. Levels of mRNA (**d**) Runx2 and (**e**) bone morphogenetic protein 2 (BMP-2) in the aortas of sham-operated animals and uremic rats with different Mg content in the diet. $^{a}P < 0.001$ versus sham group; $^{b}P < 0.01$ versus sham group; $^{c}P < 0.05$ versus sham group; $^{d}P < 0.001$ versus all groups; $^{+++}P < 0.001$ versus Mg 0.1%. GAPDH, glyceraldehyde-3-phosphate dehydrogenase. To optimize viewing of this image, please see the online version of this article at www.kidney-international.org.

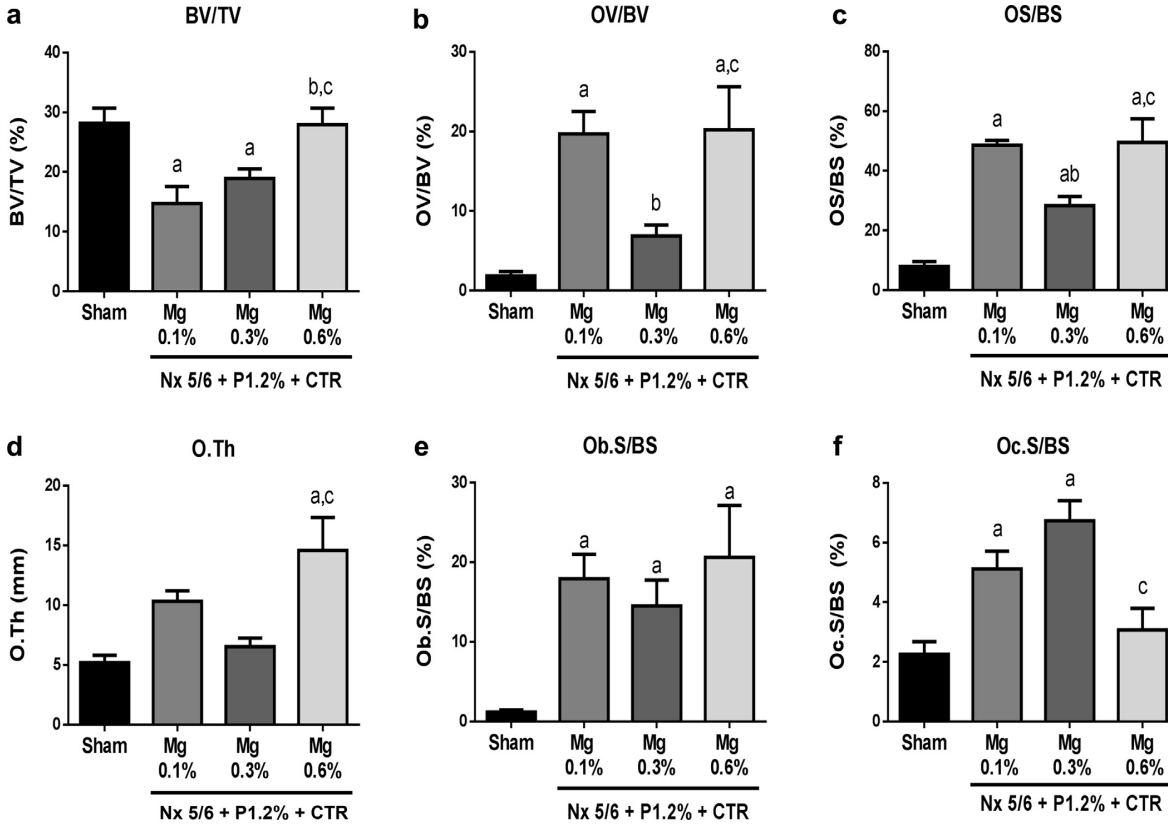

Figure 3 | Effect of dietary magnesium (Mg) supplementation on bone homeostasis. Bone histomorphometric analysis of distal femurs. (**a**) Bone volume to tissue volume (BV/TV). (**b**) Osteoid volume–to–bone volume ratio (OV/BV). (**c**) Osteoid surface–to–bone surface ratio (OS/BS). (**d**) Osteoid thickness (O.Th). (**e**) Osteoblast surface–to–bone surface ratio (Ob.S/BS). (**f**) Osteoclast surface–to–bone surface ratio (Oc.S/BS). $^{a}P < 0.05$ versus sham; $^{b}P < 0.05$ versus Mg 0.1%; and $^{c}P < 0.05$ versus Mg 0.3% .

with a lesser osteoid thickness. However, the number of osteoclasts was similar to that of uremic rats with Mg 0.1%. A higher dietary content of Mg (0.6%) maintained the high number of osteoblasts despite the marked reduction in PTH levels, and the osteoid volume increased to the same level as in rats fed Mg 0.1%. Osteoclasts were reduced to the same level as sham-operated rats. Figure 4 shows Goldner's trichrome stain with representative bone samples of each experimental group. These changes are also observed in bone histological staining (Figure 4).

Effect of Mg on vascular calcification independent of the serum phosphate. To evaluate whether the beneficial effect of Mg on VC was exclusively due to phosphate binding or a direct effect of Mg, we compared VC in nephrectomized rats fed a diet containing high P plus Mg supplementation versus normal P and no Mg supplement (P 1.2% + Mg 0.6% vs. P 0.7% + Mg 0.1%). The objective was to obtain rats with the same reduction in serum P without the addition of Mg. The results showed that a reduction in dietary P produced a decrease in serum P concentration that was similar to that obtained by Mg supplementation (0.6%) (Figure 5a). Despite similar serum P, the content of Ca and P in the aorta was significantly less in the group of rats fed P 1.2% + Mg 0.6% than P 0.7% + Mg 0.1% (Figure 5b and c). These results suggest that Mg may have a direct protective effect against VC.

Whether the benefit of Mg supplementation was only due to P binding was further evaluated by analysis of data presented in the previous experiments. In this secondary analysis in nephrectomized rats with similar elevation in serum P concentration, the degree of VC reduced by dietary Mg was assessed. Among rats with dietary Mg supplementation, only rats with serum P concentration within the 50th to 95th percentile were selected (7.28–12.86 mg/dl). These rats were compared with rats on Mg 0.1% with the same range of serum P concentration. By design, the mean serum P was high and similar for all groups (Figure 6a). The Ca and P contents in the aorta were significantly reduced in rats receiving Mg supplementation in the diet (Figure 6b and c). These data provide supporting evidence that dietary Mg supplementation reduced VC by other mechanisms besides the reduction of the serum P levels.

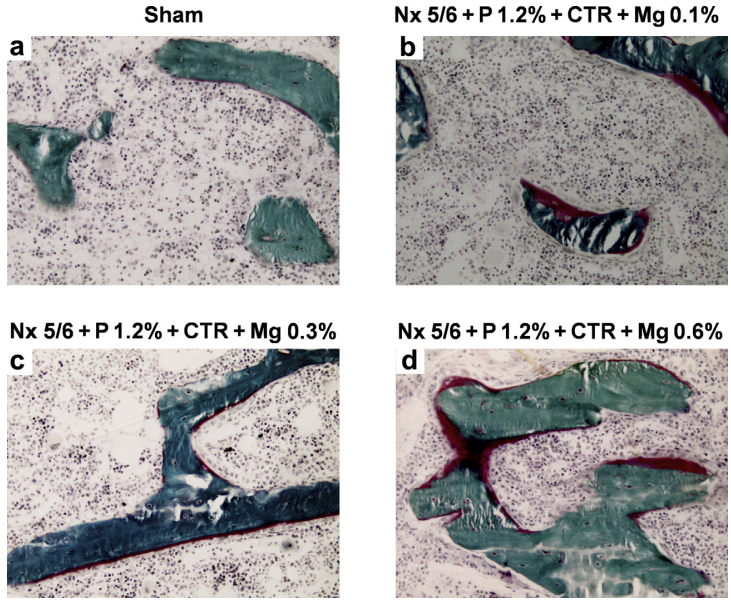

Figure 4 | Histological slides of trabecular distal femurs stained with Goldner's trichrome stain. (**a**) Sham. (**b**) 5/6 nephrectomy (Nx 5/6) + phosphate (P) 1.2% + calcitriol (CTR) + magnesium (Mg) 0.1%. (**c**) Nx 5/6 + P 1.2% + CTR + Mg 0.3%. (**d**) Nx 5/6 + P 1.2% + CTR + Mg 0.6%. Green: calcified bone; red: osteoid. Original magnification ×200. To optimize viewing of this image, please see the online version of this article at www.kidney-international.org.

Finally, to demonstrate the effect of Mg independent of its phosphate binder action we administered Mg i.p. in our model of vascular calcification. Compared with vehicle-treated rats, rats receiving i.p. Mg had higher serum Mg concentration, comparable to that obtained by oral loading (diet containing Mg 0.6%). The addition of parenteral

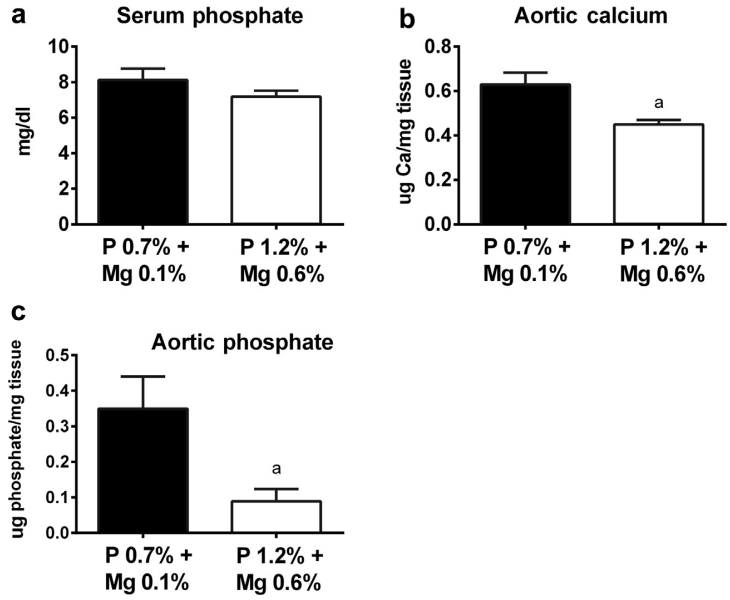

Figure 5 | Effect of dietary magnesium (Mg) on vascular calcification independent of phosphate (P), part 1. Levels of (**a**) serum P, (**b**) aortic calcium (Ca), and (**c**) aortic P in 5/6-nephrectomized rats with low P in the diet (P 0.7% + Mg 0.1%) versus dietary Mg supplementation with high P (P 1.2% + Mg 0.6%). $^{a}P < 0.05$ versus 5/6-nephrectomized rats with low P in the diet. Mean serum P levels in sham animals were 6.5 ± 0.3 mg/dl, not statistically different in comparison with the other groups.

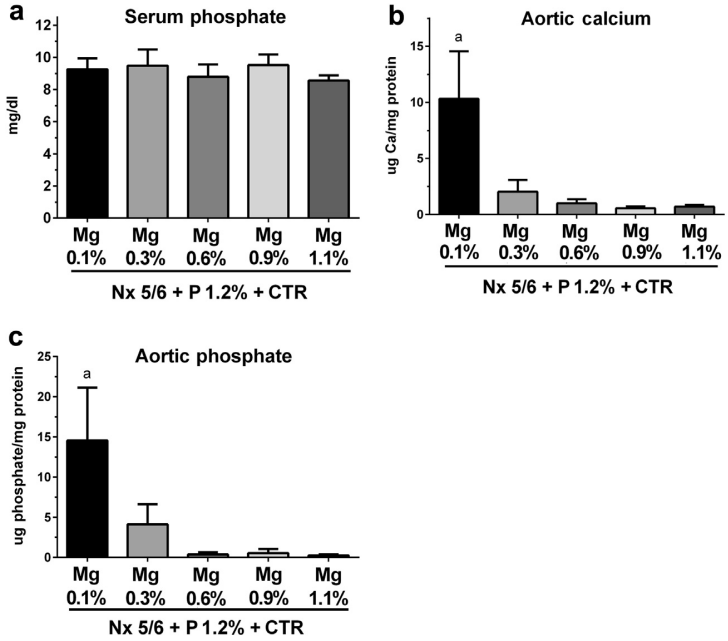

Figure 6 | Effect of dietary magnesium (Mg) on vascular calcification independent of phosphate (P), part 2. Levels of (**a**) serum P, (**b**) aortic calcium (Ca), and (**c**) aortic P in 5/6-nephrectomized rats with different dietary Mg supplementation and with serum P ranging from mean to 95th percentile. $^{a}P < 0.05$ versus all groups.

Mg did not significantly modify serum phosphate, ionized calcium, or serum creatinine (Table 3). I.p. administration of $MgSO_4$ significantly reduced aortic content of calcium (Figure 7a) and phosphate (Figure 7b). This is also shown by von Kossa staining (Figure 7c).

Changes in blood pressure. Blood pressure (BP) values measured in sham-operated and nephrectomized rats on P 1.2% + Mg 0.1% or P 1.2% + Mg 0.6% diets are shown in Figure 8. Independent of diet, nephrectomized rats had higher BP than did sham-operated rats. Among nephrectomized rats, the higher-Mg diet resulted in significantly lower values of both systolic and diastolic BP.

Experiment 2: Effect of dietary Mg intake on progression of VC

The second part of the study was designed to determine whether in nephrectomized rats on a normal Mg diet (0.1%) with established VC the progression of VC could be halted or even reversed by increasing the dietary Mg intake (Figure 1). Survival rates in rats with calcification during the 42 days of Mg supplementation are shown in Figure 9. At day 28, mortality rate in rats fed Mg 0.1% was greater than 50% (11 of 21), while the mortality rate in rats on the Mg 0.6% was only 28% (5 of 18; $P < 0.04$) (Figure 9a). By day 42, none of the rats fed Mg 0.1% survived (0 of 3); by contrast, 75% of the rats (3 of 4) fed Mg 0.6% were alive at day 42 ($P < 0.03$) (Figure 9b).

Table 3 | Biochemical parameters related to the effect of $MgSO_4$ i.p. on renal function and vascular calcification

Parameter	Sham + Mg 0.1%	Nx + veh	Nx + $MgSO_4$
Magnesium (mg/dl)	2.4 ± 0.09	2.8 ± 0.29	3.4 ± 0.59[a,b]
Phosphate (mg/dl)	4.95 ± 0.51	9.74 ± 1.13[a]	8.25 ± 1.15[a]
Ionized calcium (mmol/l)	1.20 ± 0.028	1.07 ± 0.099[a]	1.05 ± 0.039[a]
Creatinine (mg/dl)	0.43 ± 0.016	0.88 ± 0.211[a]	1.04 ± 0.229[a]

Mg, magnesium; Nx, nephrectomy; veh, vehicle.
[a]$P < 0.05$ versus sham plus Mg 0.1%.
[b]$P < 0.05$ versus Nx plus veh.

Blood chemistry from rats at days 14 and 28 is shown in Table 3. At day 28, serum Mg levels remained unchanged in rats fed a normal-Mg diet, but they were increased in rats fed Mg 0.6%: 3.1 ± 0.2 mg/dl versus 2.3 ± 0.2 mg/dl ($P < 0.05$). From days 14 to 28, in rats fed Mg 0.1%, the serum Ca decreased, and both PTH and serum P increased (Table 4). In rats fed Mg 0.6%, the serum iCa, PTH, and P did not change from days 14 to 28.

At day 28, the aortic Ca content was significantly lower in rats receiving Mg 0.6%, (7 ± 0.9 mg/g tissue) than in rats fed Mg 0.1%(14.9 ± 1.9 mg/g tissue). Furthermore, the aortic Ca content observed at day 28 in the rats fed a high-Mg diet (7 ± 0.9 mg/g tissue) was also significantly lower than at day 14: 14.3 ± 2.1 mg/g tissue, indicating that higher dietary Mg intake not only halted but also reversed VC (Figure 10a). The aortic P content showed the same trend as aortic Ca; the values in the group on a high-Mg diet at day 28 were lower than in the Mg 0.1% group at days 14 and 28

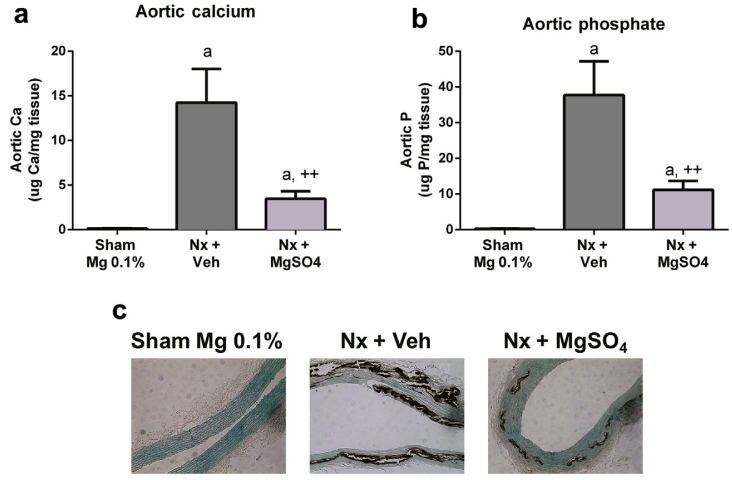

Figure 7 | Effect of i.p. administration of magnesium (Mg) on vascular calcification. (**a**) Calcium (Ca) and (**b**) phosphate levels in aortic tissue, respectively, in sham-operated + Mg 0.1% rats, 5/6-nephrectomized (Nx) rats on a diet containing 1.2% P and 0.1% Mg with calcitriol replacement and receiving vehicle (Nx + Veh), and Nx + $MgSO_4$ (vehicle + $MgSO_4$ i.p., 30 mg/kg body weight). (**c**) von Kossa staining from aortas. $^{a}P < 0.001$ versus sham; $^{++}P < 0.01$ versus Nx + Veh. To optimize viewing of this image, please see the online version of this article at www.kidney-international.org.

(37.8 ± 4.23 mg/g tissue and 51 ± 6.5 mg/g tissue, respectively) (Figure 10b). Results of von Kossa–stained sections of the aorta were consistent with mineral quantification. Thus, marked deposition of brown-stained pigments were evident in the rats fed normal Mg, while the rats fed high Mg showed a staining that was less marked than both with Mg 0.1% in the diet at 14 or 21 days (Figure 10c).

The beneficial effect of higher dietary Mg intake on tissue calcification was also evident in the stomach and lung (Figure 11). An increase in dietary Mg resulted in significantly lower Ca content in both the lung (1.3 ± 0.2 vs. 10.4 ± 3.4 mg/g tissue) and the stomach (2.6 ± 0.4 vs. 9.3 ± 1.4 mg/g tissue). After supplementation with Mg, the P content in the stomach and lung changed in parallel with Ca.

As reported above, 3 of the 4 rats alive in the high-Mg group at day 28 remained alive at day 42. The biochemical profile (creatinine, iCa, and Mg) of these 3 surviving rats was similar to that of the rats on high Mg at day 28, but they had significantly lower serum P (6.2 ± 0.7 mg/dl) and PTH (12 ± 3 pg/ml). Aortic calcification in these rats was similar to the values found at day 28 (7.4 ± 2.1 mg/g tissue). Notably, both gastric Ca (0.4 ± 0.2 mg/g tissue) and pulmonary Ca (0.6 ± 0.1 mg/g tissue) were much lower at day 42 than at day 28 (2.6 ± 0.4 mg/g tissue).

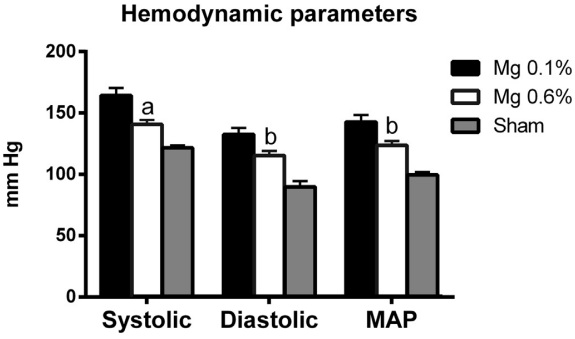

Figure 8 | Changes in blood pressure. Values in mm Hg of systolic blood pressure, diastolic blood pressure, and mean arterial pressure (MAP) in the 5/6 nephrectomy + phosphate 1.2% + calcitriol + magnesium 0.1% group (Mg 0.1%, black bars), the 5/6 nephrectomy + phosphate 1.2% + calcitriol + magnesium 0.6% group (Mg 0.6%, white bars), and the healthy rat group (sham, gray bars). $^{a}P < 0.001$ and $^{b}P < 0.01$ versus Mg 0.1% group.

In vitro studies

As shown in Figure 12, stimulation of human umbilical vein endothelial cells (HUVECs) with tumor necrosis factor alpha (TNF-α) increased both mRNA (Figure 12a) and protein expression of bone morphogenetic protein 2 (BMP-2) (Figure 12b). Treatment with Mg resulted in a dose-dependent decrease in mRNA and protein expression of BMP-2 in HUVECs exposed to TNF-α. Changes in the nuclear p65 fragment of NF-κB paralleled those of BMP-2 (Figure 12b).

DISCUSSION

The results from the present study in uremic rats demonstrate that dietary Mg supplementation reduces VC and other soft tissue calcification. We found that high dietary Mg in 5/6-nephrectomized rats produced a significant decrease in serum P and PTH that only partially explains the reduction of VC; for the same level of serum P, VC was significantly reduced in Mg-supplemented rats. The beneficial effects of Mg on VC are partly mediated by an effect independent of its

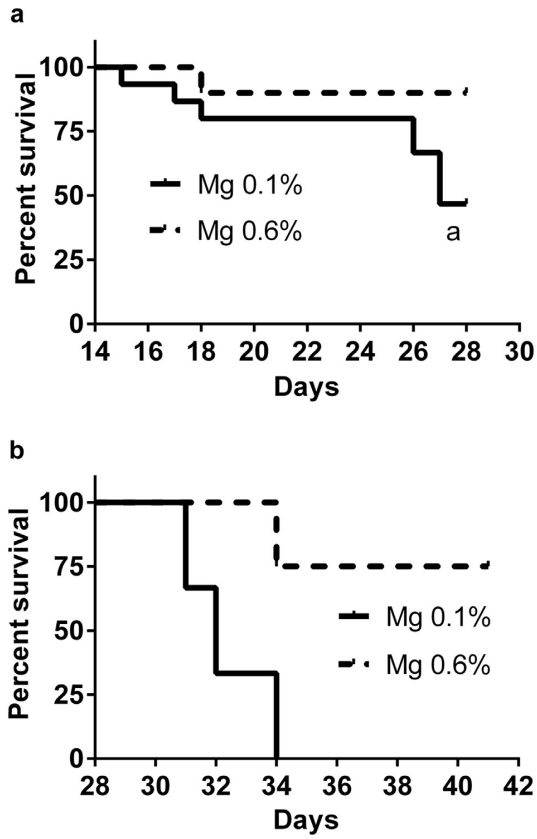

Figure 9 | Kaplan–Meier curves of survival in uremic rats with calcifications fed normal (0.1%) or moderately high (0.6%) magnesium (Mg) diets. (**a**) Survival at 14 to 28 days in the 5/6 nephrectomy + phosphate 1.2% + calcitriol + Mg 0.1% group (11 of 21 dead, continuous line) and 5/6 nephrectomy + phosphate 1.2% + calcitriol + Mg 0.6% group (5 of 18 dead, interrupted line). $^{a}P < 0.05$. (**b**) Survival from 28 to 42 days in the 5/6 nephrectomy + phosphate 1.2% + calcitriol + Mg 0.1% group (continuous line) and the 5/6 nephrectomy + phosphate 1.2% + calcitriol + Mg 0.6% group (interrupted line). All rats on the Mg 0.1% diet (3 of 3) were dead at this time, whereas 75% of rats on the Mg 0.6% diet survived (3 of 4; $P < 0.05$).

Table 4 | Experiment 2: effect of dietary magnesium on reversibility of aortic calcification, biochemical parameters in the study groups at killing (see text for details)

		Day 28	
Parameter	Day 14	Mg 0.1%	Mg 0.6%
Magnesium (mg/dl)	2.4 ± 0.17	2.3 ± 0.25	3.1 ± 0.23[a,c]
Ionized calcium (mmol/l)	1.22 ± 0.04	1.06 ± 0.06[a]	1.20 ± 0.03[c]
PTH (pg/ml)	284 ± 55	1401 ± 312[b]	177 ± 79[c]
Phosphate (mg/dl)	10.9 ± 1.00	16.7 ± 2.73[b]	11.3 ± 0.01[d]
Creatinine (mg/dl)	1.9 ± 0.15	1.8 ± 0.2[a]	1.9 ± 0.22

Mg, magnesium; PTH, parathyroid hormone.
[a]$P < 0.05$ versus day 0.
[b]$P < 0.001$ versus day 0.
[c]$P < 0.05$ versus Mg 0.1% at day 14.
[d]$P < 0.01$ versus Mg 0.1% at day 14.

phosphate binder action. Moderate (0.3%) but not higher (0.6%) supplementation of Mg had a positive effect on bone histomorphometry. Improvement in VC was also associated with a reduction in BP and protection of renal function. Moreover, in uremic rats that had developed VC, the addition of Mg to the diet appeared to decrease calcifications and mortality.

In nephrectomized rats on a normal Mg 0.1% diet, CrCl was lower than in nephrectomized rats fed higher Mg concentrations. Hyperphosphatemia with marked vascular and soft-tissue calcification probably contributed to the worsening of renal failure. Increasing dietary Mg to 0.3% resulted in a lower serum P and the virtual elimination of aortic and stomach calcification, and this was associated with better control of renal function. Further increases in dietary Mg intake progressively decreased PTH, with eventual normalization of its values. In the nephrectomy plus Mg 0.6% group, normalization of PTH was observed even though mild hyperphosphatemia persisted. Dietary Mg supplementation reduces P absorption, which is a key factor for control of hyperparathyroidism; in addition, there is a direct inhibitory effect of Mg on parathyroid cell function.[25–28] We are not aware of any previous study resulting in a marked reduction in PTH by Mg loading or hypermagnesemia in uremic animals with secondary hyperparathyroidism enhanced by P loading. The hyperphosphatemia should have been reduced by the high dietary Mg intake because Mg is an effective P binder.[29,30] The increase in serum iCa concentration in rats ingesting Mg supplements may be explained by the reduction in serum P concentration, which increases the calcemic effect of PTH.[31,32] Furthermore, with dietary Mg supplements bone resorptive activity is maintained despite the reduction in PTH levels. Finally, it should be considered that with oral Mg, there is a chelant effect on phosphate increasing calcium availability that in the presence of calcitriol might promote its absorption. Moreover, this concept is also supported by the data in Table 3, which demonstrate that serum phosphate was not reduced by i.p. magnesium and iCa remained decreased. Serum calcitriol values were lower in nephrectomized than in sham-operated rats, but were not different among nephrectomized rats. As such, calcitriol should not have resulted in differences in intestinal Mg, Ca, and P absorption and PTH and FGF23 values. In nephrectomized rats, FGF23 values were much greater than in sham-operated rats, but among nephrectomized rats, no discernible reason could be ascertained for the wide variation in FGF23 values.

Our data show an inverse association between soft-tissue calcification and creatinine clearance. Calcification was reduced by the Mg 0.3% diet, and this was associated with improvement in renal function. Further increase in dietary Mg had limited additional beneficial effect on calcification, but it improved renal function. This suggests that the beneficial effect of Mg on renal function may not be fully

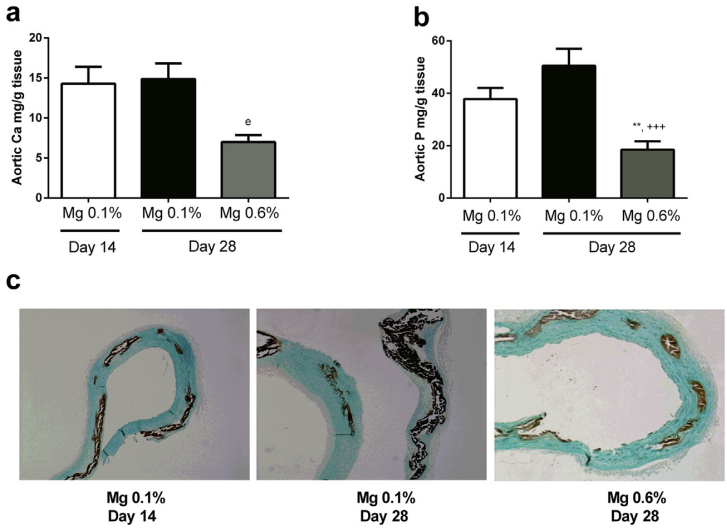

Figure 10 | Effect of dietary magnesium (Mg) on reversibility of aortic calcification. (**a**) Aortic calcium (Ca) content at days 14 and 28 in rats fed normal (0.1%) and moderately elevated (0.6%) Mg. (**b**) Aortic phosphate (P) content at days 14 and 28 in rats fed normal (0.1%) and moderately elevated (0.6%) Mg. (**c**) von Kossa staining of the aorta at days 14 and 28 in rats fed normal (0.1%) and moderately elevated (0.6%) Mg. $^{e}P < 0.01$ versus all groups; $^{**}P < 0.01$ versus Mg 0.1% at day 14; $^{+++}P < 0.001$ versus Mg 0.1% at day 28. To optimize viewing of this image, please see the online version of this article at www.kidney-international.org.

explained by the reduction in calcification. Recent studies by Sakaguchi *et. al*[10] show that an excess load of P has a negative effect on renal function, and Mg directly protects the kidney from the deleterious effect of high P. In our experimental rats, dietary supplementation of Mg may have protected kidney function through a reduction in intestinal absorption of P, thus preventing a potential deleterious effect of high P on renal tubular cells.

Two different methods were used to evaluate calcification of the aorta and stomach: direct measurement of Ca and P after tissue dissolution in formic acid and histological staining for CaP. Both methods yielded similar results. In nephrectomized rats fed Mg 0.1%, extensive calcifications were seen in the aorta and stomach. If dietary Mg is increased to 0.3% or higher, aortic and stomach calcifications were 20- to 40-fold less than on the Mg 0.1% diet, and values were not different from sham-operated rats. In addition, we also found that dietary Mg supplementation prevented the expression of an osteochondrogenic phenotype of VSMC induced by uremia and a high-P diet (Figure 2d and e). Similar results have been obtained in previous *in vitro* and animal studies in which Mg inhibited calcification in VSMC.[20,22,33,34] Clinical studies have also suggested that Mg supplementation may have a favorable effect on VC and disease.[14,22] *In vivo*, it is difficult to separate the direct effect of dietary Mg intake on calcification from that on the reduction in serum P. However, even though serum P was reduced in rats fed the Mg-supplemented diets, high levels of serum phosphate persisted even with the highest Mg diet.

In uremic rats fed P 1.2% and Mg 0.1%, serum PTH was elevated and bone histology showed features of high bone turnover. Bone histology appears to be improved with 0.3% dietary Mg supplementation; osteoid accumulation was reduced compared with that in rats fed Mg 0.1%, and bone homeostasis improved. However, despite a marked reduction on PTH in rats receiving the Mg 0.6% diet, osteoblast activity was maintained while osteoclast activity was reduced. At the same time, osteoid volume and thickness increased, suggesting a decrease in mineralization activity. Moreover, these data suggest a stimulating effect of high Mg on osteoblastogenesis independent of PTH.

Moreover, regression of extraskeletal calcification was observed in rats fed a high-Mg diet that had persistently elevated serum P. In addition, comparison of rats with similar serum P levels and fed different levels of dietary Mg showed that the protective effect of dietary Mg on VC was not exclusively due to the P-binding effect. For a similar serum P concentration, more Mg in the diet was associated with less vascular accumulation of Ca and P.

Results from our study with parenteral Mg administration demonstrate that Mg reduces, in part, VC independently of its actions as a phosphate binder. The experiments in which Mg was administered parenterally provide compelling evidence of a protective effect on VC independent of any phosphate-binding actions. However, the reduction of VC was less accentuated after Mg given i.p. than in the diet. Overall, it seems that oral Mg supplementation offers advantages over parenteral Mg administration because it combines direct and

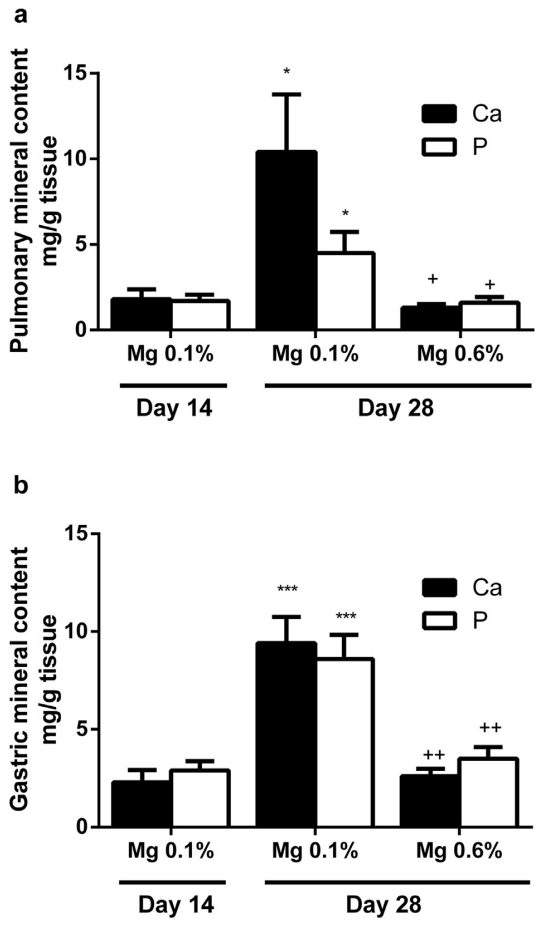

Figure 11 | Effect of dietary magnesium (Mg) on reversibility of soft-tissue calcification. (**a**) Pulmonary mineral content at days 14 and 28 in rats fed normal (0.1%) and moderately elevated (0.6%) Mg. (**b**) Gastric mineral content at days 14 and 28 in rats fed normal (0.1%) and moderately elevated (0.6%) Mg. $^{***}P < 0.001$ versus Mg 0.1% at day 14; $^{*}P < 0.05$ versus Mg 0.1% at day 14; $^{++}P < 0.01$ versus Mg 0.1% at day 28; and $^{+}P < 0.05$ versus Mg 0.1% at day 28.

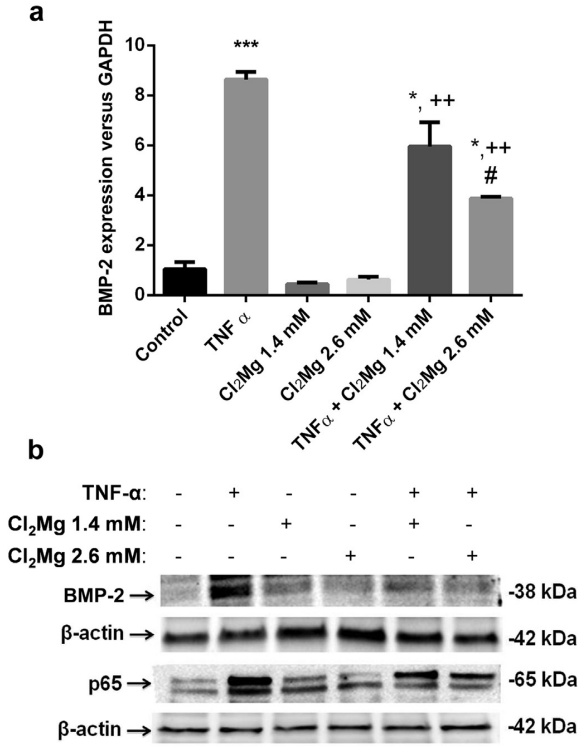

Figure 12 | *In vitro* effect of magnesium (Mg) on human umbilical vein endothelial cells (HUVECs) exposed to tumor necrosis factor alpha (TNF-α). Stimulation of HUVECs with TNF-α increased both (**a**) mRNA and (**b**) protein expression of BMP-2 and nuclear p65 fragment from NF-κB. Treatment with Mg resulted in a dose-dependent decrease in mRNA and protein expression of BMP-2 in HUVECS exposed to TNF-α. $^{***}P < 0.001$ versus control; $^{*}P < 0.05$ versus control; $^{++}P < 0.01$ versus TNF-α; and $^{\#}P < 0.05$ versus TNF-α + Cl_2Mg 1.4 mM. GAPDH, glyceraldehyde-3-phosphate dehydrogenase.

indirect (P-binding) effects; the administration of Mg i.p. did not help to control serum P or Cr.

Our study also shows that in uremic rats, a high-P diet promotes VC, which is associated with an increase in BP. Dietary Mg supplementation was accompanied by a reduction in BP that could be explained by the marked diminution in VC. However, our experimental design does not allow for the determination of whether the decrease in BP is due to decreased VC, improved renal function, or both. In addition, other mechanisms, such as a direct effect of Mg on BP, cannot be excluded. There are a number of studies showing an association between low serum Mg concentration and hypertension.[35,36] The effect of Mg supplementation on hypertension is controversial, and clear evidence from randomized controlled clinical trials is lacking.[37]

In vitro studies were performed to evaluate the protective effects of Mg on VC independent of its phosphate-binder action. Our results also support a beneficial effect of Mg at the endothelial level. TNF-α–stimulated endothelial microparticles, which are rich in BMP-2, have been shown to enhance VSMC osteogenesis and calcification.[38] Our data, showing that exposure to Mg prevents the increased expression of BMP-2 and p65–NF-κB by TNF-α, provides an additional mechanism by which Mg may protect against inflammation and VC. With respect to inflammation, the decrease of p65–NF-κB induced by Mg suggests an anti-inflammatory effect, which could be also related to less VC. Other groups have shown *in vivo*[39] and *in vitro*[40] that Mg supplementation also decreases NF-κB levels.

In our study, the regression in VC promoted by Mg occurred with a parallel decrease in serum biochemical parameters related to secondary hyperparathyroidism. PTH

levels were significantly lower in rats at day 28 than day 14. Partial regression of cardiac and pulmonary calcifications[41] and complete resorption of abdominal soft-tissue calcification[42] have been described in hemodialysis patients after parathyroidectomy. Thus, the marked suppression of PTH observed in our uremic rats after dietary Mg supplementation may have influenced VC regression. The contribution of high PTH levels on vascular and coronary calcifications in uremic rats has been described by Neves *et al.*[43]

In addition to improving the parameters of mineral metabolism, Mg could also have promoted regression of VC by direct mechanisms. Although the mechanistic pathways involved in a regression of VC are not fully understood, a Ca-sensing receptor–mediated effect has been postulated in a study with calcimimetics.[44] Mg is able to interact with Ca-sensing receptor; it may share some common mechanisms with calcimimetics in its capacity to prevent VC.[28] Urinary Ca excretion as assessed by Ca-to-Cr ratio tended to increase in rats with dietary Mg supplementation, and it reached statistical difference in the group of rats receiving the highest percentage of Mg in the diet (1.1%). In this group of rats, PTH was low and tubular reabsorption of Ca was likely reduced as a result. In addition, there are clinical and experimental data suggesting that Mg load reduces distal tubular reabsorption of Ca through TRPV5.[45]

Our study shows for the first time that dietary Mg intake is able to reverse already-established vascular and soft-tissue calcifications. Certainly, the data suggest that a 0.6% Mg diet may reverse VC. However, it should be emphasized that VCs were not measured in the same rats. Therefore, with this experiment a definite reversal of VC cannot be demonstrated.

The experimental rat model has limitations, especially the short period of time to achieve vascular and soft-tissue calcifications; however, the model reproduces with precision the changes in renal function, mineral metabolism, hypertension, and VC observed in patients with advanced renal failure. Despite the severity of the process, moderate dietary Mg supplementation was able to not only prevent the development of VC but also halt its progression. The results obtained in this model should help to generate hypotheses for testing in prospective clinical trials. A noninterventional study by Sakaguchi *et al.*[13] showed that in hemodialysis patients, hypomagnesemia was a significant predictor of mortality.

To date, there is not an effective therapeutic approach to achieve VC regression. There have been previous reports in the literature about the use of compounds and chelating agents such as sodium thiosulfate to treat or slow the progression of calcifilaxis.[46–48] Calcimimetics have also been reported to be useful for the treatment of VC in animal models.[49] In the ADVANCE study, the administration of cinacalcet plus low-dose vitamin D to hemodialysis patients resulted in attenuation of VC.[50] Serum P concentration also decreases when using calcium-free P binders to treat VC; the protective effect of sevelamer or lanthanum carbonate have been widely described.[51,52] Several studies in animal models have shown that the use of bisphosphonates reduces arterial calcifications in nephrectomized rats.[53,54] Clinical studies in CKD patients have also shown a beneficial effect of bisphosphonates on VC.[55] Although there is an association between low Mg levels and CVD, a beneficial effect of Mg supplementation has not been adequately tested in clinical trials.[56,57] The CALMAG study reported the efficacy of Ca and Mg salts as a P binder in hemodialysis patients. De Francisco *et al.* concluded that the administration of Mg had a good tolerability profile, suggesting that Mg supplementation is safe.[30] Other clinical trials with Mg supplementation have been performed in the context of type 2 diabetes[58] and depression,[59] demonstrating the efficacy and safety of Mg supplementation. Moreover, our study shows that the beneficial effect of Mg was observed in rats on the most moderate Mg-supplemented diet (0.3%).

In conclusion, we have shown that in 5/6-nephrectomized rats, increased dietary Mg prevents and even reverses vascular and other soft-tissue calcification, and has positive effects on mineral metabolism parameters, BP, renal function, and mortality. These beneficial effects of Mg are partly mediated independently of its action as a phosphate binder.

METHODS

Animals

Healthy 9- to 10-week-old male Wistar rats without any genetic modifications weighing 250 to 300 g were used. This strain was chosen on the basis of its feasibility to reproduce CKD features. Animals were purchased from Charles River (Wilmington, MA) and individually housed in 33.5 × 56 × 19 cm cages with 450 cm^2 floor area per rat while applying a 12-hour light-dark cycle. Before entering the study, rats were given *ad libitum* access to a standard diet (Ca 0.8%, P 0.6%, and Mg 0.1%). Appropriate measures were taken to ensure animal welfare and to address the basic behavioral and physiological needs of rats. Killing was accomplished by aortic puncture and exsanguination under general anesthesia (20 mg/kg thiopental sodium i.p.). All experimental protocols were reviewed and approved by the Ethics Committee for Animal Research of the University of Cordoba, and all rats received humane care in compliance with the guiding principles in the Guide for the Care and Use of Laboratory Animals, Eighth Edition.

5/6 nephrectomy

Uremia was induced by 5/6 nephrectomy, a 2-step procedure that reduces the original functional renal mass by five-sixths. On the basis of our previous studies, animals were anesthetized using xylazine (5 mg/kg i.p.) and ketamine (80 mg/kg i.p.). In the first step of the nephrectomy, a 5- to 8-mm incision was made on the left mediolateral surface of the abdomen. The left kidney was exposed, and the 2 poles (two-thirds of renal mass) were ablated. The kidney was inspected and returned to an anatomically neutral position within the peritoneal cavity. The abdominal wall and skin incisions were closed with sutures, and the rat was placed back into its home cage. After 1 week of recovery, the animal was reanesthetized and a 5- to 8-mm incision was made on the right mediolateral surface of the abdomen. The right kidney was exposed and unencapsulated, the renal pedicle was clamped and ligated, and the kidney was removed. The ligated pedicle was returned to a neutral anatomical position and the abdomen and skin incisions closed with suture materials.

Phentanyl (0.2 mg/kg) was used as an analgesic agent. An additional group of nonuremic sham-operated rats that underwent the same surgical manipulation without renal ablation was also studied.

Experimental design

The *in vivo* studies included 2 experiments: experiment 1 was designed to study the effect of dietary Mg supplementation on prevention of VC, and experiment 2 evaluated the effect of Mg on reversibility of calcifications (Figure 1). Rats were randomly assigned to different experimental groups to determine the effect of dietary Mg on VC in rats with renal failure. The total number of animals used was 108 in experiment 1 and 49 in experiment 2.

Experiment 1: effect of increasing dietary Mg intake on the development of VC. One day after the second kidney surgery, rats were fed a high-P diet (0.6% Ca and 1.2% P). The animals received 20 ng/48 h/rat i.p. calcitriol (Calcijex; Abbott, Madrid, Spain), to control hyperparathyroidism and favor VC. Rats were randomly divided into groups (n = 10–14) that were fed diets with differing Mg contents: 0.1%, 0.3%, 0.6%, 0.9%, and 1.1% for 14 days. Sham-operated rats receiving a normal diet containing 0.1% Mg and 0.6% P and without calcitriol administration were used as controls. All animal feed was purchased from Altromin Spezialfutter (Lage, Germany). Mg was added as magnesium carbonate.

Because the addition of Mg to the diet resulted in a reduction in serum P, an additional protocol was designed to evaluate the separate effects of dietary Mg and serum P on VC. The objective was to analyze aortic mineral content in rats with the same reduction in serum P with and without the addition of dietary Mg. Additional experimental rats were treated as in the previous experimental groups (with same dose of calcitriol), but these rats were fed diets with a different P and Mg content (a 5/6 nephrectomy group on a diet containing P 0.7% and Mg 0.1% and a 5/6 nephrectomy group on a diet containing P 1.2% and Mg 0.6%). Animals were placed in metabolic cages 3 days before killing to collect 3 24-hour urine samples. After 2 weeks, all rats were killed 24 hours after having received the last dose of calcitriol. Following killing, the thoracic aorta and stomach were removed and stored to measure Ca and P content.

An additional experiment was performed to evaluate the effect of Mg given parenterally on vascular calcification. This experiment was conducted to determine the effect of Mg independent of its phosphate-binding action. The 5/6-nephrectomized rats on 1.2% P diet and calcitriol replacement received 30 mg/kg $MgSO_4$ diluted in 5% dextrose (n = 10) or vehicle (n = 10) over 14 days. $MgSO_4$ was administered every 12 hours to maintain constant high levels of serum Mg. Rats in the control group following the same protocol received vehicle (dextrose). At the end of the experiment, animals were placed in metabolic cages before killing, and 24-hour urine samples were collected. All rats were killed 24 hours after having received the last dose of calcitriol. Following killing, blood and the thoracic aorta were removed and stored to measure Ca and P content and for von Kossa staining.

Experiment 2: effect of dietary Mg intake on reversibility of VC. A second experiment was performed to determine whether the VC observed in nephrectomized rats on normal Mg diet (0.1%) could be reversed by increasing Mg supplementation. Thus, rats used in this study were subjected to the same protocol described in experiment 1: they were nephrectomized; fed a diet with 0.6% Ca, 1.2% P, and 0.1% Mg; and treated with calcitriol (20 ng/48 h/rat i.p.). Rats (n = 49) were monitored for 14 days to allow for the development of soft-tissue calcification. At day 14, 10 animals were killed to quantify calcification in the aorta and other soft tissues as well as to measure biochemical parameters before starting Mg supplementation. The remaining rats were randomly assigned to 2 experimental groups and placed on a diet with 0.6% Ca, 1.2% P, and either normal (0.1%) Mg (n = 21) or moderately high (0.6%) Mg (n = 18). The original design aimed to kill half of the rats in each group 14 days later (day 28). However, due to high mortality (mainly in the rats fed Mg 0.1%), only 7 rats on Mg 0.1% and 9 on Mg 0.6% were killed. The remaining rats, 3 in the Mg 0.1% group and 4 in the Mg 0.6% group, were monitored for an additional 14-day period for a total of 42 days of experimental period. Then all the remaining rats were killed (Figure 1). Following killing, the thoracic aorta, stomach, and lungs were removed and stored.

Assessment of vascular and soft-tissue calcification

Vascular and soft-tissue calcification was assessed by microscopy and by measurement of Ca and P tissue content. To avoid sampling bias, the same section of the aorta from every animal was selected for each assessment: the cranial one-third for histology and the middle one-third for Ca and P quantification. The cranial part of the thoracic aorta and samples of stomach and lung were fixed in 10% buffered formalin and subsequently sectioned and stained by the von Kossa method to assess mineralization according to standard protocols. The extent of calcification (von Kossa staining) was evaluated blindly by 3 independent observers. The middle part of the aorta was demineralized in 10% formic acid, and the Ca and P contents were measured in the supernatant. The organs (aorta, stomach, and lungs) were placed into separate 30-ml tubes, and 20 ml 150 mM HCl were added to each tube. The tubes were mixed by inversion for 24 hours at room temperature, and Ca and P were measured in the acid extract.[60] Ca and P were measured in the aortas of killed rats and those found dead.

Runx2 and BMP-2 expressions by RT-PCR

Total RNA from the thoracic aorta was extracted using the RNeasy Fibrous Tissue Kit from Qiagen (Hilden, Germany). The expression of mRNA was examined by quantitative real-time PCR (RT-PCR) using the Light Cycler thermal cycler system (Roche Diagnostics, Indianapolis, IN). RT-PCR was carried out in 1 step, using the QuantiTect SYBR Green RT-PCR kit (Qiagen) following the manufacturer's protocol. BMP-2 and Runx2 primers were designed with Oligo 7 software (Oligosoft, Bangalore, India), and the sequences were the following: Fwd-Runx2: 5′-CGGGAATGATG AGAA CTACTC-3′ and Rwd-5′-GCGGTCAGAGAACAAACTAGGT-3′; Bmp2: Fwd-5′-AGGAGGCAAAGAAAAGGAACGGAC-3′ and Rwd-5’-GGAAGCAG CAACGCTAGAAGACAG-3′. Results were normalized to glyceraldehyde-3-phosphate dehydrogenase expression that was used as a housekeeping gene. Glyceraldehyde-3-phosphate dehydrogenase sequence was the following: Fwd-5′TGATGACATCA AGAAGGTGGTGAAG-3′and Rwd-5′-TCCTTGGAGG CCATGT GGGCCAT-3′. Quantification of relative expression was determined by the 2Δ(ΔCT) method.

Bone histology and histomorphometric analysis

After killing, right femurs were dissected and placed in 70% ethanol. Subsequently, femurs were cut at the middle and distal bones, dehydrated in alcohol, treated with xylene, and embedded in 75% methyl methacrylate, 25% dibutyl phthalate, and 2.5% weight/volume benzoyl peroxide. Histomorphometric parameters were evaluated in undecalcified 5-μm sections treated with modified Masson-Goldner trichrome staining. Briefly, slices were fixed with

50% ethanol under pressure, then were rehydrated and stained with hematoxylin-ferric chloride 1:1, cleared with 1% HCl, and turned blue with $LiCO_3$. After rinsing with water, slices were stained with Goldner trichrome dye for 20 minutes and then rinsed with 1% acetic acid. Subsequently, samples were stained with safranin for 5 minutes and dehydrated with ethanol and mounted. Green-stained areas were considered to be mineralized bone, and red-stained areas measuring at least 1.5 μm were considered to be osteoid. Bone histomorphometric parameters were assessed in cancellous bone within the secondary spongiosa under ×200 magnification as previously described,[61] and derived indices were determined by standard calculations.[62]

Measurement of blood pressure in nephrectomized rats on dietary Mg supplementation

The effect of dietary Mg supplementation (0.6%) on BP in 5/6-nephrectomized rats on a 1.2% diet was evaluated. The 5/6 nephrectomy was performed according to the protocol previously described; after the second nephrectomized rats were randomly assigned to receive diets containing P 1.2% plus Mg 0.1 % or P 1.2% plus Mg 0.6%. At day 10, systolic, diastolic, and mean arterial pressures were measured using a Panlab LE 5001 pressure meter (Harvard Apparatus, Holliston, MA).

Biochemical determinations

Blood for biochemical analyses was obtained from the abdominal aorta at the time of killing. Blood for measurements of iCa levels was collected in heparinized syringes and measured immediately in a Ciba-Corning 634 ISE Ca^{2+}/pH analyzer (Essex, UK). Serum was separated by centrifugation and stored at –20°C until further analysis. Serum and urine creatinine, Ca, P, and Mg were measured by spectrophotometry (BioSystems SA, Barcelona, Spain). Serum PTH levels were quantified according to the vendor's instructions using a rat PTH (1–34) immunoradiometric assay kit (Immunotopics, San Clemente, CA). Calcitriol was measured with a radioreceptor assay (Immunodiagnostic Systems, Boldon, UK). FGF23 levels were determined using an intact FGF23 enzyme-linked immunosorbent assay kit (Kainos Laboratories, Tokyo, Japan). The collected urine was centrifuged (1500 rpm for 5 minutes), volume was measured, and an aliquot was saved for Ca, P, Mg, and creatinine measurement (BioSystems SA).

In vitro studies

To investigate the influence of Mg on expression of osteogenic proteins by endothelial cells, HUVECs (Cell Systems/Clonetics, Solingen, Germany) were cultured at 37°C, 5% CO_2 with endothelial cell medium (LONZA, Hopkinton, MA), plus endothelial cell growth supplements (EGM, LONZA) and 10% fetal calf serum (Invitrogen Molecular Probes, Eugene, OR). HUVECs from 2 to 9 passages were used. HUVECs were stimulated by addition of TNF-α (Sigma-Aldrich, St. Louis, MO) (20 ng/ml) over 36 hours. The optimal concentration and time of TNF-α was established based on preliminary results obtained from concentration- and time-dependent effects of TNF-α on intracellular BMP-2 expression in HUVECs. Two concentrations of Cl_2Mg (1.4 and 2.6 mM), alone or in combination with TNF-α, were also added. Treatments were performed on 5 independent cultures.

Total RNA from HUVECs was extracted using Trizol reagent (Sigma-Aldrich), and the expression of mRNA was examined as described earlier.

BMP-2 and p65–NF-κB Western blots

Cytosolic proteins were isolated from cultured cells using lysis buffer A, containing *N*-2-hydroxyethylpiperazine-*N*′-2-ethanesulfonic acid (10 mmol/l), KCl (10 mmol/l), ethylenediamine tetraacetic acid (0.1 mmol/l), ethyleneglycol-bis-(β-aminoethylether)-*N*,*N*,*N*′,*N*′-tetraacetic acid (0.1 mmol/l), dithiothreitol (1 mmol/l), phenylmethylsulfonyl fluoride (0.5 mmol/l), protease inhibitor cocktail (70 mg/ml; Sigma-Aldrich), Igepal CA-630 (0.5%), and pH 7.9. The suspension was centrifuged, and the supernatant was stored. Protein concentration was determined by the Bradford method (Bio-Rad Laboratories, Munich, Germany). Once separated by electrophoresis in Ready Gel Tris-HCl 4% to 20% (Bio-Rad Laboratories), proteins were transferred to nitrocellulose membranes. Human anti–BMP-2 (sc-137087, Santa Cruz Biotechnology, Dallas, TX) and anti–p65-NF-κB (sc-109, Santa Cruz Biotechnology) were used as primary antibodies. Visualization of immune complexes was performed using horseradish peroxidase-conjugated secondary antibody (goat anti-mouse IgG-HRP, sc-2060, Santa Cruz Biotechnology) and the ECL Advance Detection Reagents (GE Healthcare Bio-Sciences, Uppsala, Sweden). Protein levels were quantified using the image analysis software Quantity One 4.4.0 (Bio-Rad Laboratories) and were normalized to β-actin levels.

Statistics

Values are expressed as the mean ± SEM. Sample size and the power of a contrast of hypothesis were calculated with statistical software (GRANMO; IMIM, Barcelona, Spain). The difference between means of more than 2 groups was assessed by analysis of variance followed by Duncan's *post hoc* analysis. Comparison of means from 2 different groups was evaluated by unpaired *t*-test. A P value of <0.05 was considered significant. Survival curves were analyzed by Mantel–Cox test.

DISCLOSURE

SS is an employee of Fresenius Medical Care. MR has received honoraria for lectures from Abbott, Amgen, Fresenius, and Shire. All the other authors declared no competing interests.

ACKNOWLEDGMENTS

This work has been partially supported by a Spanish government grant from the Programa Nacional I+D+I 2008-2011 from the Instituto de Salud Carlos III (PI14/00638 and PI14/00467) with cofinancing from European Funds (FEDER); Consejería de Economía, Innovación, Ciencia y Empleo from the Junta de Andalucía (CVI-7925); Fresenius Medical Care; EUTOX; and REDINREN from Instituto de Salud Carlos III.

Grant support

NV and JMD are supported by Consejería de Economía, Innovación, Ciencia y Empleo from the Junta de Andalucía (CVI-7925). MER is a recipient of a "Sara Borrell" research contract from the National Institute of Health Carlos III. YA and JRM are senior researchers supported by the Nicolás Monardes Programme, Consejeria de Salud-SAS (Junta de Andalucia).

SUPPLEMENTARY MATERIAL

Figure S1. Effect of dietary magnesium (Mg) on prevention of gastric calcification. (**A**) Calcium gastric content in the study groups of experiment 1. (**B**) Phosphate (P) gastric content in the study groups of experiment 1. $^{a}P < 0.001$ versus sham group; $^{b}P < 0.01$ versus sham group; $+++P < 0.001$ versus Mg 0.1%; and $++P < 0.01$ versus Mg 0.1%.

Supplementary material is linked to the online version of the paper at www.kidney-international.org.

REFERENCES

1. Lipsky MS, Mendelson M, Havas S, Miller M. *American Medical Association Guide to preventing and treating heart disease: essential information you and your family need to know about having a healthy heart*. 1st ed. Hoboken, NJ: John Wiley & Sons, Inc.; 2008:145–147.
2. Song Y, Liu S. Magnesium for cardiovascular health: time for intervention. *Am J Clin Nutr*. 2012;95:269–270.
3. Larsson SC. Urinary magnesium excretion as a marker of heart disease risk. *Am J Clin Nutr*. 2013;97:1159–1160.
4. Qu X, Jin F, Hao Y, et al. Magnesium and the risk of cardiovascular events: a meta-analysis of prospective cohort studies. *PLoS One*. 2013;8:e57720.
5. Liao F, Folsom AR, Brancati FL. Is low magnesium concentration a risk factor for coronary heart disease? The Atherosclerosis Risk in Communities (ARIC) Study. *Am Heart J*. 1998;136:480–490.
6. Ascherio A, Rimm EB, Hernan MA, et al. Intake of potassium, magnesium, calcium, and fiber and risk of stroke among US men. *Circulation*. 1998;98:1198–1204.
7. Chakraborti S, Chakraborti T, Mandal M, et al. Protective role of magnesium in cardiovascular diseases: a review. *Mol Cell Biochem*. 2002;238:163–179.
8. London GM, Pannier B, Marchais SJ, et al. Calcification of the aortic valve in the dialyzed patient. *J Am Soc Nephrol*. 2000;11:778–783.
9. Tin A, Grams ME, Maruthur NM, et al. Results from the Atherosclerosis Risk in Communities study suggest that low serum magnesium is associated with incident kidney disease. *Kidney Int*. 2015;87:820–827.
10. Sakaguchi Y, Iwatani H, Hamano T, et al. Magnesium modifies the association between serum phosphate and the risk of progression to end-stage kidney disease in patients with non-diabetic chronic kidney disease. *Kidney Int*. 2015;88:833–834.
11. Spiegel DM, Farmer B, Smits G, et al. Magnesium carbonate is an effective phosphate binder for chronic hemodialysis patients: a pilot study. *J Ren Nutr*. 2007;17:416–422.
12. Spiegel DM, Farmer B. Long-term effects of magnesium carbonate on coronary artery calcification and bone mineral density in hemodialysis patients: a pilot study. *Hemodial Int*. 2009;13:453–459.
13. Sakaguchi Y, Fujii N, Shoji T, et al. Hypomagnesemia is a significant predictor of cardiovascular and non-cardiovascular mortality in patients undergoing hemodialysis. *Kidney Int*. 2014;85:174–181.
14. Kanbay M, Yilmaz MI, Apetrii M, et al. Relationship between serum magnesium levels and cardiovascular events in chronic kidney disease patients. *Am J Nephrol*. 2012;36:228–237.
15. Ishimura E, Okuno S, Kitatani K, et al. Significant association between the presence of peripheral vascular calcification and lower serum magnesium in hemodialysis patients. *Clin Nephrol*. 2007;68:222–227.
16. Tzanakis I, Pras A, Kounali D, et al. Mitral annular calcifications in haemodialysis patients: a possible protective role of magnesium. *Nephrol Dial Transplant*. 1997;12:2036–2037.
17. Tzanakis IP, Papadaki AN, Wei M, et al. Magnesium carbonate for phosphate control in patients on hemodialysis. A randomized controlled trial. *Int Urol Nephrol*. 2008;40:193–201.
18. Turgut F, Kanbay M, Metin MR, et al. Magnesium supplementation helps to improve carotid intima media thickness in patients on hemodialysis. *Int Urol Nephrol*. 2008;40:1075–1082.
19. Montes de OA, Guerrero F, Martinez-Moreno JM, et al. Magnesium inhibits Wnt/beta-catenin activity and reverses the osteogenic transformation of vascular smooth muscle cells. *PLoS One*. 2014;9:e89525.
20. Montezano AC, Zimmerman D, Yusuf H, et al. Vascular smooth muscle cell differentiation to an osteogenic phenotype involves TRPM7 modulation by magnesium. *Hypertension*. 2010;56:453–462.
21. Kircelli F, Peter ME, Sevinc OE, et al. Magnesium reduces calcification in bovine vascular smooth muscle cells in a dose-dependent manner. *Nephrol Dial Transplant*. 2012;27:514–521.
22. Salem S, Bruck H, Bahlmann FH, et al. Relationship between magnesium and clinical biomarkers on inhibition of vascular calcification. *Am J Nephrol*. 2012;35:31–39.
23. Ennever J, Vogel JJ. Magnesium inhibition of apatite nucleation by proteolipid. *J Dent Res*. 1981;60:838–841.
24. Peralta-Ramirez A, Montes de OA, Raya AI, et al. Vitamin E protection of obesity-enhanced vascular calcification in uremic rats. *Am J Physiol Renal Physiol*. 2014;306:F422–F429.
25. Massry SG, Coburn JW, Kleeman CR. Evidence for suppression of parathyroid gland activity by hypermagnesemia. *J Clin Invest*. 1970;49:1619–1629.
26. Cholst IN, Steinberg SF, Tropper PJ, et al. The influence of hypermagnesemia on serum calcium and parathyroid hormone levels in human subjects. *N Engl J Med*. 1984;310:1221–1225.
27. Brown AJ, Zhong M, Ritter C, et al. Loss of calcium responsiveness in cultured bovine parathyroid cells is associated with decreased calcium receptor expression. *Biochem Biophys Res Commun*. 1995;212:861–867.
28. Rodriguez-Ortiz ME, Canalejo A, Herencia C, et al. Magnesium modulates parathyroid hormone secretion and upregulates parathyroid receptor expression at moderately low calcium concentration. *Nephrol Dial Transplant*. 2014;29:282–289.
29. Delmez JA, Kelber J, Norword KY, et al. Magnesium carbonate as a phosphorus binder: a prospective, controlled, crossover study. *Kidney Int*. 1996;49:163–167.
30. De Francisco AL, Leidig M, Covic AC, et al. Evaluation of calcium acetate/magnesium carbonate as a phosphate binder compared with sevelamer hydrochloride in haemodialysis patients: a controlled randomized study (CALMAG study) assessing efficacy and tolerability. *Nephrol Dial Transplant*. 2010;25:3707–3717.
31. Rodriguez M, Martin-Malo A, Martinez ME, et al. Calcemic response to parathyroid hormone in renal failure: Role of phosphorus and its effect on calcitriol. *Kidney Int*. 1991;40:1055–1062.
32. Somerville P, Kaye M. Evidence that resistance to the calcemic action of parathyroid hormone in rats with acute uremia is caused by phosphate retention. *Kidney Int*. 1979;16:552–560.
33. Louvet L, Buchel J, Steppan S, et al. Magnesium prevents phosphate-induced calcification in human aortic vascular smooth muscle cells. *Nephrol Dial Transplant*. 2013;28:869–878.
34. De Schutter TM, Behets GJ, Geryl H, et al. Effect of a magnesium-based phosphate binder on medial calcification in a rat model of uremia. *Kidney Int*. 2013;83:1109–1117.
35. Witteman JC, Willett WC, Stampfer MJ, et al. A prospective study of nutritional factors and hypertension among US women. *Circulation*. 1989;80:1320–1327.
36. Ascherio A, Rimm EB, Giovannucci EL, et al. A prospective study of nutritional factors and hypertension among US men. *Circulation*. 1992;86:1475–1484.
37. Jee SH, Miller ER III, Guallar E, et al. The effect of magnesium supplementation on blood pressure: a meta-analysis of randomized clinical trials. *Am J Hypertens*. 2002;15:691–696.
38. Buendia P, Montes de OA, Madueno JA, et al. Endothelial microparticles mediate inflammation-induced vascular calcification. *FASEB J*. 2015;29:173–181.
39. Dowling O, Chatterjee PK, Gupta M, et al. Magnesium sulfate reduces bacterial LPS-induced inflammation at the maternal-fetal interface. *Placenta*. 2012;33:392–398.
40. Liu Z, Zhang J, Huang X, et al. Magnesium sulfate inhibits the secretion of high mobility group box 1 from lipopolysaccharide-activated RAW264.7 macrophages in vitro. *J Surg Res*. 2013;179:e189–e195.
41. Di LC, Gallieni M, Bestetti A, et al. Cardiac and pulmonary calcification in a hemodialysis patient: partial regression 4 years after parathyroidectomy. *Clin Nephrol*. 2003;59:59–63.
42. Sabeel A, Al-Homrany M. Complete resorption of massive soft tissue calcification in a hemodialysis patient after parathyroidectomy. *Am J Nephrol*. 2000;20:421–424.
43. Neves KR, Graciolli FG, dos Reis LM, et al. Vascular calcification: contribution of parathyroid hormone in renal failure. *Kidney Int*. 2007;71:1262–1270.
44. Mendoza FJ, Lopez I, Canalejo R, et al. Direct upregulation of parathyroid calcium-sensing receptor and vitamin D receptor by calcimimetics in uremic rats. *Am J Physiol Renal Physiol*. 2009;296:F605–F613.
45. Bonny O, Rubin A, Huang CL, et al. Mechanism of urinary calcium regulation by urinary magnesium and pH. *J Am Soc Nephrol*. 2008;19:1530–1537.
46. Lei Y, Grover A, Sinha A, et al. Efficacy of reversal of aortic calcification by chelating agents. *Calcif Tissue Int*. 2013;93:426–435.
47. Delmez JA. Efficacy and safety of a new kappa-opioid receptor agonist for the treatment of uremic pruritus. *Nat Clin Pract Nephrol*. 2006;2:358–359.
48. Yonova DH, Vazelov ES, Trendafilov II, et al. First impressions of cardiovascular calcification treatment in hemodialysis patients with a

new dialysis fluid containing sodium thiosulphate (STS). *Int J Artif Organs*. 2014;37:308–314.
49. Lopez I, Mendoza FJ, Guerrero F, et al. The calcimimetic AMG 641 accelerates regression of extraosseous calcification in uremic rats. *Am J Physiol Renal Physiol*. 2009;296:F1376–F1385.
50. Raggi P, Chertow GM, Torres PU, et al., ADVANCE Study Group. The ADVANCE study: a randomized study to evaluate the effects of cinacalcet plus low-dose vitamin D on vascular calcification in patients on hemodialysis. *Nephrol Dial Transplant*. 2011;26:1327–1339.
51. Nikolov IG, Joki N, Nguyen-Khoa T, et al. Lanthanum carbonate, like sevelamer-HCl, retards the progression of vascular calcification and atherosclerosis in uremic apolipoprotein E-deficient mice. *Nephrol Dial Transplant*. 2012;27:505–513.
52. Block GA, Spiegel DM, Ehrlich J, et al. Effects of sevelamer and calcium on coronary artery calcification in patients new to hemodialysis. *Kidney Int*. 2005;68:1815–1824.
53. Tamura K, Suzuki Y, Hashiba H, et al. Effect of etidronate on aortic calcification and bone metabolism in calcitriol-treated rats with subtotal nephrectomy. *J Pharmacol Sci*. 2005;99:89–94.
54. Price PA, Roublick AM, Williamson MK. Artery calcification in uremic rats is increased by a low protein diet and prevented by treatment with ibandronate. *Kidney Int*. 2006;70:1577–1583.
55. Toussaint ND, Elder GJ, Kerr PG. Bisphosphonates in chronic kidney disease; balancing potential benefits and adverse effects on bone and soft tissue. *Clin J Am Soc Nephrol*. 2009;4:221–233.
56. Chertow GM, Correa-Rotter R, Block GA, et al. Baseline characteristics of subjects enrolled in the Evaluation of Cinacalcet HCl Therapy to Lower Cardiovascular Events (EVOLVE) trial. *Nephrol Dial Transplant*. 2012;27:2872–2879.
57. Mortazavi M, Moeinzadeh F, Saadatnia M, et al. Effect of magnesium supplementation on carotid intima-media thickness and flow-mediated dilatation among hemodialysis patients: a double-blind, randomized, placebo-controlled trial. *Eur Neurol*. 2013;69:309–316.
58. Rodriguez-Moran M, Guerrero-Romero F. Oral magnesium supplementation improves insulin sensitivity and metabolic control in type 2 diabetic subjects: a randomized double-blind controlled trial. *Diabetes Care*. 2003;26:1147–1152.
59. Barragan-Rodriguez L, Rodriguez-Moran M, Guerrero-Romero F. Efficacy and safety of oral magnesium supplementation in the treatment of depression in the elderly with type 2 diabetes: a randomized, equivalent trial. *Magnes Res*. 2008;21:218–223.
60. Price PA, Faus SA, Williamson MK. Warfarin-induced artery calcification is accelerated by growth and vitamin D. *Arterioscler Thromb Vasc Biol*. 2000;20:317–327.
61. Erben RG, Glösmann M. Histomorphometry in rodents. *Methods Mol Biol*. 2012;816:279–303.
62. Dempster DW, Compston JE, Drezner MK, et al. Standardized nomenclature, symbols, and units for bone histomorphometry: a 2012 update of the report of the ASBMR Histomorphometry Nomenclature Committee. *J Bone Miner Res*. 2013;28:2–17.

Calcimimetics Maintain Bone Turnover in Uremic Rats despite the concomitant decrease in Parathyroid Hormone concentration

Journal:	*Kidney International*
Manuscript ID	KI-11-17-1709.R2
Article Type:	Basic Research
Date Submitted by the Author:	n/a
Complete List of Authors:	Díaz-Tocados, Juan Miguel; Instituto Maimonides de Investigacion Biomedica de Cordoba, Metabolismo del Calcio. Calcificacion Vascular; Hospital Universitario Reina Sofia; Universidad de Cordoba Facultad de Medicina y Enfermeria Rodriguez Ortiz, Mª Encarnacion; Instituto de Salud Carlos III; Instituto de Investigacion Sanitaria de la Fundacion Jimenez Diaz, Nephrology Almaden, Yolanda; Instituto Maimonides de Investigacion Biomedica de Cordoba, Lipids and atherosclerosis; Hospital Universitario Reina Sofia, Internal Medicine Pineda, Carmen; Universidad de Cordoba Facultad de Veterinaria, Medicina y cirugia animal Martínez, Julio Manuel; Instituto Maimonides de Investigacion Biomedica de Cordoba, Metabolismo del Calcio. Calcificacion Vascular; Hospital Universitario Reina Sofia; Universidad de Cordoba Facultad de Medicina y Enfermeria Herencia, Carmen; Instituto Maimonides de Investigacion Biomedica de Cordoba, Metabolismo del Calcio. Calcificacion Vascular; Hospital Universitario Reina Sofia; Universidad de Cordoba Facultad de Medicina y Enfermeria Vergara, Noemi; Instituto Maimonides de Investigacion Biomedica de Cordoba, Metabolismo del Calcio. Calcificacion Vascular; Hospital Universitario Reina Sofia; Universidad de Cordoba Facultad de Medicina y Enfermeria Pendon-Ruiz de Mier, M Victoria; Instituto Maimonides de Investigacion Biomedica de Cordoba, Metabolismo del Calcio. Calcificacion Vascular; Hospital Universitario Reina Sofia; Universidad de Cordoba Facultad de Medicina y Enfermeria Santamaría, Rafael; Instituto Maimonides de Investigacion Biomedica de Cordoba, Nefrología. Daño celular en la inflamación crónica; Hospital Universitario Reina Sofia, Servicio de Nefrología (Red in Ren) Rodelo-Haad, Cristian; Hospital Universitario Reina Sofia, Nephrology Casado-Díaz, Antonio; Instituto Maimonides de Investigacion Biomedica de Cordoba, Fisiopatología del sistema endocrino de la vitamina D. Biotecnología y envejecimiento; Hospital Universitario Reina Sofia, Unidad de gestión clínica de endocrinología y nutrición Lorenzo, Victor; Nephrology Section, University Hospital of Canary Islands, Santa Cruz de Tenerife, Canary Islands, Spain,

	Carvalho, Catarina; Universidade do Porto Instituto de Investigacao e Inovacao em Saude; INEB; Hospital de Braga Frazao, Joao; Universidade do Porto Instituto de Investigacao e Inovacao em Saude; INEB; Centro Hospitalar de Sao Joao EPE, Nefrología Felsenfeld, Arnold; West Los Angeles VA Medical Center, Nephrology Section 111L Richards, William; Amgen, Inc., Metabolic Disorders Aguilera-Tejero, Escolastico; University of Cordoba, Medicina y Cirugia Animal Rodriguez, Mariano; Hospital Universitario Reina Sofia, Nephrology; Instituto Maimonides de Investigacion Biomedica de Cordoba, Lopez, Ignacio; Universidad de Cordoba Facultad de Veterinaria, Medicina y cirugia animal Muñoz-Castañeda, Juan R; Instituto Maimónides de Investigación Biomédica de Córdoba/Hospital Universitario Reina Sofia/Universidad de Cordoba, Servicio de Nefrología (Red in Ren), GC13. Metabolismo del calcio. Calcificación Vascular Cordoba, Cordoba, ES
Subject Area:	Mineral and Bone Disorders
Keywords:	parathyroid hormone, bone, mineral metabolism, chronic kidney disease

Calcimimetics Maintain Bone Turnover in Uremic Rats despite the concomitant decrease in Parathyroid Hormone concentration

Juan M. Díaz-Tocados[1,2,3,4,#], María E. Rodríguez-Ortiz[4,5,#], Yolanda Almadén[1,6,7], Carmen Pineda[3,8], Julio M. Martínez-Moreno[1,2,3,4], Carmen Herencia[1,2,3,4], Noemi Vergara[1,2,3,4], M. Victoria Pendón-Ruiz de Mier[1,2,3,4], Rafael Santamaría[1,2,3,4], Cristian Rodelo-Haad[1,2,3,4], Antonio Casado-Díaz[1,3,9,10], Víctor Lorenzo[11], Catarina Carvalho[12,13,14], João M. Frazão[13,14,15], Arnold J. Felsenfeld[16], William G. Richards[17], Escolástico Aguilera-Tejero[3,8], Mariano Rodríguez[1,2,3,4,*], Ignacio López[3,8,+], Juan R. Muñoz-Castañeda[1,2,3,4,+].

[1]Maimonides Institute for Biomedical Research (IMIBIC), Cordoba, Spain. [2]Nephrology Service, Reina Sofia University Hospital, Cordoba, Spain. [3]University of Cordoba, Spain, [4]Spanish Renal Research Network (REDinREN), Institute of Health Carlos III, Madrid, Spain. [5]Laboratory of Nephrology, Health Research Institute-Jiménez Diaz Foundation, Madrid, Spain. [6]Internal Medicine Service, Reina Sofia University Hospital, Cordoba, Spain. [7]Spanish Biomedical Research Networking Centre consortium for the area of Physiopathology of Obesity and Nutrition (CIBEROBN), Institute of Health Carlos III, Madrid, Spain. [8]Department of Medicine and Animal Surgery, Cordoba, Spain. [9]Clinical Management Unit for Endocrinology and Nutrition, Reina Sofia University Hospital. [10] Network for Cooperative Research on Ageing and Fragility (RETICEF) & Spanish Biomedical Research Networking Centre consortium for the area of Frailty and Healthy Ageing (CIBERFES), Institute of Health Carlos III, Madrid, Spain. [11]University Hospital of Tenerife, Nephrology Service, Canary Islands, Spain. [12] Braga Hospital, Department of

Nephrology, Portugal, [13]Institute of Investigation and Innovation in Health (I3S), University of Porto, Portugal. [14]National Institute of Biomedical Engineer (INEB), University of Porto, Portugal. [15]Department of Nephrology, São João Hospital Center, Porto, Portugal. [16]Department of Medicine, Veterans Affairs Greater Los Angeles Healthcare System and the David Geffen School of Medicine, University of California, Los Angeles, California, USA. [17]Amgen Research Thousand Oaks Ca, USA.

[#]These authors share the first authorship. [+]These authors share the last authorship.

Running title: PTH-independent Effects of Calcimimetics in Bone

*Correspondence: Mariano Rodríguez: marianorodriguezportillo@gmail.com. Maimonides Institute for Biomedical Research (IMIBIC). Nephrology Service, Reina Sofia University Hospital, Av. Menendez Pidal, Postal Code 14004, Cordoba, Spain.

ABSTRACT

Calcimimetics (CMs) are used to decrease parathyroid hormone (PTH) secretion in uremic patients with secondary hyperparathyroidism. Decreased PTH should be associated with a reduction in bone turnover. However, bone cells express calcium sensing receptor (CaSR) and the direct *in vivo* effect of CMs on these cells has not been defined. In this study, we evaluate the direct bone effects of CaSR activation by CM (AMG 641) *in vivo* and *in vitro*. Normal and 5/6 nephrectomized (Nx) rats were divided in subgroups that underwent parathyroidectomy followed by a constant subcutaneous infusion of PTH during treatment with vehicle or CM.

CM administration to normal rats with clamped PTH increased osteoblasts and osteoid volume. In Nx rats elevated PTH concentration led to reduced bone volume and increased bone turnover. CM administration to Nx animals decreased plasma PTH while bone cell activity remained similar to the vehicle Nx group. In Nx rats with PTH clamp (PTHx6), CM administration increased osteoblasts number, osteoid surface and bone formation as compared with vehicle. A higher dose of PTH1-34 (PTHx9) caused an increase in bone turnover that was not altered by the administration of CM.

In UMR cells CM induced Erk1/2 phosphorylation and the expression of osteoblastic genes. The addition of a calcilytic resulted in the opposite effect. Moreover, CM promoted the osteogenic differentiation and mineralization of human bone marrow mesenchymal stem cells.

In conclusion, calcimimetic administration has a direct anabolic effect on bone that counteracts the concomitant decrease in PTH levels.

Keywords: calcimimetic, parathyroid hormone, bone, CaSR, mineral metabolism, chronic kidney disease.

INTRODUCTION

Patients with renal insufficiency develop secondary hyperparathyroidism (SHPT). High levels of parathyroid hormone (PTH) are associated with negative outcomes and play a key role in the development of Chronic Kidney Disease-Mineral and Bone Disorder (CKD-MBD). Excess PTH increases bone turnover and, as SHPT progresses, osteitis fibrosa develops[1]. However, due to bone resistance to PTH, normal or moderately increased PTH concentration is not sufficient to maintain normal bone turnover[2]. Therefore, an excessive suppression of PTH may exacerbate adynamic bone disease.

Calcimimetics (CMs) are used to reduce high PTH levels in dialysis patients[3]. CM's act as positive allosteric modulator of the calcium sensing receptor (CaSR) expressed on the parathyroid gland [4] to reduce PTH levels, which is accompanied by decreased bone turnover as evidenced in clinical studies[5,6].

Bone cells also possess functionally active CaSR[7] and a question that needs to be addressed is whether CMs have a direct effect on bone turnover independent of what would correspond to the reduction in PTH. *In vitro* studies have demonstrated that an increase in extracellular calcium (Ca) activates the osteoblast CaSR resulting in downstream cell signaling (Erk1/2 phosphorylation) to induce osteoblast proliferation, osteoblastic gene expression and calcification[8]. This response is abrogated by the addition of a CaSR antagonist [8,9]. Additionally, some authors indicate that CaSR is also expressed in osteoclasts, monocytes and osteoclast precursors[10–12]. In 1999, Kanatani M. et al showed *in vitro* that CM administration inhibited osteoclastic differentiation in osteoclast precursor cells derived from spleen cells[13]. Despite all this information, the action of CM on bone independent of its modulation on PTH levels has not been investigated in the context of CKD.

Therefore, the aim of the present study was to evaluate a direct effect of CMs *in vivo* using normal and uremic rats in experimental models with parathyroidectomy (PTX) and clamped PTH level so the action of CMs on bone could be isolated from that of PTH. Additionally, the direct activation of the CaSR in osteoblasts by CMs was investigated *in vitro*.

RESULTS

In vivo effects of CM in rats with normal renal function

Biochemical parameters:

As shown in Table 1, blood ionized Ca was decreased in PTX rats compared with sham-operated rats ($p<0.05$). PTH replacement (PTX-PTH) restored the serum Ca concentration and the administration of calcimimetic (PTX-PTH-CM) did not decrease serum Ca levels. Serum P concentration was significantly increased in the PTX group as compared with Sham ($p<0.05$). PTX-PTH and PTX-PTH-CM rats had normal serum P concentration ($p<0.05$ vs PTX group). The decrease in serum $1,25(OH)_2D_3$ was non-significant in PTX and PTX-PTH groups. In rats treated with CM the concentration of $1,25(OH)_2D_3$ was increased ($p<0.05$ vs all groups) while plasma levels of FGF23 were reduced significantly ($p<0.05$) from 129±20 to 88±14 pg/ml.

Bone histomorphometry analysis:

Bone Volume (BV/TV) was similar in all four groups (Fig. 1a). In PTX rats, osteiod volume, osteoid surface and the bone surface covered by osteoblasts (OV/BV, OS/BS and Ob.S/BS, respectively) were significantly reduced after 28 days (Fig. 1b, c, d). Additionally, the osteoclast surface was decreased without changes in the eroded surface (Fig. 1e and f). PTH replacement (PTX-PTH) restored bone histomorphometric parameters to values similar to those found in sham-operated animals. The administration of CM (PTX-PTH-CM) did not alter bone parameters as compared with Sham and PTX-PTH groups. Representative microphotographs are shown in Supplementary Figure S1.

In vivo effects of CM in uremic rats

After 28 days of experimentation, body weight increased in all groups of Nx rats and body weight gain was no significantly different among the Nx groups. The gain in body weight observed in Sham rats was slightly higher than in Nx rats (Supplementary Figure S2).

Biochemical parameters:

As shown in Table 2, serum concentration of creatinine was significantly increased ($p<0.05$) in all Nx groups with no differences among them. In parathyroidectomized Nx rats, PTH infusion in an amount 6-fold the normal replacement dose (Nx-PTX-PTHx6) was sufficient to maintain serum Ca at a level similar to Nx rats. However, a significant increase in iCa levels was observed in both Nx-PTX-PTHx9 groups (^{d} $p<0.05$ vs Nx-PTX-PTHx6) that was not altered by the administration of CM. The increase in serum P concentration observed in Nx rats was not altered by parathyroidectomy. CM administration in the Nx-PTX-PTHx6-CM group maintained serum P at a level not significantly different from the Sham group. As expected intact rat PTH was elevated in 5/6 Nx rats and decreased with the administration of CM. Additionally, PTH1-34 levels in animals with PTH replacement were compared with PTH1-34 levels of Nx group. Table 2 shows that in Nx-PTX-PTHx6 treated animals the PTH1-34 levels did not reach levels observed in the Nx group. However, in Nx-PTX-PTHx9, PTH1-34 levels increased significantly with respect to Nx and Nx-PTX-PTHx6 groups (^{d} $p<0.05$ vs Nx-PTX-PTHx6). The serum level of $1,25(OH)_2D_3$ was similar in all groups. Finally, plasma FGF23 was higher in the Nx groups than in Sham animals (^{a} $p<0.05$) and CM administration decreased FGF23 levels in Nx animals (^{b} $p< 0.05$ vs Nx group). Nx- PTX- PTHx6 rats had lower FGF23 levels than those found in Nx group. Whereas a higher dose of PTH (Nx-PTX-PTHx9) increased FGF23 levels significantly. In rats with PTH infusion, the addition of CM did not change FGF23 levels.

Bone histomorphometry analysis:

Except for BV/TV which was reduced when compared with Sham rats ($p<0.001$) (Fig. 2a), all bone parameters were increased in Nx rats (Fig. 2b-h). In Nx rats with intact parathyroid glands treated with CM bone turnover was maintained despite a 4-fold reduction in PTH levels (from 540 to 144 pg/ml).

In Nx-PTX-PTHx6 rats treated with vehicle, that had relatively low levels of 1-34 PTH bone turnover was reduced. The high dose of PTH (Nx-PTX-PTHx9) produced a significant increase in bone turnover when compared to Nx-PTX-PTHx6 vehicle group, resulting in higher values of osteoid volume (OV/BV), OS/BS, ObS/BS, ES/BS, OcS/BS, MS/BS and BFR/BS (Fig. 2).

In the Nx-PTX-PTHx6 group CM administration (Nx-PTX-PTHx6-CM) increased osteoid surface (OS/BV), osteoblasts surface (Ob.S/BS) and osteoclasts surface (Oc.S/BS). With respect to bone formation, the addition of CM to Nx-PTX-PTHx6 rats produced an increase in mineralizing surface (MS/BS, 30.9±2.24 vs 21.3±5.00 %, $p<0.05$, Fig.2g) and BFR/BS (379±55 vs 253±81 %/year, $p<0.01$, Fig.2h) as compared to Nx-PTX-PTHx6-vehicle group. In conditions of very high PTH levels (Nx-PTX-PTHx9), CM administration (Nx-PTX-PTHx9-CM) did not alter bone cell activity (Fig. 2). No differences in cortical bone area and thickness were observed among all animal groups (Supplementary Fig. S3 **a** and **b**).

With respect to mineralization, as compared with Sham animals, Nx group showed higher mineral apposition rate and mineralization lag time ([a] $p<0.05$ vs Sham group, Fig. 3a and 3b) and lower mineralizing surface related to osteoid surface and an adjusted apposition rate (Fig. 3c and 3d, [a] $p<0.05$ vs Sham group). The Nx-PTX-PTHx9 group showed a significant increase in mineral apposition rate, mineralization lag time and osteoid thickness as compared with the Nx-PTX-PTHx6 group (Fig. 3a, b and e respectively). However, as

compared with the corresponding vehicle, CM administration did not induce significant changes in the mineralization parameters in any experimental condition (Fig. 3).

Representative samples of Goldner's trichrome staining of undecalcified bone from the four groups of rats are shown in Fig. 4. In Sham animals, an almost quiescent state of bone cells with normal mineralization was observed. Nx groups showed an increased bone cell activity with high number of osteoblasts and osteoclasts on the bone surface, accompanied by an increase in bone formation. CM treatment did not alter bone cell activity and mineralization was similar in Nx rats with intact parathyroid glands. In Nx-PTX-PTHx6 animals a lower bone turnover and bone formation respect to Nx group was observed. In these conditions, treatment with CM increased the number of osteoblasts and osteoclasts as well as mineralization and bone formation. In Nx-PTX-PTHx9 group bone turnover and mineralization was similar to that observed in the Nx group, and CM administration did not modify bone cells activity and bone formation.

Figure 5 shows in consecutive bone slices, that CM increases the number of bone cells positive for phospho-Erk1/2 (both in cytoplasm and nuclei). To further confirm that the Erk1/2 phosphorylation was triggered in osteoblasts, staining for osteocalcin in consecutive slices was performed and matched. The phospho-Erk1/2 positive cells were also positive for osteocalcin staining illustrating that CM promotes Erk1/2 phosphorylation of osteoblasts. The phospho-Erk1/2 immunostaining was quantified and expressed as percentage relative to the total number of osteoblasts.

Modulation of CaSR, by CM and calcilytic, regulates the expression of osteoblast markers in UMR 106 cells

To evaluate the direct effect of positive allosteric modulation of CaSR on the osteoblastic phenotype, CM was added to UMR106 cells in a medium with a low Ca concentration (0.5

mM), which in turn mimics the "*in vivo*" effects of CM decreasing PTH with the resulting reduction in serum Ca concentration. The addition of CM did not modify significantly PCNA protein expression nor affected the CaSR expression in UMR 106 cells (Fig. 6a). CaSR activation by CM led to an increase in Erk1/2 phosphorylation (Fig. 6b), demonstrating that in these cells CaSR is functional and modulated by CM. Confocal microscopy showed nuclear translocation of phosphorylated Erk1/2 induced by CM (Supplementary Figure S4). After 48 hours of treatment, CM (100μM) significantly increased ($p<0.05$ vs all groups) the expression of the osteogenic markers Runx2, Osterix and Osteocalcin (Fig. 6 c, d and e respectively). Finally, negative allosteric modulation of the CaSR by the calcilytic Calhex 231 reduced the Erk1/2 phosphorylation (Fig. 7a) which was accompanied by down-regulation of the ostegenic gene expression of Osterix (Fig. 7b), Runx2 (Fig. 7c) and Osteocalcin (Fig. 7d) (a $p<0.05$ vs Control).

CM increases osteoblastic differentiation and mineralization of human bone marrow mesenchymal stem cells

Human bone marrow mesenchymal stem cells (MSC) were differentiated into osteoblasts in a medium with a low Ca concentration (Ca 0.5 mM). After 21 days, Ca deposition (Fig. 8a) and number of mineralization nodules were increased in osteoblasts cultured with CM 100 μM (Fig. 8b). Addition of CM increased the expression of the early osteoblast markers Runx2 and Osterix (Fig. 8c and d respectively) and mature osteoblast markers such as osteocalcin (Fig. 8e). Furthermore, CM addition enhanced the expression of BMP2 (Fig. 8f), a well-known pro-osteogenic factor. Both, undifferentiated MSC and MSC differentiated into osteoblasts expressed CaSR (Fig. 8g).

DISCUSSION

The present study was designed to determine whether CMs directly affect bone cell activity. Our study showed that CM produced an increase in bone cell activity, as evidenced by *in vivo* and *in vitro* experiments. The CM effect was direct and independent of that from a reduction in PTH induced by CM. This explains the observation that in uremic rats with intact parathyroid glands the administration of CM maintained bone turnover despite the reduction of PTH level.

To evaluate a direct effect of CM on bone *in vivo* in Nx rats, it was necessary to clamp the serum PTH concentration using continuous delivery of PTH1-34 at 6 and 9- fold the replacement dose by subcutaneous miniosmotic pumps in previously PTX rats. The *in vivo* results demonstrated that CM increased bone cell activity. As compared with Nx group, the Nx-PTx-PTHx6 group presented a low bone cell activity which was likely due to relatively low levels of PTH as illustrated by the lower levels of PTH1-34. In this setting of low bone turnover (PTH6x), CM administration increased bone cell activity and bone mineralization. While osteoblast activity was higher in the Nx-PTX-PTHx6-CM group than in the Nx-PTX-PTHx6 receiving vehicle, the bone volume remained similar. This could be explained by the increased osteoclast activity (Oc.S/BS) in the Nx-PTX-PTHx6-CM.

However, PTHx9 rats showed a very high bone turnover which was not further increased by CM administration. CM administration did not significantly affect cortical bone. More prolonged experiments may be required to assess whether CM has any effect on cortical bone.

With equal amounts of PTH infusion, in both normal and Nx rats, the administration of CM increased the bone surface covered by osteoblasts and the bone formation rate. In contrast to previous studies[5,14,15], we did not find significant differences between vehicle or

calcimimetic administration in any PTH condition, indicating that the treatment with CM did not produce abnormal mineralization.

In normal renal function PTX rats with PTH infusion CM administration increased $1,25(OH)_2D_3$ levels, which likely results from reduced serum FGF23 levels in the PTX-PTH-CM as compared with the PTX-PTH group. Furthermore, elevated $1,25(OH)_2D_3$ levels might also contribute to the increased bone anabolism observed in this group. In a previous article[15] it was shown that serum levels of FGF23 may be markedly reduced when serum calcium concentrations decrease below 8-8.5 mg/dl (which corresponds to 1.0 – 1.06 mM of ionized calcium). The reduction in FGF23 in the PTX-PTH-CM group could be related in part to the moderate reduction in serum calcium observed in these rats. Activation of the CaSR is known promote calciuria[16]. In our Nx rats with clamped PTH the production of FGF23 was not modified by CM because FGF23 synthesis is mainly determined by the reduction of renal function and by phosphate load.

In a previous study, Khoshniat S et al reported that extracellular calcium is necessary to promoted phosphate-dependent Erk1/2 signaling activation in osteoblasts *in vitro*. This occurs independent of CaSR and it is related with calcium phosphate precipitates which was associated with an increased expression of *Osteopontin* (*OPN*) and *Matrix Gla Protein* (*MGP*) that are associated with a decrease in mineralization[17]. In our *in vitro* experiments in osteoblasts cultured with normal phosphate concentration, the addition of calcimimetic induced the Erk1/2 phosphorylation with an associated increase in both, osteogenic genes expression and matrix mineralization as assessed by the amount of calcium in the mineralized matrix. Thus, our data also support that the CaSR activation may not be involved in the decreased mineralization induced by calcium phosphate precipitates due to high levels of calcium and phosphate.

To confirm the direct effect of the CM on osteoblasts, CM was added to UMR cells, an osteoblast cell line in culture. In these cells, the activation of CaSR by CM led to the phosphorylation of Erk1/2 triggering the expression of osteogenic genes. By contrast, in UMR 106 cells, the calcilytic compound Calhex 231 inhibited Erk1/2 phosphorylation and reduced the expression of osteogenic genes which further support the role of CaSR on osteoblast activity. Furthermore, when human bone marrow MSC were differentiated into osteoblasts and cultured with CM increased matrix mineralization together with an up-regulation of osteogenic genes were observed. Taken together all these results indicate that positive allosteric modulation of the CaSR in bone cells participates in the maintenance of bone turnover.

Our results suggest that the activation of CaSR by CM in osteoblasts promotes bone turnover independently of PTH. In the context of CKD, our results are consistent with other studies. Wada et al reported that the calcimimetic R-568 reduced PTH levels and ameliorated osteoitis fibrosa in uremic rats. However, bone cell activity was not significantly different than in rats receiving vehicle[18]. In a similar animal model, over-suppression of PTH by CM, produced no significant differences in the surface of bone covered by osteoclast, although the number of osteoblasts was significantly reduced[19]. Given the reduced bone responsiveness to PTH in uremia[20], it is important to maintain PTH levels sufficiently high to sustain bone turnover. In this context, our results suggest that CaSR activation of bone cells with a CM may act to maintain bone turnover when PTH is reduced.

The relevance of CaSR activity on bone health was evaluated by Xue Y. et al in rodents null for PTH and CaSR. In these animals, the anabolic effects of PTH were more greatly reduced in $PTH^{-/-}$ $CaSR^{-/-}$ as compared with $PTH^{-/-}$[21]. Likewise, another study showed that

high dietary Ca increased bone formation in both wild type and $PTH^{-/-}$ mice, but these effects were absent in $PTH^{-/-}$ $CaSR^{-/-}$ double knockout mice[22]. Similarly, osteoblast specific ablation of CaSR attenuated the anabolic action of PTH[14]. All these findings support an important role of CaSR activation in bone cell activity. Conversely, a study by Dvorak et al[23] reported that constitutive activation of the bovine parathyroid CaSR in mature osteoblasts of mice without other systemic changes in serum Ca^{2+} and PTH led to bone loss through an increase in bone resorption. In this case, CaSR activation was not associated with an altered renal function or changes in mineral metabolism parameters such as P, 1,25-OH_2D_3 or FGF23 which likely modulate bone activity; in addition, the role of CaSR on early osteoblasts was not quantified. Whether the structure and function of CaSR in parathyroid glands is the same that CaSR in bone is controversial. Regardless, additional studies still need to be performed to characterize specific aspects of the role of CaSR on bone cell activity in normal physiological states.

A clinical study called Bonafide was conducted to assess bone histomorphometric changes after treatment with the calcimimetic cinacalcet in a cohort of dialysis patients. The study reported a reduction in PTH levels after 12 months of treatment. The reduction of PTH was accompanied by decreased bone turnover and bone formation. However, only a modest correlation between changes in PTH and the reduction in bone activity existed, suggesting that other factors besides the change in PTH may have influenced bone turnover. An excessive dose of vitamin D at the beginning of the study might have affected the results[5]. Of interest, a recent pre-clinical study which looked at the effect of the calcimimetic Parsabiv™ (Etelcalcetide) on SHPT in subtotal Nx rats showed that Etelcalcetide administration decreased plasma PTH levels, but histomorphometric analysis showed that the osteoblast and osteoclast bone surface remained similar to vehicle[24].

Extracellular Ca is the natural activator of the CaSR. In fact, high extracellular Ca has been shown to promote osteoblast maturation and proliferation[8,25]. The hypercalcemic effect of PTH may potentiate the bone anabolic effect of PTH. The administration of CM to dialysis patients causes a reduction in PTH and a concomitant decrease in the plasma Ca concentration. It is important to know whether the action of CM on the CaSR could potentially compensate for the moderate reduction in plasma Ca concentration on bone cells. Thus, we performed an experiment to evaluate *in vitro*, the effect of CM on bone cells in the presence of a low Ca concentration. UMR106 cells and osteoblasts-derived from MSC cultured in low Ca conditions showed an increase in the expression of osteogenic genes when treated with CM. Moreover, the increased osteoblastic genes were associated with the activation of the Erk1/2 pathway. Of note, mineralization was enhanced in MSC differentiated into osteoblasts with CM suggesting an active role of the CaSR in mineralization. Our study is the first to demonstrate that despite low calcium, CM increases maturation, differentiation and mineralization of osteoblast-like cells.

In conclusion, this is the first *in vivo* study to show that, in uremic rats, the administration of a calcimimetic directly increases bone cell activity and bone formation rate, an effect that is observed despite the concomitant decrease in PTH levels.

METHODS

In vivo experiments

Male Wistar rats weighing 200-250 g were housed with a 12h/12h light/dark cycle and given *ad libitum* access to standard diet, 0.6% Ca, 0.6% phosphate (P) and tap water. Animal care and experimental procedures were approved by Research and Ethics Committees of IMIBIC/Reina Sofia University Hospital in accordance with Directive 2010/63/EU of the European Parliament and with institutional guidelines for the care and use of laboratory animals and the Declaration of Helsinki. Human samples of bone marrow mesenchymal stem cells were collected after obtaining the corresponding signed informed consent.

Total PTX was performed as previously reported with the aid of a dissecting microscope[26]. One week after PTX, rats were anesthetized using sevofluorane (Abbott, Madrid, Spain) and blood (0.7 ml) was drawn by puncture of the jugular vein to measure serum Ca levels. PTX was considered successful in rats with ionized Ca levels below 0.8 mM.

In vivo effects of CM in rats with normal renal function

Subsequently, a miniosmotic pump (ALZET model 2ML4 purchased from Charles River Laboratories, Barcelona, Spain) was implanted subcutaneously between the shoulders. The osmotic pump was loaded with rat PTH (rat PTH1-34 fragment, Sigma Aldrich Co., St Louis, MO, USA) diluted in isosmotic saline with 2% cysteine (pH 1.4) in aseptic conditions. Two subgroups of PTX rats received the amount of PTH1-34 infused that allowed to maintain serum calcium close to the physiological range (PTH1-34, 0.022 µg/100g per hour) through the miniosmotic pumps, one of them in combination with calcimimetic AMG 641 (1.5 mg/kg/48 h, subcutaneously) and the other one received vehicle. The physiological dose of PTH (0.022 µg/100g per hour) was previously defined by its ability to maintain a normal

range of serum ionized calcium values (1.15-1.25 mM) in PTX rats fed a 0.6% Ca and 0.6% P diet[27] .

In rats with normal renal function the following experimental groups were included: Sham operated (Sham, n=6), Parathyroidectomized rats (PTX, n=7), Parathyroidectomized rats plus PTH replacement (PTX-PTH, n=5) and Parathyroidectomized rats and PTH replacement plus CM (PTX-PTH-CM, n=6).

The calcimimetic AMG 641 was reconstituted in Captisol (Ligand Pharmaceuticals, Inc. San Diego, CA) 12% p/v, pH 3. The control animals received only Captisol as vehicle. The calcimimetic AMG 641 (chemical name: (1R)-N-((6-(methyloxy)-4′-(trifluoromethyl)-3-biphenylyl)methyl)-1-phenylethanamine) is an arylalkylamine with a molecular weight of approximately 400 g/mol, the half-life is approximately 3-fold longer than cinacalcet and has a large volume of distribution. This compound triggers Erk1/2 phosphorylation in the absence of calcium; therefore, it would referred as an allosteric agonist rather than strict allosteric modulator[19,28]. The dose of AMG 641 administered to the rats has showed to be efficient to decrease PTH levels in Nx rats[29].

In vivo effects of CM in uremic rats

To assess the effects of the CM on bone in animals with renal insufficiency and intact parathyroid glands, a second experiment was performed in uremic rats. Uremia was induced by 2-step subtotal nephrectomy (Nx) as previously described[26]. After the second surgery, the standard diet was switched to a moderately high phosphate diet (0.6% Ca and 0.9% P) (Nx group). An additional group of Nx rats was treated with CM (1.5 mg/kg/48h; subcutaneously) (Nx-CM). To determine whether the administration of AMG641 (CM) exerts PTH-independent effects on bone, several additional groups of Nx rats underwent total PTX receiving a constant infusion of a 6-fold (0.132 µg/100g per hour) or 9-fold (0.198 µg/100g

per hour) dose of rat recombinant PTH1-34 through ALZET osmotic pumps in combination with vehicle or CM (1.5 mg/kg/48 h, subcutaneously). Therefore, final experimental groups were the following: Sham (Sham, n=6), 5/6 Nephrectomized rats (Nx, n=7), 5/6 Nephrectomized rats plus AMG641 (Nx-CM, n=6), 5/6 Nephrectomized plus Parathyroidectomy and PTH replacement x6 (Nx-PTX-PTHx6, n=8), 5/6 Nephrectomized plus Parathyroidectomy and PTH replacement x6 plus CM (Nx-PTX-PTHx6-CM, n=5), 5/6 Nephrectomized plus Parathyroidectomy and PTH replacement x9 (Nx-PTX-PTHx9, n=5), 5/6 Nephrectomized plus Parathyroidectomy and PTH replacement x9 plus CM (Nx-PTX-PTHx9-CM, n=6).

Body weight of Sham animals and the different experimental groups with reduced renal function was measured twice a week. On day 28, twenty-four hours after the last dose of CM had been administered, blood was obtained by aortic puncture under general anesthesia (sodium tiopenthal, i.p) and femurs were dissected to study bone histomorphometry.

Blood Biochemistry

Blood for measurements of ionized Ca levels was collected in heparinized syringes and immediately analyzed using a Ciba-Corning 634 ISE Ca^{2+}/pH Analyzer (Ciba-Corning, Essex, England). Afterwards, serum was separated by centrifugation and stored at -20° C. Serum P and creatinine were measured by spectrophotometry (Biosystems SA, Barcelona, Spain). Serum concentrations of active vitamin D (1,25-OH_2D_3) were measured by radioimmunoassay (IDS kit, Boldon, UK) and Serum intact PTH levels were assayed using enzyme-linked immunosorbent assay (ELISA) kit (Immutopic, San Clemente, CA, USA). Infused PTH was not recognized by PTH assay. The plasma concentration of the PTH (1-34) fragment, was measured with a specific ELISA kit (Phoenix Pharmaceuticals, Inc.

Burlingame, CA, USA). Plasma levels of circulating intact FGF23 were determined using an ELISA kit (Kainos Laboratories, Tokyo, Japan).

Bone Histomorphometry

Bone mineralization was assessed only in uremic rats. Double calcein labeling (25 mg/kg) was administered at days 9 and 2 before sacrifice. At sacrifice, right femurs were dissected and placed in 70% ethanol. Subsequently, femurs were dehydrated in alcohol, cleared with xylene, and embedded in 75% methyl methacrylate, 25% dibutyl phthalate and 2.5% w/v benzoyl peroxide. Histomorphometric parameters were evaluated in undecalcified 5-µm sections of the distal bone treated with modified Masson-Goldner trichrome staining. Briefly, slices were fixed with 50% ethanol with pressure, then rehydrated and stained with hematoxylin-ferric choride 1:1, cleared with 1% HCl, and turned blue with $LiCO_3$. After rinsing with water, slices were stained with Goldner trichrome dye for 20 minutes and then rinsed with 1% acetic acid. Subsequently, samples were stained with safranin for 5 minutes, dehydrated with ethanol and mounted. Green stained areas were considered as mineralized bone and red stained areas measuring at least 1.5 µm were considered as osteoid.

Bone histomorphometric parameters were assessed in cancellous bone within the secondary spongiosa (0.25mm distance from endocortical bone and growth plate) under 200x magnification using OsteoMeasure™ software (OsteoMetrics, Decatur, IL, USA) and derived indices were determined by standard calculations[30]. The bone dynamic parameters were calculated by measurement of the single and double fluorescent calcein labelling lines in undecalcified 10-µm serial sections. Analysis of cortical bone was performed in axial sections of the femoral midshaft according to the method reported by Erben RG[31].

The following parameters were analyzed: BV/TV: Bone Volume/Tissue Volume, OV/TV: Osteoid Volume/Tissue Volume, OS/BS: Osteoid Surface/Bone Surface, Ob.S/BS:

Osteoblast Surface/Bone Surface, ES/BS: Eroded Surface/Bone Surface, Oc.S/BS: Osteoclast Surface/Bone Surface, BFR/BS: Bone Formation Rate/Bone Surface, MS/BS: Mineralizing Surface/Bone Surface, Osteoid Thickness (O.Th), Mineralizing Surface related to Osteoid Surface (MS/OS), mineral apposition rate (MAR), adjusted apposition rate (Aj.AR), mineralization lag time (Mlt) and osteoid maturation time (Omt), Ct.B.Ar: Cortical Bone Area, Ct.Th: Cortical Thickness.

Bone immunohistochemistry

Consecutive decalcified bone sections were used to analyse: Goldner´s trichrome staining, phospho-Erk1/2 immunostaining, osteocalcin immunostaining and absence of antibody. Bone slices from 5-µm sections were deacrylated in a 1:1 mixture of xylene and chloroform for 30 minutes and rehydrated with graded ethanol. Subsequently, samples were decalcified with 14% EDTA, pH 7.4 for 1 hour and rinsed with distilled water for 10 minutes. Then, immunohistochemistry was performed using the Novolink Polymer detection System kit (Leica Biosystems Newcastle Ltd, UK) according to the manufacturer's instructions. Anti-phospho-p44/42 MAPK (4370, Cell Signaling Technology Inc., Danvers, MA) was used as primary antibody at 1:400. Anti-human/rat Osteocalcin antibody was purchased from R&D Systems (Minnesota, USA) and it was used at concentration of 10 µg/ml. Finally, PBS was used to perform a negative immunostaining to substrate background. Image were taken in a Leica DM2000 LED microscope with a Leica MC190 HD camera using the Leica Application Suite 4.8.0 software.

In vitro experiments

To test the effects of the treatment with CM in mature osteoblasts, we used the rat osteosarcoma cell line UMR106 (ATCC, Manassas, VA, USA) which displays osteoblastic

properties. UMR106 cells were culture in calcium-free DMEM (Gibco™, Grand Island, NY, USA), supplemented with 10% FBS (Lonza Inc., Walkersville, MD, USA), 2mM ultraglutamine (Lonza), 1mM sodium pyruvate (Lonza), 20mM HEPES (Sigma-Aldrich), 100 U/ml penicillin, 100µg/ml streptomycin and calcium chloride (Sigma-Aldrich) to adjust the calcium concentration at 0.5mM. Once cells reached ~90% confluence, CM (1 µM and 100µM) or Calhex 231 hydrochloride (1 and 10 µM) were added to the medium. Protein samples were collected after 6 hours of treatment for western blot analysis. RNA samples were obtained after 48 hours of treatment for gene expression quantification.

Additionally, human mesenchymal stem cells (MSC) were obtained from excess bone marrow collected during diagnosis or routine follow-up of patients on the Hematology service of the Reina Sofía University Hospital. These MSC from the iliac crest were isolated by their plastic adherence properties. 750µl of total bone marrow aspirate were cultured in 75cm^2 flasks (NUNC A/S, Roskilde, DE, USA) with αMEM (Sigma-Aldrich) containing 15% FBS, 2mM ultraglutamine, 100U/ml penicillin, 100µg/ml streptomycin and 1ng/ml of basic fibroblast growth factor, (PeproTech EC Ltd, London, UK) in a humidified atmosphere of 5% CO_2 at 37ºC. Fresh α-MEM supplemented as above and with 10% FBS added after 24 hours and replaced every 3 days. Once 85-90% confluent, cells were collected using Trypsin-EDTA (Lonza), seeded into 6-well plates (NUNC A/S) at 13000 cells/cm^2 and cultured with calcium-free DMEM supplemented as described above and under osteogenic stimuli based on 1µM dexamethasone (Sigma-Aldrich), 10mM β-glycerol phosphate (Sigma-Aldrich CO.) and 200µM ascorbic acid (Bayer, Barcelona, Spain). Additionally, 100µM of CM was added to osteogenic media with low Ca (0.5mM) throughout differentiation. After 21 days, protein and RNA samples were collected for analysis.

Protein extraction and Western blot analysis

Total protein will be isolated from cells in a lysis buffer, containing 20mM Tris/HCl, 150mM NaCl, 1mM EDTA, 0.5mM PMSF, 70µg/ml Protease Inhibitor Cocktail (Sigma-Aldrich), 0.5% Igepal CA-630 (Sigma-Aldrich), 1µl/ml Phosphatase Inhibitor Cocktail 2 and 1µl/ml Phosphatase Inhibitor Cocktail 3 (Sigma-Aldrich), pH 7.6. Suspension will be centrifuged and supernatant (protein extract) will be stored at -80ºC. Protein concentration will be determined by Bradford assay (Bio-Rad Laboratories, Hercules, CA, USA). To determine specific proteins content, 50µg of total protein will be analyzed by immunoblotting using antibodies for CaSR (ab19347, Abcam plc., Cambridge, UK) at 2µg/ml, p44/42 MAPK (4695, Cell Signaling Technology) at 1:1000, phospho-p44/42 MAPK (4370, Cell Signaling Technology) and PCNA (sc-56, Santa Cruz Biotechnology) at 1:200 were used as primary antibodies, and horseradish peroxidase-conjugated goat anti-mouse and goat anti-rabbit (Santa Cruz Biotechnology Inc., Dallas, TX) at 1:10000 were used as secondary antibodies. β-actin (sc-47778, Santa Cruz Biotechnology) at 1:500 was used as loading control.

Gene expression quantification

Total RNA was extracted using TRI reagent (Sigma-Aldrich) and final concentration was quantified by spectrophotometry (ND-1000, Nanodrop Technologies, Wilmington, DE, USA). Isolated RNA samples were treated with DNase amplification grade (Sigma-Aldrich) and Real-time PCR was assayed with 50ng of DNAse-treated RNA using SensiFAST SYBR No-ROX One-Step Kit (Bioline, London, UK). Primers for PCR are shown in supplementary information (Supplementary Table S1). PCR amplification was performed using Lightcycler 480 (Roche Molecular Biochemicals, Indianapolis, IN). The expression of target genes was normalized to the expression of with the $2^{-\Delta\Delta Ct}$ method using GAPDH as housekeeping control.

Confocal immunofluorescence

UMR cells were cultured on glass coverslips in 6-well plates. Once cells reached 90% confluence, cells were treated with CM (100 μM) or a similar volume of vehicle (DMSO) and after 6 hours, cells were processed for immunofluorescence staining of phospho-Erk1/2. Briefly, cells were rinsed with PBS, fixed with cold methanol for 20 minutes and subsequently rinsed with PBS three times. Fixed cells were incubated in the diluted antibody in 1% BSA (Sigma-Aldrich) and PBS. Phospho-Erk1/2 primary antibody (Cell signaling Technology Inc; dilution 1:500) was incubated O/N at 4ºC. Subsequently, cells were washed with PBS and incubated with Alexa Fluor 488 anti-rabbit (Invitrogen; 1:500 dilution) diluted in 1% BSA in PBS for 1 hour at RT. Nuclei were visualized with the nuclear stain 4',6-diamino-2-phenylindole dihydrochloride (DAPI; Invitrogen). Pictures were obtained at 400x in a Zeiss LSM 710 inverted confocal microscope (Carl Zeiss, Jena, Germany). ImageJ software (National Institutes of Health, Bethesda, MD, USA) was used to analyze the confocal images. Co-localization analysis was performed by quantifying the mean of intensity of fluorescence (phospho-Erk1/2-488) in each nucleus of the different treatments. Values are showed as fold change vs Control.

Measurement of calcium content in cultured cells

After 21 days of osteogenic differentiation, cells were decalcified by incubation in HCl (0.6 M) for 24 hours. Ca content in the supernatant was determined by the phenolsulphonephthalein method using a commercial assay (QuantiChrom™ Calcium Assay Kit, BioAssay Systems, CA, USA). Cells were washed 3 times with PBS (Sigma Aldrich) and protein content was extracted with a NaOH (0.1 M) SDS (0.1%) solution. Protein content was quantified as described above and the Ca content was normalized according to total protein.

Statistics

Values are expressed as the mean ± standard deviation (SD). The difference between means for two groups was assessed by T-test. One-way ANOVA test with tukey post hoc was used to analyze the statistical differences among three or more independent groups. Two-way ANOVA test with LSD post hoc was used to examine the influence of PTH and CM on another variable. $P<0.05$ was considered significant. IBM SPSS Statistics software (IBM, Armonk, NY, USA) was used for Two-way ANOVA statistical analysis. GraphPad Software (GraphPad Software, Inc., La Jolla, CA, USA) was used for One-way ANOVA and T-test statistical analyses and graph performance.

DISCLOSURE

W.G.R is employed by AMGEN.Inc. MR has received honoraria for lectures from Amgen, and Sanifit. JMF has received honoraria for lectures from Amgen. All the other authors declared no competing interests.

ACKNOWLEDGEMENTS

We thank Daniela Sousa from the INEB/I3S institute and the Nephrology Unit of the Hospital São João for the kind assistance with bone histomorphometry. The calcimimetic AMG 641 was a kindly gift from AMGEN. This work has been partially supported by a Spanish Government Grant from the National Program I+D+I 2008-2011 from the National Institute of Health Carlos III (PI14/00638 and PI14/00467 and PI 17/01010) with co-financing from European Funds (FEDER). JM. D-T. and N.V. are supported by Ministry of Economy, Innovation, Science and Employment from Andalusian Local Government (CVI-7925). M.E.R-O. is recipient of a "Sara Borrell" research contract from the National Institute of Health Carlos III. Y.A. and J.R.M-C. are senior researchers supported by Nicolás Monardes Programme, Ministry of Health-Andalusian Health Service (Andalusian Local Government).

Table 1. Serum mineral and biochemical parameters in the experiment with rats with normal renal function.

	Sham n=6	**PTX** n=7	**PTX-PTH** n=5	**PTX-PTH-CM** n=6
Ionized calcium (mM)	1.21±0.04	0.59±0.05[a]	1.13±0.09	1.07±0.10
Phosphate (mg/dl)	6.2±0.4	11.6±2.4[a]	5.6±0.89[b]	5.4±1.47[b]
$1,25(OH)_2D_3$ (pg/ml)	192±78	126±53	163±56	252±73[abc]
FGF23 (pg/ml)	130±76	68±16[a]	129±45[b]	88±34[c]

Data are mean±SD. ANOVA with Tukey test. [a]: $p<0.05$ vs Sham; [b]: $p<0.05$ vs PTX; [c]: $p<0.05$ vs PTX-PTH.

Table 2. Serum mineral and biochemical parameters in the experiment with rats with renal insufficiency.

	Sham n=6	**Nx** n=7	**Nx-CM** n=6	**Nx-PTX-PTHx6** n=8	**Nx-PTX-PTHx6-CM** n=5	**Nx-PTX-PTHx9** n=5	**Nx-PTX-PTHx9-CM** n=6
Creatinine (mg/dl)	0.5±0.07	0.9±0.16[a]	0.9±0.11[a]	0.9±0.08	0.9±0.11	0.9±0.11	0.85±0.10
Ionized calcium (mM)	1.21±0.04	1.10±0.05[a]	1.00±0.04[a]	1.02±0.08	1.08±0.13	1.15±0.16	1.17±0.15
Phosphate (mg/dl)	6.2±0.4	8.73±1.03[a]	7.35±0.78[a]	7.77±1.22	6.32±0.89	7.58±1.79	7.94±1.86
Intact PTH (pg/ml)	47±9.83	540±259[a]	144±98[ab]	n.a	n.a	n.a	n.a
PTH (1-34) (pg/ml)	-	386±116	-	304±65	295±27	541±141[c]	599±137
$1,25(OH)_2D_3$ (pg/ml)	192±78	159±48	131±22	162±28	158±16	153±38	152±54
FGF23 (pg/ml)	130±76	1522±574[a]	826±436[ab]	471±296	491±194	1209±626[c]	1005±343

Data are mean±SD. One-way ANOVA with Tukey post hoc test was used to analyze differences among Sham, Nx and Nx-CM groups.

[a]: $p<0.05$ vs Sham; [b]: $p<0.05$ vs Nx. Two-way ANOVA test with LSD post hoc was used to compare the PTH and CM effects on Nx-PTx groups. [c]: $p<0.05$ vs Nx-PTX-PTHx6; n.a.: not applicable.

FIGURE LEGENDS

Figure 1. Effects of CM in the bone histomorphometric parameters of normal rats undergoing PTX and clamped PTH. After 28 days, the bone volume (a) remained similar in all groups. Parathyroidectomy decreased the osteoid volume (b), osteoid surface (c), osteoblasts (d) and osteoclasts (f) activity. PTH replacement reestablished bone remodeling that was similar to sham. Treatment with CM produce a tendency to increase osteoblast activity. Bars show mean±SD. One-way ANOVA test with Tukey post-hoc. *: $p<0.05$; **: $p<0.01$. ●: Sham; ■: PTX; ▲: PTx-PTH;▼: PTx-PTH-CM.

Figure 2. Effects of CM in bone histomorphometric parameters of Nx rats and Nx rats with PTX and PTH infusion. Nx induced a reduction in the bone volume (a), and increased bone turnover (b-f). [a] $p<0.05$ vs Sham (One-way ANOVA test with tukey post hoc). In Nx rats, treatment with CM prevented the decrease in bone turnover. In Nx-PTx-PTHx6 the bone turnover was decreased while CM treatment (Nx-PTx-PTHx6-CM) increased bone cell activity. *: $p<0.05$; ** $p<0.01$ (Two-way ANOVA test with LSD post hoc). The infusion of PTHx9 significantly increased bone turnover as compared with PTHx6. [b] $p<0.01$vs Nx-PTx-PTHx6 (Two-way ANOVA test with LSD post hoc). In conditions of very high PTH, the administration of CM (Nx-PTx-PTHx9-CM) did not produce a significant further increase in bone cell activity. Bars show mean±SD. n.s: not significant. ●: Sham; ▲: Nx; ▲: Nx-CM; ■: Nx-PTX-PTHx6; ■: Nx-PTX-PTHx6-CM; ▼: Nx-PTX-PTHx9; ▼: Nx-PTX-PTHx9-CM.

Figure 3. Effects of CM on bone mineralization of Nx rats and Nx rats with PTX and PTH infusion. No significant differences were found between groups treated with vehicle or CM for osteoid thickness (**a**), mineralizing surface related to osteoid Surface (**b**), mineral apposition rate (**c**), adjusted apposition rate (**d**), mineralization lag time (**e**) or osteoid maturation time (**f**). [a]

p<0.05 vs Sham (One-way ANOVA test with tukey post hoc). [b] p<0.05 vs Nx-PX-PTHx6 (Two-way ANOVA test with LSD post hoc). n.s: no significant differences. ●: Sham; ▲: Nx; ▲: Nx-CM; ■: Nx-PTX-PTHx6; ■: Nx-PTX-PTHx6-CM; ▼: Nx-PTX-PTHx9; ▼: Nx-PTX-PTHx9-CM.

Figure 4. Representative photographs of Goldner's trichrome staining and double calcein labeling in trabecular bone. In Sham animals, an almost quiescent state of bone cells was observed (**a**), with normal mineralization (**b**). In Nx rats, an increase in bone cell activity was observed, note the high number of the cuboidal cells (osteoblasts, arrowhead) and multinucleated cells (osteoclasts, asterisk) on the bone surface (**c**), accompanied by an increase in bone formation (**d**). Nx rats treated with CM maintained similar bone cell activity (**e**) and mineralization (**f**) to Nx rats. In Nx-PTX-PTHx6 animals low bone turnover (g) and bone formation (h) with respect to Nx group were detected. Treatment with CM increased the number of osteoblasts and osteoclasts (**i**) as well as mineralization and bone formation (**j**). In Nx-PTX-PTHx9 group a similar bone turnover (**k**) and mineralization (**l**) to the Nx group was observed. In Nx-PTX-PTHx9 + CM bone cells activity (**m**) and bone formation (**n**) were also similar to those observed in their corresponding vehicle group Nx-PTX-PTHx9. Mineralized tissue is stained in green while the non-mineralized bone (osteoid) is stained in red. The distance between calcein labels (Double-head arrows) shows the bone being formed during the time interval (7 days) indicating the mineralization status. Magnification: 200x. Scale bar: 100µm. Arrowheads: Osteoblasts. Asterisks: Osteoclasts.

Figure 5. The administration of CM triggered Erk1/2 phosphorylation of osteoblasts. Osteoblasts with positive phospho-Erk1/2 staining (b and c) were counted in 3 random fields samples and were expressed as the percentage of total osteoblasts (a). Goldner's staining of undecalcified bone sections showed cuboidal osteoblasts covering osteoid on the bone surface.

Immunohistochemistry for phospho-Erk1/2 showed intense nuclear staining in osteoblasts in the Nx-CM (b), Nx-PTx-PTHx6-CM and Nx-PTx-PTHx9-CM groups (c) and scarce nuclear staining in the bone cells of the other groups. To determine that the target cells were osteoblasts, serial undecalcified bone sections were also stained for osteocalcin. Immunohistochemistry without primary antibody in undecalcified bone samples showed no positive staining. Arrows indicate nuclear phospho-Erk1/2. Magnification 1000x. Scale bar: 20μm.

Figure 6. Treatment with CM triggers CaSR downstream signaling and up-regulates osteogenic marker genes expression in low calcium conditions. Western blots of total protein extracts show positive expression of CaSR in UMR106 cell line and with CM there was a non-significant tendency to increase PCNA expression (a), while induced a manifested Erk1/2 phosphorylation (b). The gene expression of Runx2 (c), Osterix (d) and osteocalcin (e) was induced with the effective dose of CM. Bars show mean±SD. T-test. a: $p<0.05$ vs control; b: $p<0.05$ vs CM 1μM.

Figure 7. Inhibition of CaSR signaling by Calcilytics decreases osteogenesis in UMR-106 cells. Calhex administration at 10 μM reduced Erk1/2 phosphorylation (**a**). In presence of Calhex there was a significant decrease of Osterix (**b**), Runx2 (**c**) and Osteocalcin (**d**) expression.

Figure 8. Treatment with CM during osteogenic differentiation of MSC in low Ca medium increases mineralization and gene expression of osteogenic marker. Osteogenic differentiation induced matrix mineralization (**a** and **b**), and increased expression of osteogenic gene markers Runx2 (**c**), Osterix (**d**), Osteocalcin (**e**) and BMP2 (**f**). Both, MSC and MSC-derived osteoblasts expressed CaSR (**g**). Mineralization and osteogenic markers were further increased with CM addition. Low Ca was 0.5mM. [CM]= 100μM. Bars show mean±SD. T-test. a: $p<0.05$ vs MSC. b: $p<0.05$ vs OB. Magnification: 200x. Scale bar: 100μm.

Supplementary Materials

Supplementary Table S1. Sequences of the primers used for the RT-PCR.

Supplementary Figure S1. Representative photographs of Goldner's trichrome staining in trabecular bone from Sham (**a**), PTX (**b**), PTX-PTH (**c**) and PTX-PTH-CM (**d**) groups with normal renal function. As compared with the Sham group, the PTX group shows a decrease in osteoid surface and in the number of osteoblasts and osteoclasts. PTH replacement increased osteoid surface and the osteoid surface covered by osteoblasts. As compared with PTX group the administration of CM maintained bone cell activity and mineralization. Magnification: 200x. Scale bar: 100µm.

Supplementary Figure S2. Evolution of the total body weight of the different groups of rats during the experiment. * $p<0.05$ Sham vs all groups.

Supplementary Figure S3. Cortical bone analysis. Cortical Bone Area (Ct.B.Ar) (**a**) and Cortical Thickness (Ct.Th) (**b**) in the midshaft of the femurs were similar in all groups.

Supplementary Figure S4. Treatment with CM triggers phospho-Erk1/2 nuclear translocation. Immunofluorescence analysis show increased amount phospho-Erk1/2 (Green) in the nuclei of UMR cells (Blue) after 6 hours of treatment with CM (a). The amount of green pixels in the nuclei was higher in cells treated with CM than in vehicle (b). T-test *** $p<0.001$. Scale bar: 50 µm.

REFERENCES

1. Moe S, Drüeke T, Cunningham J, Goodman W, Martin K, Olgaard K, Ott S, Sprague S, Lameire N, Eknoyan G, Kidney Disease: Improving Global Outcomes (KDIGO). Definition, evaluation, and classification of renal osteodystrophy: a position statement from Kidney Disease: Improving Global Outcomes (KDIGO). *Kidney Int*. 2006;69(11):1945-1953. doi:10.1038/sj.ki.5000414.

2. Picton ML, Moore PR, Mawer EB, Houghton D, Freemont AJ, Hutchison AJ, Gokal R, Hoyland JA. Down-regulation of human osteoblast PTH/PTHrP receptor mRNA in end-stage renal failure. *Kidney Int*. 2000;58(4):1440-1449. doi:10.1046/j.1523-1755.2000.00306.x.

3. Block GA, Martin KJ, de Francisco ALM, Turner SA, Avram MM, Suranyi MG, Hercz G, Cunningham J, Abu-Alfa AK, Messa P, Coyne DW, Locatelli F, Cohen RM, Evenepoel P, Moe SM, Fournier A, Braun J, McCary LC, Zani VJ, Olson KA, Drüeke TB, Goodman WG. Cinacalcet for secondary hyperparathyroidism in patients receiving hemodialysis. *N Engl J Med*. 2004;350(15):1516-1525. doi:10.1056/NEJMoa031633.

4. Goodman WG, Frazao JM, Goodkin DA, Turner SA, Liu W, Coburn JW. A calcimimetic agent lowers plasma parathyroid hormone levels in patients with secondary hyperparathyroidism. *Kidney Int*. 2000;58(1):436-445. doi:10.1046/j.1523-1755.2000.00183.x.

5. Behets GJ, Spasovski G, Sterling LR, Goodman WG, Spiegel DM, De Broe ME, D'Haese PC. Bone histomorphometry before and after long-term treatment with cinacalcet in dialysis patients with secondary hyperparathyroidism. *Kidney Int*. 2015;87(4):846-856. doi:10.1038/ki.2014.349.

6. Yajima A, Akizawa T, Tsukamoto Y, Kurihara S, Ito A, K Study Group. Impact of cinacalcet hydrochloride on bone histology in patients with secondary hyperparathyroidism. *Ther Apher Dial Off Peer-Rev J Int Soc Apher Jpn Soc Apher Jpn Soc Dial Ther*. 2008;12 Suppl 1:S38-43. doi:10.1111/j.1744-9987.2008.00630.x.

7. Chang W, Tu C, Chen TH, Komuves L, Oda Y, Pratt SA, Miller S, Shoback D. Expression and signal transduction of calcium-sensing receptors in cartilage and bone. *Endocrinology*. 1999;140(12):5883-5893. doi:10.1210/endo.140.12.7190.

8. Yamaguchi T, Chattopadhyay N, Kifor O, Butters RR, Sugimoto T, Brown EM. Mouse osteoblastic cell line (MC3T3-E1) expresses extracellular calcium (Ca2+o)-sensing receptor and its agonists stimulate chemotaxis and proliferation of MC3T3-E1 cells. *J Bone Miner Res Off J Am Soc Bone Miner Res*. 1998;13(10):1530-1538. doi:10.1359/jbmr.1998.13.10.1530.

9. Dvorak MM, Siddiqua A, Ward DT, Carter DH, Dallas SL, Nemeth EF, Riccardi D. Physiological changes in extracellular calcium concentration directly control osteoblast function in the absence of calciotropic hormones. *Proc Natl Acad Sci U S A*. 2004;101(14):5140-5145. doi:10.1073/pnas.0306141101.

10. Yamaguchi T, Olozak I, Chattopadhyay N, Butters RR, Kifor O, Scadden DT, Brown EM. Expression of extracellular calcium (Ca2+o)-sensing receptor in human peripheral blood

monocytes. *Biochem Biophys Res Commun*. 1998;246(2):501-506. doi:10.1006/bbrc.1998.8648.

11. Kameda T, Mano H, Yamada Y, Takai H, Amizuka N, Kobori M, Izumi N, Kawashima H, Ozawa H, Ikeda K, Kameda A, Hakeda Y, Kumegawa M. Calcium-sensing receptor in mature osteoclasts, which are bone resorbing cells. *Biochem Biophys Res Commun*. 1998;245(2):419-422. doi:10.1006/bbrc.1998.8448.

12. House MG, Kohlmeier L, Chattopadhyay N, Kifor O, Yamaguchi T, Leboff MS, Glowacki J, Brown EM. Expression of an extracellular calcium-sensing receptor in human and mouse bone marrow cells. *J Bone Miner Res Off J Am Soc Bone Miner Res*. 1997;12(12):1959-1970. doi:10.1359/jbmr.1997.12.12.1959.

13. Kanatani M, Sugimoto T, Kanzawa M, Yano S, Chihara K. High extracellular calcium inhibits osteoclast-like cell formation by directly acting on the calcium-sensing receptor existing in osteoclast precursor cells. *Biochem Biophys Res Commun*. 1999;261(1):144-148. doi:10.1006/bbrc.1999.0932.

14. Al-Dujaili SA, Koh AJ, Dang M, Mi X, Chang W, Ma PX, McCauley LK. Calcium Sensing Receptor Function Supports Osteoblast Survival and Acts as a Co-Factor in PTH Anabolic Actions in Bone. *J Cell Biochem*. 2016;117(7):1556-1567. doi:10.1002/jcb.25447.

15. Richard C, Huo R, Samadfam R, Bolivar I, Miao D, Brown EM, Hendy GN, Goltzman D. The calcium-sensing receptor and 25-hydroxyvitamin D-1alpha-hydroxylase interact to modulate skeletal growth and bone turnover. *J Bone Miner Res Off J Am Soc Bone Miner Res*. 2010;25(7):1627-1636. doi:10.1002/jbmr.58.

16. Vezzoli G, Tanini A, Ferrucci L, Soldati L, Bianchin C, Franceschelli F, Malentacchi C, Porfirio B, Adamo D, Terranegra A, Falchetti A, Cusi D, Bianchi G, Brandi ML. Influence of calcium-sensing receptor gene on urinary calcium excretion in stone-forming patients. *J Am Soc Nephrol JASN*. 2002;13(10):2517-2523.

17. Khoshniat S, Bourgine A, Julien M, Petit M, Pilet P, Rouillon T, Masson M, Gatius M, Weiss P, Guicheux J, Beck L. Phosphate-dependent stimulation of MGP and OPN expression in osteoblasts via the ERK1/2 pathway is modulated by calcium. *Bone*. 2011;48(4):894-902. doi:10.1016/j.bone.2010.12.002.

18. Wada M, Ishii H, Furuya Y, Fox J, Nemeth EF, Nagano N. NPS R-568 halts or reverses osteitis fibrosa in uremic rats. *Kidney Int*. 1998;53(2):448-453. doi:10.1046/j.1523-1755.1998.00782.x.

19. Henley C, Davis J, Miller G, Shatzen E, Cattley R, Li X, Martin D, Yao W, Lane N, Shalhoub V. The calcimimetic AMG 641 abrogates parathyroid hyperplasia, bone and vascular calcification abnormalities in uremic rats. *Eur J Pharmacol*. 2009;616(1-3):306-313. doi:10.1016/j.ejphar.2009.05.013.

20. Evenepoel P, Bover J, Ureña Torres P. Parathyroid hormone metabolism and signaling in health and chronic kidney disease. *Kidney Int*. 2016;90(6):1184-1190. doi:10.1016/j.kint.2016.06.041.

21. Xue Y, Xiao Y, Liu J, Karaplis AC, Pollak MR, Brown EM, Miao D, Goltzman D. The calcium-sensing receptor complements parathyroid hormone-induced bone turnover in

discrete skeletal compartments in mice. *Am J Physiol Endocrinol Metab*. 2012;302(7):E841-851. doi:10.1152/ajpendo.00599.2011.

22. Shu L, Ji J, Zhu Q, Cao G, Karaplis A, Pollak MR, Brown E, Goltzman D, Miao D. The calcium-sensing receptor mediates bone turnover induced by dietary calcium and parathyroid hormone in neonates. *J Bone Miner Res Off J Am Soc Bone Miner Res*. 2011;26(5):1057-1071. doi:10.1002/jbmr.300.

23. Dvorak MM, Chen T-H, Orwoll B, Garvey C, Chang W, Bikle DD, Shoback DM. Constitutive activity of the osteoblast Ca2+-sensing receptor promotes loss of cancellous bone. *Endocrinology*. 2007;148(7):3156-3163. doi:10.1210/en.2007-0147.

24. Li X, Yu L, Asuncion F, Grisanti M, Alexander S, Hensley K, Han C-Y, Niu Q-T, Dwyer D, Villasenor K, Stolina M, Dean C, Ominsky MS, Ke HZ, Tomlinson JE, Richards WG. Etelcalcetide (AMG 416), a peptide agonist of the calcium-sensing receptor, preserved cortical bone structure and bone strength in subtotal nephrectomized rats with established secondary hyperparathyroidism. *Bone*. 2017;105:163-172. doi:10.1016/j.bone.2017.08.026.

25. Chattopadhyay N, Yano S, Tfelt-Hansen J, Rooney P, Kanuparthi D, Bandyopadhyay S, Ren X, Terwilliger E, Brown EM. Mitogenic action of calcium-sensing receptor on rat calvarial osteoblasts. *Endocrinology*. 2004;145(7):3451-3462. doi:10.1210/en.2003-1127.

26. Rodriguez M, Lorenzo V, Felsenfeld AJ, Llach F. Effect of parathyroidectomy on aluminum toxicity and azotemic bone disease in the rat. *J Bone Miner Res Off J Am Soc Bone Miner Res*. 1990;5(4):379-386. doi:10.1002/jbmr.5650050411.

27. Berdud I, Martin-Malo A, Almaden Y, Aljama P, Rodriguez M, Felsenfeld AJ. The PTH-calcium relationship during a range of infused PTH doses in the parathyroidectomized rat. *Calcif Tissue Int*. 1998;62(5):457-461.

28. Nemeth EF, Van Wagenen BC, Balandrin MF. Discovery and Development of Calcimimetic and Calcilytic Compounds. *Prog Med Chem*. 2018;57(1):1-86. doi:10.1016/bs.pmch.2017.12.001.

29. Lopez I, Mendoza FJ, Aguilera-Tejero E, Perez J, Guerrero F, Martin D, Rodriguez M. The effect of calcitriol, paricalcitol, and a calcimimetic on extraosseous calcifications in uremic rats. *Kidney Int*. 2008;73(3):300-307. doi:10.1038/sj.ki.5002675.

30. Dempster DW, Compston JE, Drezner MK, Glorieux FH, Kanis JA, Malluche H, Meunier PJ, Ott SM, Recker RR, Parfitt AM. Standardized nomenclature, symbols, and units for bone histomorphometry: a 2012 update of the report of the ASBMR Histomorphometry Nomenclature Committee. *J Bone Miner Res Off J Am Soc Bone Miner Res*. 2013;28(1):2-17. doi:10.1002/jbmr.1805.

31. Erben RG, Glösmann M. Histomorphometry in rodents. *Methods Mol Biol Clifton NJ*. 2012;816:279-303. doi:10.1007/978-1-61779-415-5_19.

Fig.1

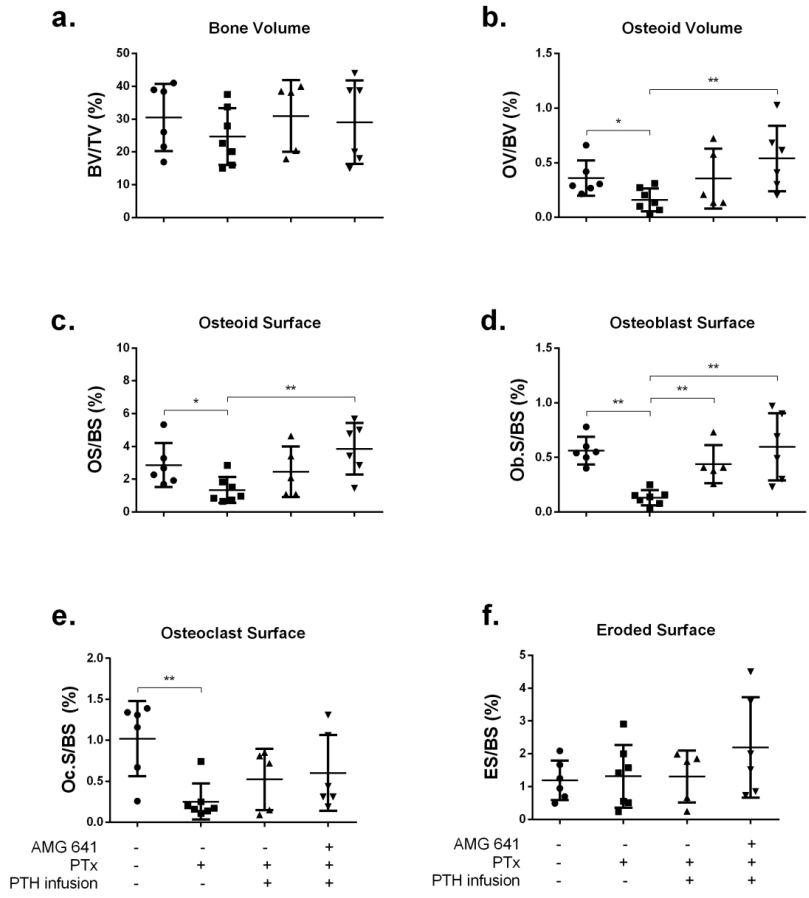

Figure 1. Bone histomorphometry normal renal function

206x243mm (300 x 300 DPI)

Fig.2

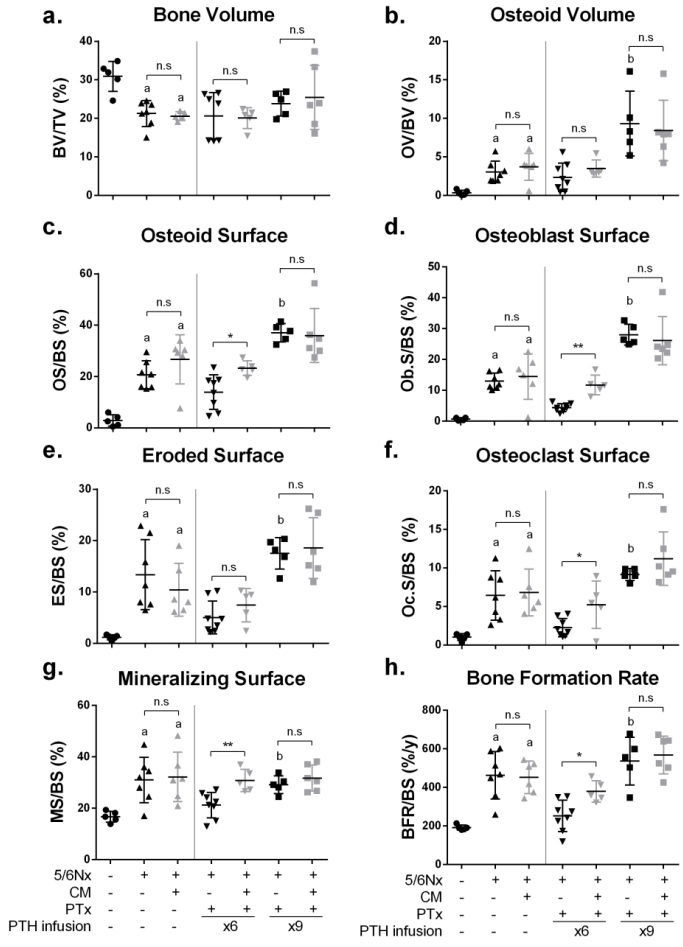

Figure 2. Bone histomorphometry 5/6Nx_TV

211x300mm (300 x 300 DPI)

Fig.3

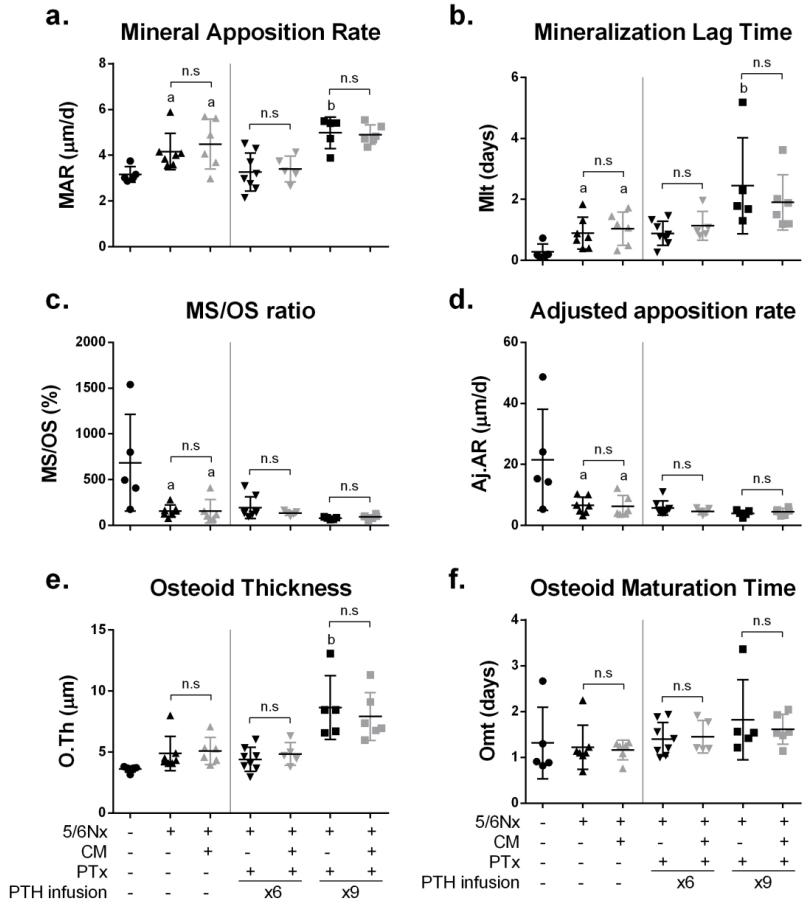

Figure 3. Bone histomorphometry 5/6Nx_M

210x252mm (300 x 300 DPI)

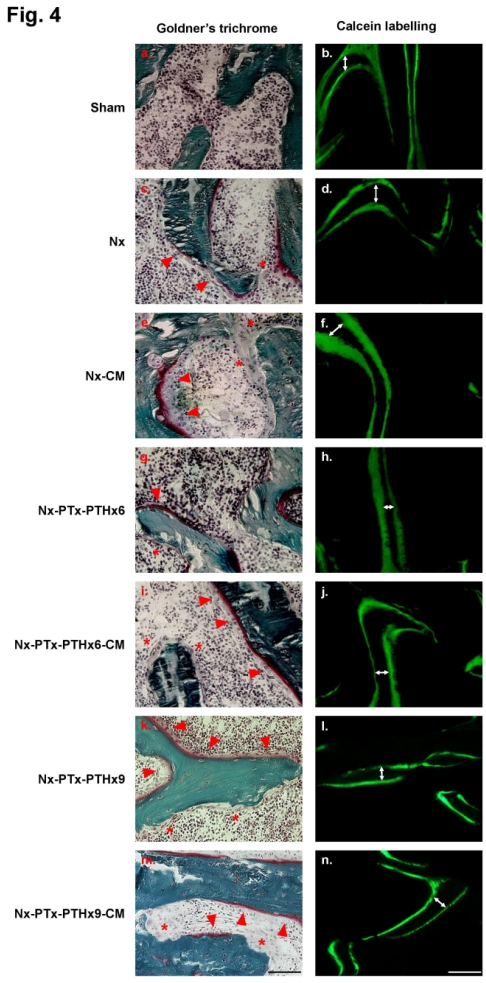

Figure 4. Representative microphotographs

190x338mm (300 x 300 DPI)

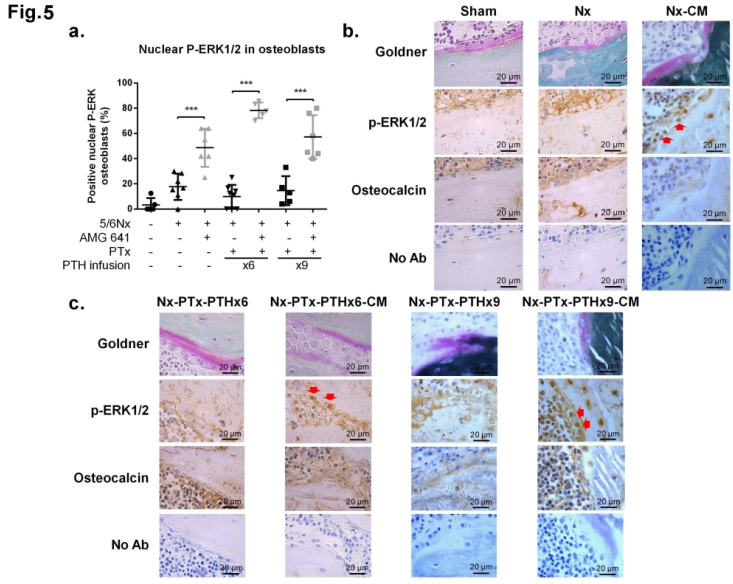

Figure 5. Bone p-ERK1/2 IHC

297x209mm (300 x 300 DPI)

Fig.6

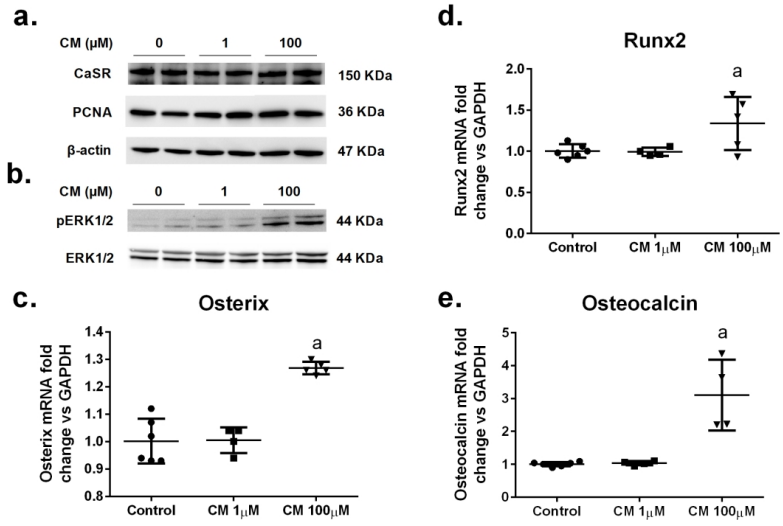

Figure 6. UMR and CM

205x147mm (300 x 300 DPI)

Fig.7

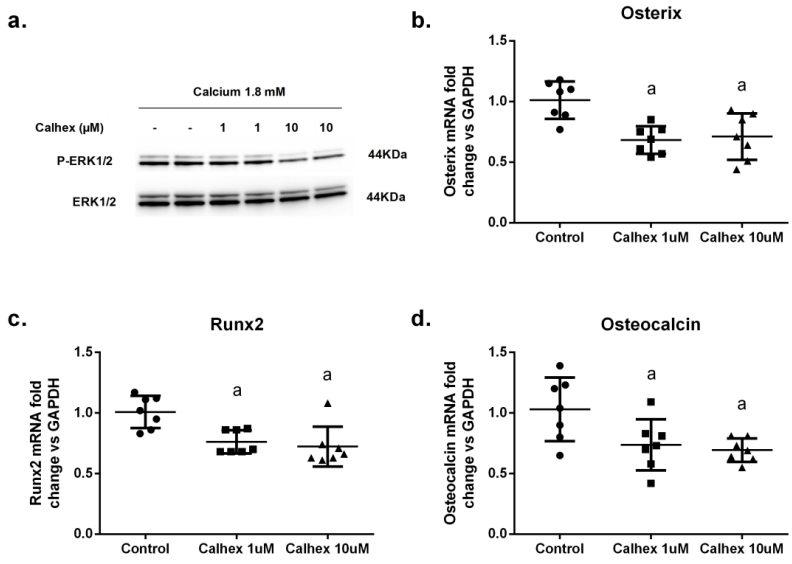

Figure 7. UMR and Calhex

261x196mm (300 x 300 DPI)

Fig.8

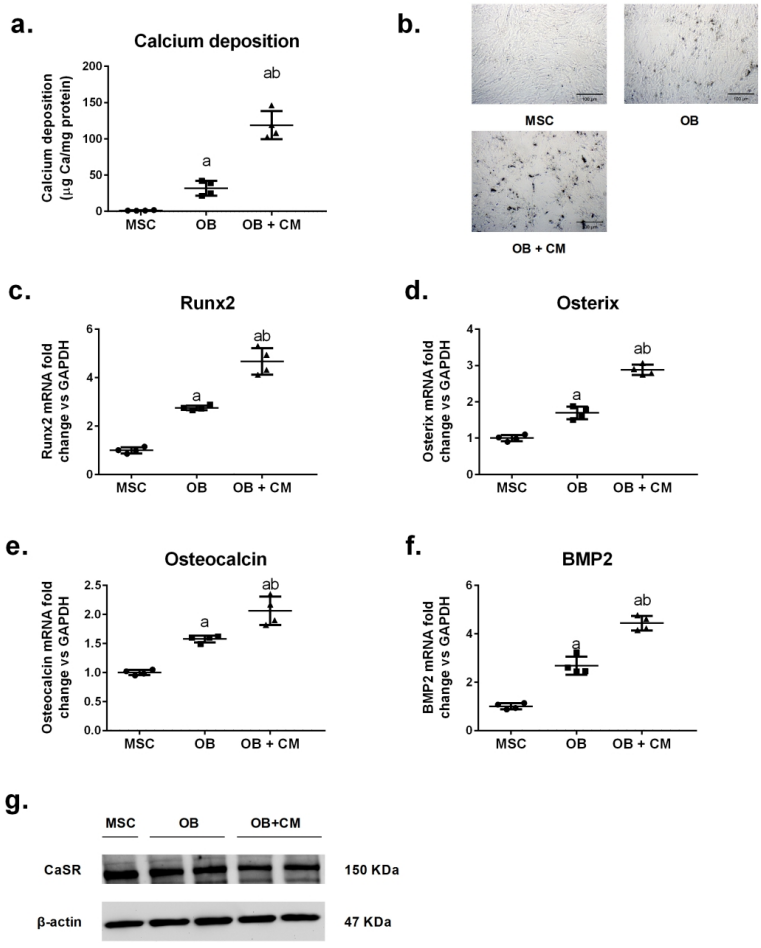

Figure 8. MSC osteogenic differentiation and CM

204x265mm (300 x 300 DPI)

SUPPLEMENTARY FIGURE S1.

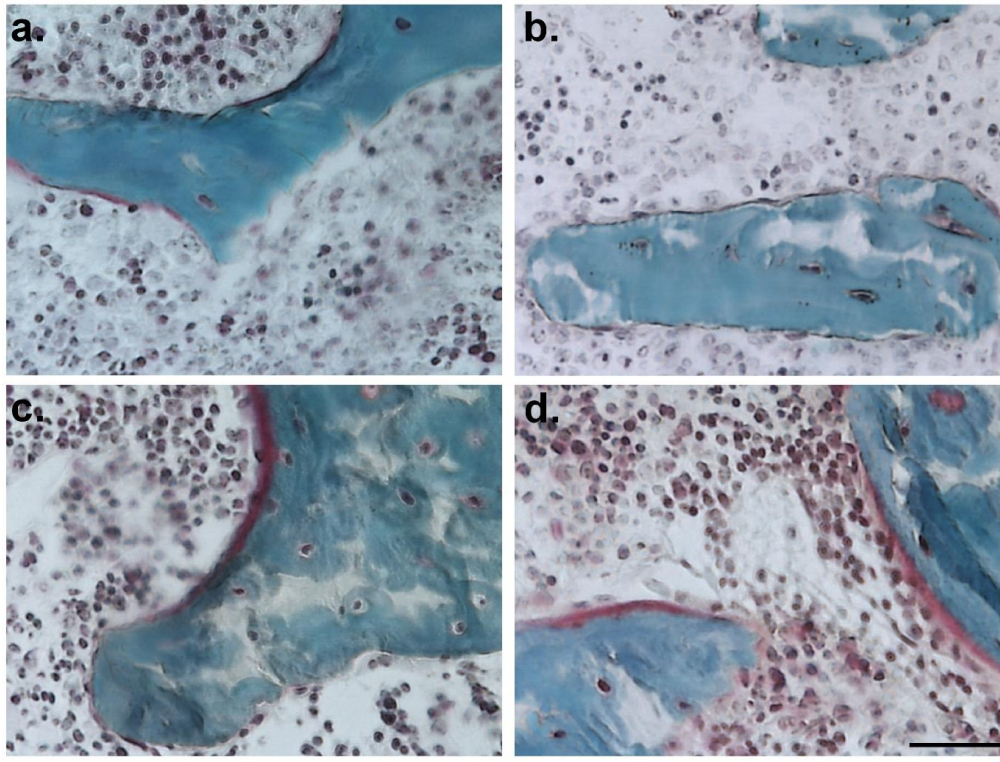

Supplementary Figure S1. Representative photographs of Goldner's trichrome staining in trabecular bone for Sham (**a**), PTX (**b**), PTX-PTH (**c**) and PTX-PTH-CM (**d**) groups with normal renal function. As compared with the Sham group, the PTX group shows a decrease in osteoid surface and in the number of osteoblasts and osteoclasts. PTH replacement increased osteoid surface and the osteoid surface covered by osteoblasts. Despite absence of PTH the administration of CM maintained bone cell activity and mineralization. Magnification: 200x. Scale bar: 100µm.

SUPPLEMENTARY FIGURE S2.

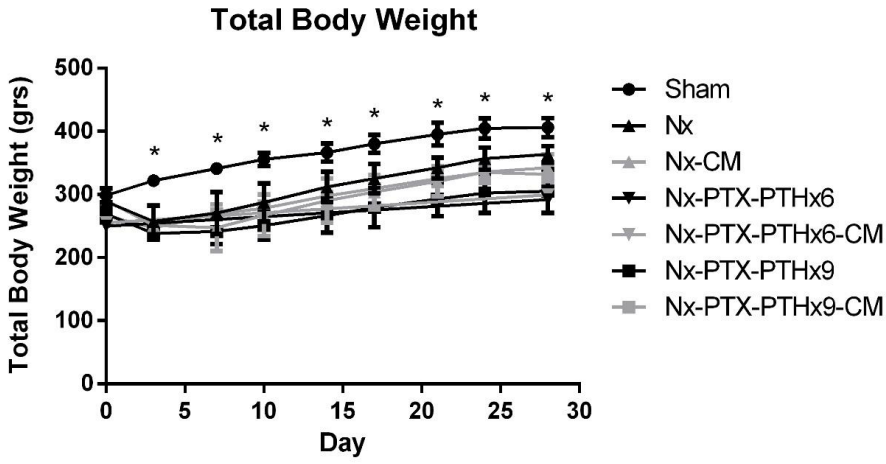

Supplementary Figure S2. Evolution of the total body weight of the different groups of rats during the experiment. * $p<0.05$ Sham vs all groups.

SUPPLEMENTARY FIGURE S3.

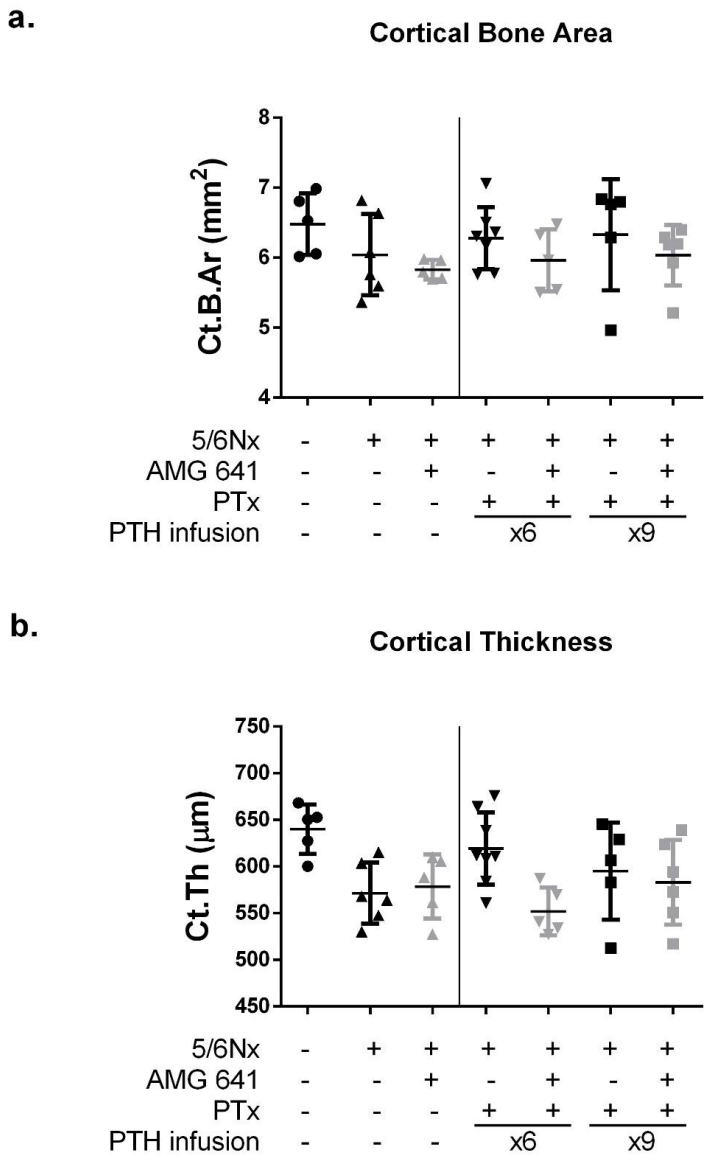

Supplementary Figure S3. Cortical bone analysis. Cortical Bone Area (Ct.B.Ar) (**a**) and Cortical Thickness (Ct.Th) (**b**) in the midshaft of the femurs were similar in all groups.

SUPPLEMENTARY FIGURE S4.

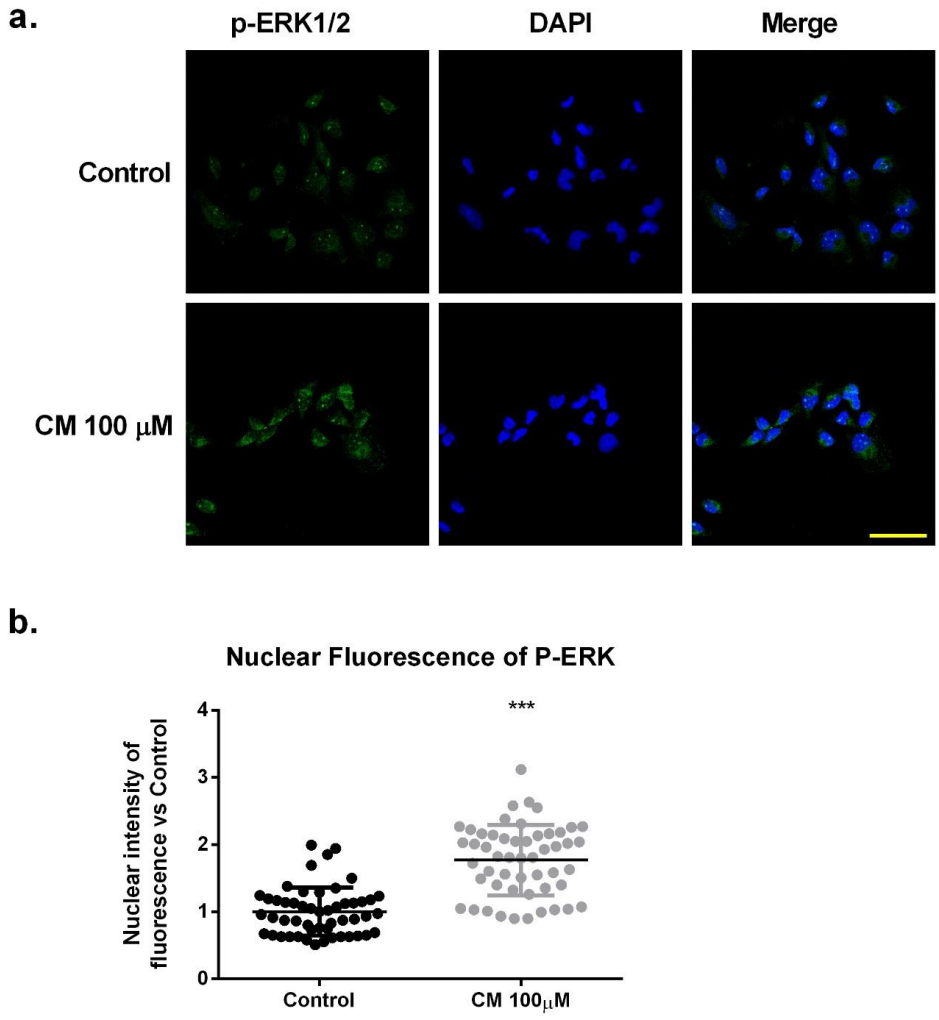

Supplementary Figure S4. Treatment with CM triggers phospho-Erk1/2 nuclear translocation. Immunofluorescence analysis show increased amount phospho-Erk1/2 (Green) in the nuclei of UMR cells (Blue) after 6 hours of treatment with CM (a). The amount of green pixels in the nuclei was higher in cells treated with CM than in vehicle (b). T-test *** $p<0.001$. Scale bar: 50 μm.

SUPPLEMENTARY TABLE S1.

	Forward primer	Reverse Primer
Rat Runx2	5'-CGGGAATGATGAGAACTACTC-3'	5'-CGGTCAGAGAACAAACTAGGT-3'
Rat Osterix	5'-GTACGGCAAGGCTTCGCATCTGA-3'	5'-TCAAGTGGTCGCTTCGGGTAAAG-3'
Rat Osteocalcin	5'-TCTGAGTCTGACAAAGCCTTCATG-3'	5'-TGGGTAGGGGGCTGGGGCTCC-3'
Rat GAPDH	5'-AGGGCTGCCTTCTCTTGTGAC-3'	5'-TGGGTAGAATCATACTGGAACATGTAG-3'
Human Runx2	5'-CCGGAGTGGACGAGGCAAGAGTT-3'	5'-AGCTTCTGTCTGTGCCTTCTGGG-3'
Human Osterix	5'-ATCTGCCTGGCTCCTTGGGACCCG-3'	5'-TGCTTTGCCCAGAGTTGTTGAGTC-3'
Human Osteocalcin	5'-GCAGAGTCCAGCAAAGGTGCAGCC-3'	5'-GCCTCCTGAAAGCCGATGTGGTCA-3'
Human BMP2	5'-AGGAGGCAAAGAAAAGGAACGGAC-3'	5'-GGAAGCAGCAACGCTAGAAGACAG-3'
Human GAPDH	5'-TGATGACATCAAGAAGGTGGTGAAG-3'	5'-TCCTTGGAGGCCATGTGGGCCAT-3'

Supplementary Table S1. Sequences of the primers used for the RT-PCR.

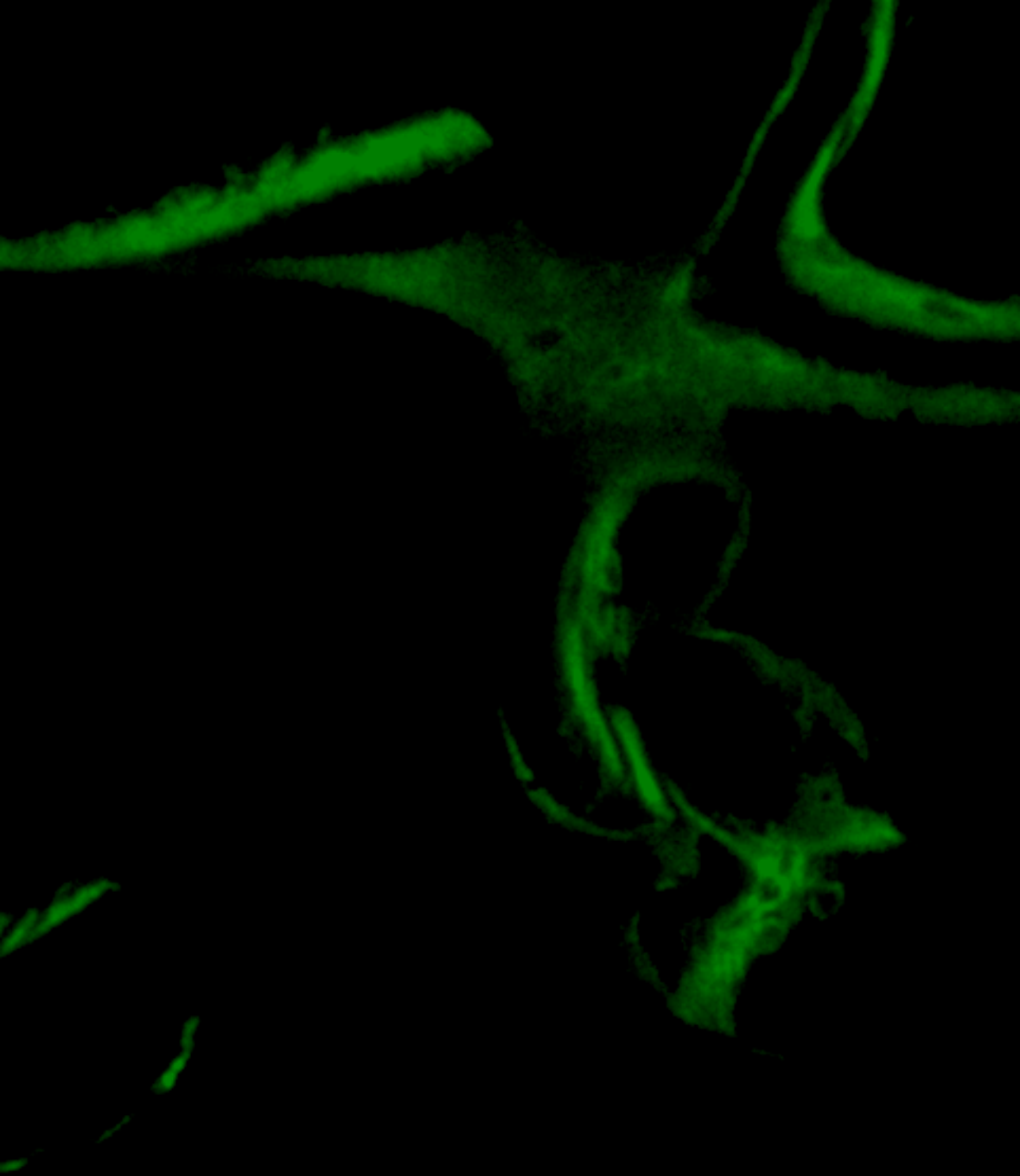

JUNTA DE ANDALUCIA

UNIVERSIDAD D CÓRDOBA

IMIBIC
INSTITUTO MAIMÓNIDES DE INVESTIGACIÓN BIOMÉDICA DE CÓRDOBA